Aspects of the Hemes and Modulation by Hydrogen Donors in Catalases from Bovine Liver, Yeast, and *Escherichia coli*

By:

Alexander P. Hillar
(BSc.(Hons), University. of Waterloo)

A thesis submitted to the Department of Biological Sciences in Partial Fulfillment of the Requirements for the Degree of Master of Science

July 1993
Brock University,
St. Catharines, Ontario, Canada

ABSTRACT

Catalase is the enzyme which decomposes hydrogen peroxide to water and oxygen. *Escherichia coli* contains two catalases. Hydroperoxidase I (HPI) is a bifunctional catalase-peroxidase. Hydroperoxidase II (HPII) is only catalytically active toward H_2O_2. Expression of the genes encoding these proteins is controlled by different regimes. HPII is thought to be a hexamer, having one heme *d* cis group per enzymatic subunit. HPII wild type protein and heme containing mutant proteins were obtained from the laboratory of P. Loewen (Univ. of Manitoba). Mutants constructed by oligonucleotide-directed mutagenesis were targeted for replacement of either the His128 residue or the Asn201 residue in the vicinity of the HPII heme crevice. His128 is the residue thought to be analogous to the His74 distal axial ligand of the heme in the bovine liver enzyme, and Asn201 is believed to be a residue critical to the function of the enzyme because of its role in orienting and interacting with the substrate molecule. Investigation of the nature of the hemes via absorption spectroscopy of the unmodified catalase proteins and their derived pyridine hemochromes showed that while the bovine and *Saccharomyces cerevisiae* catalase enzymes are protoheme-containing, the HPII wild type protein contains heme *d*, and the mutant proteins contain either solely protoheme, or heme *d*-protoheme mixtures. Cyanide binding studies supported this, as ligand binding was monophasic for the bovine, *Saccharomyces cerevisiae*, and wild type HPII enzymes, but biphasic for several of the HPII mutant proteins.

Several mammalian catalases, and at least two prokaryotic catalases, are known to be NADPH binding. The function of this cofactor appears to be the prevention of inactivation of the enzyme, which occurs via formation of the inactive secondary catalase peroxide compound (compound II). No physiologically plausible scheme has yet been proposed for the NADPH mediation of catalase activity. This study has shown, via fluorescence and affinity chromatography techniques, that NADPH binds to the T (Typical) and A (Atypical) catalases of *Saccharomyces cerevisiae*, and that wild type HPII apparently does not bind NADPH. This study has also shown that NADPH is unlike any other hydrogen donor to catalase, and addresses its features as a unique donor by proposing a mechanism whereby NADPH is oxidized and catalase is protected from inactivation via the formation of protein radical species. Migration of this radical to a position close to the NADPH is also proposed as an adjunct hypothesis, based on similar electron migrations that are known to occur within metmyoglobin and cytochrome *c* peroxidase when reacted with H_2O_2. Validation of these hypotheses may be obtained in appropriate future experiments.

ACKNOWLEDGEMENTS

First and foremost, I wish to acknowledge my M.Sc. research supervisor, Dr. Peter Nicholls. His direction, valued advice, and patience, have made my stay at Brock a tremendously fulfilling experience. As I move on, I shall always admire his razor wit, and his degree of dedication to research and teaching. I also wish to acknowledge Brenda Tattrie, our lab technician. I cannot count the number of times I have called upon her for expert advice and help in matters mundane and complex alike. I wish to thank Dr. Yousef Haj-Ahmad, my co-supervisor, for his advice and guidance. Many thanks also go to the members of my M.Sc. supervisory committee, Drs. Castle and Bruce, for their encouragement, suggestions, and good humour. I wish to thank all the members of lab H218 , both those currently working here and those now elsewhere . Their enthusiasm and openness have made the laboratory a pleasant place to work and exchange ideas. Many thanks also go to the faculty members, staff, and graduate students (and honours students), of the department of Biological Sciences. They are truly outstanding in every respect, and I count them all as friends. I also gratefully acknowledge Dr. Peter Loewen of the University of Manitoba, for providing the HPII enzyme and mutant proteins, as well as for valuable discussions, collaborations, and his interest in the NADPH binding material. Lastly, but certainly not least, I wish to acknowledge my parents for their unquestioning support of my endeavours.

> How much easier it is when one can connect with the work of great predecessors whose value is not doubted by anyone. A personal experiment, a construction whose foundations one must dig himself and whose walls one must erect himself, runs a real risk of becoming a humble hovel. But perhaps one prefers to live there rather than in a palace that has been built by others.
>
> -M.C. Escher

TABLE OF CONTENTS

LIST OF FIGURES

LIST OF TABLES

LIST OF ABBREVIATIONS

ADP	Adenosine Diphosphate
Arg	Arginine
Asn	Asparagine
Asp	Aspartate
BLC	Bovine Liver Catalase
CCP	Cytochrome *c* Peroxidase
EDTA	Ethylenediaminetetraacetic Acid
ENDOR	Electron-Nuclear Double Resonance
EPR	Electron Paramagnetic Resonance
Gln	Glutamine
HRP	Horseradish Peroxidase
HPII	*E. coli* (catalase) Hydroperoxidase II
INH	Isonicotinic Acid Hydrazide
MEOS	Microsomal Ethanol Oxidizing System
Met	Methionine
NADH	Nicotinamide Adenine Dinucleotide, Reduced form
NADPH	Nicotinamide Adenine Dinucleotide Phosphate, Reduced form
NAD	Nicotinamide Adenine Dinucleotide, Oxidized form
NADP	Nicotinamide Adenine Dinucleotide Phosphate, Oxidized form
Phe	Phenylalanine
Pro	Proline
PAGE	Polyacrylamide Gel Electrophoresis
PVC	*Penicillium vitale* Catalase
PMSF	Phenylmethylsulfonyl Fluoride
SCCA	*Saccharomyces cerevisiae* CatalaseA
SCCT	*Saccharomyces cerevisiae* Catalase T
SDS	Sodium Dodecyl Sulfate
TRIS	Tris(Hydroxymethyl)aminomethane
Thr	Threonine
Trp	Tryptophan
Tyr	Tyrosine
Val	Valine

PREFACE

A portion of the Results (Chapter III) herein reported as part of section E, and discussed at length in the Discussion (Chapter IV), contains figures and literature that have been presented in published form prior to the completion of this thesis, as an article entitled "A mechanism for the NADPH inhibition of catalase compound II formation" by A. Hillar and P. Nicholls, **FEBS Letters**, vol. **314**, no. 2, 179-182. This preface duly draws attention to this fact in lieu of externally referencing the appropriate sections of the text.

CHAPTER I. INTRODUCTION AND LITERATURE REVIEW

INTRODUCTION

Virtually all aerobically respiring organisms produce catalases. Though the physiological functions of these enzymes may be debated, they are unequalled in nature as superlative catalysts for the breakdown of the cellular oxidant, hydrogen peroxide. Periodic reviews on the subject of catalases have appeared since their systematic investigation was initiated early this century (Sumner, 1941; Nicholls and Schonbaum, 1963; Schonbaum and Chance, 1976; Jones and Wilson, 1978; Percy, 1984), and the information accumulated on these enzymes has increased our understanding of their biochemical and physiological characteristics. Present attempts to understand the control of gene expression for these enzymes and other aspects of their molecular biology (Ruis and Hamilton, 1992; Loewen, 1992) have intensified due to implications for such studies in potentially identifying the basis for genetic disorders in humans related to oxidant stresses. Such work also serves in increasing our understanding of the protective roles these enzymes may play in preventing cell aging and mitogenesis leading to cancer (Ames and Shigenaga, 1992).

Most catalases belong to a larger family of hemoprotein enzymes. However, not all catalases are heme containing, nor are all catalases structurally similar. Most catalase have molecular weights of approximately 240kda, are tetrameric, and contain heme prosthetic groups. Some catalases have molecular weights notably lower or higher than 240kda (Kikuchi-Torii *et al.* 1982), some catalases have been identified as being dimeric (Goldberg and Hochman, 1989) or hexameric holoenzymes (Loewen and Switala, 1986) and some catalases are known

to utilize manganese clusters as catalytic centres instead of hemes (Allgood and Perry, 1986; Kono and Fridovich, 1983). All catalases are capable of catalytic decomposition of hydrogen peroxide, but some also engage in peroxidation reactions. The diversity, in terms of both structure and function in these enzymes, has suggested a central role for them in cellular metabolism. An approach integrating both biochemistry and molecular biology, in conjunction with future physiological investigation of catalases, will probably provide further elucidation of the roles played by catalases, as well as their evolutionary histories.

Interest in hemoprotein enzymes, which are involved in redox reactions in the cell, has recently enjoyed greater attention in an attempt to provide a more complete picture as to how protein conformation in the vicinity of the heme dictates functionality. One of the most powerful methods developed for this type of evaluation is site-directed mutagenesis. By genetically altering selected amino acid residues incorporated into the protein via genetic engineering methodology, the importance of any given moiety can be evaluated. Work has already been done on hemoproteins, including myoglobin (Adachi *et al.* 1991; Adachi *et al.* 1993), cytochrome *c* peroxidase (Fishel *et al.* 1991; Miller *et al.* 1992), and other proteins (Mauk, 1991).

One objective of this study was based on the opportunity to investigate site-directed mutant proteins of the HPII (Hydroperoxidase II) catalase of *Escherichia coli* in which amino acid residues in the vicinity of the heme were substituted. This primarily involved spectroscopic studies of the native hemoproteins, their reduced alkaline pyridine hemochromes, and the course of titration of the various proteins with the classical heme ligands, cyanide and formate.

These studies served to characterize and compare both the mutant proteins and the wild type HPII; both to each other, and to the bovine liver catalase and the purified A and T catalases of baker's yeast. The information obtained could give some preliminary indication of the effects on catalytic function of specific amino acid alterations, and provide direct evidence concerning the postulated essential nature of conserved moieties in proximity to the heme, based on the DNA sequence homologies to other catalases. Such investigations would, at the very least, expand our understanding of general heme functionality, and provide a basis for exploring other aspects of hemoprotein structure.

The recent finding that mammalian catalase binds nicotinamide adenine dinucleotides (Kirkman and Gaetani, 1984) has initiated a re-evaluation of the physiological status of the enzyme and has raised new questions concerning the mechanism of catalysis and the redox properties of the heme. The NADPH function has been shown to be in prevention and removal of the catalase peroxide complex II (Kirkman *et al.* 1987), an inactive form of catalase produced during exposure to low levels of hydrogen peroxide. This function requires the cofactor to engage in a single electron redox step, yet NADPH and NADH are two electron donors. Kirkman and co-workers have suggested the possibility of a stabilized $NADP^{\bullet}$ radical being formed, but provide no related evidence or scheme whereby such stabilization would take place. To date, NADPH binding has been found to occur only in mammalian enzymes from several different sources and in catalases of the prokaryotes *Proteus mirabilis* and *Micrococcus lysodeikticus.*

A second objective of this thesis was to re-examine the NADPH effect on compound II formation in bovine liver catalase and the

prevention of that formation, and to classify the cofactor in terms of a scheme developed by Keilin and Nicholls (1958), to categorize a number of hydrogen donors capable of providing reducing equivalents to the peroxide compounds of catalase. It was expected that these endeavours would yield sufficient information to propose a more complete model for the mechanism of NADPH action in the catalytic cycles of mammalian catalase. The results obtained have led to a revised model for catalase catalysis, which includes the formation of a hypothetical protein radical species. Extensive evidence now exists for similar species in the reaction cycles of the analogous hemoproteins, myoglobin and cytochrome *c* peroxidase.

The availability of catalase from two sources that had not previously been characterized, with regard to NADPH binding, provided a means to accomplish a further objective of this thesis. This consisted of an examination of the nicotinamide adenine dinucleotide binding characteristics of catalase fractions purified from baker's yeast (*Saccharomyces cerevisiae*) and the HPII wild type catalase of *Escherichia coli*. Experimental evaluations were carried out via affinity chromatography and fluorimetry of the native hemoproteins. The work expands the list of catalases investigated for NADPH binding, and provides an added basis for understanding the evolutionary conservation of the dinucleotide fold in catalases. It also gives a further point of comparison to determine whether there are significant biochemical differences between the A and T isozymes of *Saccharomyces cerevisiae*.

LITERATURE REVIEW

A. CATALASE, AN OVERVIEW

i. General features of the enzyme and its kinetics

Catalase (E.C. 1.11.1.6 Hydrogen peroxide: hydrogen peroxide oxidoreductase) is the enzyme that dismutes H_2O_2 to water and O_2. The overall reaction (1) is shown below :

$$2H_2O_2 \longrightarrow 2H_2O + O_2 \qquad (1)$$

Catalases are almost invariably heme containing proteins. Most are large, globular enzymes over 200 kilodaltons in molecular weight, comprising four identical, single polypeptide chain subunits. To date, catalases have been isolated from a large number of prokaryotic and eukaryotic sources, with the enzyme isolated from beef liver (BLC) probably the best characterized in terms of general biochemical, kinetic, and structural data.

The early history of catalase investigations is inextricably linked with the history of hydrogen peroxide itself. The French chemist Louis-Jacques Thénard (1777-1857) discovered hydrogen peroxide in 1818. He found that a number of substances could break down hydrogen peroxide to water and oxygen by the process now recognized as catalysis. He also observed this reaction when hydrogen peroxide was added successively to animal tissues: the first description of catalase action. Despite his work, however, Thénard could not conceive of the catalytic principle (Jones and Wilson, 1978). It was the work of Schönbein and others some half a century later, that would usher in the concept of catalytic activity mediated by biological molecules (Sumner,1941). At

the beginning of the twentieth century, Loew's work on the tobacco plant led to the rudimentary purification of an enzyme which he termed catalase (the name is archaic; it stems from the enzyme concept of Schönbein, who erroneously attributed the dismutation of H_2O_2 to be a universal property of enzymes). After Loew (1901), Issajew (1904) was the first to report findings regarding the catalase of brewer's yeast (*Saccharomyces cerevisiae*). Issajew accredited G. Senter with initial reports of the characterization of catalase from mammalian blood. In 1923, Warburg proposed that catalase was an iron containing enzyme, due to the observation of its inhibition by cyanide. This was later shown to be correct by the work of Zeile and Hellström, who demonstrated the hematin nature of the enzyme; Stern (1936) subsequently showed that the prosthetic group of beef liver catalase was ferriprotoporphyrin IX (also see Nicholls and Schonbaum, 1963). In 1937, BLC became one of the first proteins to be successfully crystallized (Sumner and Dounce, 1937), a feat which has since been repeated for many other catalases (Percy, 1984; Jouve *et al.* 1991). Biochemical and kinetic analyses of the enzymes from mammalian and prokarytic sources were the major foci of investigations on catalases carried out by the laboratories of Keilin and Hartree, Theorell, Chance, and others. The discoveries made by Keilin and Hartree (1936) and later Chance (1947) of the peroxidatic mode of reaction and the first reaction intermediate of catalase (though this had been observed earlier by Stern (see Nicholls and Schonbaum, 1963), respectively, changed consideration of catalase from a role of peroxide remover to that of ethanol oxidizer. The debate as to what role catalase plays physiologically is still unresolved.

Catalases typically have molecular weights between 220 kd. and 385 kd., with BLC and the majority of investigated catalases having a molecular weight of approximately 240 kd. Most catalases are comprised of four identical heme-containing subunits. In the case of the BLC, the amino acid sequence is known, based on direct protein sequencing (Schroeder *et al.* 1982), and for other catalases it is known by inference from the corresponding gene (Hartig and Ruis, 1986; Okada *et al.* 1987; Cohen *et al.* 1988; Haas *et al.* 1991, von Ossowski *et al.* 1991)). Crystal structures of the BLC and *Penicillium vitale* (PVC) enzymes have recently been solved to atomic resolution (Murthy *et al.* 1981; Reid *et al.* 1981; Vainshtein *et al.* 1986). Variations in subunit number are known to occur predominantly in catalases from prokaryotic sources. *Escherichia coli* and *Bacillus subtilis* produce catalases apparently containing subunits some 20kd. larger than those of BLC, and these may associate as hexamers (Loewen, 1992). *Lactobacillus plantarum* and *Thermoleophilum album* produce catalases containing manganese redox centres, instead of heme groups, in each of the subunits, which associate as hexamers or tetramers, respectively (Allgood and Perry, 1986; Kono and Fridovich, 1983). *Klebsiella pneumoniae* produces three catalases, one of which exists in dimer form (Goldberg and Hochman, 1989). The catalase from *Aspergillus niger*, although containing four subunits, has been shown to be a glycoprotein with a molecular weight of 345-385 kd. (Mosavi-Movahedi *et al.* 1987; Kikuchi-Torii *et al.* 1982)

Fig. 1A shows the secondary and tertiary structure of an individual subunit of BLC, with Fig. 1B showing the entire catalase molecule, indicating the intersubunit relationships. Each subunit in BLC has 506 residues and the structure has been arbitrarily subdivided by

Fita and Rossmann (1985A) into four principal domains: (1) the amino terminal extension "arm" of the catalase subunit, which interacts with a two-fold related subunit neighbour, (2) the eight stranded β-barrel region consisting of two four-stranded anti-parallel β sheets, (3) the wrapping domain comprising little distinct secondary structure, apart from the "essential" α helix, and lastly, (4) the carboxy terminal domain, containing four α helices on the outer edge of the subunit molecule. Each catalase subunit in BLC also binds one molecule of NADPH tightly (Kirkman and Gaetani, 1984) in the region near the "hinge" between two subunits, formed by the knotting of the amino "arm" of one subunit into the loop formed in the wrapping domain of the other (indicated by the arrow in Fig. 1A). Interaction of two of these knotted units forms the functional globular protein, which has been described as roughly dumbbell shaped (Fita and Rossman, 1985A)(Fig. 1B). In *Penicillium vitale* catalase, crystalline structure has been compared to that of the BLC enzyme (Melik-Adamyan *et al.* 1986), no evidence for bound NADP/ NADPH is apparent, but there is instead an additional "flavodoxin-like" domain at the carboxy terminus consisting of approximately 150 extra residues. This structure consists of five short amino acid sequences that adopt a β sheet conformation (Vainshtein *et al.* 1986).

The tertiary structures of the BLC and PVC protein subunits are similar. The flavodoxin-like region of the PVC provides the major topological point of significant departure between the two enzymes, in that it nestles in the same crevice as that between the α helical and β barrel domains which comprise the NADPH binding site in the BLC (Melik-Adamyan *et al.* 1986). This difference, however, has rather important consequences for the structure of the main substrate channel

through the tetramer to the heme group. The channels in both proteins are some 20 Å long, but the opening to the channel is blocked in PVC by the flavodoxin-like domain. Similarly, the channel in PVC which has its aperture at a position corresponding to the BLC amino terminal helix, is likewise probably blocked, or at least presenting major steric constraints to entering substrates. In terms of the detailed secondary structure of the BLC compared to that of PVC, precise description of domains, as indicated above, is difficult. Vainshtein *et al.* (1986) did not consider the amino terminal arm and the hinge region of the subunits to be distinct domains, since they lack elements of the secondary structure domains characterized for BLC. Crystallographic data, used in conjunction with a computer program to compare the position of atoms for the BLC vs. PVC subunits, have yielded results in which some 458 of the 506 α carbons of the subunit backbone were structurally and topologically equivalent (Melik-Adamyan *et al.* 1986). The chief differences between the two enzymes occur in three specific regions: the short amino terminal arm, the flavodoxin-like domain, and an extra loop structure (that would also partially block the BLC major heme channel) of the β- barrel domain of PVC . There are also two areas of difference in the outer wrapping domains of the PVC subunit in which five and four residue amino acid insertions occur, respectively (Melik-Adamyan *et al.* 1986).

Protoheme is the prosthetic component of the active site of BLC. Each subunit contains one non-covalently bound protoporphyrin IX group having one atom of ferric iron in a high spin (paramagnetic) state in the resting enzyme. All the heme groups in catalase are well buried, some 20Å from the molecular centre and separated by at least 31Å from the

Figure 1. Structural features of bovine liver catalase.
(**A**) Adopted from Fita and Rossmann (1985A). Aspects of the secondary and tertiary structure of the BLC subunit, showing the position of the NADPH(double arrowhead) and heme prosthetic groups (single arrowhead). (**B**) Adopted from Melik-Adamyan *et al* (1986). Representation of the catalase molecule showing the subunit interactions.

Figure 1

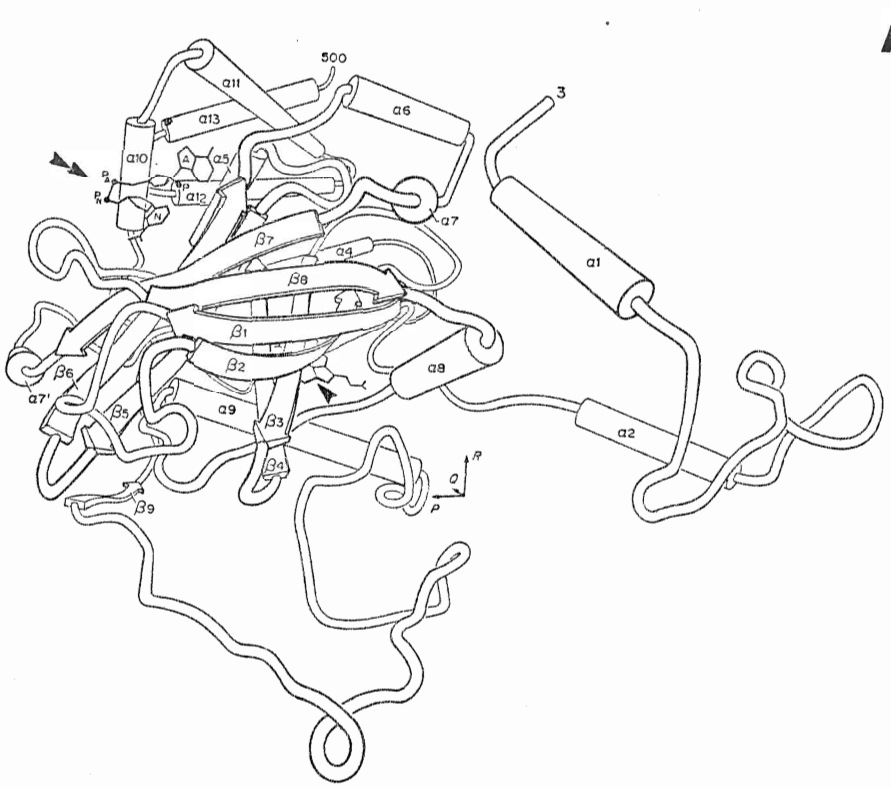
A
500
3
α11
α13
α6
α10
α5
α12
α7
β7
α4
β8
α1
β1
β2
α8
β6
α7'
β5
α9
β3
α2
β4
β9
Q
P
R
B
P
Q
R

nearest iron atom in another related subunit (Fita and Rossmann, 1985A). Heme ring vinyl and methyl groups interact with the protein mainly through van der Waals' interactions with non-polar side chains. The propionate groups are involved in a network of charge-charge interactions as well as in hydrogen bonding. These interactions also involve up to three water molecules. It has been suggested that binding of the heme provides a degree of structural integrity to the rather flexible wrapping domain of the protein (Fita and Rossmann, 1985A)

The heme pocket of BLC is strongly hydrophobic in character. The distal side of the heme is primarily defined by a surrounding β barrel domain "wall", which also interacts with the porphyrin pyrrole rings, (A)I, (B)II, and (C)III, and with the amino terminal arm residues of the adjoining subunit. The distal side of the heme also defines the catalytic site, with the main heme channel opening into this cavity and the "essential" distal histidine occurring at position 74. The residues on this side of the heme considered to be of functional/structural importance by Fita and Rossmann (1985A) include His-74, Asn-147, Val-73, Phe-152, and Phe-160. The positions of the side chains of these residues in relation to the heme, and of important residues on the proximal side, are shown in Fig. 2. The imidazole ring of the distal histidine is almost parallel to the plane of the heme. This implicates this residue in enzyme function; it restricts the entrance of molecules to the redox centre and may play some direct role in pre-orienting the molecules that do enter the heme crevice, in conjunction with the Thr-114 side chain situated across from it.

The important proximal residues are all associated with the essential α^9 helix that contains the heme proximal ligand (see Fig. 2) and lies almost parallel to the heme plane. Extensive hydrogen bonding

of the oxygen of the phenolate group on the Tyr-357 by the nitrogen atoms of Arg-353 occurs, as well as interactions involving His-217, Val-145, and a water molecule (W2). These serve the function of maintaining the iron atom in close association with the deprotonated tyrosine phenolate oxygen and preserving its low redox potential (Fita and Rossmann, 1985A).

In order to understand the mechanisms of hemoproteins more fully, it is extremely important to have detailed information regarding the axial ligands of the hemes. As has been pointed out, the proximal ligand in BLC, occupying the fifth co-ordination position of the iron, is Tyr-357 (Reid *et al.* 1981; Fita and Rossmann, 1985A). A tyrosine phenolate group serving as the proximal ligand is unusual in hemoproteins other than catalase. This position is usually occupied by a histidine residue (e.g., His-170 in horseradish peroxidase (Dunford, 1991); His-175 in cytochrome *c* peroxidase (Bosshard *et al.* 1991), and His-93 in metmyoglobin (Takano, 1977)). Studies by Adachi *et al.* (1993), in which the His-93 of recombinant human metmyoglobin was replaced with either tyrosine or cysteine residues via site-directed mutagenesis, have indicated that the identity of the proximal axial ligand in hemoproteins largely influences the nature of the absorption spectrum and coordination of the heme iron, as the His-93-Tyr mutant gave spectra very similar to those of catalase and other high spin iron heme proteins. Iron-tyrosinate co-ordination is apparently common among the catalases, as resonance Raman spectroscopy has indicated tyrosinate ring modes in BLC, *Aspergillus niger* catalase, *Micrococcus luteus* catalase (Sharma *et al.* 1989), and in HPII catalase of *E. coli* (Dawson *et al.* 1991). Resonance Raman spectroscopy also suggests

Figure 2. The heme environment in a subunit of BLC.
Biograf™ generated representation of the heme and relative positions of certain important amino acid residues implicated in the catalytic functions in a subunit of the enzyme. Only side chains of the residues shown (**A**). Distal side of the heme, perpendicular perspective on the heme. Note positions of the His-74 and Asn-147, implicated in coordination of the substrate for reaction at the heme iron. (**B**). Proximal side of the heme, perpendicular perspective (reverse of that in **A**). Note the position of the Tyr-357 phenolate group, the fifth ligand of the heme iron.

Figure 2

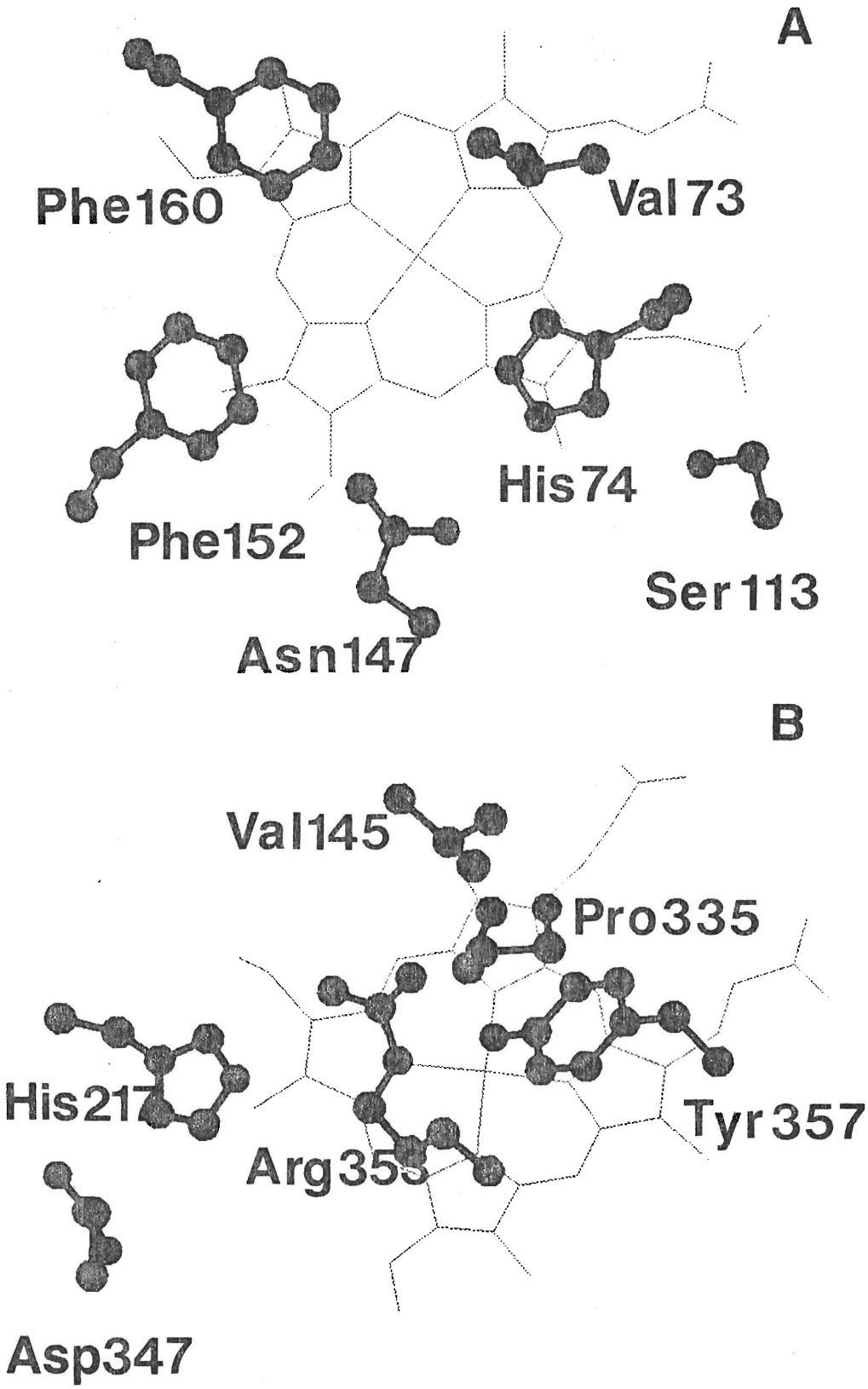
A
Phe160
Val73
His74
Phe152
Ser113
Asn147
B
Val145
Pro335
His217
Tyr357
Arg355
Asp347

that the heme iron in these catalases is high-spin and pentacoordinate (Chuang *et al.* 1988; Sharma *et al.* 1989), a finding that contradicts earlier assumptions that the sixth coordination position of catalase ferriheme is occupied by a water or hydroxide molecule (arguments in Schonbaum and Chance (1976) and Jones and Wilson (1978)). ^{1}H and ^{19}F NMR spectra obtained by Oakes (1986), however, show that a water molecule *is* present in the vicinity of the heme, though it is located some 3.6- 3.8Å from the heme iron and is hydrogen bonded to His-74 and Asn-147. As these residues are critical to function of the enzyme, it is apparent that such a water molecule is still mechanistically important, since binding of the substrate to the active site requires its displacement.

The reactions of catalase with classical heme ligands are spectroscopically similar to those of other hemoproteins. Native catalases are, however, not dithionite-reducible to the ferrous state. This probably reflects the fact that the catalase hemes are buried in the protein. The reaction of native catalase with cyanide was investigated in detail by Chance (1949), and shown to occur independently at each of the four hemes in the tetrameric molecule. The spectral shifts observed for this reaction are consistent with a change in heme iron coordination number from high spin (5/2) with five unpaired electrons to low spin (1/2) with one unpaired electron. High spin complexes may also be formed through ligand reactions at the heme, and common species observed to react this way include formate, acetate, fluoride, and azide. All the catalase-ligand complexes form via reaction of the protonated forms of the compounds with the enzyme. The equilibrium constant for reaction in each case is proportional to

the amount of undissociated acid present (Nicholls and Schonbaum, 1963)

Detailed studies of the reaction of catalase with H_2O_2 have produced the following rate law:

$$-\frac{d[H_2O_2]}{dt} = k_0[\text{catalase}][H_2O_2] \qquad \text{(eq. 1)}$$

where [catalase] is the concentration of tetrameric enzyme,and k_0 is independent of pH in the range of 4.7-10.5, at concentrations of H_2O_2 below 0.1M (Jones and Wilson, 1978). The high specific activity of catalases as well as their inactivation by prolonged contact with H_2O_2 complicates the kinetic analysis by restricting the useful enzyme concentrations to the nanomolar range and by requiring relatively rapid measurement techniques. Above a concentration of 0.1M H_2O_2, catalase has been shown to have Michaelis-Menten type saturation kinetics when suitable techniques such as the rapid quenched flow method are employed. A K_m of 1.1M H_2O_2 was found for BLC at 20^oC (Ogura, 1955). The k_0 (Eq. 1) for various catalases typically falls in the range of 0.6 to 6.0×10^7 M^{-1} s^{-1}.

The observation by Chance (1947) of a change in absorption spectra of catalase to which H_2O_2 had been added constituted the first identification of the active reaction intermediate, which was named catalase peroxide complex I (now usually abbreviated as compound I). This species has a distinct absorption, with a Soret band of approximately 12% less the intensity than that for the native enzyme as well as reduced and slighty shifted peaks in the visible spectrum. Investigation of the kinetics of this compound by Chance were comprehensive, and led to his proposal that catalatic action of catalase

(i.e. the decomposition of H_2O_2) is a special case of a peroxidatic mechanism and represented by two separate and sequential reactions, (2) and (3):

$$\text{Catalase} + H_2O_2 \longrightarrow \text{Compound I} + H_2O \qquad (2)$$

$$\text{Compound I} + H_2O_2 \longrightarrow \text{Catalase} + O_2 + H_2O \qquad (3)$$

By this mechanism, the catalase ferric (Fe^{III}) heme iron is oxidized by an initial complexation (which may be reversible) and reaction with a peroxide to give an intermediate (compound I) whose oxidation state is formally two oxidizing equivalents above that of the resting enzyme. For convenience, the oxidation level of this intermediate is often represented by placing the oxidation equivalents on the reaction centre iron (i.e.Fe^{V}), although, as will be discussed shortly, this representation is not structurally or mechanistically accurate. This species, via reaction with a second molecule of peroxide, or with a molecule of some other suitable reductant (e.g., ethanol, formate), is reduced back to the resting ferricatalase, completing the redox cycle of the enzyme. The initial reaction is extremely rapid with H_2O_2 as the substrate, with a specfic velocity constant of approximately $1.0 \times 10^7 M^{-1}s^{-1}$ per hematin enzyme (Nicholls and Schonbaum, 1963). The second reaction is of the same order of magnitude as the first when the substrate is H_2O_2, but is approximately three orders of magnitude less when the substrate is a low molecular weight alcohol or formate (Chance, 1950B).

The reduction of compound I back to ferricatalase may occur as either a single two-electron equivalent redox step or as two one-electron equivalent redox steps.The classification of donors to

compound I as being either one-electron or two-electron is based upon the criterion of whether catalase peroxide compound II is detected during the reaction. Catalase peroxide compound II is a semi-reduced species of formal oxidation state IV, sometimes referred to as the "ferryl" species. Compound II has a unique spectrum compared to those of both ferricatalase and compound I, characterized chiefly by a broader, less intense, and slightly red-shifted Soret peak and a distinctive visible band at 565 nm. Compound II is a catalytically inactive species of catalase, but once formed, it decays spontaneously, even in the absence of exogenous reductants. This reduction implies the existence of donor group(s) present on the catalase protein, usually referred to as the endogenous donor(s). As has been pointed out in earlier reviews (Nicholls and Schonbaum,1963; Schonbaum and Chance, 1976; Jones and Wilson, 1978), the classification of electron donors on the basis of compound II formation is inconclusive with respect to the mechanisms. The absence of detectable compound II may not mean that none is formed, but rather that the ratio of the second to first reduction rates may be extremely high. Furthermore, the term one or two-electron donor, used here, is equally inconclusive, since such a term does not distinguish species on a chemical or mechanistic basis. Nicholls and Schonbaum (1963) have suggested that the term hydrogen donor be employed instead. Compound I may undergo reaction with added azide or hydroxylamine to form ferrocatalase, which is three oxidizing equivalents below that of compound I, and one below the resting enzyme (Nicholls and Schonbaum, 1963). Azide and hydroxylamine are in a unique class in being able to react as three electron equivalent donors to compound I.

A scheme presented by Keilin and Nicholls (1958) classified reductants of compounds I and II according to their spectrophotometrically observable reactions. The scheme comprises six groups of hydrogen donors as follows: Group 1, ascorbate and ferrocyanide; Group 2, phenols; Group 3, alcohols and formic acid; Group 4, nitrite; Group 5, azide and hydroxlamine; and Group 6, hydrogen peroxide. Reactions of these donor groups are summarized in Fig. 3. The Group 1 donors reduce compound I to compound II without reducing compound II to ferricatalase. They are thus a class of one electron donors. Group 2 donors reduce compound I to compound II and compound II to ferricatalase. Rates of the compound I reduction are approximately thirty times greater than those with compound II. Their participation in the compound II to ferricatalase reduction suggests that they be considered as two-electron donors. Group 3 donors reduce compound I to free ferricatalase. In the presence of continuously generated H_2O_2, they will prevent the formation of compound II by maintaining a low steady state concentration of compound I. Thus, these donors also prevent inactivation of the enzyme by eliminating compound II formation without themselves reacting with compound II. The Group 4 donor, nitrite, will react with both compound I and compound II to give ferricatalase. As such, nitrite reacts with compound I in a two-electron and with compound II in a one-electron redox step. The reaction with compound I does not produce detectable compound II as an intermediate, and thus resembles the action of the Group 3 donors in this case. Group 5 donors have been considered briefly above. They are potent inhibitors of catalase, and when reacted with catalase in the presence of peroxides, form an inactive ferrous derivative of catalase

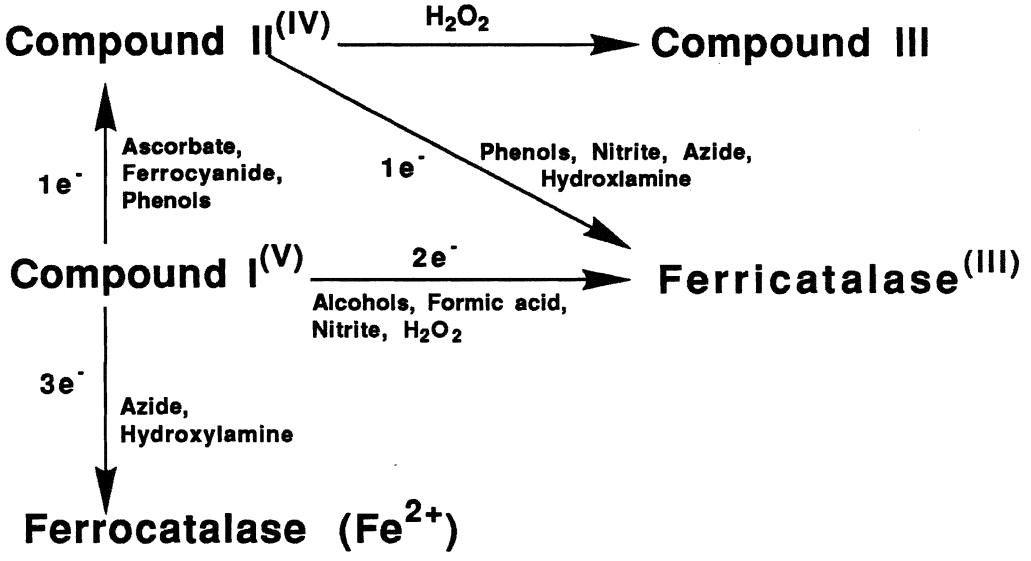

Figure 3. Scheme of hydrogen donor reactions with catalase-peroxide compounds.
After Keilin and Nicholls (1958)

having a characteristic spectrum with absorption bands at 587nm and 559nm. The reactions of azides and hydroxylamine with catalase are more complex than alluded to here, but a detailed consideration of these other reactions are beyond the scope of this review. Finally, the Group 6 donor, hydrogen peroxide, which is the reductant in the catalatic reaction of the enzyme, engages in the rapid two-electron redox step to reduce compound I back to ferricatalase. It is accorded its own group as a donor because it forms yet a third spectroscopically distinct but inactive compound of catalase (compound III) via the addition of large amounts of H_2O_2 to compound II. Not included in this scheme is the compound aminotriazole. It is mentioned here because although this substance catalyzes the decomposition of compound II, it does not promote the formation of compound II from compound I and has been demonstrated not to engage in donor reactions with catalase (Nicholls, 1962). Also absent from this scheme are the large organic molecules that were reported to be donors, such as guaiacol, which have been shown by Sichak and Dounce (1986) to engage in catalytic reactions with a denatured form of BLC, but not enzymatic reactions.

Various substances inhibit the catalytic reactions of catalase. The majority of classical inhibitors are also characteristic heme ligands, such as cyanide, fluoride, and azide. At low substrate concentrations, the inhibition observed is classically noncompetitive, because the H_2O_2 both decomposes the enzyme substrate complex as well as forms it. At much higher concentrations of substrate (>1.1M), the inhibition observed takes on a classically competitive form, as compound I accumulates. Progressive inhibition by some inhibitors, such as acetate and fluoride, but not cyanide and formate, is also observed during the course of the catalatic reaction. This is due to the

effects that some of these compounds have in promoting formation of compound II, as well as other inactive catalase compounds (Nicholls and Schonbaum, 1963). Aminotriazole is an unusual catalase inhibitor in that it is a substance, apart from organic solvents and other denaturation agents, that irreversibly inhibits the enzyme in the presence of hydrogen peroxide, by reacting with compound I. The finding that the aminotriazole-inhibited catalase species formed could still react with much reduced catalatic activity, as well as form complexes with ligands such as cyanide, has suggested that the aminotriazole is bound to the enzyme via an irreversible reaction with some moiety on the protein (Nicholls, 1962).

ii. The catalase reaction mechanism

The cycles of the peroxidatic reactions of catalase are summarized in Fig. 4, which also indicates the change in the formal oxidation state of the enzyme during the cycles. The noncatalytic reactions with reductants that form compound III, ferrocatalase, and other catalase derivatives, are not included in the figure.

Though no comprehensive mechanism for all the reactions of catalase exists, Fita and Rossmann (1985A) have modelled a detailed mechanism for the formation and reduction of the methyl hydroperoxide catalase compound I, by utilizing a computer graphics system. The model draws upon the crystallographic data available for the enzyme and also incorporates features from the model of peroxidatic catalysis by cytochrome *c* peroxidase (CCP) proposed by Poulos and Kraut (1980). Aspects of the model which have been investigated recently will be included here.

Figure 4. Catalytic reaction cycles of catalase.
Adopted from Kirkman *et al* (1987). Scheme showing the principal redox reactions of the enzyme.

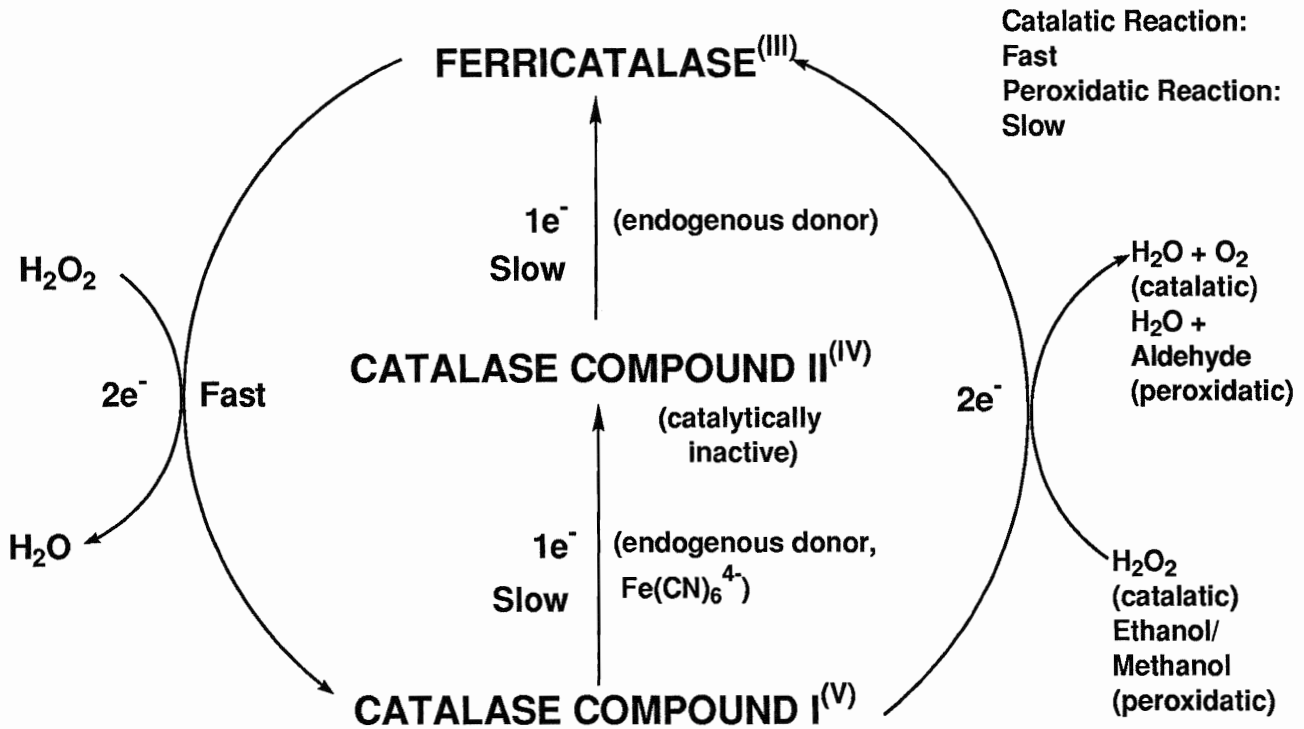
FERRICATALASE(III)
Catalatic Reaction:
Fast
Peroxidatic Reaction:
Slow
1e-
Slow
(endogenous donor)
H2O2
2e-
Fast
CATALASE COMPOUND II(IV)
(catalytically
inactive)
2e-
H2O + O2
(catalatic)
H2O +
Aldehyde
(peroxidatic)
H2O
1e-
Slow
(endogenous donor,
Fe(CN)6 4-)
H2O2
(catalatic)
Ethanol/
Methanol
(peroxidatic)
CATALASE COMPOUND I(V)

Figure 4

The initial step in the formation of compound I is the entrance of the peroxide molecule to the heme crevice on the heme's distal side (see Fig. 5,a). The peroxide is sterically constrained to move between the His-74 and Asn-147 residues before interaction with the heme iron. These residues are believed to pre-orient the substrate and then interact with it via hydrogen bonding as the catalase-peroxide complex is produced. In the case of CCP, two water molecules are displaced from the heme pocket as the coordination of the peroxide takes place. This is analogous to the water molecule that may be displaced from its position co-ordinated to the His-74 and Asn-147 of catalase (Oakes, 1986) when the peroxide becomes co-ordinated to the heme iron.

The actual reaction of the co-ordinated peroxide-catalase complex to form the compound I intermediate has been described by Dunford (1991) in the analogous case of the reaction of horse radish peroxidase (HRP) to operate via an electron " push-pull" mechanism (see Fig. 5). The initial push is the flow of two electrons toward the ferric heme iron from the deprotonated oxygen atom of the peroxide that is coordinated to the heme, the proton being abstracted by the imidazole nitrogen of the His-74 (Fig. 5, b). This push is generated by the ferric iron in association with the phenolate group of the proximal Tyr-357. The subsequent pull comes as the cleavage of the O-O bond takes place, generated by the electrostatic interactions of the terminal peroxide oxygen with the His-74 imidazole and the terminal peroxide hydrogen with the Asn-147 amine groups. The hydrogen abstracted by the imidazole ring of the histidine is thus attached to the distal peroxide oxygen via the flow of electrons away from the heme, forming a

Figure 5. Mechanism of the formation of catalase compound I. Based upon the scheme of Bosshard *et al* (1991). Note that the formation of a protein radical species is unsubstantiated for catalase (i.e. formation of e). Please see text for details.

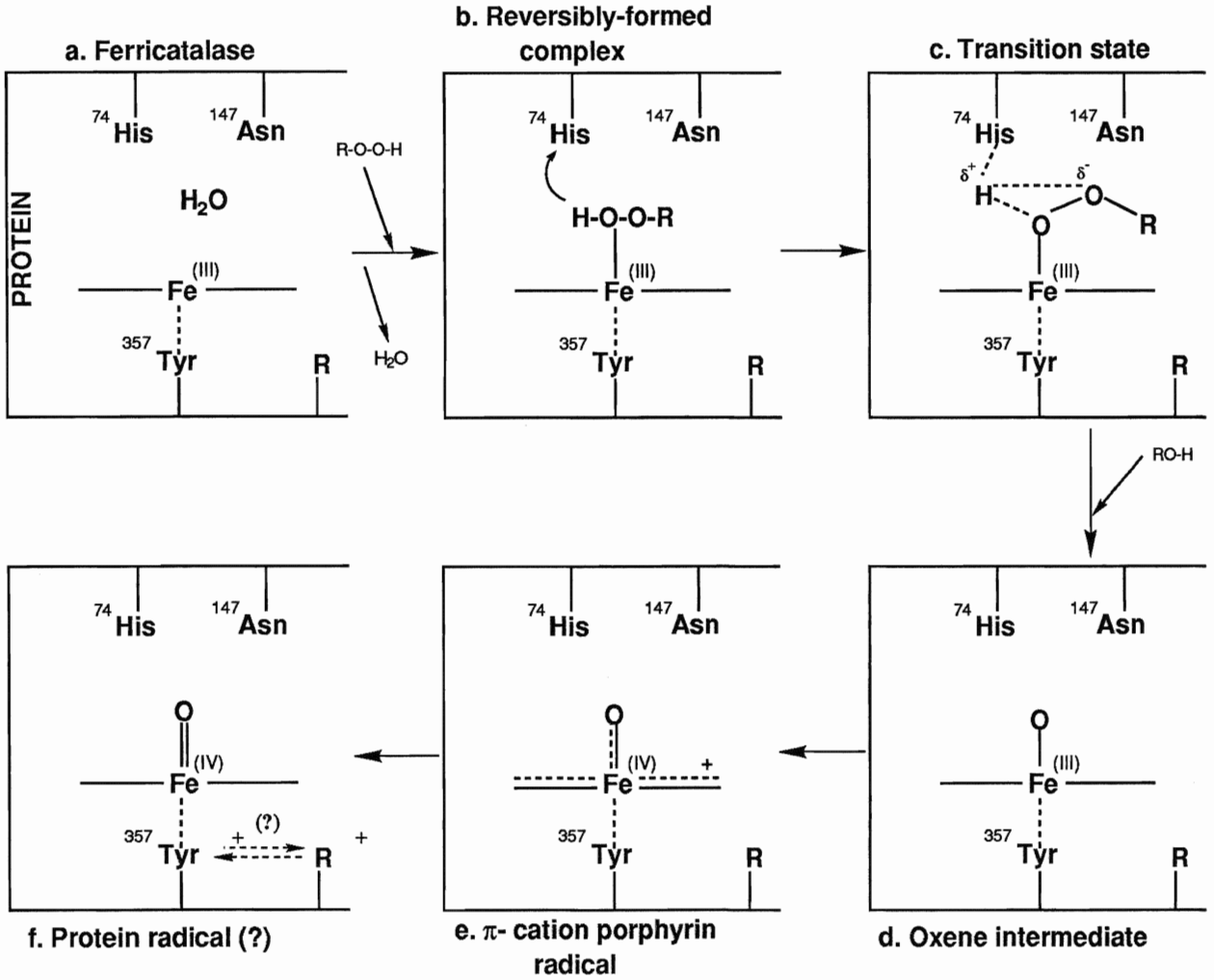
a. Ferricatalase
b. Reversibly-formed complex
c. Transition state
PROTEIN
74 His
147 Asn
H2O
Fe (III)
357 Tyr
R
R-O-O-H
H2O
H-O-O-R
δ+
δ-
RO-H
d. Oxene intermediate
e. π- cation porphyrin radical
f. Protein radical (?)
O
(IV)
(?)

Figure 5

molecule of water (Fig. 5, c), and an oxo-iron heme species (Fig. 5, d-f). This mechanism of compound I formation is generally applicable to peroxidases and has been reiterated in less detailed form in a recent review (Ortiz de Montellano, 1992).

Compounds I of catalase and peroxidases can be represented in terms of a formal oxidation state of the heme iron (i.e. Fe^{V}). The more likely chemical form of compound I is an oxyferryl iron at a formal oxidation level of IV in conjunction with a π-cation porphyrin radical (i.e. Fe^{IV}=O and a porphyrin radical [Fig. 5, e]). Indeed, initial structural investigations of compounds I of HRP and catalase via EPR and coulometric techniques, as well as analysis of synthetic heme systems, suggested that these were the correct representations of the chemical species (Dolphin *et al.* 1971). Problems arising in these investigations due to photoinduced conversions of the compounds, however, later cast some doubt on the initial characterizations (Chuang and Van Wart, 1992). Recently, more sensitive studies employing resonance Raman spectroscopy (Chuang and Van Wart, 1992), under conditions which eliminate the formation of photoproducts, have confirmed the validity of the original findings, and suggest that π-cation radical porphyrin species are the predominant ground state configurations for the compound I species of HRP and BLC as well as compound II species of these and other enzymes (Palanappian and Terner, 1990).

The formation of compound I via the two electron oxidation of catalase and peroxidases by peroxides, is a well characterized reaction, with the majority of features of the reaction being equivalent among these enzymes. Differences become apparent, however, upon comparing the reductions of compound I of catalase with the same process in peroxidases. Catalases "prefer" two-electron reduction

mechanisms for compound I while peroxidases preferentially carry out the reduction through one electron steps, thus forming compound II species in the process. The specific structural characteristics of the heme pockets as well as the residues involved in the reactions are likely to play a role in producing this difference between these systems.

The model of catalase compound I reduction proposed by Fita and Rossmann (1985A), which assumed the reductant to be a molecule of ethanol (i.e. a two electron donor for compound I reduction), was also analyzed via a computer graphics program. The model reaction proceeds in two phases. Initially, the sterically constrained ethanol is positioned via co-ordination of its C2 hydrogen to the oxyferryl heme oxygen and the His-74 and Asn-147 side chains. Abstraction of the hydrogen from the C2 carbon to bond with the oxo-iron oxygen weakens the oxo-iron bond, and increases the nucleophilic character of the His-74 imidazole N. Though the second step of the reaction is mechanistically less clear, acetaldehyde and a water molecule are formed by a reaction whereby the hydroxyl associated with the iron is reduced, possibly by a hydride transfer reaction, with a simultaneous oxidation of the ethanol to an aldehyde. The catalatic reaction would be similar, with the obvious features that the H_2O_2 molecule is less sterically constrained (Fita and Rossmann, 1985A) propose two possible binding modes for the substrate), that the rate of the reaction is great, and that the final products of the reaction are a water molecule and an oxygen molecule.

The stability of the compound II species formed in peroxidases, can be understood by an examination of the model mechanism for HRP (Dunford, 1991). It is formed by the removal of the porphyrin radical by

reduction and concomitant proton transfer to the distal histidine residue of the heme, as shown in Fig. 6. The proton transfer allows a coordination via hydrogen bonding by the oxygen bound to the heme iron with the protonated His-42 imidazole nitrogen. The process thus removes a potentially reactive species while stabilizing the oxyferryl heme. The parallel stacked orientation of the imidazole ring of the His-74 in catalases prevents this type of interaction. As catalase compound II may be formed via addition of the appropriate one-electron reductants or through electron transfer from an endogenous donor on the apoprotein, it must be concluded that the compound II species of catalases, will show some similarity to that of horseradish peroxidase, as proposed in Fig. 5. The interaction with a protonated side chain suggested in the case of HRP is, however, doubtful for catalase, due to its distance from the iron and the planarity of the His-74 imidazole; but a one-electron reaction could certainly generate a radical species either on the porphyrin or on the as yet uncharacterized endogenous donor species.

iii. Biosynthesis, localization, and physiological function

The intracellular localization and biosynthesis of catalase has been investigated extensively for the hepatocytes of rat liver, chiefly through the work of de Duve and Lazarow (reviewed in Lazarow and Fujiki, 1985). A detailed sequence of biosynthetic steps for catalase can be traced from cytoplasmic translation to final tetrameric assembly of the enzyme in the mammalian peroxisome, the main repository of catalase in eukaryotic cells. Peroxisomes, sometimes called microbodies, microperoxisomes, or in the case of fatty seeds of

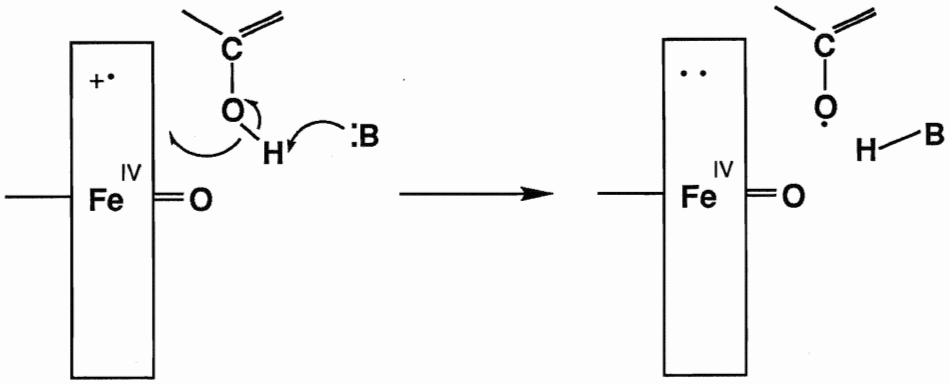

Figure. 6. Proposed mechanism for the one-electron reduction of compound I to compound II of HRP via a phenol.

Adopted from Dunford (1991). In catalase, the position of the distal basic group (imidazole of His-74) is not close enough to the heme plane to allow interaction of the abstracted proton with the oxygen bound to the iron.

plants, glyoxysomes, are subcellular particles of approximately 0.5μm in diameter, surrounded by a single membrane, and having a finely granular matrix which sometimes includes a dense crystalloid or polytubular core. The term peroxisome specifically refers to the biochemical rather than the morphological features of these particles, emphasizing the close association of catalase with H_2O_2 producing oxidases in the organelles (de Duve, 1974).

Messenger RNA encoding the liver catalase amino acid sequence is found in normal rats and in rats in which peroxisome proliferation has been stimulated, in some cases consisting of up to 89% of the total cellular mRNA. Cell free translation products of the mRNAs are of identical size (66 kda) to the subunits of mature rat catalase, based on their migration patterns in SDS-PAGE (Lazarow and Fujiki, 1985). The encoded polypeptide is translated as an apomonomer to the extent of 13μg/ g/ liver tissue. The apomonomer has a half life between 35-50min (de Duve, 1974; Lazarow and Fujiki, 1985). The apomonomer is imported into the peroxisomes via a posttranslational mechanism which apparently does not modify the polypeptide primary structure. Heme groups are bound to the apomonomer subunits within the peroxisomes. These heme containing precursors of catalase have half-lives between 12-17min and amount to 4μg/ g/ liver (de Duve, 1974; Lazarow and Fujiki, 1985). Both the heme-containing and heme free monomers are susceptible to denaturation by solvents that do not denature mature catalase. In the final step of biosynthesis, the catalase tetramer is formed within the peroxisomes to give the active enzyme. Mature rat liver catalase has a half-life on the order of 1.5 days (de Duve, 1974).

Though the steps of catalase biosynthesis are known in detail, it is still unclear as to where in the cell the translation of the polypeptide monomers take place. The theory that the polypeptides are translationally co-translocated into the endoplasmic reticulum and then conveyed to the peroxisomes is in contrast with the evidence that the catalase apomonomer is recovered primarily in the cytoplasmic rather than the microsomal fraction (de Duve, 1974). A modified version of this theory proposes that newly synthesized apomonomers are released into the cytosol, taken up posttranslationally by the endoplasmic reticulum, and then translocated to peroxisomes. Such a process requires that cis-acting targeting signals exist within the imported proteins, since the apomonomers of catalase are not proteolytically processed either during or after import into peroxisomes (Lazarow and Fujiki, 1985). Targeting sequences in one eukaryote may be recognized by another, as has been demonstrated by the import of *Hansenula polymorpha* alcohol oxidase into the peroxisomes of *Saccharomyces cerevisiae* (Distel *et al.* 1987) and the import of *Saccharomyces cerevisiae* catalase A into peroxisomes of *Hansenula polymorpha* (Hansen and Roggenkamp, 1989). A C-terminal sequence, Ser-Asp-Leu, has been identified by Gould and coworkers (1989) to be sufficient for peroxisomal import of certain proteins, though such a C-terminal sequence is not present in all peroxisomal proteins. For example, it is absent in both BLC and *Saccharomyces cerevisiae* catalase A (SCCA). Hartig *et al.* (1990) have shown that the targeting signal for SCCA is located at neither the C-terminal nor the N- terminal region of the apomonomer, and favour the hypothesis that an internal, highly conserved, sequence of amino acids, is responsible for the peroxisomal targeting of the majority of eukaryotic catalases,

perhaps in conjunction with chaperonins or other unfoldase type proteins.

The final assembly of the heme containing monomers of catalase is perhaps the least understood aspect of the process of catalase biosynthesis. The monomers that finally form catalase must be heme containing, as demonstrated by the treatment of rats with allylisopropylacetamide, which inhibits heme metabolism but does not prevent the apomonomers from entering and accumulating in the peroxisomes (Sugita *et al.* 1982). The heme containing monomers, however, need not be in the peroxisomes in order to form active catalase. This has been shown in cases of persons with Zellweger Syndrome, who lack hepatic peroxisomes, but still have normal levels of catalase in the cytosol of the hepatocytes (Lazarow and Fujiki, 1985), and in the case where recombinant rat catalase was successfully expressed in *E. coli* (which contains no peroxisomes), and found to have almost identical characteristics to those of the authentic enzyme (Furata and Hayashi, 1990).

Catalase is almost ubiquitous in aerobic cells containing a cytochrome system. In animals it is found most abundantly in liver, kidney, and erthrocytes, and is least abundant in connective tissue (Percy, 1984). More recently, catalase has also been found in rat heart mitochondria (Radi *et al.* 1991). Levels of catalase activity from different tissues have been shown to be quite variable in a number of mammalian species. The level of catalase activity in one tissue of a given species often does not reflect the activity in any other tissue of that species (Jones and Masters, 1976). In plant peroxisomes, catalase is found not only in the matrix, as with animal peroxisomes, but also in the polytubular core or nucleoid of the organelles (Tolbert, 1978).

A puzzling aspect of catalases, is that in a number of species, more than a single type of catalase has been identified. The heterogeneity initially observed in erythrocyte catalase purified from human blood (Cantz *et al.* 1968) was eventually found to be an artefact, considered to be due to oxidation of the enzyme during purification (Morikofer-Zwez *et al.* 1969). Goth (1991) has shown that blood may contain at two catalase charge isoforms, the erythrocyte and the serum catalases (which occurs in the case of certain diseases), having different electrophoretic mobilities. Various treatments, such as exposure to dialyzable serum ligands, NADPH, and protection of SH groups, did not alter the electrophoretic mobilities of the catalases, but dilution at 20 times or greater progressively decreased erythrocyte catalase mobility until it was similar to that of serum catalase. The author concludes that the formation of the catalase charge isoforms is caused by a reversible conformational change due to matrix effects of the serum. Among micro-organisms, however, *E. coli*, *Klebsiella pneumoniae*, *Mycobacterium* species, and *Saccharomyces cerevisiae* all possess more than one catalase. The hydroperoxidase enzymes (HPI and HPII) of *E. coli* and the T (Typical) and A (Atypical) catalase enzymes of *Saccharomyces cerevisiae*, will be considered in more detail in the following sections. The T (Temperature sensitive) and M catalases of species of *Mycobacterium* are different in kinetics and resistance to inhibitors as well in characteristic temperature sensitivities (Wayne and Diaz, 1988). The three catalases of *Klebsiella pneumoniae* show great diversity in terms of stability in ethanol-chloroform and different regimes of pH. Of the three, two are tetrameric, protoheme enzymes, while one is a dimeric, chlorin heme-containing enzyme, of lesser molecular weight than the former two proteins (Goldberg and

Hochman, 1989). Plants also have multiple forms of catalase; in some cases the subunits differ only in charges on the proteins, but in cotton, maize, and some other plants, a multiple gene system is employed for catalase (Ni *et al.* 1991; Scandalios, 1991). The only multiple gene system for catalase suggested to exist in animals , is for *Drosophila melanogaster* (Bewley *et al.* 1986). Multiple catalase gene systems are likely to be intrinsic to regulation of gene expression of the organisms that utilize them, as well as important in mediating the physiological functions of the cell.

iv. Physiological function

The precise physiological function of catalase is not known. The protective effect of the catalatic action of the enzyme in removing hydrogen peroxide generated in the cell, has long been considered a prime candidate for the function of the enzyme, even before its support within the peroxisome concept of de Duve (Böck *et al.* 1980). The demonstration by Keilin and Hartree (1945) that catalase also catalyses the oxidation of hydrogen donors, such as low molecular weight alcohols however, suggests that the peroxidatic function of the enzyme may also be important *in vivo*. That H_2O_2 may be decomposed mainly by the co-operative glutathione peroxidase and glutathione reductase system which is found primarily in the cytoplasmic fraction (though up to 30% is found in the mitochondrial matrix) of the cell, and the fact that catalase has a relatively low affinity for H_2O_2 (K_m: 1.1M), are the principal arguments for the peroxidatic function of catalase. However, proponents of the catalatic function contend that the enzyme is preferentially responsible for H_2O_2 decomposition *in peroxisomes*,

as a detoxication system separate from cytosolic or mitochondrial systems that eliminate H_2O_2 (Böck *et al.* 1980).

Since two major pathways in the cell contribute to H_2O_2 decomposition, it is fair to ask what contribution each makes. Of course the removal of H_2O_2 will also depend on where and at what rate the peroxide is formed. By selectively inhibiting either catalase or glutathione reductase via treatment of cultured rat hepatocytes with aminotriazole or 1,3-bis(2-chloroethyl)-1-nitosourea (BCNU), respectively, Starke and Farber (1985) investigated the effect of hydrogen peroxide, generated slowly by glucose and glucose oxidase, on cell killing. They found that catalase inhibition or glutathione reductase inhibition both contribute to increased cell killing by hydrogen peroxide, via an antioxidant insensitive mechanism in the case of inhibited catalase, and via a mechanism sensitive to antioxidants for the case of inhibited glutathione reductase. This suggests that both catalase and the glutathione peroxidase/ reductase systems are active in preventing H_2O_2 toxicity in hepatocytes. Oshino and Chance (1977) have commented that the compartmentalization of catalase and the glutathione cycling system in eukaryotic cells re-emphasizes the unique aspects of each as a hydrogen peroxide detoxifier, and imply that the co-operation of the two enzymes is important. They propose that the glutathione peroxidase/reductase system is optimized at extremely low H_2O_2 concentrations in vivo, and that the elimination of higher concentrations of H_2O_2 via catalase serves to mediate this activity. This view is also supported by Radi *et al.* (1993) for the case of mitochondrial catalase. These workers noted no reduced glutathione dependent metabolism of high levels of H_2O_2 in rat heart mitochondria, suggesting that catalase is the key enzyme in

removing toxic concentrations of H_2O_2. In certain species of microorganisms, including *Escherichia coli*, glutathione peroxidase is absent. Though other metabolic alternatives, apart from catalase mediated hydrogen peroxide decomposition, may be responsible for protecting these cells from oxidant stresses, it is unclear to what extent such processes are involved. An *in vivo* study of catalase in *Micrococcus lysodeikticus* by Chance (1952), demonstrated that compound I was formed within these cells and that a hydrogen donor was present. The steady state observed in this study was essentially that of the catalatic reaction, though Nicholls and Schonbaum (1963) have pointed out that the H_2O_2 present may have been formed exogenously through a photooxidation reaction. Ma and Eaton (1992) have investigated the toxicity of exogenously added H_2O_2 to dilute and concentrated suspensions of *E. coli* cells that were either catalase-containing or catalase deficient. Unfortunately, the concentration of peroxide added was probably too high (1mM) in the dilute suspensions to give a result of physiological relevance, though colonial aggregations of both the catalase containing and catalase deficient strains showed increased tolerance to peroxide challenge. P. Nicholls (personal communication), has indicated that the specific rate of the catalatic reaction in *E. coli* cells however, is likely to be similar to the rate obtained for the same reaction in erythrocytes, if one assumes the catalase concentration and cell dimensions are comparable, and that exogenous H_2O_2 is a factor in cell death of free living *E. coli.* Eisenstark and Perrot (1987) suggest that though exogenous H_2O_2 may influence the survivorship of *E. coli,* and perhaps of other microorganisms, when it is generated as a photoproduct of exposure to near ultraviolet light, there is no direct evidence of a correlation

between near-UV sensitivity and H_2O_2 sensitivity in several strains of normal, catalase-overproducing, and catalase-deficient, *E. coli* cells.

A number of arguments against a protective role for catalase have been advanced. As mentioned above, the presence of catalase in microorganisms, sometimes at high intracellular levels, does not necessarily result in the protection of these cells from toxic exposure to H_2O_2. Similarly, hemoglobin from erythrocytes is not protected by catalase when exposed to H_2O_2 generated slowly by a glucose oxidase/ glucose system (Nicholls and Schonbaum, 1963).

The argument that the process of aging results from (a) increased frequencies of cellular oxidations and (b), the progressive slowing of gene expression producing antioxidant enzymes such as catalase, may be of some relevance. Orr and Sohal (1992) have recently reported that catalase overexpressing strains of transgenic *Drosophila melanogaster*, which lack the ability to metabolize H_2O_2 via the glutathione peroxidase/ reductase system, show increased resistance to exogenously administered H_2O_2, although protection against other forms of oxidative stress (hyperoxia/paraquat treatments) was not enhanced. Guemouri *et al.* (1991) have observed that there is no significant reduction of blood catalase activity levels for humans below age 65. Above the latter age, loss of catalase activity parallels loss of activity for many other enzymes. The argument that increasing oxidative damage in the cell is due to a lack of toxicity mediating enzymes such as catalases, is therefore equivocal.

The most interesting argument against the protective role of the catalatic mechanism, however, is the medical condition in humans known as acatalasemia, a heritable syndrome in which catalase is deficient in one or more body tissues. Japanese-type acatalasemia is

often complete, in that the absence of the enzyme is found to affect all body tissues, whereas Swiss type acatalasemia only affects the erythrocytes, with higher than normal levels of catalase often found in liver and kidney. Japanese type acatalasemia is caused by a defective posttranscriptional processing error resulting in the lack of gene expression (Wen *et al.* 1990), whereas it is generally assumed that the Swiss variant of the disease is produced by one or more point mutations that destabilize the protein, resulting in its rapid breakdown in erythrocytes. The only clinical symptomology of the disease is an increased tendency to develop dental infections, with no apparent deficiencies in the metabolism of the affected individual (Nicholls and Schonbaum, 1963). Dispensing with the catalase-peroxidase gene has recently been shown to be of advantage to the microorganisms *Mycobacterium tuberculosis* and *Mycobacterium smegmatis*. Loss or inactivation of the gene makes the affected strain resistant to the drug isonicotinic acid hydrazide (INH), the drug of choice in treatment of uncomplicated cases of tuberculosis (Zhang *et al.* 1992). These observations make it difficult to reconcile catalase to a role of protective agent against peroxide toxicity, though it is not clear whether another metabolic pathway may be sufficient to accomplish the same functions *in vivo*.

The theory that catalase may have a peroxidatic physiological function was, as mentioned previously, first suggested by Keilin and Hartree (1945). The peroxidatic reaction of catalase *in vivo* however, requires the presence of both hydrogen peroxide and a physiological hydrogen donor. A likely candidate for this donor would be ethanol, which has been shown to be present in rat liver at a concentration of 0.4μmole/ g (de Duve, 1974). Chance *et al.* (1974) have noted that if

catalase is to carry out ethanol oxidation in the cell, not only must a high H_2O_2 flux exist, but the molar ratio of ethanol to H_2O_2 must exceed 1000. This group and others (Sies, 1974) have investigated the effect of ethanol on the steady state of the catalase reaction intermediate, compound I, and the effect of inhibitors in hemoglobin free perfused rat livers, using sensitive spectrophotometric techniques. The specific rate at which peroxidatic reaction with ethanol occurred was calculated to be $1.3 \times 10^3\ M^{-1}s^{-1}$ for the catalase of rat liver, when the simplifying model of a triple steady state equation was employed. This requires that H_2O_2 concentration, the intermediate (compound I) concentration, and concentration of infused ethanol be taken as constants. The rate calculated is very similar to that calculated by Chance for the *in vitro* analysis of the kinetics of catalase compound I in presence of constantly generated H_2O_2 (Chance, 1950A).

If catalase does have a role in alcohol oxidation in the cell, as Chance and others have suggested, the extent of this role is uncertain, since alcohol dehydrogenase and cytochrome P-450 (Ingelman-Sundberg and Jörnvall, 1984) are also involved in this pathway. Chance *et al.* (1974) resolved the alcohol oxidation due to catalase from that due to alcohol dehydrogenase and other systems by titration of perfused rat liver with either methanol or ethanol. The reaction rates of compound I with methanol and with ethanol are very similar. As methanol will only be oxidized by catalase compound I in the system, while ethanol will be oxidized by catalase, by alcohol dehydrogenase, and by other components of the system, the difference in calculated rates gives the physiological contribution by catalase to the oxidation rate of ethanol. At high ratios of ethanol to methanol, perfused rat liver preferentially

oxidizes ethanol by alcohol dehydrogenase and other systems. An oxidation rate of 17μmoles/min/100g body weight was obtained when perfused rat liver was saturated with ethanol. The contribution estimated by the authors for the catalase dependent oxidation rate was 0.8μmoles/min/100g body weight under experimental conditions. Under conditions of normal intracellular ethanol load, the contribution of catalase to the process of ethanol oxidation is, therefore, significant. A more recent study of alcohol dehydrogenase deficient deermice (*Peromyscus maniculatus*) by Handler *et al.* (1986), in which any possible residual catalase activity was carefully eliminated by pretreatment with aminotriazole, and cytochrome P-450 activity was likewise absent, the oxidation of ethanol was undetectable due to inhibition of the peroxidatic action of catalase. In agreement with the results obtained by Chance *et al.* (1974), metabolism of ethanol by catalase in alcohol dehydrogenase positive strains of deermouse was found to be a minor component of the ethanol oxidation system under normal conditions. The observation that alcohol dehydrogenase negative strains of deermice were still able to eliminate ethanol at 25% of the basal rate after treatment with aminotriazole, suggests that other mechanisms of ethanol elimination occur in the perfused mouse liver. The authors favour the existence of other physiological processes accounting for this activity, which may include the often controversial NADPH dependent microsomal ethanol oxidation system (MEOS) of Lieber and DeCarli (see Thurman *et al.* (1972) for a discussion and rebuttal).

The evidence suggesting the involvement of catalase in the physiological oxidation of ethanol is equivocal. In contrast to the claims of Handler *et al.* (1986), both *in vitro* and *in vivo* studies of

alcohol dehydrogenase deficient deermice have indicated that catalase plays only a minor role in ethanol metabolism, implying a functional MEOS (Alderman *et al.* 1987: Alderman *et al.* 1989). Van der Zel *et al.* (1991), conclude that catalase is not the major system employed by alcohol dehydrogenase deficient *Drosophila melanogaster* larvae in the oxidation of ethanol. They admit, however, that the enzyme may be important for this purpose in certain tissues and at certain times during development, since throughout its evolution, this species has presumably fed on fermenting plant matter, which often contains levels of ethanol to concentrations as high as 0.69M.

A consensus as to the physiological function of catalase has not yet been reached, and functions of the enzyme have been suggested other than the protective and ethanol oxidation roles. Vuillaume *et al.* (1988) suggested that catalase may be implicated in the synthesis of nucleotide triphosphates from nucleotide diphosphates in phosphate buffer; the added phosphate was not derived from the buffer, but apparently from the NADPH bound to the catalase. But until catalase dependent ATP synthesis can be demonstrated to conform to enzymatic reaction parameters *in vitro* and verification of the process can be obtained *in vivo*, the reported results must be cautiously interpreted. Perhaps there is no unique role for catalase, as has been suggested by Nicholls and Schonbaum (1963). The enzyme may be a "fossil", with a peripheral and largely dispensable role in the contemporary organism. The fact that it duplicates the function of enzymes in the same metabolic pathways, that it is generally inducible, and that acatalasemics and strains of *Mycobacterium* are largely unaffected or even at a selective advantage by its loss, suggests that the physiological need for such an enzyme is facultative at best.

B. CATALASES OF BAKER'S YEAST (*Saccharomyces cerevisiae*)

In contrast to the case of BLC and other mammalian catalases, the catalases of *Saccharomyces cerevisiae* are not well characterized biochemically, nor is there a crystallographic structure or chemically determined amino acid sequence available for either enzyme. This is unusual when one considers the amount of work that has recently been done by several laboratories on the molecular biology of the enzymes. The preliminary characterization of *Saccharomyces cerevisiae* as catalase containing was done by Issajew (1901) and later duplicated by von Euler *et al.* (see Brown, 1953). The work of Brown (1953), in the laboratory of Theorell, indicated that the partially purified enzyme was similar in many respects to the analogous enzymes from other eukaryotes. Both the absorption spectrum of the native and the cyanide liganded species showed Soret and visible peaks in similar positions. The prosthetic group of the enzyme was shown to be protoheme, and cyanide and azide were shown to be effective in inhibition of enzyme activity. The enzyme preparation obtained, however, was found to be less stable than the catalases from mammalian blood or liver, with progressive rapid inactivation apparent both at room temperature and at lower pH.

Seah and Kaplan (1973) and Seah *et al.* (1973), succeeded in achieving the purification of the yeast catalase to homogeneity. Their procedure led to the identification of two separate catalase fractions, which were differentiated by their elution order from the final hydroxlapatite fractionation step. The first fraction to elute was

named catalase A (Atypical) and the second to elute was named catalase T (Typical). The T catalase was indeed typical, in that its absorbance spectrum and SDS-PAGE profile were very similar to other eukaryotic catalases. Its subunit molecular weight was 61 kd., implying a native enzyme molecular weight of 244 kd. The specific rate constant of the enzyme fraction T was also consistent with that of other catalases, being 7.7 x $10^6 M^{-1}s^{-1}$, when converted from the archaic units of specific activity for catalase, *kat f.* via the equation:

$$kat.\ f. = \frac{520k_1'}{e} \qquad \text{(eq. 2)}$$

where *e* is the molecular mass of enzyme per hematin and k_1' is in the units $M^{-1}s^{-1}$ (Nicholls and Schonbaum, 1963). The A catalase had an unusual SDS-PAGE profile. It apparently contained subunits of only 45 kda molecular weight with other bands present indicating peptides of even lower molecular weight, and it had a lower specific activity than the T catalase, at only 4.3 X $10^6 M^{-1}s^{-1}$ after conversion from *kat f.* units. This however, is likely to have been the result of the unusually low heme to protein ratio reported for the enzyme. The authors suggested that this fraction may have contained some proteolytically modified catalase as well. The characterization of the two catalase fractions on the basis of their biochemical differences led to their initial classification as isoforms. Immunological cross-reaction was not observed between the two catalase proteins (Seah *et al.* 1973; Zimniak *et al.* 1976), substantiating this initial classification. It was not until the work of Ammerer *et al.* (1981) that the two yeast catalases were shown to be genetically distinct isozymes.

Unicellular eukaryotes like *Saccharomyces cerevisiae* offer great advantages for the investigation of catalases, because of their suitability for genetic studies. Studies focusing on the regulation of catalase genes in microorganisms have turned out to be valuable in two ways: (i) in general, levels of catalase are controlled according to functional need, and regulatory studies provide information concerning *in vivo* functions of the enzymes and (ii) catalase genes are useful model systems, which can provide insights into mechanisms of gene expression control in other eukaryotic organisms (Ruis and Hamilton, 1992).

Since the discovery that baker's yeast produces two catalase isozymes, much work has been done in an attempt to better understand the molecular genetics of this system. The catalase T protein of *S. cerevisiae* is encoded by the gene *CTT1* (Spevak *et al.* 1983), and the A protein by the gene *CTA1* (Cohen *et al.* 1985). Both functional catalases are present under conditions of aerobic growth, but not produced under conditions of fermentation. Induction of both catalases by O_2 is related to the role of heme as an inducer of gene expression. As at least two heme biosynthetic enzymes require oxygen, it is not surprising that anaerobic cultures of *S. cerevisiae* do not produce catalase apoproteins either. The heme mediated transcription activator protein known as HAP1 (Heme Activator Protein) has been characterized along with the heme control regions for the *CTT1* gene and an analogous region upstream of the *CTA1* sequence.

As the catalase A protein is localized to the peroxisomes of yeast cells (Susani, 1976), the findings that glucose represses, and growth on fatty acids induces, expression of the *CTA1* gene, is not surprising. The phenomena are apparently linked by a role of the transcription

activator ADR1(Alcohol Dehydrogenase Regulator). This protein was originally characterized as a regulator of the gene encoding alcohol dehydrogenase II of *S. cerevisiae* . This factor not only mediates the derepression of *CTA1* but also affects several other genes, including those encoding proteins involved in peroxisomal fatty acid β-oxidation and in peroxisome assembly (Ruis and Hamilton, 1992). A variety of fatty acids, oleic acid especially, induced the rapid proliferation of peroxisomes in *Saccharomyces cerevisiae* (Veenhuis *et al.* 1987). Such proliferation did not occur in the presence of methanol and other carbon sources usually associated with the proliferation of such microbodies in other yeasts (Verduyn *et al.* 1988). This gives evidence that catalase A plays some role in β-oxidations of fatty acids and lipids as part of peroxisomal metabolism. Elucidation of the role of peroxisomal proliferators in *Saccharomyces cerevisiae* may also provide information of medical significance.In mammalian hepatocytes, peroxisomal proliferation may enhance carcinogenic effects as a result of reactive oxygen species formed through stimulation of β-oxidations, assuming that peroxisome proliferation in mammalian liver and in yeast is controlled by related mechanisms (Ruis and Hamilton, 1992).

Though heme/ O_2 control of gene expression is common to both catalases A and T , the cytosolic T catalase (the only cytosolic catalase) is under the control of different transcription factors as well as factors affecting its translation. Hemin is known to induce the production of the HAP1 (Heme Activator Protein). HAP1 acts as positive transcriptional regulator at two distinct sites upstream of the *CTT1* gene. The *CYC1* gene, which encodes the mitochondrial iso-1-cytochrome *c* protein, also binds HAP1 at a control region characterized for that gene. Winkler *et al.* (1988) have suggested that

HAP1 may be involved in the co-ordinate control of expression for a number of related redox proteins that include catalase T (and A) and iso-1-cytochrome *c*. Whether hemin is a true HAP1 ligand, and how HAP1 is activated, remain to be elucidated. Hemin is also effective in regulation of catalase T gene expression at the translational level. Translation of yeast catalase mRNA in a cell-free system isolated from a heme-deficient mutant of *Saccharomyces cerevisiae* was inefficient although translation of most other mRNAs was comparable to that of a system from heme-containing cells (Ruis and Hamilton, 1992).

Derepression of the catalase T gene through nutrient starvation is part of a pleiotropic response of yeast cells that is mediated by a signal pathway involving a number of proteins, including regulators of adenylate cyclase and cAMP dependent protein kinases. Mutations resulting in decreased adenylate cyclase activities lead to increased *CTT1* expression. Conversely strains with high levels of constitutive adenylate cyclase activity have both extremely low catalase T levels and a reduced response to nitrogen starvation (Ruis and Hamilton, 1992). Experiments carried out by Belazzi and co-workers (1991) demonstrated that derepression of *CTT1* transcription via nitrogen starvation is rapid and direct and that a cAMP independent alternative system of signalling occurs in *Saccharomyces cerevisiae*. In addition, this study also showed that subjecting the cells to the added stress of heat shock under conditions of oxygenation and nutrient starvation, causes the dramatic synergistic increase of transcription level for the *CTT1* gene. Heat shock induced maximal transcription within 30min. when cells were moved from 28 degrees to 37 degrees (Wieser *et al.* 1991), This makes the control of the *CTT1* gene a special case, with mediation of three separate controlling mechanisms. As well, another

region of the promoter, located between 220 and 280 bp upstream of the *CTT1*, is suggested to consist of several functional elements that exert negative control on gene expression, as elimination of these DNA elements causes increased expression under both repressed and derepressed conditions (Belazzi *et al.* 1991). This region thus also contributes to the synergism exhibited by the gene promoter

As the *CTT1* and *CTA1* genes of *Saccharomyces cerevisiae* show intrinsically different mechanisms of transcriptional and, to some extent, translational expression (apart from the common oxygen stress response mediated by heme and HAP1 gene product), this provides some explanation for the requirement of two separate catalases. One is inherently involved only in catabolic functions in the peroxisomes, and one is involved in similar functions only under conditions of physiological stress in the cytosol. Ruis and Hamilton (1992) have remarked that under conditions of optimal growth, with little or no significant stress, catalase T biosynthesis would be extremely wasteful energetically when increasing the cell population. When growth is curtailed or no longer possible, the protection of cells against damage expected from stress factors will increase survival probability. The elaborate control of the *CTT1* gene, has been hypothesized by the same authors to be of selective value, in that a system with multiple synergistic components provides a flexible response to a variety of physiological stresses.

C. HYDROPEROXIDASES OF *Escherichia coli*

The prokaryote *Escherichia coli* contains two hydroperoxidases with catalase-like properties. These two enzymes, now known as HPI (Hydroperoxidase I) and HPII (Hydroperoxidase II), are both heme containing proteins. HPI is a tetrameric hemoprotein having a molecular mass of 337 kd., or 84 kd. per individual subunit (Claiborne *et al.* 1979). It is thus larger than the conventional eukaryotic catalases which usually have molecular weights of about 240 kd. The holoenzyme apparently only contains two heme prosthetic groups, both being protoheme. The enzyme functions as both a catalase and as a broad specificity peroxidase (Claiborne and Fridovich, 1979). HPII is an unconventional catalase that has been recently characterized as a hexameric hemoprotein with a native molecular mass of 540 kd., and an estimated subunit mass of some 92 kd. (Loewen and Switala, 1985). This contrasts with the original characterization of the protein by Claiborne and co-workers as a 312 kd. tetramer with 78kd. subunits (Claiborne *et al*, 1979). Even more unusual is the fact that the enzyme contains not protoheme prosthetic groups, but heme d_{cis} groups, stereoisomers of a prosthetic group of the *E. coli* anaerobic terminal oxidase complex (comparison of protoheme and heme d_{cis} structure shown in Fig. 7) (Chiu *et al.* 1989). HPII is only functional as a catalase, and has been found to be 6-fold more active catalatically than HPI (Claiborne *et al.* 1979). HPI is found in both the periplasmic space associated with the inner membrane of *E. coli* cells and the cytosol, while HPII remains in the cytosol (Heimberger and Eisenstark, 1988). The differences in localization, catalytic ability, and structure of these enzymes imply functional differences between them.

Figure 7

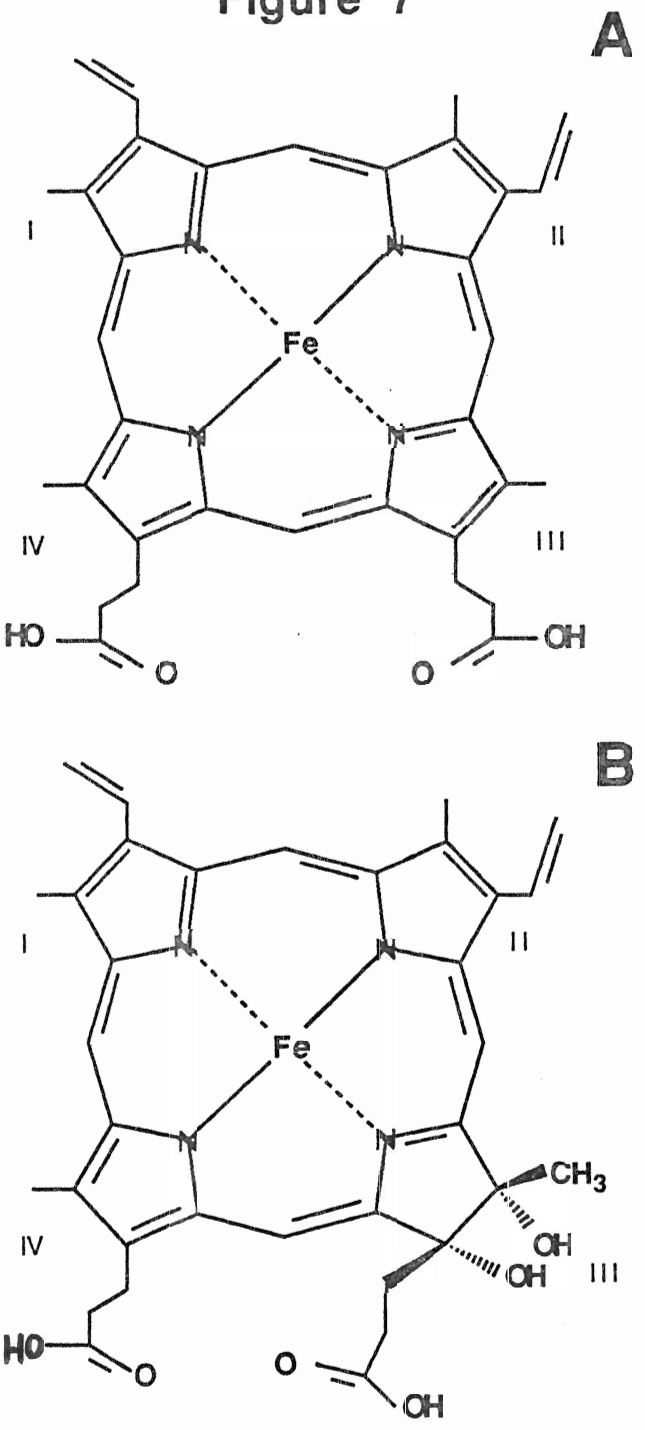

Figure 7. Structures of protoheme and heme d_{cis}.
Pyrrole rings numbered as per Fita and Rossmann (1985A). (**A**) Structure of protoheme (ferriprotoporphyrin IX) (**B**) Structure of heme d_{cis}.

Escherichia coli contains two catalase genes which may be activated to express the hydroperoxidases, HPI and HPII. Similarity of the deduced amino acid sequence of HPI to that of *Bacillus stearothermophilus* peroxidase possibly indicates that HPI has evolved as a peroxidase and not as a true catalase. The HPII amino acid sequence, in contrast, very much resembles those of eukaryotic catalases, and it is thought to have evolved as a true catalase (Loewen, 1992). In addition to differences in the structure and function of the mature enzymes, genetic control of biosynthesis for the catalases is also secured via different mechanisms in *Escherichia coli*, a theme that seems to be comparable in *Escherichia coli* and *Saccharomyces cerevisiae*.

HPI subunits are encoded by *katG* on the *E. coli* chromosome (Loewen *et al.* 1985B). This gene is expressed constitutively even under anaerobic conditions, when HPII is not (Claiborne *et al.* 1979). HPI catalase is further inducible by addition of H_2O_2 to the growth medium, but such induction also gives rise to a variety of other proteins including an alkyl hydroperoxidase. Of these proteins, nine are known to be under the control of the *oxyR* gene product at the level of transcription in both *E. coli* and *Salmonella typhimurium* (Loewen, 1992). The binding requirements for the OxyR protein remain uncharacterized because the *oxyR*, *ahpC* (alkyl hydroperoxidase), *ahpF*, and *katG* promoter sequences have little similarity. Moreover, transcription observed for a mutant in which there was only one base pair substitution suggests the involvement of some of the other (as yet uncharacterized) proteins that are transcribed in response to the presence of H_2O_2. The mechanism of activation of the OxyR protein has recently been shown to be by oxidant action on the protein itself (Storz

et al. 1990). By oxidizing the protein directly, the stimulus thus effects enhanced transcriptional activity and genes are transcribed whose proteins constitute at least part of the protective response. The change in oxidation state of the protein alters its conformation and allows it to interact efficiently with its target promoters (Loewen, 1992). It is assumed that of the 32 other proteins produced in response to the stress induced by exogenous oxidants, most also have functions in the mediation of the cellular response. Apart from the alkyl hydroperoxidase from the *ahp* genes of *E. coli*, none has yet been identified.

HPII subunits are encoded by the *katE* locus of the *E. coli* chromosome. The gene has been cloned and sequenced and has been shown to be independent of the *oxyR* locus (Loewen *et al.* 1985A) The catalase-hydroperoxidase which the gene expresses is biosynthesized normally under conditions of slow growth, beginning upon entry of cultures into stationary phase, and during growth on citric acid cycle intermediates (Loewen, 1992). The synthesis of HPII, however, requires the mediation of *katF,* whose gene product is very similar to a σ transcription factor. The transcription factor is a broad spectrum activator known to regulate expression of a group of genes, including *katE* itself, *xthA,* involved in DNA repair, *bolA*, involved in cell morphology change, *appA*, involved in phosphate metabolism, *pex*, involved in starvation protection functions, and possibly other loci as yet uncharacterized (Loewen, 1992).

Though entrance into stationary growth phase or starvation results in *katF* expression, the mere presence in the cell of the gene product is not sufficient to start *katE* transcription, suggesting that another factor regulating the biosynthesis of HPII must be involved. In

addition, expression of *katF* under artificial starvation conditions could be prevented by uncouplers, inhibitors of electron transport, and by lowering pH. This effect did not occur when electron transport was inhibited, or proton motive force was reduced, in rich growth media. In fact, the expression of *katF* is stimulated under these conditions (Loewen, 1992). This finding has led to the proposal by Loewen (1992) that *katF* expression is sensitive to the reduction in membrane potential that occurs as a result of nutrient depletion or slower metabolism. How the cell senses ΔpH or some electron carrier mediated effect, however, remains to be determined.

The catalases of *E. coli* are thus quite similar to those of *Saccharomyces cerevisiae*, with respect to the mode of regulation. Both the *E. coli* HPI and the *S. cerevisiae* catalase A are induced through oxidant stresses, independently of the other catalase present in the respective cells. The *CTA1* gene, however, is expressed through mediation of the heme and HAP1 protein in the cell, whereas only the OxyR protein mediates the transcription of the *katG* locus. HPII and *S. cerevisiae* catalase T are both induced under conditions of nutrient stress, with the possibility of synergistic enhancement of transcription due to heat shock factors and oxidant stress in the case of the *CTT1* gene. But only the enhancement of *katF* transcription has been noted as necessary for expression at the *katE* locus, though other factors could be involved (these could include heat shock or other oxidant sensitive factors). There are striking similarities between a unicellular eukaryote and a unicellular prokaryote. Certain aspects of the less characterized system in *E. coli* could actually be analogous to the regulatory mechanism employed by *S. cerevisiae* cells.

D. CATALASE- NADPH INTERACTIONS

The discovery that BLC tightly binds NADPH was the unexpected finding of Kirkman and Gaetani (1984). They were trying to identify NADP(H) binding proteins in an attempt to understand better the regulation of the pentose phosphate pathway in erythrocytes. Their study showed that tetrameric human and bovine catalases bind one molecule of NADPH per subunit and that the binding of reduced dinucleotides is highly favoured over the oxidized forms. NADPH had the lowest observed dissociation constant (less than 10nM) followed by NADH, NADP+, and NAD+. This work allowed for the re-interpretation of available crystallographic data on the BLC enzyme. Earlier analyses showed a region of extra density located in what was analogous to the PVC "hinge" region of the protein, but this region was simply interpreted as a carboxyl terminal extension to the polypeptide. The evidence for NADP bound to the protein made clear that the extra density corresponded extremely well to one molecule of the cofactor occupying a small cleft between the "hinge" region and the β- barrel domain (Fita and Rossmann, 1985B). The NADPH was found to be unusual in that it adopted a right-handed helix folded conformation when bound to the catalase, whereas the majority of nicotinamide adenine dinucleotide cofactors bind to proteins in their extended conformations, which has been explained to occur due to electrostatic interactions that exist between the protein residues and the bases of the bound NADPH (Fita and Rossmann, 1985B). The helical folding of the NADP on catalase puts the nicotinamide ring roughly parallel to the adenine ribose, with the actual binding site on the protein near the carboxyl ends of two α helices, the α5 and α10. The phosphate groups of the NADPH are positioned furthest from the protein while the two

bases are closest to the residues of the helices. That the unusual conformation of bound NADPH is related to its function, may thus be implied.

It is now known that catalase of human, bovine, and canine origins are all NADPH-binding (Kirkman *et al.* 1987). In the original investigation by Jouve and co-workers (Jouve *et al.* 1986), the evidence for an ability of *Proteus mirablis* catalase to bind NADPH was equivocal. Re-evaluation of this catalase later revealed that it did indeed show binding behaviour (Jouve *et al.* 1989). Cystallography has confirmed the presence of one molecule of NADPH bound to each catalase monomer for BLC and for the catalase of *Micrococcus lysodeikticus* (Jouve *et al.* 1991). Recent work by this group has shown that catalase isolated from potato tubers (*Solanum tuberosum*) is not NADPH binding (Beaumont *et al.* 1990), athough a search for NADPH binding in other plant catalases has not been conducted. Among the moulds, neither *Aspergillus niger* (Kirkman and Gaetani, 1984) nor *Penicillium vitale* (Fita and Rossmann, 1985B) catalases bind NADPH, and in fact, in view of their subunit and protein structures, they would not be expected to bind dinucleotides. This list reflects the current information available concerning the phenomenon of NADPH binding to catalases.

Upon the discovery that mammalian catalases bind NADPH, three hypotheses regarding the function of the cofactor were presented (Kirkman and Gaetani, 1984). The first suggested that the NADPH is implicated in an enzymatic activity of catalase that is separate from that of the usual catalatic/peroxidatic modes. This hypothesis remains tenable because the physiological function of catalase in the cell is still unclear. Evidence for various possible functions of the enzyme

were presented above (**I.A**.iv). If catalase engages in other reactions for which NADPH is required, this would necessitate re-examination of the enzyme to identify the reactions that obligately utilize both it and the cofactor. The proposal of Vuillaume *et al.* (1988) suggesting that the enzyme may cause concerted synthesis of triphosphonucleotides would be one such reaction; but that investigation could not substantiate that the reaction proposed was indeed enzyme catalyzed.

The second hypothesis proposed that NADPH serves to prevent and reverse the progressive inactivation of catalase by its substrate, H_2O_2. Whether this could occur directly via the reaction of the cofactor as a hydrogen donor, or allosterically via a change in the conformation of the protein between NADPH bound and free forms was not established. This hypothesis has been tested (Kirkman *et al.* 1987). Results obtained utilizing an NADPH regenerating system added to an *in vitro* mixture in which catalase compound II formation was favoured (via slow generation of H_2O_2 using glucose/ glucose oxidase), indicated that the NADPH could both prevent and reverse accumulation of the inactive catalase species without reacting rapidly with compound I. Based on this result, Kirkman *et al.* (1987) have proposed a scheme for NADPH modulation of the catalytic reactions of catalase, shown in Fig. 8. According to this scheme, NADPH acts as a unique one electron donor in reducing compound II back to ferricatalase. The authors readily admit, however, that NADPH acting as a one electron donor is not physiologically likely, as NADPH is normally a preferential two electron donor. They therefore propose that the apoprotein stabilizes NADPH, allowing it to form a free radical species which reduces compound II in two successive one electron reactions. Eaton *et al.* (1974) had also noted a protective effect on catalase activity of NADPH

when added to hemolysates incubated with ascorbate, but were unaware of the binding interaction of the cofactor. In contrast, Orii *et al.* (1989) performed direct spectral examinations of hemoglobin-free perfused rat livers and suggested that compound II formed in liver cells is accumulated to a level comparable to that of compound I. Comparisons of the reflectance spectra for the rat livers and the absorbance spectra for purified bovine liver catalase treated to give a high proportion of compound II did indeed show similarity. The suggestion made by this group is that, *in vivo*, one electron donors present in the liver, not NADPH *per se,* modify catalase activity. As the spectral changes indicative of the decomposition of compound II were more rapid for the liver enzyme, this was also interpreted as supporting this mode of compound II depletion. Hydrogen donors such as NADPH/NADH and o-dianisidine, protect catalase from destruction of the heme-protein interaction mediated by the reaction of t-butyl hydroperoxide (tBOOH) with the enzyme under aerobic conditions *in vitro*. The cause of this destruction is thought to involve the attack of peroxyl or alkoxyl radicals formed subsequent to the reaction of the tBOOH to form an unstable porphyrin radical species (Pichorner *et al.* 1993). Similar protective effects of NADH have been observed for cytochrome P450 reactions with organic hydroperoxides (Cadenas and Sies, 1982). Of possible relevance is the additional finding of Mashino and Fridovich (1988), that *in vitro*, catalase activity is lost more rapidly when NADPH is *bound* to the enzyme, upon treatment with monochloroamine, a powerful oxidizing agent. The authors suggest that the oxidant probably enters the NADPH binding folds on the protein and oxidizes the cofactor directly. Unfortunately,

Figure 8. Scheme for NADPH protection of catalase from inactivation due to compound II formation.

Scheme of Kirkman *et al* (1987), proposing NADPH oxidation to NADP+ via the intermediate formation of an NADP radical species stabilized by the protein. Also note the postulated reversibility of the compound I reduction to compound II.

Figure 8

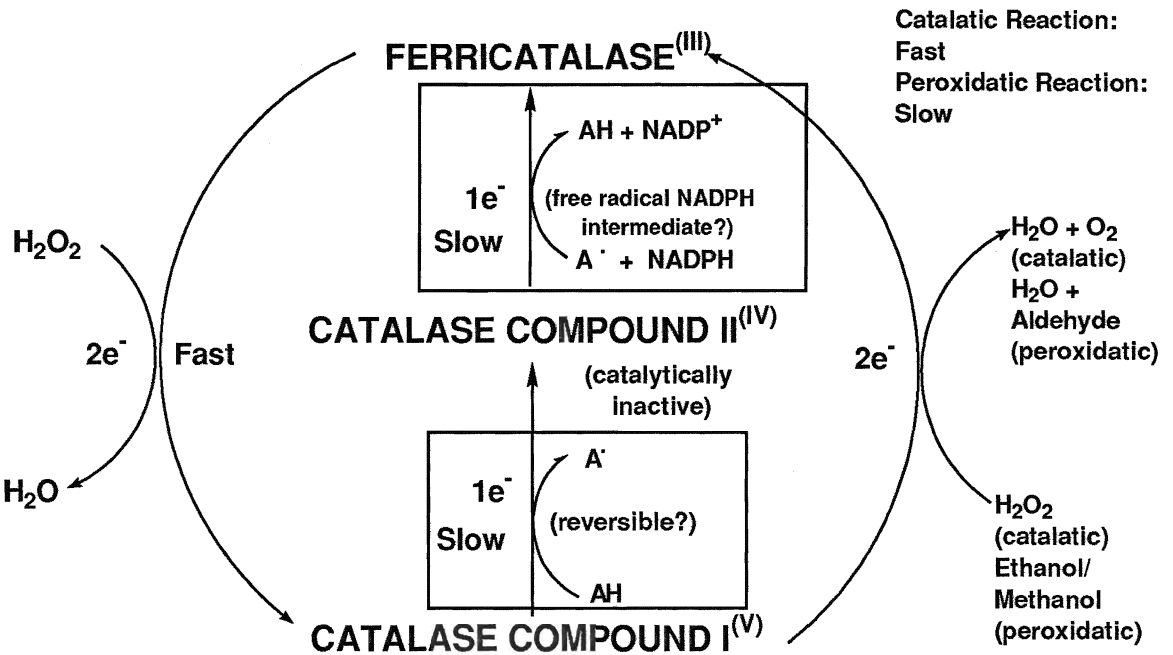
Catalatic Reaction:
Fast
Peroxidatic Reaction:
Slow
FERRICATALASE(III)
AH + NADP+
1e-
Slow
(free radical NADPH
intermediate?)
A · + NADPH
CATALASE COMPOUND II(IV)
(catalytically
inactive)
A·
1e-
Slow
(reversible?)
AH
CATALASE COMPOUND I(V)
H2O2
2e-
Fast
H2O
2e-
H2O + O2
(catalatic)
H2O +
Aldehyde
(peroxidatic)
H2O2
(catalatic)
Ethanol/
Methanol
(peroxidatic)

this interaction is not selective, as side reactions which produce ^{-}OCl ions and HOCl also occur, causing the presumed inactivation of the enzyme by ligating to the hemes.

The third hypothesis regarding the function of NADPH proposed that catalase is a regulatory enzyme allowing the glutathione reductase/ peroxidase system to operate at higher efficiencies under conditions of peroxidative stress within erythrocytes. The argument of Kirkman and Gaetani (1984) for this was that $NADP^{+}$ release from catalase occurs under conditions of peroxidative stress. The latter may be induced by certain drugs, which cause the glutathione reductase/ peroxidase mechanism to deplete cellular NADPH, presumably in both the unbound and catalase-bound forms, and stimulate the further operation of this mechanism via a higher NADPH flux through activity of glucose-6-phosphate dehydrogenase. This hypothesis seems difficult to reconcile with the facts that NADPH is tightly bound to catalase and not readily exchanged to be oxidized by the glutathione metabolizing system. The eukaryotic catalase is largely sequestered away from the bulk of the glutathione system in peroxisomes. The hypothesis may be supported however, as suggested by Kirkman and Gaetani (1984); cells should be investigated by subjecting them to peroxidatic stress for catalase-NADH complexes and elevated levels of cytosolic NADP.

If hemoproteins were exposed to oxidative stresses that give rise to a number of species capable of destroying the catalytic function via chemical modification of the heme, or the surrounding protein, or both; then the original role of reducing species such as NADH/ NADPH bound to catalase may have been prevention of the physical destruction of the heme or the protein. Oxidative stresses would, however, be more relevant in the contemporary bacterium rather than in the mammal,

since the latter has a homeostatically controlled intercellular environment. Though this may explain the lack of deleterious effects in the acatalasemic man, it does not explain why mammalian catalases still retain NADPH, nor does it explain how the role of the cofactor may have changed in the evolutionary history of catalase.

CHAPTER II. MATERIALS AND METHODS

Unless otherwise stated, laboratory chemicals were acquired through Sigma Chemical Co., St. Louis, Missouri. K_2HPO_4, $CHCl_3$, NaS_2O_4, $K_4Fe(CN)_6$, HCOONa, and KCN were products of BDH Chemicals, Etobicoke, Ontario. 95% ethanol and 1N NaOH were from Caledon Laboratories, Georgetown, Ontario. KH_2PO4 was from J.T. Baker Ltd., Phillipsburg, New Jersey. NH_4SO_4 was from Fisher Scientific, Nepean, Ontario. Sodium dodecyl sulfate (SDS) (sodium salt) was from Aldrich Chemicals, Milwaukee, Wisconsin. Chemicals employed were of AnalaR™ or similar quality throughout.

1. Sources of Catalase

i. Bovine liver catalase

Bovine liver catalase employed was the Sigma C-100 product. The catalase was normally used as supplied, by diluting the concentrated semicrystalline suspension in the buffer appropriate to the given investigation (usually pH 6.5 or pH 7.0, 50mM potassium phosphate), followed by centrifugation for 5min. in a clinical centrifuge at high speed to remove insoluble material before use. For fluorescence studies, the protein was also filtered on a Sephadex G-25 column (1.5 x 10cm) in 50mM potassium phosphate buffer, pH 7.0. Concentrations of catalase were estimated spectrophotometrically using a millimolar extinction coefficient of 3.24×10^2 cm^{-1} @ 405nm (Samejima and Yang, 1979; Jones *et al*, 1982), or reported in hematin units using a millimolar extinction coefficient of 1.20×10^2 cm^{-1} @406nm (Nicholls and Schonbaum, 1963)

ii. Purification of Catalase from baker's yeast

The procedure described here was essentially that of Seah and Kaplan (1973) with modifications. All procedures were carried out at 4°C.

Step 1. Preparation of the crude extract

60g. of commercial active dry baker's yeast (Fleischmann's Ltd., Etobicoke, Ontario) were placed in a standard blender. The blender was operated at high speed for three periods of fifteen seconds. The resultant fine powder was then added to 200ml. of 50mM TRIS-HCl, 1mM EDTA, 0.1% PMSF at pH 8.0. The mixture was stirred for 30 min. Portions of approximately 50ml of the mixture were transferred to 250ml Polyvinyl chloride centrifuge bottles. Glass beads (0.4-0.5mm diameter) were added to the bottles in the proportions of 1g per ml. of the mixture. The bottles were placed on a sidearm shaker and agitated at highest speed setting for 2 hours. The bottles were then placed in an International Equipment Corporation Superspeed Centrifuge (#872 rotor) and centrifuged at 7,000 RPM for 30min. Supernatant collected was then again centrifuged at 7,000 RPM for 15min. The resultant mixture, with glass beads and debris removed, was designated the crude extract.

Step 2. Ethanol-chloroform treatment:

One volume of a mixture of ethanol and $CHCl_3$ (1:1, v/v) was added to 5 volumes of crude extract in a 250ml. separatory funnel which was then subjected to three periods of vigorous shaking for 15 sec; the stopper was opened between periods. The contents were spun at 10,000 RPM for 30min. in a Sorvall RC-5 Superspeed Centrifuge

(DuPont Instruments Ltd.) in an SS-34 rotor in jacketed 30ml Corex® centrifuge tubes; the top, aqueous layer, was removed, and the dense, middle layer of denatured protein and bottom layer of organic solvent were discarded.

Step 3. First Ammonium Sulfate Fractionation:

Solid $(NH_4)_2SO_4$ was added to 40% saturation. The precipitate collected by centrifugation (as in step 2, 10,000 RPM, 30min) was discarded, and the supernatant was brought to 60% saturation. The precipitate was collected and dissolved in 5 mM potassium phosphate buffer, pH 7.0.

Step 4. Second Ammonium Sulfate Fractionation:

Solid $(NH_4)_2SO_4$ was added to 45% saturation. The calculation assumed that none was carried over when the second precipitate of step 3 (above) was resuspended in buffer. The precipitate collected by centrifugation (as in step 2, 10,000 RPM, 30min.) was discarded, and the supernatant was again brought to 60% saturation. The precipitate was dissolved in 1 to 2 ml. of the same buffer as in Step 2 and reserved.

Step 5. Sephadex G-75 Chromatography:

The solution from step 4 was passed over a column (1.5cm x 30cm) of Sephadex G-75 pre-equilibrated with 5mM potassium phosphate, pH 7.0. Elution was again with 5mM potassium phosphate, pH 7.0, utilizing a very slow flow (approximately 1 ml. per 20min.) and collecting 1.5ml aliquots. Catalase activity appeared with the initial protein peak. Tubes with catalase activity were pooled, and the enzyme

was precipitated with $(NH_4)_2SO_4$ (80% saturation), collected by centrifugation (as in step 2), and taken up in a small volume (1.5 to 2.0 ml) of 5mM potassium phosphate, pH 7.0. The resulting brown solution was desalted by passing over a column (0.9cm x 15cm) of Sephadex G-25, coarse mesh, and eluting with 5mM potassium phosphate, pH 7.0. Aliquots (1.5ml) were collected, and those with catalase activity were pooled.

Step 6. Hydroxylapatite Chromatography:

Hydroxylapatite separation of the eluted catalase mixture was carried out in the following way. Hydroxylapatite (HTP dry gel, Bio-Rad Laboratories, Richmond, Ca.) was rehydrated in 0.1M potassium phosphate (pH7.0) and packed to a 2.0x 5.0cm column. The pooled catalase active fractions from the Sephadex G-75 step were applied to this column. Protein was eluted stepwise with 20ml 0.1M potassium phosphate (pH 7.0) and 30ml each of 0.15M, 0.20M and 0.30M potassium phosphate (pH 8.0). Catalase A was eluted with 0.15M, and catalase T with 0.20M-0.30M concentrations of buffer. The fractions thus collected were tested for activity (spectrophotometric assay as per procedure #4, this chapter), concentrated by means of Centriprep-30 centrifugal concentrators (Amicon, Beverley, Mass.) in a clinical centrifuge to approximately 0.5-1ml total volumes, and then stored frozen (-20 C) as recommended.

Concentrations of the *Saccharomyces cerevisiae* enzymes were estimated spectrophotometrically using millimolar extinction coefficients per hematin of 100 cm^{-1} @408nm and @406nm for the A and

T catalases, respectively, based on Sharma *et al* (1989)(cf. Seah *et al*, 1973).

iii. *Escherichia coli* catalase HPII proteins and HPII site-directed mutant proteins

The catalase HPII proteins and the site-directed mutant proteins used in the investigations described were generous gifts from the laboratory of Dr. P.C. Loewen, University of Manitoba. The mutants were constructed (von Ossowski *et al*, unpublished) using the techniques of oligonucleotide directed mutagenesis employing the plasmid pAMkatE72 containing the *katE* gene. The latter specifies the HPII catalase of *E. coli*. Growth conditions, harvesting of cells, and isolation and purification of HPII and the mutant proteins are after the procedure of Loewen and Switala (1986). The lyophilized material received was directly dissolved in 50mM potassium phosphate buffer, pH 7.4 or pH 7.0. Insoluble material was removed by centrifugation, and pH adjustments made as required with 500mM monobasic/ dibasic potassium phosphate stocks. HPII catalase concentrations were estimated using a millimolar extinction co-efficient per hematin of 1.18×10^2 cm^{-1} @405nm (Dawson *et al*, 1991) or via direct protein determinations utilizing procedure # 3, this chapter.

2. Heme characterization

Heme characteristics were investigated by the preparation of reduced pyridine hemochromes according to the guidelines recommended by Fuhrhop and Smith (1975). In a typical case, 100µl. pyridine was added to a 100µl. aliquot of the sample dissolved in 50mM

potassium phosphate, pH 6.5 in a serological tube . This mixture was gently swirled for approximately one minute to allow for protein denaturation, before the addition of a 50µl aliquot of 1N NaOH. Samples of the prepared mixture were then diluted with distilled water. Absorbance spectra were obtained of samples in blackwalled semi-micro cuvettes (0.5ml.) by a DU series 50 spectrophotometer (Beckman Instruments Ltd., Irvine, Ca.) with microbeam attachment linked to a Comptech™ 286-AT PC system with Beckman's Dataleader™ software package installed. Reduced pyridine hemochrome spectra were obtained by the reduction of the cuvette samples with a few crystals of sodium dithionite, and absorption spectra were then taken again. Results were output to a Roland plotter.

3. Protein Determination

Protein concentration was generally determined by the method of Bradford (1976), utilizing the Coomassie blue-protein complex system, according to the specifications of the manufacturer (Bio-Rad Laboratories) and employing the BSA standard supplied for construction of the standard curve. Absorbance of the samples and standards were measured in triplicate in a DU-7HS (Beckman Instruments) spectrophotometer at 595nm.

4. Assay for Catalase Activity

Assays were conducted after the method of Beers and Sizer (1952). In the general case, to 2.0ml of 50mM potassium phosphate buffer, pH 6.5, in a 3.0ml quartz cuvette 50µl. of a 1M solution of H_2O_2

was added. The H_2O_2 concentration was determined spectrophotometrically using an extinction coefficient at 240nm of 39.4 $M^{-1}cm^{-1}$(Nelson and Kiesow, 1972). To this cuvette in a spectrophotometer (DU-50 or DU-7HS system as in procedure #2, this chapter) set to a wavelength of 240nm, an aliquot of sample was added estimated to bring the final concentration of catalase to approximately 1nM. The absorbance of the mixture was monitored for a period of usually between 10 and 12 minutes. Pseudo-first order rate constants for the samples examined were calculated as (see also Appendix A):

$$k_1 = \frac{\ln 2}{t_{\frac{1}{2}}}$$

where $t_{\frac{1}{2}}$ is the time taken for the absorbance level of hydrogen peroxide to decay to half its initial value. Specific first order rate constants were then calculated as:

$$k_1' = \frac{k_1}{[\text{catalase hematin}]}$$

in units of $M^{-1}s^{-1}$.

5. Polyacrylamide gel electrophoresis and staining

Polyacrylamide gel electrophoresis was performed in the SDS denaturing system described by Laemmli (1970) utilizing the Mini-Protean II slab gel apparatus as specified by the manufacturer (Bio-Rad Laboratories). The acrylamide concentration used was 12%. Gel slabs were loaded with approximately 25µg. protein per sample well estimated using the protein determination procedure given in #3, this

chapter. Running conditions used a voltage setting of 200V in a TRIS-glycine buffer, pH 8.3. Staining for protein utilized the Coomassie blue staining system as specified by the manufacturer.

6. Titration of catalase proteins with heme ligands

Potassium cyanide and sodium formate were made up in glass distilled water as 1.0M and 6.0M stock solutions, respectively. Serial dilutions of these stocks were prepared fresh daily by diluting with appropriate amounts of the buffer used for preparation or predilution of the given protein to be titrated. The catalase proteins to be titrated were prepared in 50mM potassium phosphate, pH 6.5. Temperatures were 25 degrees, unless otherwise stated. Estimates of the protein concentrations were made spectrophotometrically utilizing the molar absorption coefficients given in section #1 for the Soret absorbance band of the given catalase.

7. Affinity Chromatography

Affinity chromatography of catalase proteins was carried out utilizing the Affi-gel Blue® Affinity Chromatography Gel according to the major specifications of the manufacturer (Bio-Rad Laboratories, Richmond, Ca.). The column matrix is the blue Cibacron™ F3GA dye linked to agarose as shown in Fig. 9A. The dye is a synthetic analogue of NADPH in open conformation, as shown in Fig. 9B. In theory, any protein capable of binding dinucleotides (i.e., possessing the dinucleotide "fold" (Thompson *et al*, 1975)) will thus bind the column, and be eluted via treatment with either high salt concentrations or with dinucleotides.

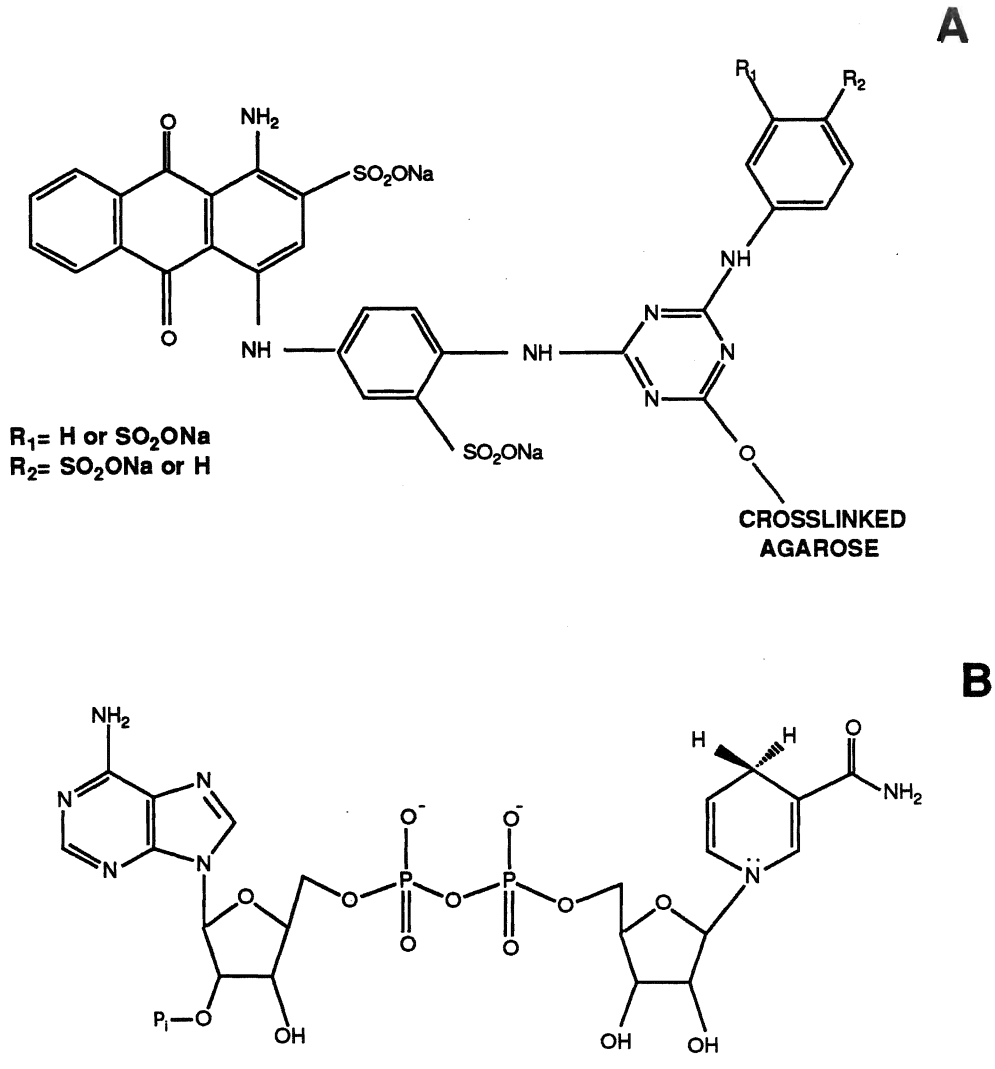

Figure 9. Comparison between structure of Cibacron® F3GA dye and NADPH.

(**A**) Structure of Cibacron® F3GA dye. The dye is crosslinked as shown to the matrix, which may be agarose or dextran, to give the chromatography gel. (**B**) Structure of NADPH

Preparation of chromatography column

Affi-gel Blue® gel was prepared by dilution of the storage buffer with 10mM TRIS-HCl, pH 7.4, and then packed to a 1.1x 1.5cm column and equilibrated with the same buffer, followed by a 2.5ml wash of 1mM NaN_3 and a subsequent wash of at least 10 bed volumes of the starting buffer before use.

Loading and elution of protein samples

For each elution , approximately 300μg. protein per sample to be evaluated was loaded onto the column in a total of from 0.2ml to 0.55ml volumes, diluted as required to achieve the correct total protein in the aliquots (based on absorbance at 280nm). The column was washed with 10ml of starting buffer (10mM TRIS-HCl, pH 7.4 or potassium phosphate, 50mM, pH 7.0), followed by 2.5ml of starting buffer to which 1mM ADP had been added. The column was then again washed with 10 ml of starting buffer, followed by 1ml starting buffer containing 10 μM NADPH. The column was once again washed with 10ml of starting buffer, and finally washed with a second aliquot of the NADPH containing buffer, to ensure no appreciable hemoprotein could be further displaced. Hemoprotein was eluted in 0.5ml fractions, and monitored at 405nm for heme and at 340nm after the point of NADPH addition, so that the NADPH elution could be followed.

8. Fluorescence

Fluorescence emission spectra were obtained as follows. Samples were diluted in 20mM TRIS-HCl, pH 8.0 containing 0.1mM EDTA as in the procedure of Lowry *et al* (1957). Fluorimetric emission spectra of

prepared samples (at least 2ml) containing approximately 0.2μM catalase protein (estimated from the extinction at 405nm, see section #1) in a 3ml quartz fluorimetric cell were usually obtained in the range of 360nm to 560nm. Excitation was at 340nm (the NADPH near-ultraviolet maximum) in a Perkin-Elmer model LS-50 luminescence spectrometer linked to a MacComp™ 386SX computer equipped with Perkin Elmer's FLDM™ data manipulation system. Conditions included the "low stir" setting at 30C for all spectra obtained. Results were output to an Epson dot-matrix printer. Emission spectra were averages of three accumulated spectra per sample.

9. Catalase secondary peroxide compound formation/depletion experiments

Spectrophotometry was carried out at 435nm with a Beckman DU-50 instrument with computer linked system as described in section. #2. Results were plotted on a Roland plotter. Semi-micro (1ml, 1cm.) quartz cuvettes with black sidewalls were usually employed. For all time course traces and spectra, the standard system was 10mM potassium phosphate, pH 6.5. Glucose oxidase was the *Aspergillus* enzyme (Sigma, type X) prepared as a concentrated stock in 50mM potassium phosphate and diluted to approximately 2-3nM in the sample buffer used. D-Glucose (BDH, Poole, Dorset, U.K.) was utilized as a 0.2M stock in distilled water. Catalase hematin (BLC, SCCT, SCCA) was determined from the stock employed in each case. Potassium ferrocyanide was prepared as a 10mM stock solution in glass distilled water and frozen until used.

CHAPTER III. RESULTS

A. Spectral and Kinetic characterization of the Catalase Proteins

i. Spectroscopy of BLC, SCCT, and SCCA proteins

Figure 10 shows the absorbance of bovine liver catalase in the Soret (Fig. 10A) and visible (Fig. 10B) regions as well as the absorbance of the SCCT and SCCA proteins purified from dried baker's yeast. For comparison, the spectrum of HPII catalase of *E. coli* is also shown. The spectra have been factor adjusted for approximate absorbance equality at 750nm, to permit visual inspection (full scale absorbances and heme concentrations as specified in the figure legend).

The Soret maximum for the BLC is at 403nm. This value is at an unusually short wavelength for the bovine enzyme. The Soret peak is usually reported at 405nm (Nicholls and Schonbaum, 1963). But the 403nm peak was found consistently among samples of the commercially obtained enzyme. It is here ascribed to the nature of the commercial preparation, perhaps due to high proportions of bile pigments in such material. The visible portion of the BLC spectrum (Figure 10B), however, shows no such deviation. The maxima for BLC are at 622nm for the principal band and at 540nm and 500nm for the accessory bands as reported previously (Nicholls and Schonbaum, 1963).

Absorbance maxima for the SCCT protein occur in the Soret region, at 405nm, and in the visible region, at 630nm, at 535 and at 505 nm. Similarly, absorbance maxima for the SCCA protein occur in the Soret region, at 405nm, and in the visible region, at 630 nm, and 535nm, with the band at 505nm being indistinct and possibly due to

Figure 10. Absorption spectra of Bovine Liver, *Saccharomyces cerevisiae* , and *E. coli* HPII catalases.
Spectra of BLC (4.3μM hematin, solid line), SCCA (3.2μM hematin, large broken line), SCCT(16.1μM hematin, small broken line), and HPII wild type (4.5μM hematin, dotted line) in (**A**) the Soret and the visible (**B**) regions. Spectra have been scaled for approximate absorbance equality at 750nm. Original full scale absorbances were 0.52, 0.33, 1.65, and 0.55 respectively, in (**A**), and 0.10, 0.07, 0.33, and 0.11 respectively, in (**B**). Samples in 50mM potassium phosphate, pH 7.0, 25 degrees.

Figure 10

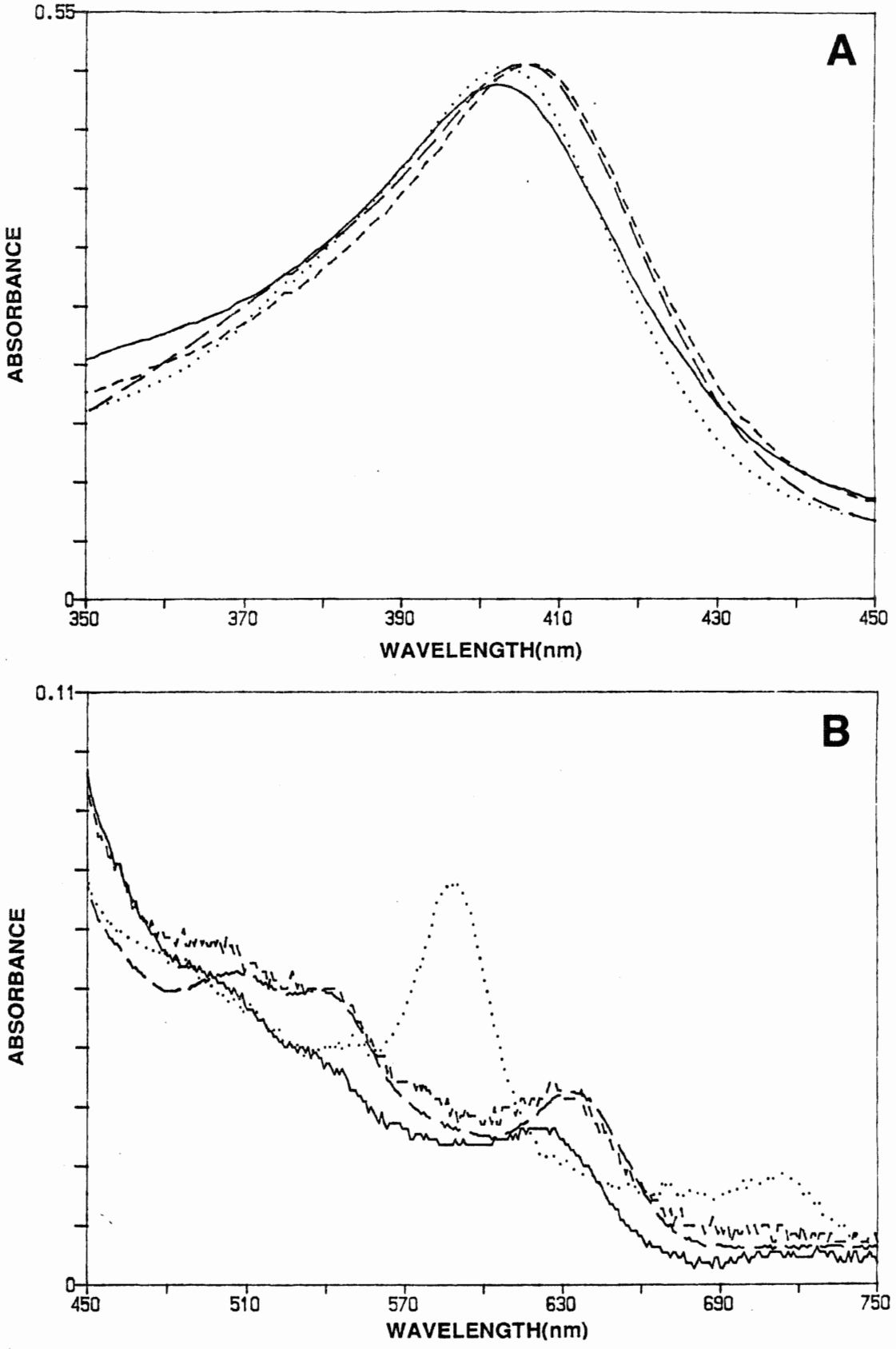
A
0.55
0
ABSORBANCE
350
370
390
410
430
450
WAVELENGTH(nm)
B
0.11
0
ABSORBANCE
450
510
570
630
690
750
WAVELENGTH(nm)

contamination by the presence of a residual amount of SCCT protein. These observations agree reasonably with spectra obtained previously (Seah and Kaplan, 1973). Comparing the spectrum for catalases isolated from *Saccharomyces cerevisiae* with that of BLC, the similarity of both the positions of the bands in the Soret and in the visible regions and the relative intensities of those bands suggests that the proteins of these two eukaryotic species have their heme prosthetic groups (protoheme IX) in common.

ii. Spectroscopy of HPII wild type and HPII mutant proteins

Figure 10 also shows the spectrum of HPII in the Soret and the visible regions. The spectrum of the protein corresponds reasonably to that described earlier (Claiborne *et al,* 1979). The Soret band is at 403nm. The predominant maxima in the visible region are at 588nm and at 712nm. The spectrum of the wild type protein thus contrasts with those of the BLC and SCC proteins (Fig. 10). It also differs from the spectra of some HPII site-directed mutant proteins (Figs. 11 and 12). The site-specific mutant proteins comprise two general families. One family (shown in Fig. 11) contains two mutants in which the histidine 128 residue of the HPII protein subunit has been replaced. This is a residue in the heme pocket distal to the heme analogous to His-74 of BLC , which is highly conserved and implicated in functionality of the enzyme. The two mutants substitute the histidine with either alanine or with asparagine and are hereafter termed H128A and H128N respectively.The second family (spectra shown in Fig. 12) consists of three mutants in which the asparagine residue at subunit residue 201of HPII has been replaced. This residue is also in the heme pocket. Studies

Figure 11. Absorption spectra of HPII wild type protein versus Histidine 128 mutant proteins.
Spectra of HPII wild type (dotted line), H128A (solid line), and H128N (broken line) proteins in (**A**) the Soret and (**B**) the visible regions. Spectra scaled for absorbance equality at 750nm. Full scale absorbances: 0.60, 0.59, and 0.36 for spectra in **A** and 0.15, 0.15, and 0.090 for spectra in **B** respectively. Samples in 50mM potassium phosphate, pH 7.0. 25 degrees.

Figure 11

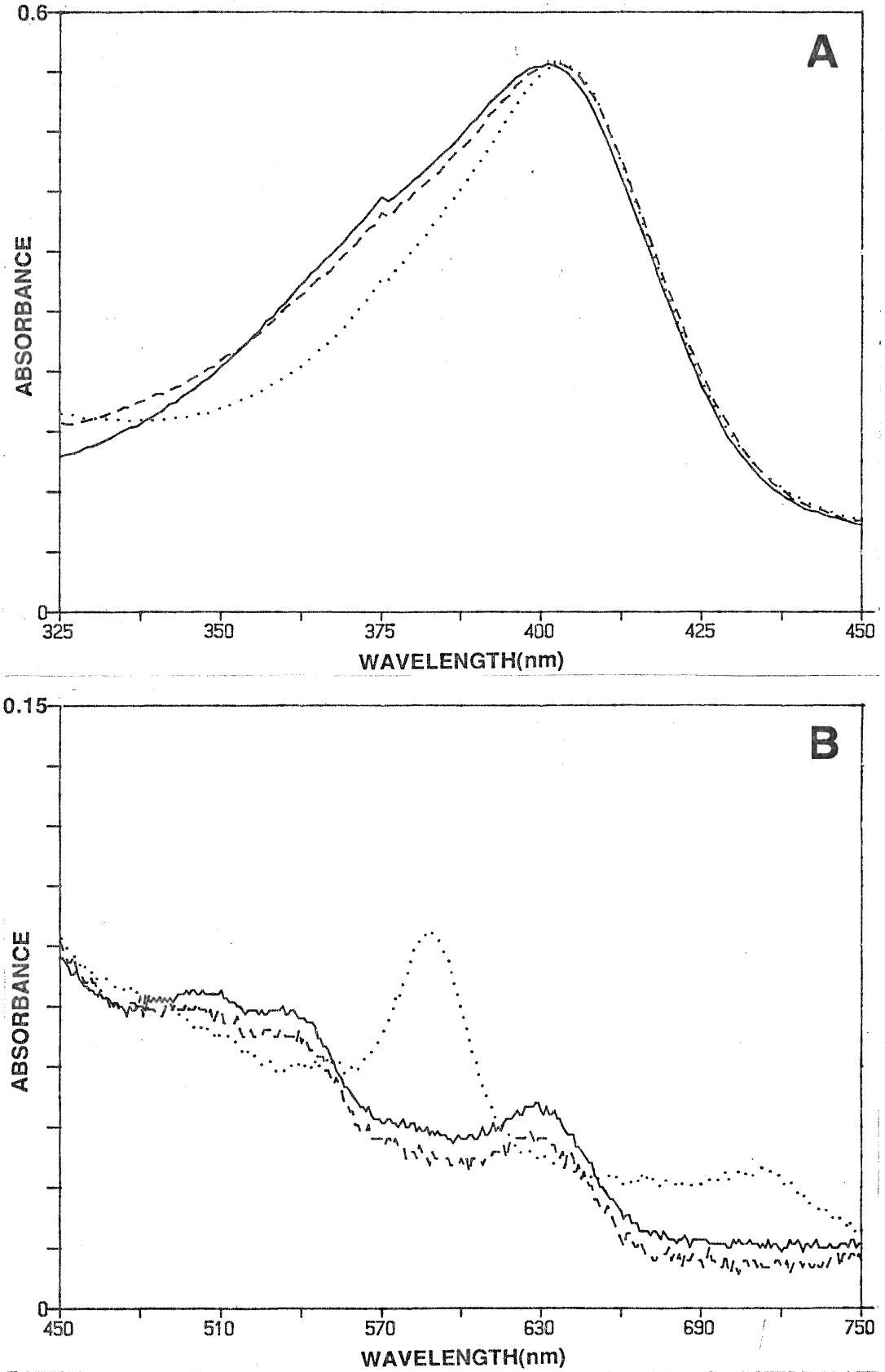
A
0.6
0
ABSORBANCE
325
350
375
400
425
450
WAVELENGTH(nm)
B
0.15
0
ABSORBANCE
450
510
570
630
690
750
WAVELENGTH(nm)

of the analogous Asn 147 in bovine liver catalase implicate it in co-ordination by hydrogen bonding to the substrate and, therefore, in catalytic activity. The three mutant proteins substitute asparagine for histidine, alanine, or glutamine, and will be hereafter referred to as N201H, N201A, and N201Q, respectively.

H128A and H128N mutant protein spectra are compared to that of the wild type HPII protein in Fig. 11. Fig 11A shows the Soret, and Fig. 11B the visible region. All spectra are adjusted to the same absorbance level at 750nm. The mutant proteins show asymmetry of their Soret maxima compared to the wild type protein. The maxima in this region are 403nm for the wild type and H128N proteins, and 401nm for the H128A protein. The visible spectra (Fig. 11B) however, show that this family of mutant proteins contains a different heme prosthetic group compared to that of wild type protein, presumably a *d* type heme. The visible maxima for both H128 mutants fall at 630nm for the 'α' bands and at 535nm and 505nm for the subsidiary bands, a situation remarkably similar to that of the protoheme IX containing BLC and spectrally almost identical to the *Saccharomyces cerevisiae* catalases (cf. Fig. 10).

Spectra of the N201 mutant proteins are shown in Figure 12. These have a high degree of variability compared to the wild type HPII. The N201Q mutant protein has a Soret maximum similar to the wild type, and the N201H and N201A mutants have maxima in the same region that are distinctly asymmetric. The visible spectra show more diagnostic features. With maxima at 585nm and at 705nm, N201Q has a spectrum largely similar to that of the wild type protein, suggesting the incorporation of the usual heme *d*, but it also has a shoulder accessory to the 585nm band in the region of 620nm that is not

Figure 12. Absorption spectra of HPII wild type protein versus Asparagine 201 mutant proteins.
Spectra of HPII wild type (solid line), N201Q(large broken line), N201A(small broken line), and N201H (dotted line) in (**A**) the Soret and(**B**) the visible regions. Spectra scaled for the approximate absorbance equality at 750nm. Full scale absorbances: 0.60, 0.31, 0.34and 0.42 for spectra in (**A**) and 0.15, 0.078, 0.085 and 0.11 for spectra in (**B**), respectively. Samples in 50mM potassium phosphate, pH 7.0. 25 degrees.

Figure 12

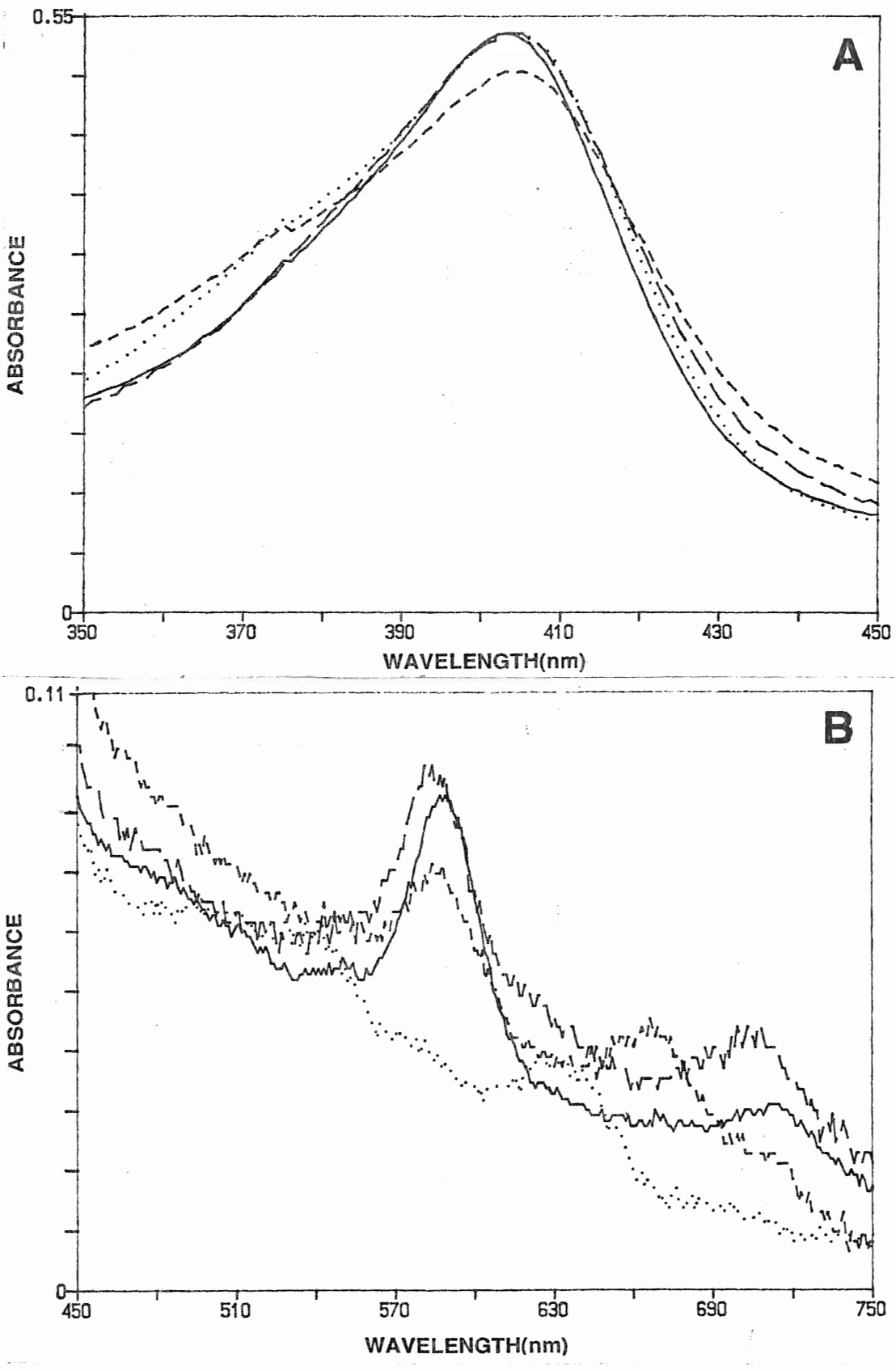
A
0.55
0
ABSORBANCE
350
370
390
410
430
450
WAVELENGTH(nm)
B
0.11
0
ABSORBANCE
450
510
570
630
690
750
WAVELENGTH(nm)

apparent in the wild type spectrum. The N201H mutant protein has a spectrum with maxima at 630nm,535nm, and 505nm, and a shoulder to the main band at 579nm, suggesting the presence of a heme more like protoheme IX than the *d* type heme (compare with spectra of BLC, Fig. 10). The spectrum of the N201A mutant protein has two maxima, at 585nm and at 665nm, resembling the spectrum of the HPII wild type protein but with the 712nm maximum occurring at a blue-shifted wavelength. Heme composition of this mutant protein would thus seem to be intermediate between that in N201Q and N201H, suggesting a heterogeneous heme population.

iii. Catalatic activity of catalase proteins

Fig. 13 shows some representative time courses in which the decomposition of H_2O_2 by catalase is followed at 240nm (see Materials and Methods for details on this activity assay). A data summary and calculations for specific pseudo-first order rate constants for all experiments are shown in Appendix A. Table I compares the specific first order rate constants (per hematin) of the wild type and site-directed mutant proteins of HPII with those of the protein fractions isolated from dried baker's yeast and BLC. Some of the HPII N201x mutants are slightly active toward hydrogen peroxide compared to the H128x site-directed mutants, but all function poorly compared to the wild type activity. The calculated specific rate constants for the *Saccharomyces cerevisiae* catalases indicate that the enzymes are comparable in activity to BLC.

B. Physical characterization of the catalase proteins

i. Denaturing polyacrylamide gel electrophoresis of SCCT and SCCA proteins

Figure 14 shows the results of a SDS-denaturing polacrylamide gel electrophoresis (conditions described in Materials and Methods). The gel compares the relative mobilities of BLC (lane a) under these conditions with mobilities of fractions obtained during the purification of catalases from dried baker's yeast (lanes b to f). The band pattern for BLC (lane a) indicates some protein overloading, with band heterogeneity possibly due to small proportions of contaminating proteins present. Lanes b to f show total protein present at stages in the purification process of the *S. cerevisiae* catalases. The penultimate step is represented by the pattern of bands seen in lane d (Sephadex G-75 fractionated and desalted catalase mixture before final fractionation). The major portion of the catalase present prior to the hydroxylapatite column chromatography step carried out appears to be SCCA based on the band pattern seen. Fractions "A" and "T" (lanes e and f respectively) show that the denatured "T" protein runs principally as subunits of approximately 66 kd while the "A" fraction runs principally as subunits of approximately 42 kd. This is in reasonable agreement with previous findings concerning the relative mobility of the catalases from *Saccharomyces cerevisiae* in SDS-PAGE systems (Seah and Kaplan, 1973), which reported relative mobilities corresponding to 60kd and 45kd for the T and A catalases, respectively. The unusually small subunit size for the A catalase subunit by SDS-PAGE is presumably due to autolysis, since the corresponding

Figure 13. Representative assays for catalase activity. Decomposition of H_2O_2 by catalase monitored at 240nm. H_2O_2 at 20mM in potassium phosphate, pH 7.0, 25 degrees, in a final volume of 2.5ml. Catalase additions were 13nM hematin N201Q mutant protein for trace **a**, 13nM hematin N201H for trace **b**, 13nM hematin N201A for trace **c**, 13nM HPII wild type protein for trace **d**, and 2.5nM hematin BLC for trace **e**.

Figure 13

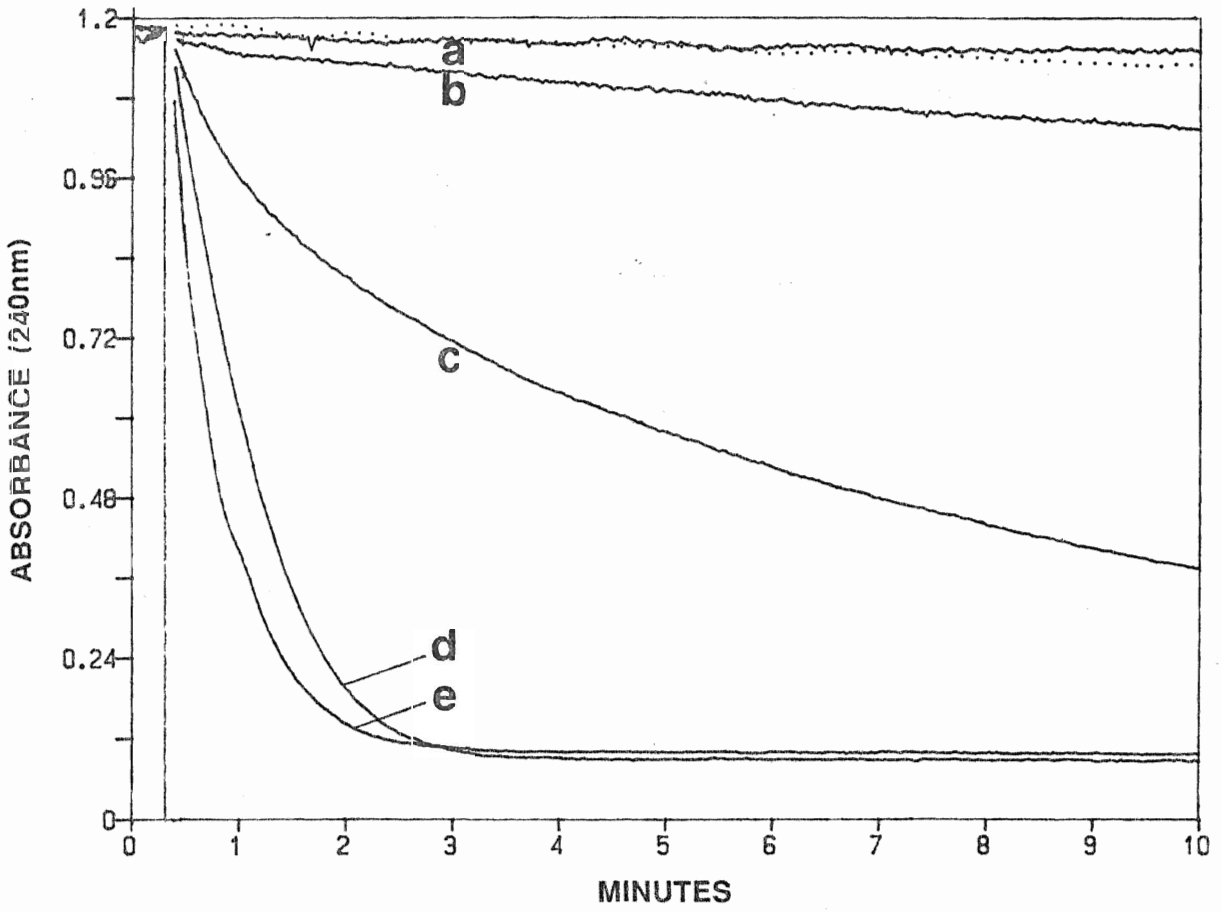
1.2
0.96
0.72
0.48
0.24
0
ABSORBANCE (240nm)
a
b
c
d
e
0
1
2
3
4
5
6
7
8
9
10
MINUTES

TABLE I. Catalatic activities of catalases.
Activity assay conditions as specified in Fig. 13. Parameters and method of calculating specific rate constants are given in Appendix A/ Materials and Methods. Specific rate constants per molar hematin concentration. Apart from value calculated for N201H, all specific rate constants are averages of at least two assays.

CATALASE	SPECIFIC ACTIVITY ($M^{-1}s^{-1}$)	ACTIVITY RELATIVE TO BLC	ACTIVITY RELATIVE TO HPII WILD TYPE
Bovine Liver	6.4×10^6	100%	533%
Saccharomyces A	6.2×10^6	97%	516%
Saccharomyces T	6.6×10^6	103%	550%
HPII wild type	1.2×10^6	19%	100%
HPII N201Q	-	<<0.1%	<<0.1%
HPII N201A	1.9×10^5	3%	16%
HPII N201H	1.7×10^4	0.3%	1.4%
HPII H128A	-	<<0.1%	<<0.1%
HPII H128N	-	<<0.1%	<<0.1%

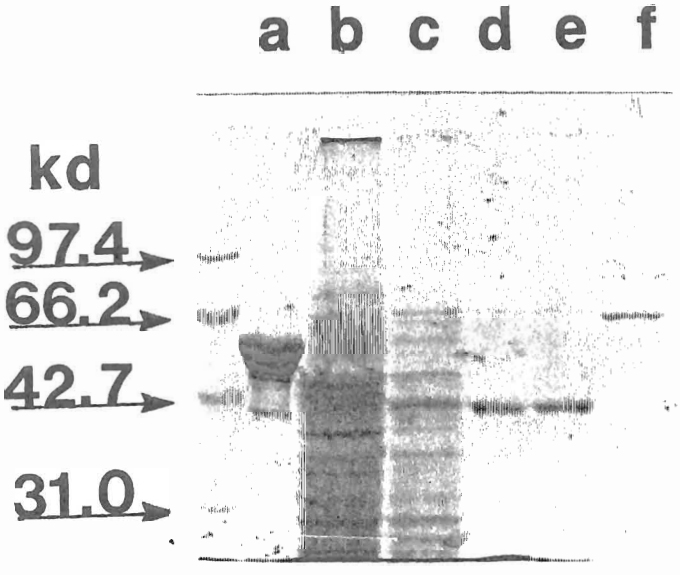

Figure. 14. SDS-PAGE characterization of *Saccharomyces* catalases.
Polyacrylamide electrophoretogram stained with Coomassie blue protein stain. Running conditions and gel composition as described in Methods and Materials, procedure #5. Estimated 25µg. protein per lanes **a-c**, 4-5µg. protein per lanes **d-f**. Molecular weight standard sizes as indicated in leftmost lane. Lanes **b** through **f** were loaded with protein obtained during a typical yeast catalase purification. Lanes: **a**) bovine liver catalase, **b**) crude extract from purification of *Saccharomyces cerevisiae* catalases, **c**) ethanol/chloroform fraction, **d**)G-75 Sephadex isolated fraction, **e**) hydroxyapatite isolated SCCA fraction and **f**) hydroxyapatite isolated SCCT fraction.

structural gene codes for a protein of 58.5kd molecular mass (Cohen *et al*, 1988).

ii.Heme group characterization of the catalase proteins

Figure 15 shows the spectra of the reduced alkaline pyridine hemochromes of BLC, SCCA, and SCCT reduced with an excess of dithionite (for details of the preparation, please see Materials and Methods). The spectra are scaled to identical absorbance levels for the α band maximum in the visible region. The dithionite reduced pyridine hemochrome α absorption bands in the visible region are at 555nm, with β bands at 524nm, and have a sharpened Soret peak at 417nm, which closely approximate the diagnostic positions of the reduced alkaline hemochrome α, β, and Soret bands for protoheme IX at 557nm, 526nm, and 419nm respectively (Fuhrhop and Smith, 1976). Pyridine hemochromes for both *Saccharomyces* catalases prepared by Seah and Kaplan (1973) and co-workers gave a result implying that the prosthetic group was protoheme. Earlier work by Brown (1953) also showed the presence of protoheme in *Saccharomyces cerevisiae* catalase, though the preparations used were not purified to homogeneity. The results shown here clearly indicate that both isolates obtained have the characteristic α and β bands of protoheme IX. The two catalases of baker's yeast thus incorporate *b* type hemes.

Figure 16 compares the reduced pyridine hemochromes of the HPII wild type and certain mutant proteins (please see Materials and Methods). The multiplicity of absorbance spectra for the mutant proteins as compared to the HPII wild type protein is again apparent . The HPII wild type hemochrome has a broad band with a maximum at

Figure 15. Absorption spectra of reduced alkaline pyridine hemochromes for BLC, SCCT, and SCCA.
3μM hematin BLC (solid line), 3.5μM hematin SCCT (large broken line), and 1.5μM SCCA (dotted line) reduced alkaline pyridine hemochromes in (**A**) the full spectrum and (**B**) the visible region. Spectra scaled for absorbance equality of the α band maxima of the spectra at 555nm. Full scale absorbances of untreated proteins were 0.56, 0.6, and 0.44 for spectra in (**A**), and 0.14, 0.15, 0.11. for spectra in (**B**). Preparation of reduced pyridine hemochromes as described in Materials and Methods.

Figure 15

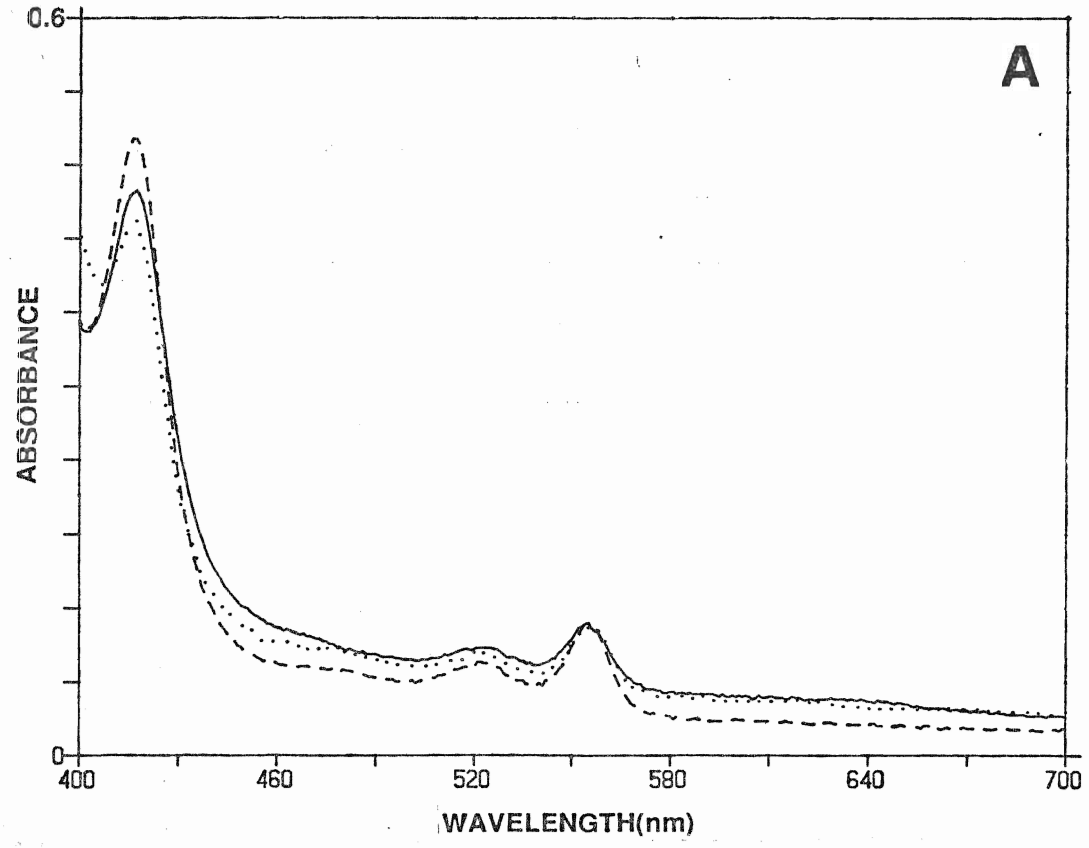
A
0.6
0
ABSORBANCE
400
460
520
580
640
700
WAVELENGTH(nm)

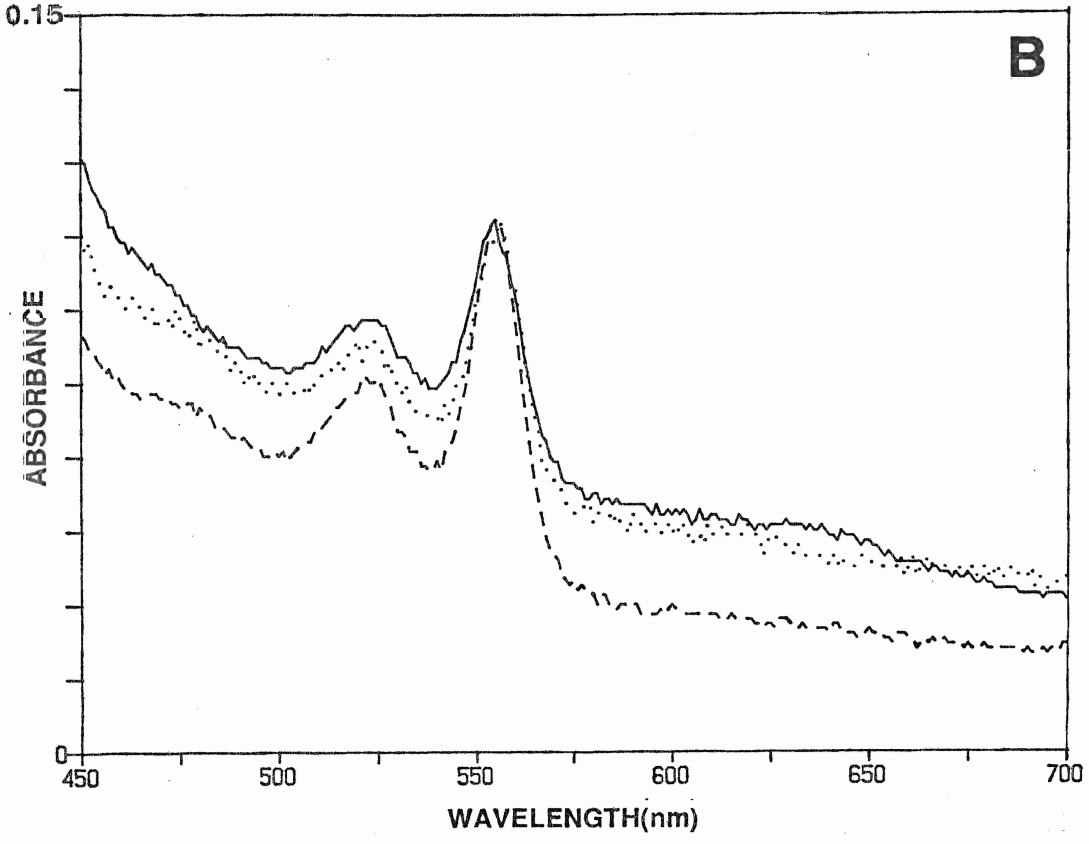
B
0.15
0
ABSORBANCE
450
500
550
600
650
700
WAVELENGTH(nm)

approximately 603nm with several additional bands at 557nm and 525nm as well as a broad band at 489nm. Previous observations of the pyridine hemochromes of the HPII protein (Barrett, 1956; Chiu *et al*, 1989) reported only that the oxidized acidic hemin gave a band at 603nm, and that the reduced alkaline pyridine hemochrome had a band at approximately 615nm. The results shown, assuming the shoulders seen in the spectra are not *bona fide* components of the heme d spectrum, suggest that a mixture of hemes may be present even in the population of wild type protein, comprising a heme *d* or analogue and a protoheme. The other spectra in Figure 16 imply that among the mutant proteins, mixtures of hemes in various proportions exist. The reduced pyridine hemochrome spectra for the H128A and H128N mutants apparently indicate that these proteins contain protoheme IX exclusively. The reduced pyridine hemochrome spectra for the N201H mutant shows a mixture primarily of protoheme with heme *d* in lesser proportion, and an extra band apparent having a maximum at 588nm. The reduced pyridine hemochrome spectrum for the N201Q mutant protein is strikingly similar to that of the wild type HPII hemochrome, with the same absorbance peak at 603nm, with shoulders at 557nm, and 525nm indicating incorporation of heme *d*, but probably protoheme as well.

Figure 16. Absorption spectra of reduced alkaline pyridine hemochromes for HPII wild type and mutant proteins.
Reduced alkaline pyridine hemochromes of HPII wild type (dotted line spectrum), H128A and H128N mutant proteins (broken line spectra **a** and **b**, respectively), N201Q, N201A, and N201H mutant proteins (solid line spectra **c**, **d**, and **e** respectively). Preparation of reduced pyridine hemochromes as described in Materials and Methods. Concentrations of the proteins were 4.3μM hematin for the HPII wild type protein, 4.6μM and 4.0 μM hematin for the H128A and H128N proteins, respectively, and 2.3μM, 2.5μM, and 3.2μM hematin for the N201Q, N201a, and the N201H proteins, respectively.

Figure 16

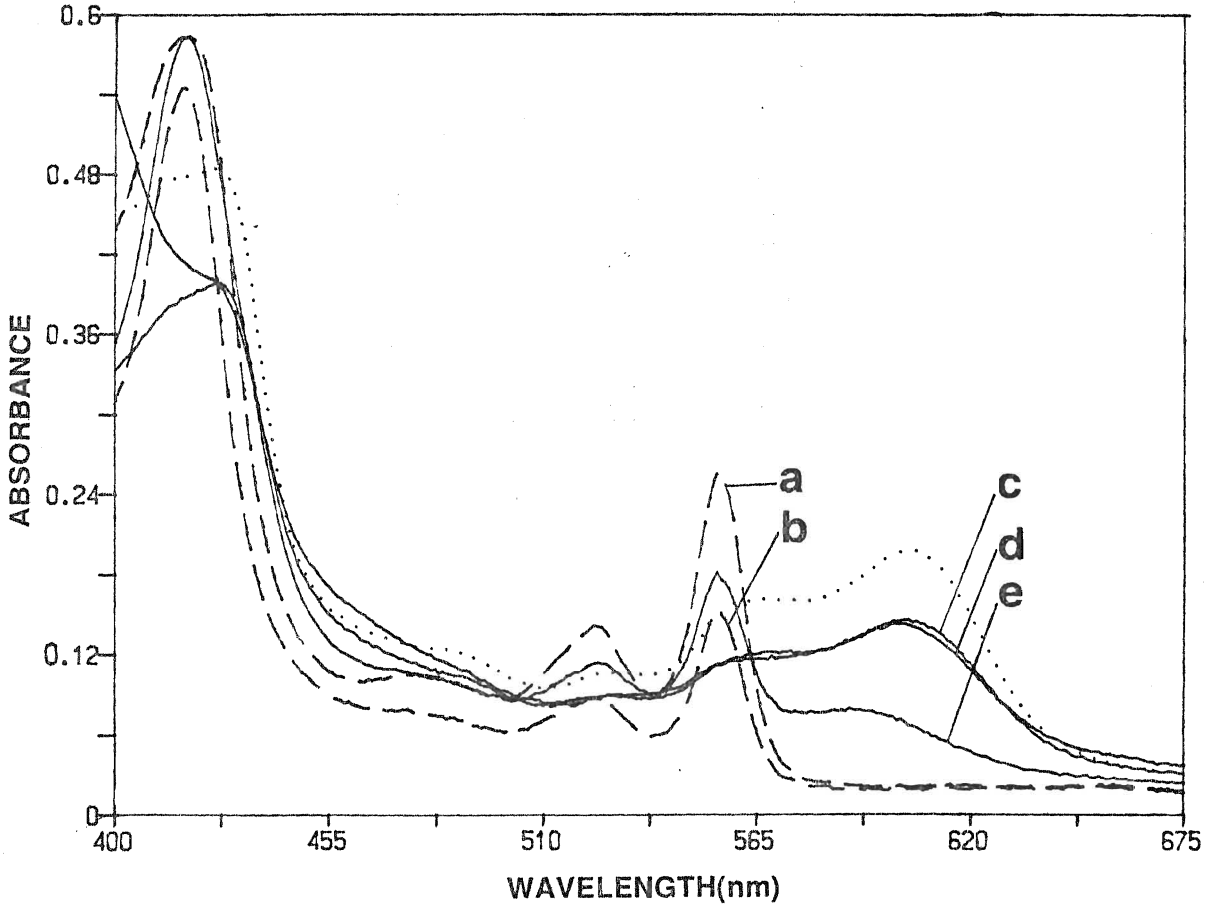
0.6
0.48
0.36
0.24
0.12
0
ABSORBANCE
400
455
510
565
620
675
WAVELENGTH(nm)
a
b
c
d
e

C. Effects of Heme ligands on Catalase Proteins

i. BLC, SCCT and SCCA cyanide and formate complexes

Figure 17A shows the effect on the absorbance spectrum of fully titrating the BLC protein with the heme ligand, cyanide. The spectral shifts produced by cyanide at pH 6.5 are typical of a change in spin state of the heme iron from the high spin pentacoordinate condition to the low spin hexacoordinate condition due to covalent ligation of the HCN group. A red shift of the Soret band is noted and the α band in the visible region is replaced by two blue-shifted bands.

Figure 17B shows the effect of formate on the absorbance spectrum of BLC. The slight red-shift and intensification of the Soret maximum as well as the slight blue shifting of the visible bands in the spectrum are indicative of a high spin ligand effect.

Difference spectra are shown in Figure 18 of the catalase-cyanide (Fig. 18A) and the catalase-formate (Fig. 18B) complexes of BLC. These difference spectra were obtained at increasing concentrations of the ligands, by subtracting the free catalase spectrum. The maximum and minimum at 428nm and at 400nm in the difference spectrum of cyanide-catalase, were used to generate titration data for secondary plots. The maximum at 405nm minus the minimum at 436nm were used to generate titration data for the binding of catalase by formate. Titration plots generated using these wavelength pairs are shown in Appendix B.

Similar absolute absorbance spectra of the SCCT-cyanide complex and representative difference spectra for the titration of SCCT with cyanide minus the spectrum of unliganded enzyme are shown in Figures

Figure 17. Effects of cyanide and formate on the spectrum of BLC.

BLC at 15μM hematin in 50mM potassium phosphate, pH 6.5., temperature 25 degrees (**A**) Original spectrum (solid line) versus spectrum of catalase-HCN (broken line) at a concentration of 2.6mM KCN. (**B**) Original spectrum (solid line) versus spectrum of catalase-HCOOH (broken line) at a concentration of 22.0mM HCOONa.

Figure 17

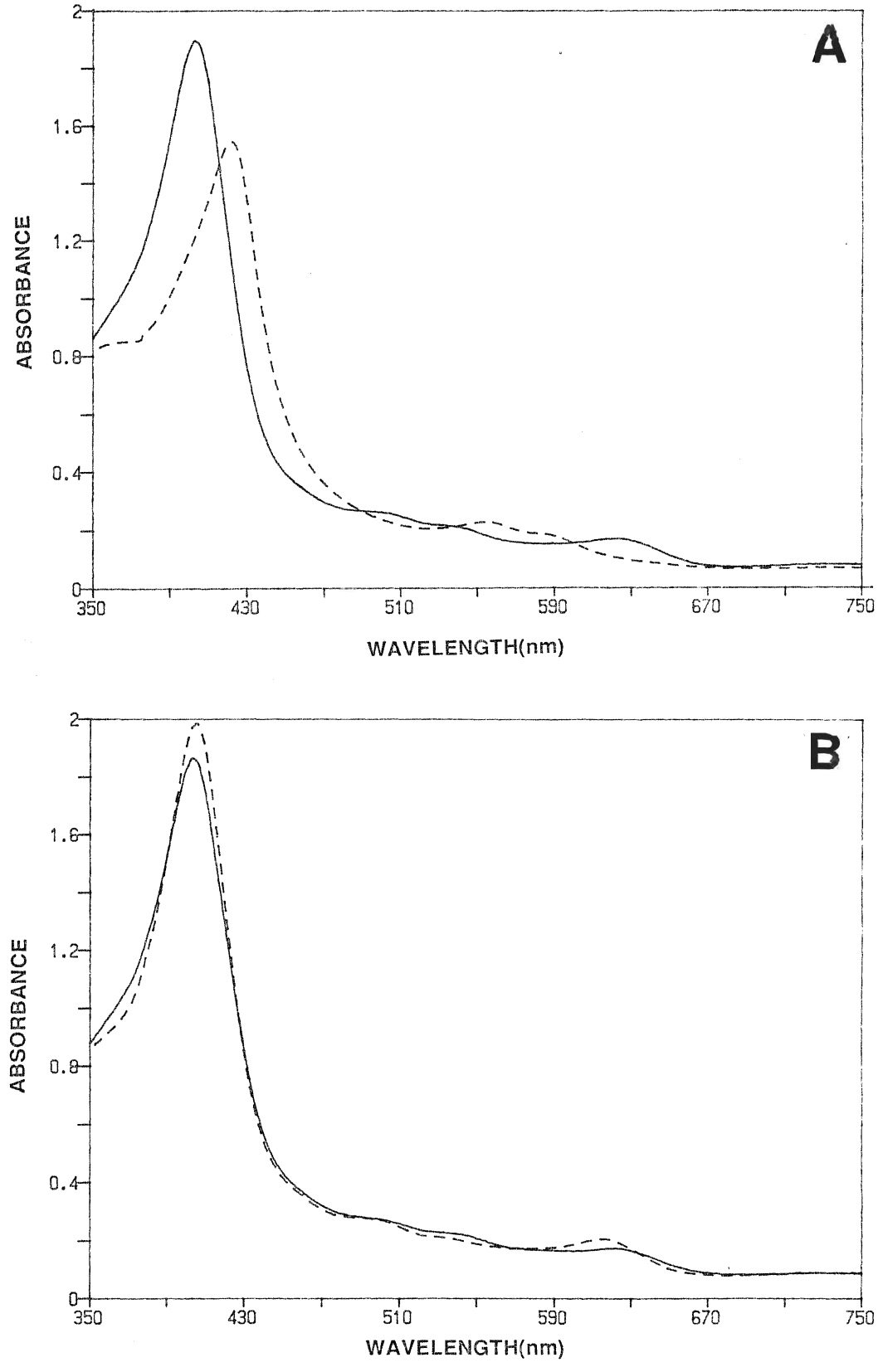
A
B
ABSORBANCE
WAVELENGTH(nm)
0
0.4
0.8
1.2
1.6
2
350
430
510
590
670
750

Figure 18. Representative difference spectra for titration of BLC with cyanide and formate.
Conditions as described in Fig. 16. (**A**) Difference spectra for BLC-HCN titration complexes at increasing concentrations of added ligand (**a**:3.2μM, **b**: 8.4μM, **c**: 16.3μM,**d**: 32μM,**e**: 151μM,**f**: 665μM,**g**: 2.64mM) minus the spectrum for the untitrated enzyme. (**B**) Difference spectra for BLC-HCOOH titration complexes at increasing concentrations of added ligand (**a**: 0.12mM, **b**: 1.5mM, **c**: 22mM) minus the spectrum for the untreated enzyme. Conditions as specified for titrations in Materials and Methods.

Figure 18

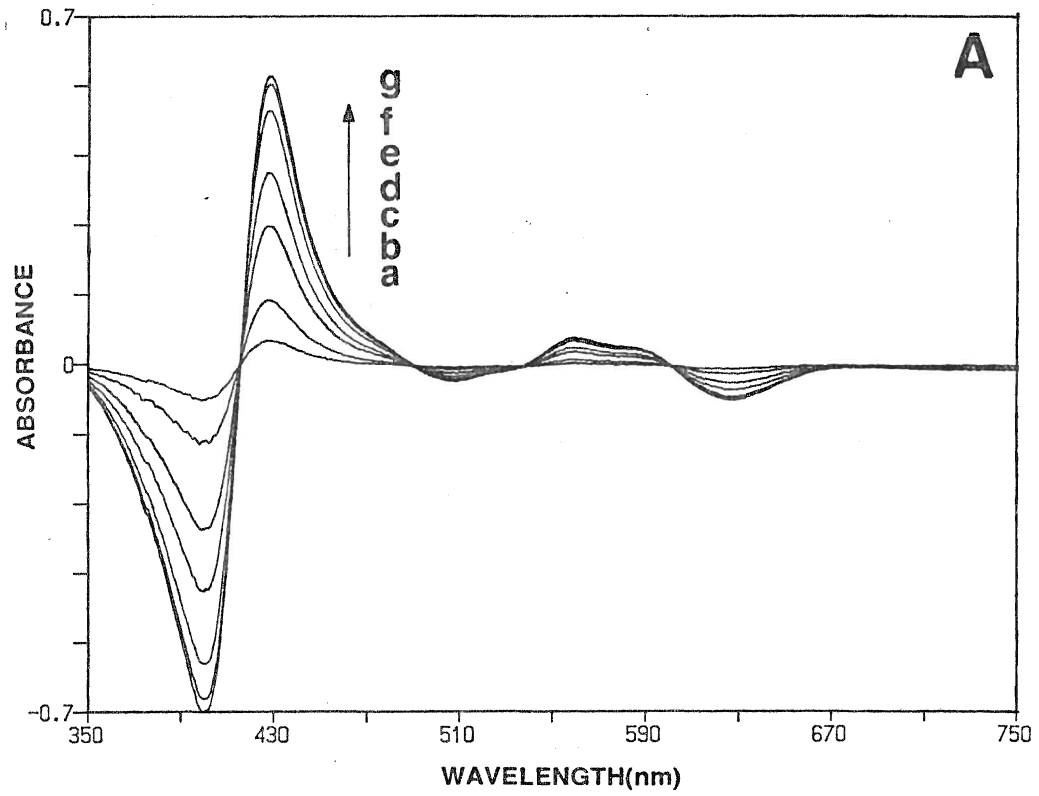
A
0.7
0
-0.7
ABSORBANCE
g
f
e
d
c
b
a
350
430
510
590
670
750
WAVELENGTH(nm)

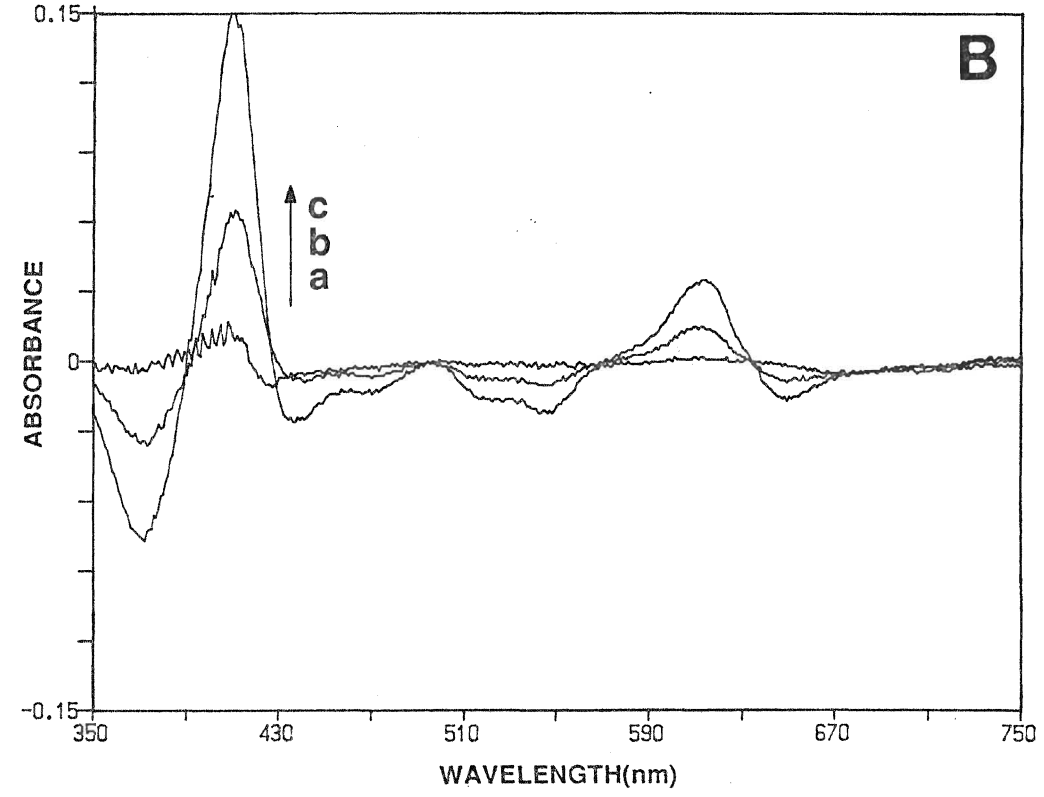
B
0.15
0
-0.15
ABSORBANCE
c
b
a
350
430
510
590
670
750
WAVELENGTH(nm)

Figure 19. Absolute/Difference spectra for titration of SCCT with cyanide.
(**A**) Absolute spectrum of the untitrated catalase (3μM hematin) (solid line) versus spectrum of SCCT-HCN complex at a concentration of 11.5mM (broken line) (**B**) Difference spectra for SCCT-HCN titration complexes at increasing concentrations of added ligand (**a**: 6.7μM, **b**: 16.6μM, **c**: 83.3μM, **d**: 177μM, **e**: 564μM, **f**: 2.1mM, **g**: 11.5mM) minus the untitrated enzyme. Conditions as specified for titrations in Materials and Methods.

Figure 19

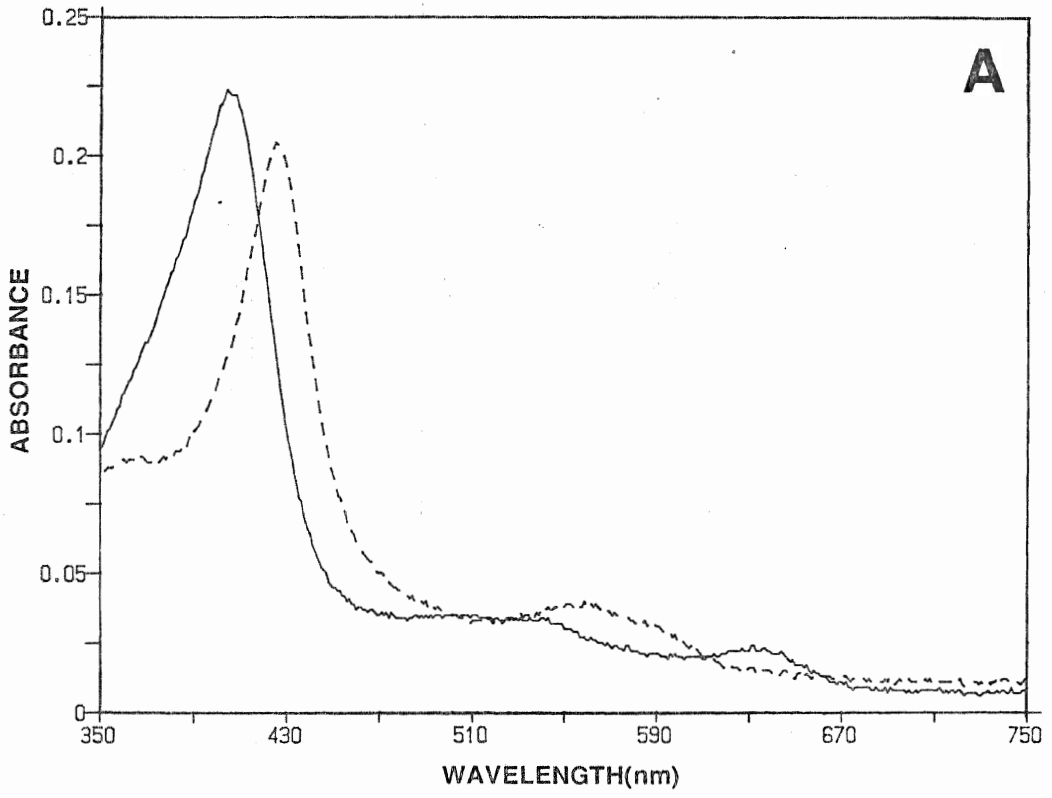
A
0.25
0.2
0.15
0.1
0.05
0
ABSORBANCE
350
430
510
590
670
750
WAVELENGTH(nm)

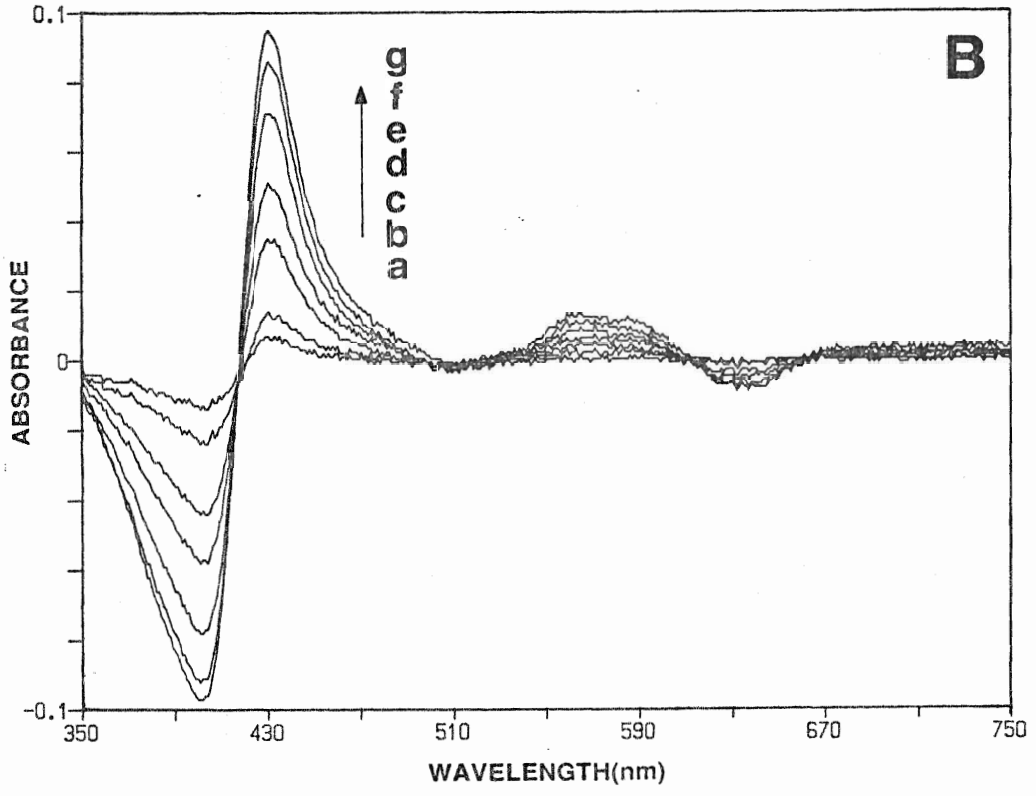
B
g
f
e
d
c
b
a
0.1
0
-0.1
ABSORBANCE
350
430
510
590
670
750
WAVELENGTH(nm)

19A and 19B, respectively. Absolute absorbance spectra of the SCCA-cyanide complex and representative difference spectra in the Soret region for the titration of SCCA with cyanide minus the spectrum of unliganded enzyme are shown in Figures 20A and 20B, respectively. The titration plots generated using appropriate wavelength pairs are shown in Appendix B. The formate complexes for these proteins, shown in Figs. 21A (SCCT) and 21B (SCCA), were typically not as distinct as those for the BLC enzyme. These catalases were, therefore, not titrated with formate.

Replotting the data obtained for the titration of BLC with cyanide yields a double reciprocal plot as indicated in Figure 22A. Rearrangement of this data in logarithmic fashion yields a typical Hill plot as in Figure 22B. The estimated cyanide dissociation constant from the Hill plot slope intercept for log(a/1-a) =0 is 12 μM. The double reciprocal plot and the Hill plot for the titration of BLC with formate are shown in figures 23A and 23B. From Figure 23B the apparent K_d of formate for the BLC at pH 6.5 was estimated to be between 3-5 mM. Comparable manipulation of data for the titrations of SCCT and SCCA proteins, as shown in Figs. 24 and 25, respectively, yielded the estimated dissociation constants of 110μM and 11μM.Cyanide affinity is greater for the SCCA by about one order of magnitude as compared to the SCCT. From initial studies of formate binding, it would seem that though both purified isolates display low affinities, that of SCCT is slightly greater.

ii. Cyanide and formate complexes of HPII wild type and mutant proteins

Figures 26A and 26B show the spectra of the cyanide and formate complexes, respectively of the HPII wild type protein. Here, as wasseen

Figure 20. Absolute/Difference spectra for titration of SCCA with cyanide.
(**A**) Absolute spectrum of the untitrated catalase (1μM hematin) (solid line) versus spectrum of SCCA-HCN complex at a concentration of 4.1mM (broken line) (**B**) Difference spectra in the Soret for SCCA-HCN titration complexes at increasing concentrations of added ligand (**a**: 11.3μM, **b**: 35.8μM, **c**: 133μM, **d**: 255μM, **e**: 499μM, **f**: 4.1mM) minus the untitrated enzyme. Conditions as specified for titrations in Materials and Methods.

Figure 20

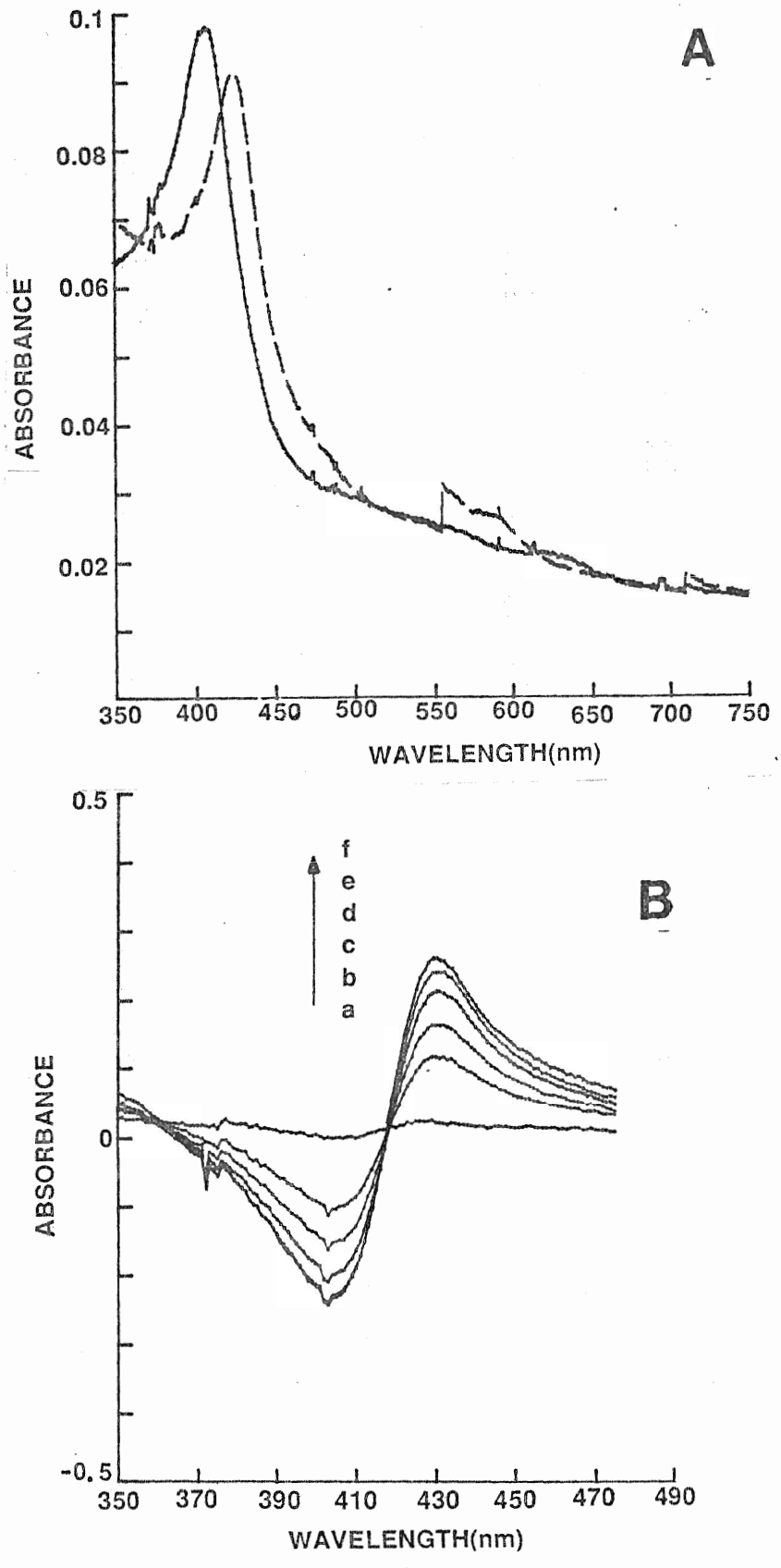
A
0.1
0.08
0.06
0.04
0.02
ABSORBANCE
350
400
450
500
550
600
650
700
750
WAVELENGTH(nm)
B
0.5
0
-0.5
f
e
d
c
b
a
ABSORBANCE
350
370
390
410
430
450
470
490
WAVELENGTH(nm)

Figure 21. Formate complexes of SCCT and SCCA proteins. (**A**) Absolute spectrum of SCCT-HCOOH complex formed by addition of 333mM HCOONa (broken line) versus the spectrum of untreated protein (solid line) at a concentration of 3μM hematin. All samples in 50mM potassium phosphate, pH 6.5, 25 degrees. (**B**) Absolute spectrum of SCCA-HCOOH complex formed by addition of 343mM HCOONa (broken line) versus spectrum of untreated protein (solid line) at a concentration of 5μM hematin.

Figure 21

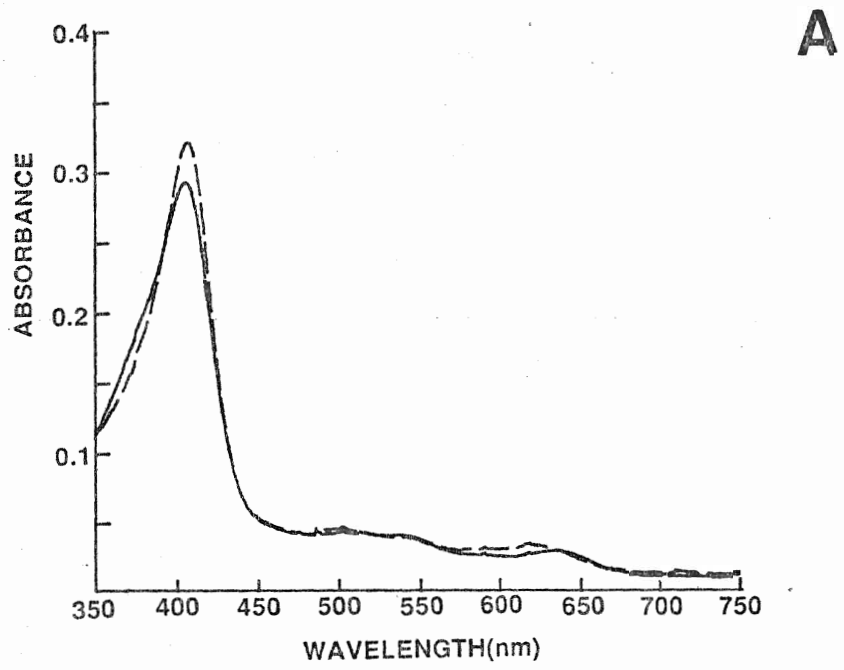
A
0.4
0.3
0.2
0.1
ABSORBANCE
350
400
450
500
550
600
650
700
750
WAVELENGTH(nm)

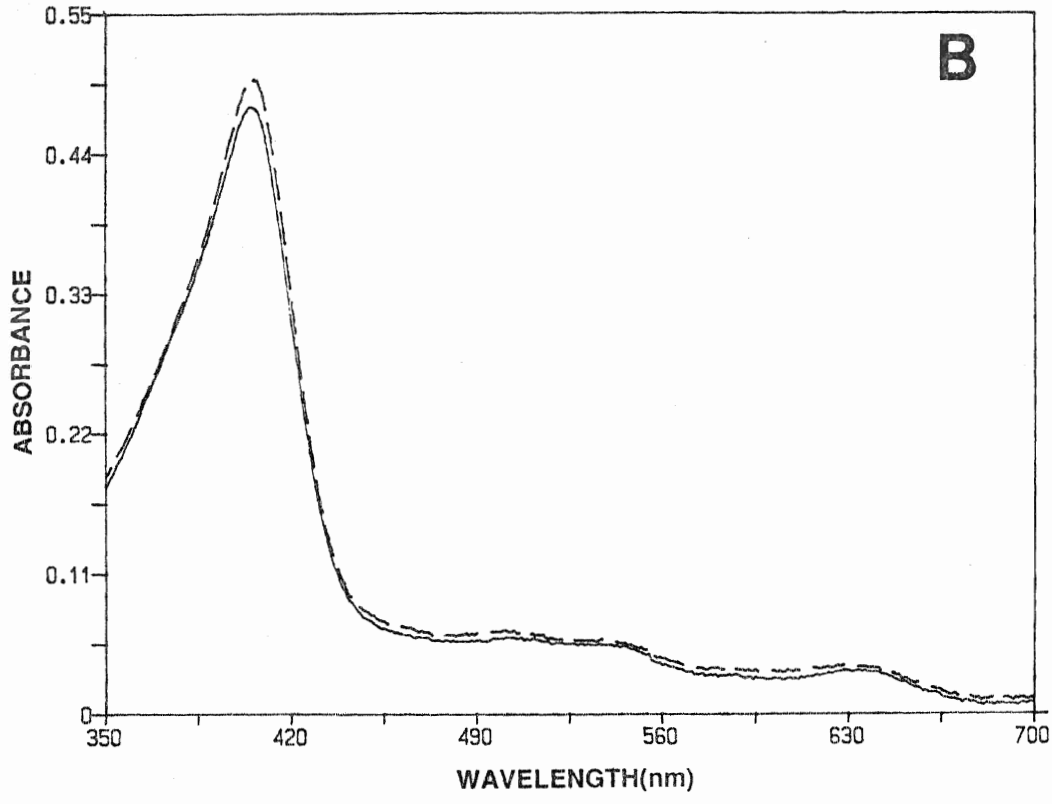
B
0.55
0.44
0.33
0.22
0.11
0
ABSORBANCE
350
420
490
560
630
700
WAVELENGTH(nm)

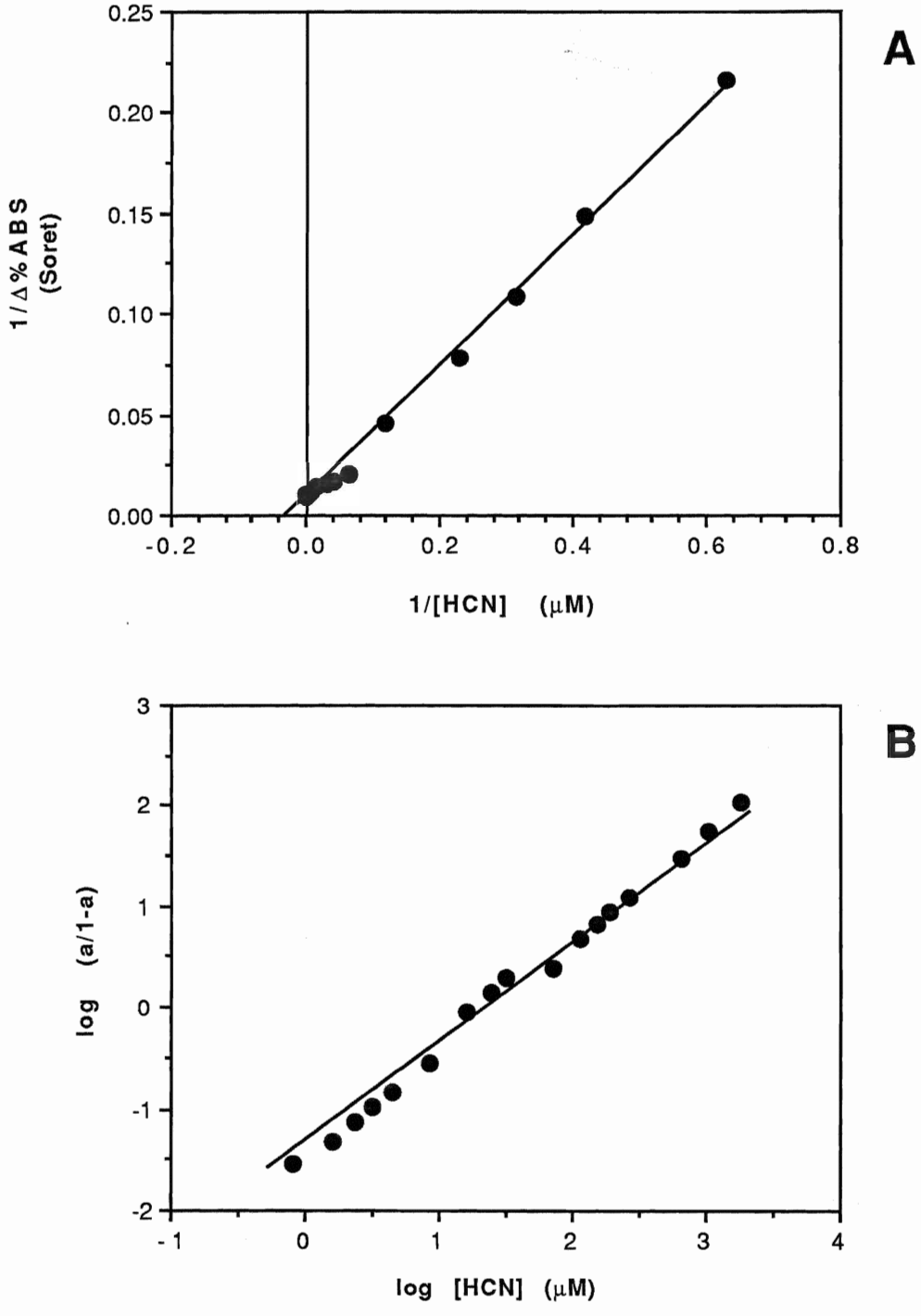

Figure 22. Titration of BLC with cyanide: secondary plots. (**A**) Double reciprocal plot of Soret wavelength derived data versus concentration of HCN. (**B**) Hill Plot of Soret wavelength derived data versus concentration of HCN. Hill slope shown.

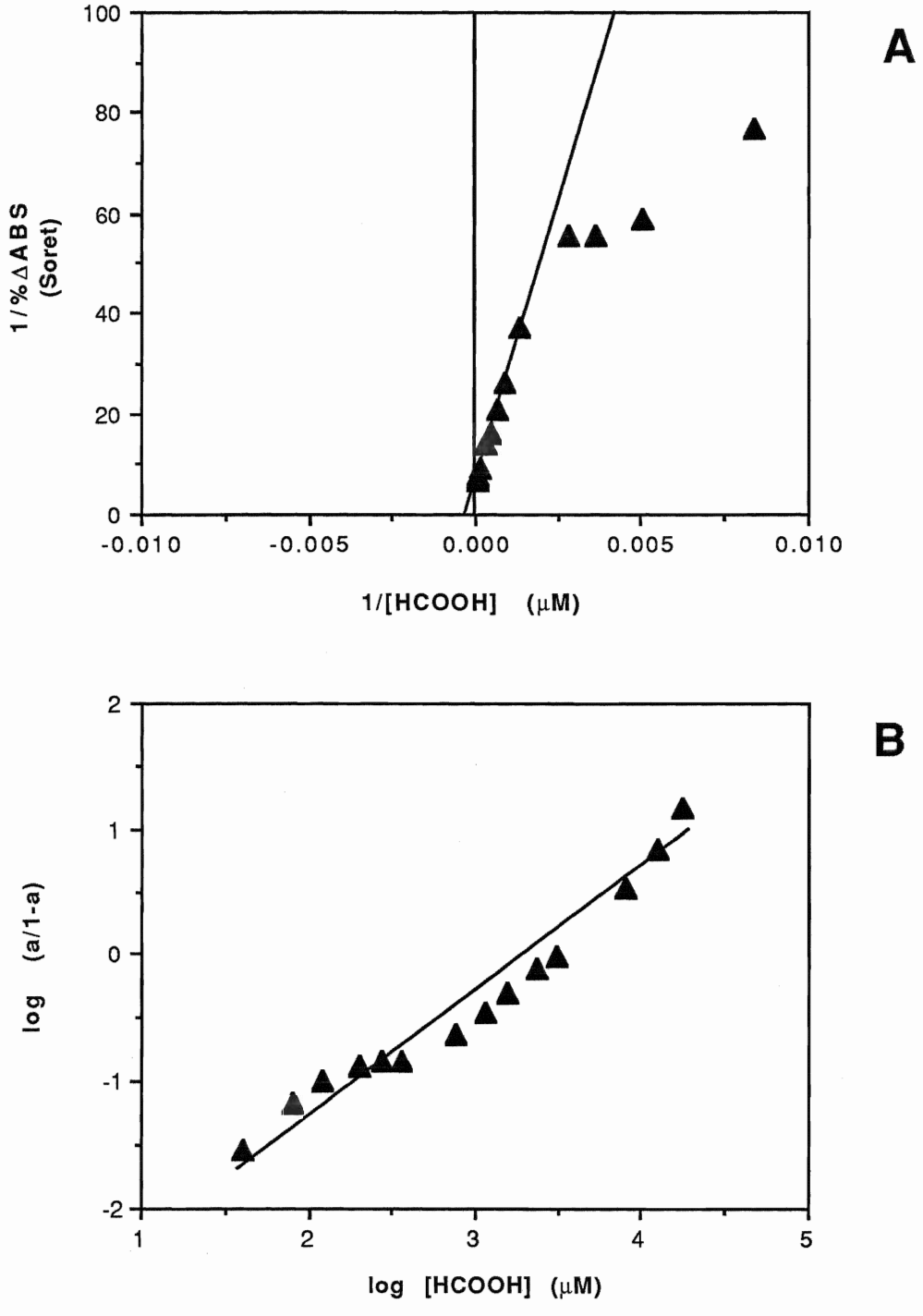

Figure 23. Titration of BLC with formate: secondary plots. **A**) Double reciprocal plot of Soret wavelength derived data versus concentration of HCOOH (**B**) Hill Plot of Soret wavelength derived data versus concentration of HCOOH. Hill slope shown.

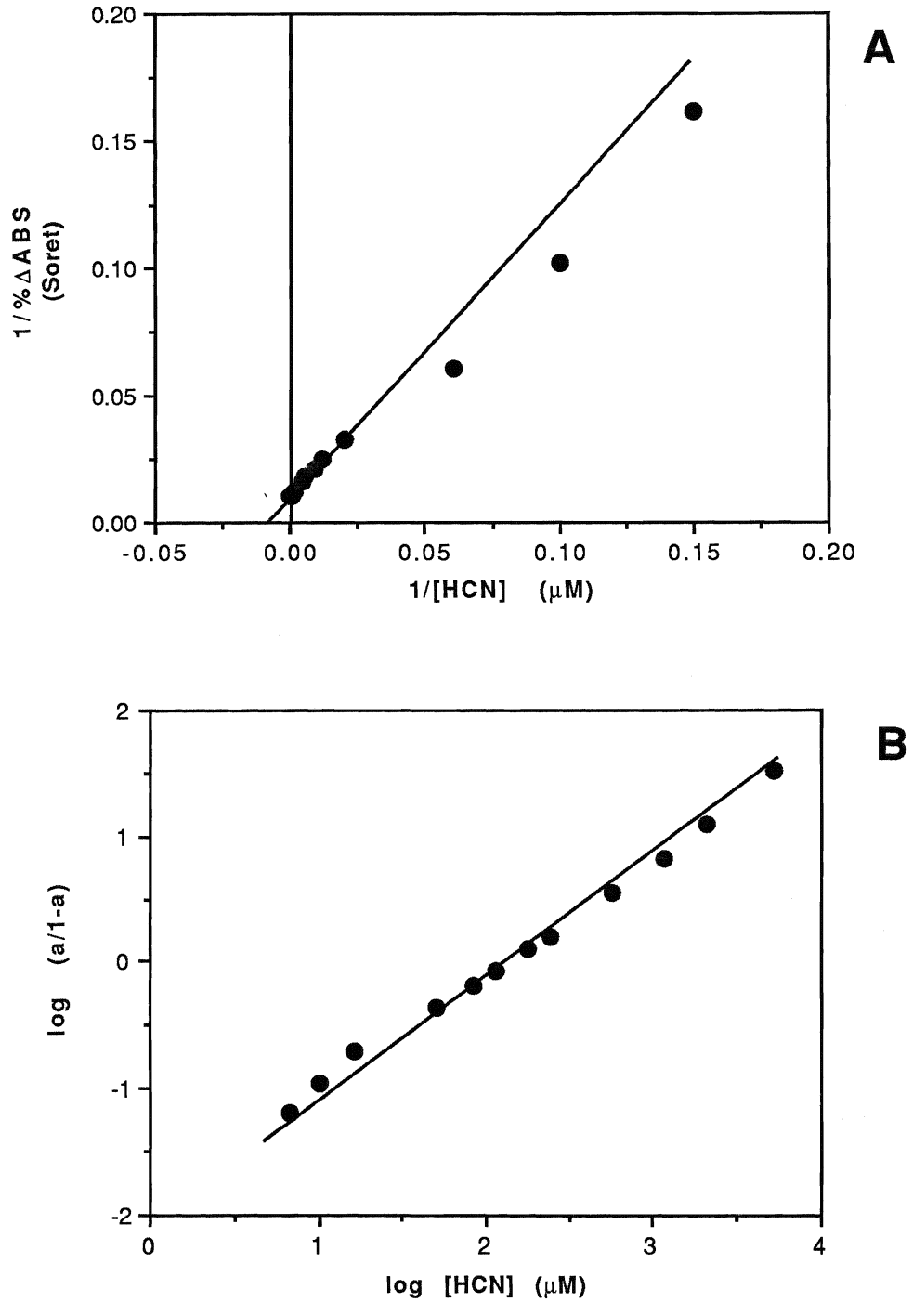

Figure 24. Titration of SCCT with cyanide: secondary plots. (**A**) Double reciprocal plot of Soret wavelength derived data versus concentration of HCN. (**B**) Hill Plot of Soret wavelength derived data versus concentration of HCN. Hill slope shown.

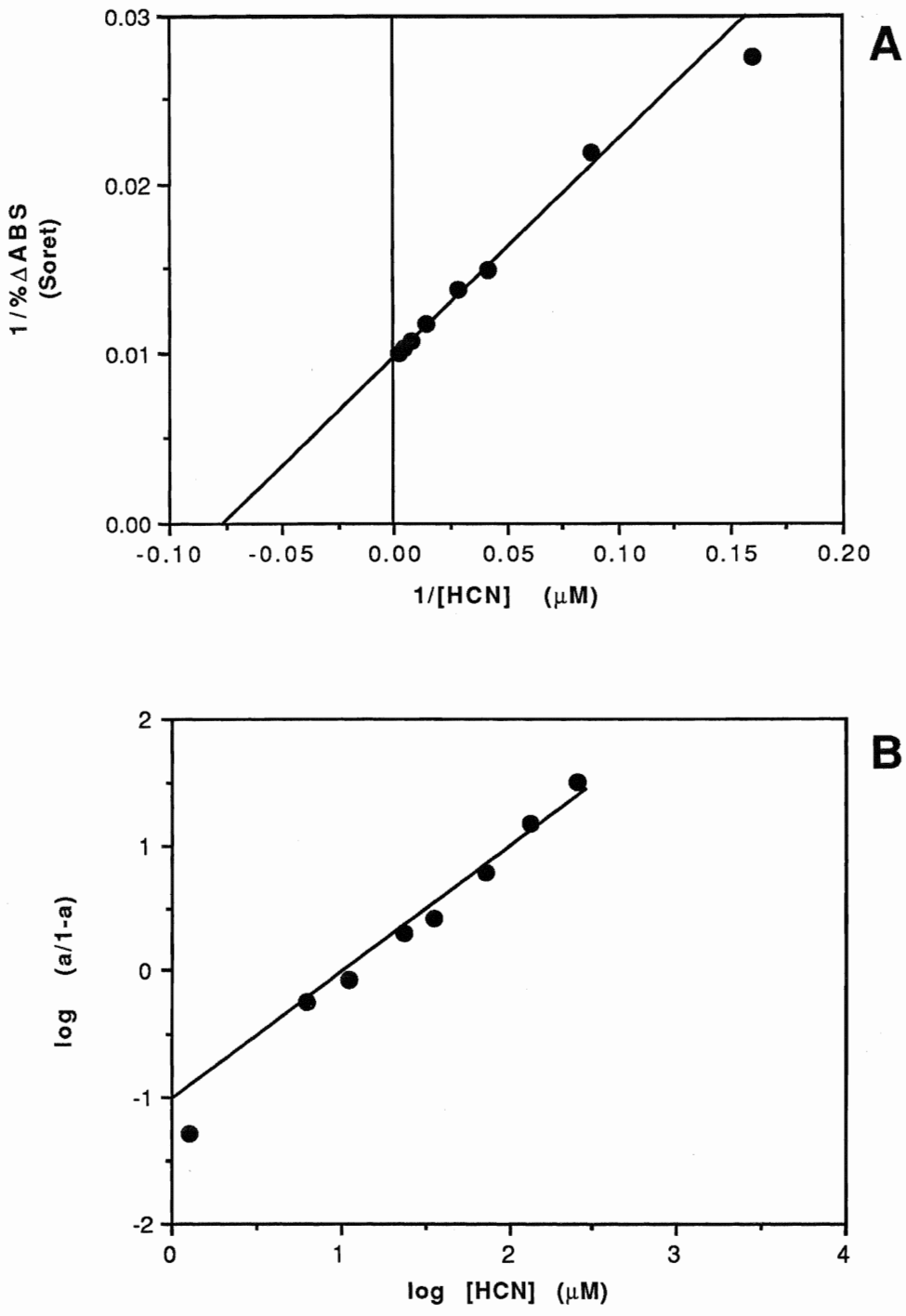

Figure 25. Titration of SCCA with cyanide: secondary plots. (**A**) Double reciprocal plot of Soret wavelength derived data versus concentration of HCN. (**B**) Hill Plot of Soret wavelength derived data versus concentration of HCN. Hill slope shown.

Figure 26. Effects of cyanide and formate on the spectrum of HPII wild type protein.
Approximately 5μM HPII wild type protein in 50mM potassium phosphate, pH 6.5, 25 degrees. (**A**) Original spectrum (solid line) versus HPII wild type-HCN complex (broken line) at a concentration of 7.8mM added ligand. (**B**) Original spectrum (solid line) versus HPII wild type-HCOOH complex (broken line) at a concentration of 2.1M added ligand.

Figure 26

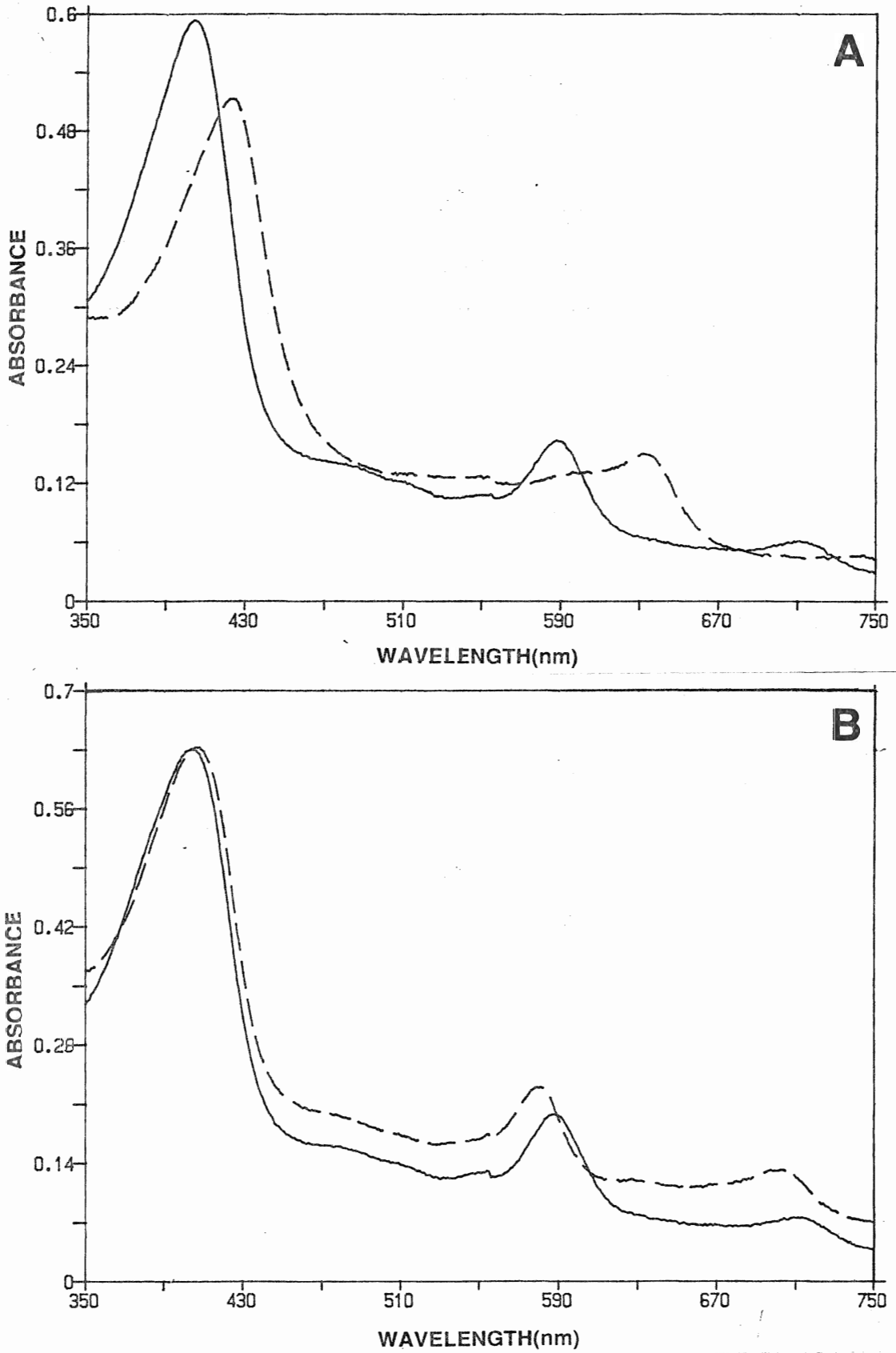
A
0.6
0.48
0.36
0.24
0.12
0
ABSORBANCE
350
430
510
590
670
750
WAVELENGTH(nm)
B
0.7
0.56
0.42
0.28
0.14
0
ABSORBANCE
350
430
510
590
670
750
WAVELENGTH(nm)

Figure 27. Representative difference spectra for titration of HPII-wild type protein with cyanide and formate.
(**A**) Difference spectra for HPII-CN titration complexes at increasing concentrations of added ligand (**a**: 6.6μM, **b**: 9.9μM, **c**: 16.4μM, **d**: 49μM, **e**: 271μM, **f**: 7.84mM) minus the untreated enzyme. at 10μM hematin (**B**) Difference spectra for HPII- HCOOH titration complexes at increasing concentrations of added ligand (**a**:2.46mM, **b**: 20.3mM, **c**: 57.3mM, **d**:241mM) minus the untreated enzyme. at 5μM hematin. Conditions as specified for titrations in Materials and Methods.

Figure 27

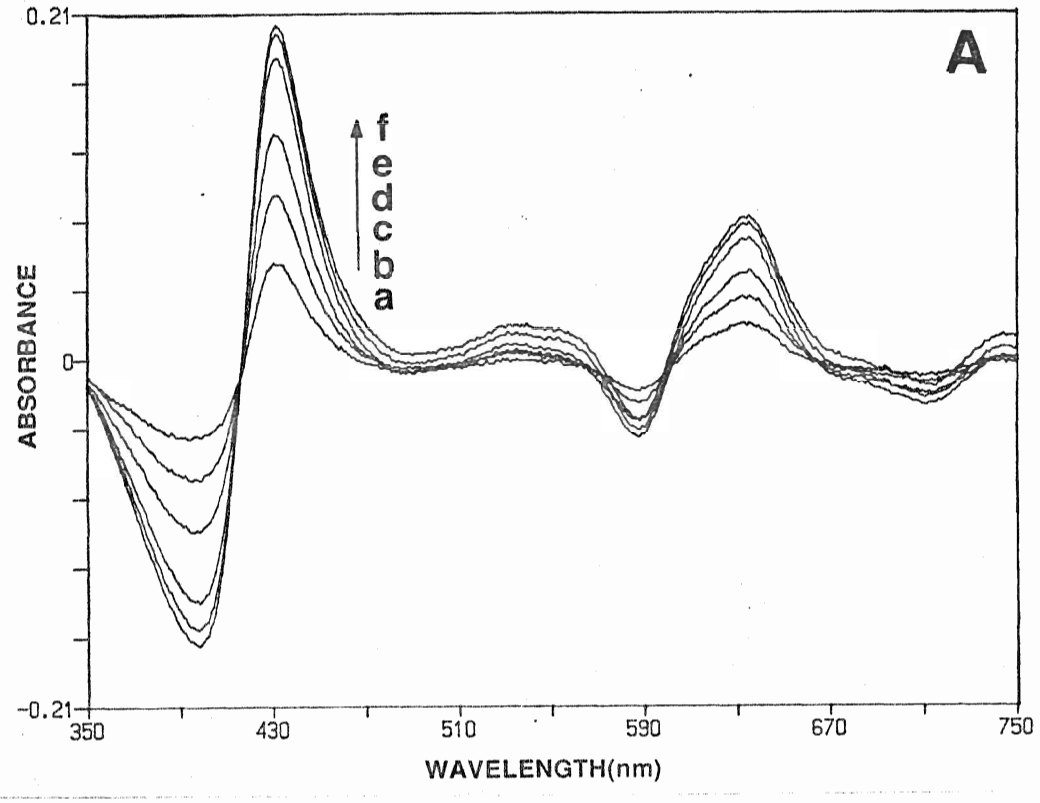
0.21
0
-0.21
ABSORBANCE
A
f
e
d
c
b
a
350
430
510
590
670
750
WAVELENGTH(nm)

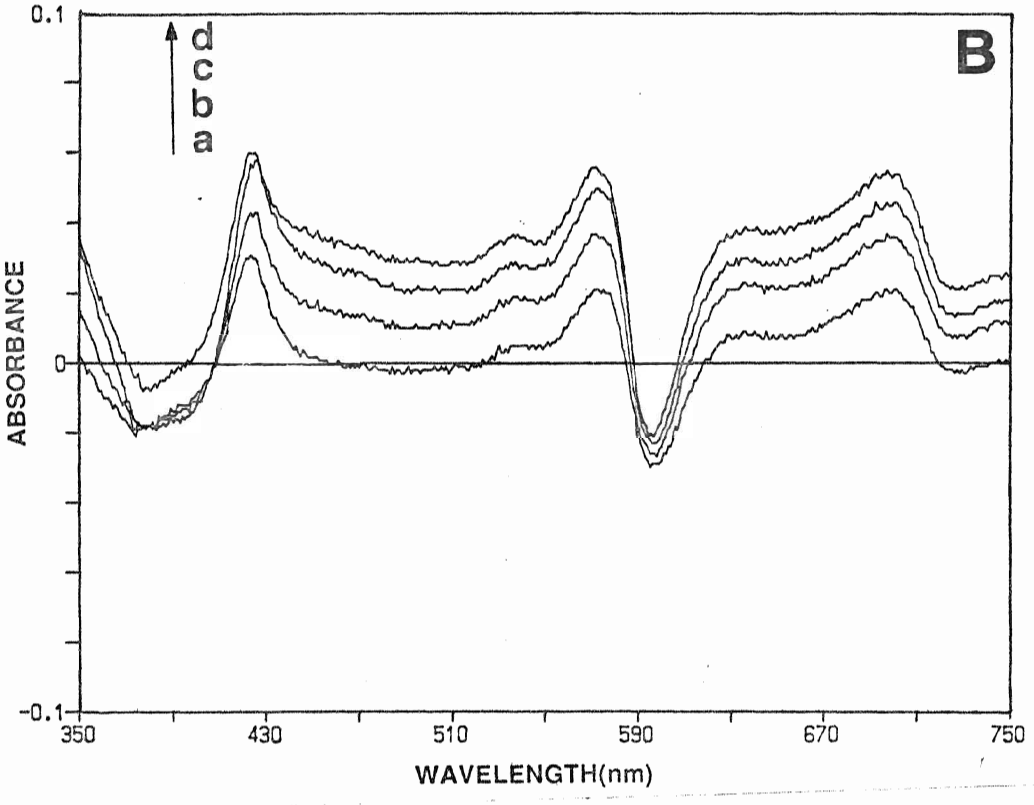
0.1
0
-0.1
ABSORBANCE
B
d
c
b
a
350
430
510
590
670
750
WAVELENGTH(nm)

in the spectra of the complexes of cyanide and formate with BLC, the typical shifts of the Soret maxima and the formation of the new blue shifted visible bands are apparent. Representative difference spectra for both heme ligand complexes at increasing ligand concentrations minus free enzyme, are shown in figure 27A, for cyanide; and Fig. 27B, for formate. Titration plots for the wavelength pairs used are shown in Appendix B.

Figure 28A shows a double reciprocal plot of the secondary data generated from a titration of HPII wild type protein with cyanide at pH 6.5, and Fig. 28B the corresponding Hill plot. Figures 29A and 29B show the double reciprocal plot and the Hill plot for titration of HPII wild type protein with formate at pH 6.5. Dissociation constants estimated from these secondary data are summarized in TABLE II.

Binding of cyanide and formate to the HPII site-directed mutant proteins is notably different from the cases already presented. Figures 30A-C show the cyanide complexes of the N201 mutant proteins.In all the mutant proteins, cyanide binding is significantly weaker than for the wild type HPII protein. The binding of formate is weaker still, with the formate complexes of some of the N201 mutant proteins shown in Figure 31A-B. Full titrations were not possible with the N201 mutant proteins due to these small spectral shifts, and spectral shifts were not observed with formate for the H128 mutant proteins nor for the N201H mutant.

Titration of the N201 mutant proteins of HPII with cyanide at near neutral pH (pH 6.5) resulted in spectral shifts similar to those seen for the HPII wild type catalase. Representative difference spectra for the titration of the N201Q mutant with cyanide are shown in Figure 32. The spectral shifts are not monophasic during the course of

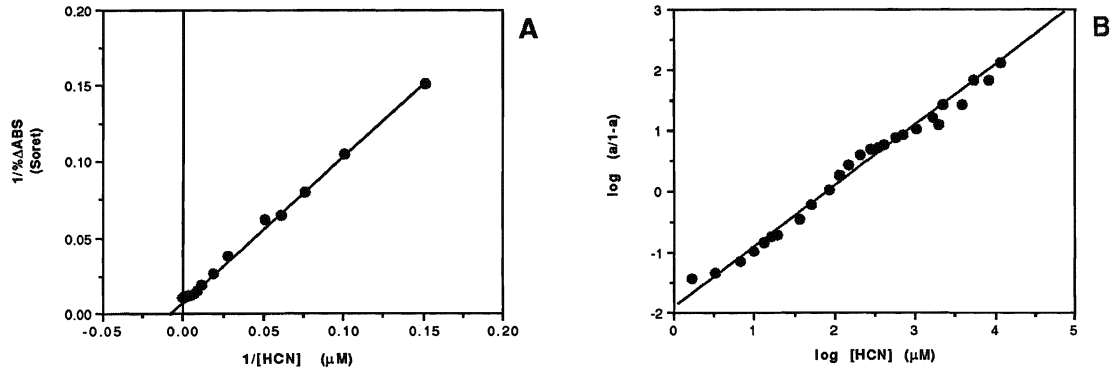

Figure 28. Titration of HPII wild type with cyanide: secondary plots.
(**A**) Double reciprocal plot of Soret wavelength derived data versus concentration of HCN. (**B**) Hill plot of Soret wavelength derived data versus concentration of HCN. Hill slope shown.

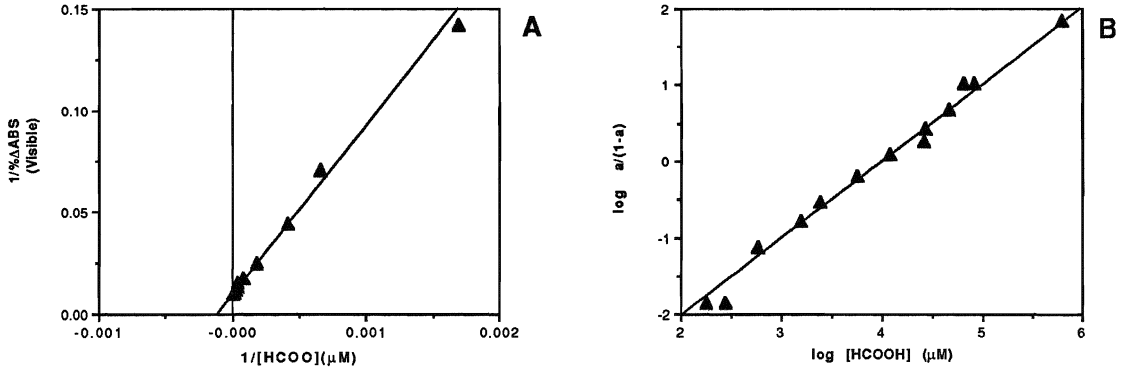

Figure 29. Titration of HPII wild type protein with formate: secondary plots.
(**A**) Double reciprocal plot of Soret wavelength derived data versus concentration of HCOONa (**B**) Hill plot of Soret wavelength derived data versus concentration of HCOONa. Hill slope shown.

Figure 30. Cyanide complexes of HPII N201 mutant proteins. (**A**) 5μM hematin N201H in 50mM potassium phosphate, pH 6.5, 25 degrees. Spectrum of untreated protein (solid line) versus spectrum of protein to which was added KCN to 14.1mM (broken line). (**B**) 3.9μM hematin N201A. Conditions as in A. Spectrum of untreated protein (solid line) versus spectrum of protein to which was added KCN to 39mM (broken line). (**C**) 3.8μM hematin N201Q. Conditions as in A. Spectrum of untreated protein (solid line) versus spectrum of protein to which was added KCN to 52mM (broken line).

Figure 30

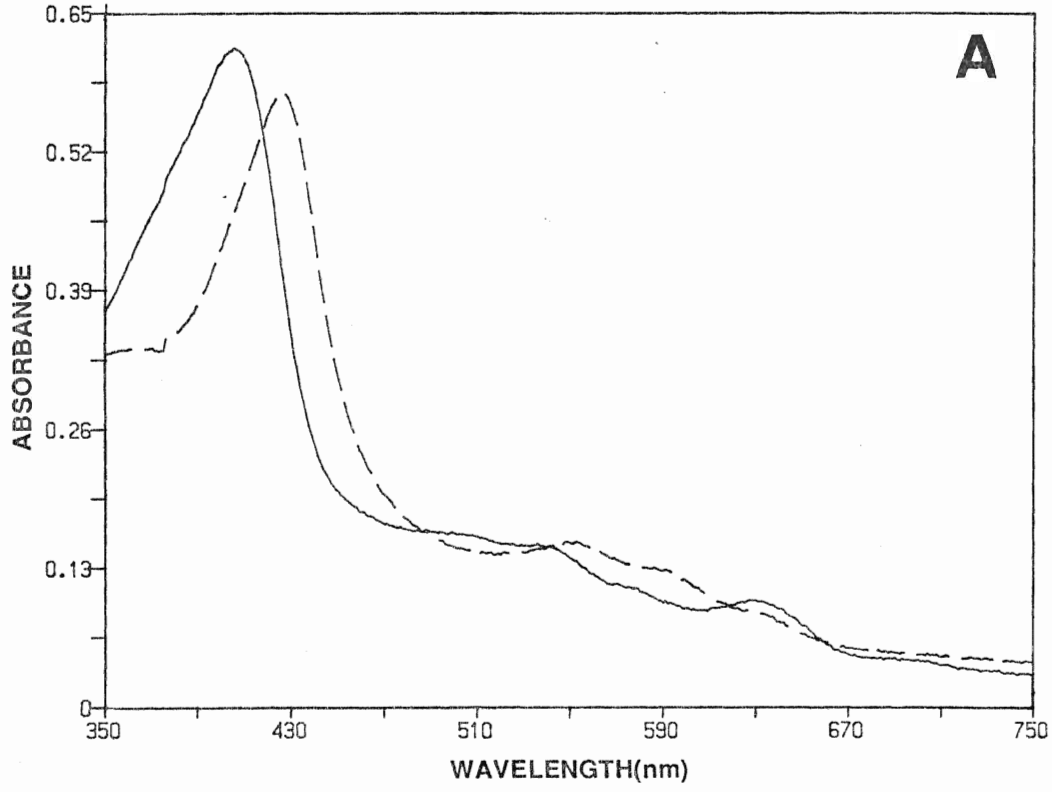
A
0.65
0.52
0.39
0.26
0.13
0
ABSORBANCE
350
430
510
590
670
750
WAVELENGTH(nm)

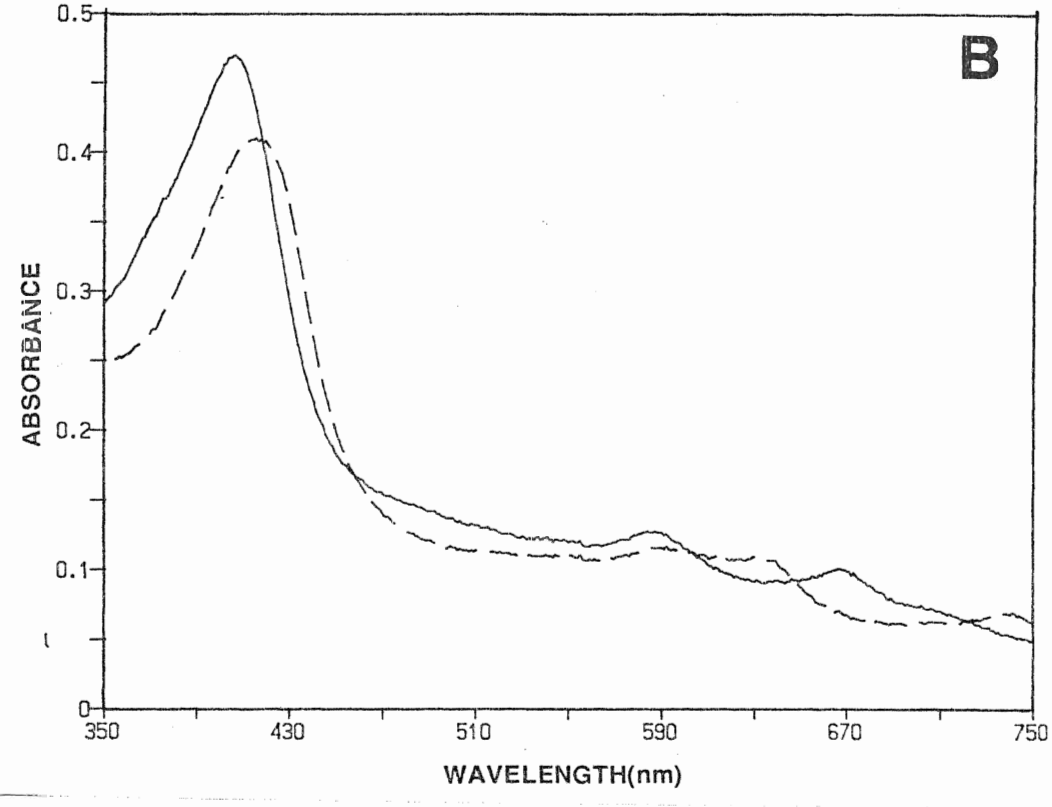
B
0.5
0.4
0.3
0.2
0.1
0
ABSORBANCE
350
430
510
590
670
750
WAVELENGTH(nm)

Figure 30

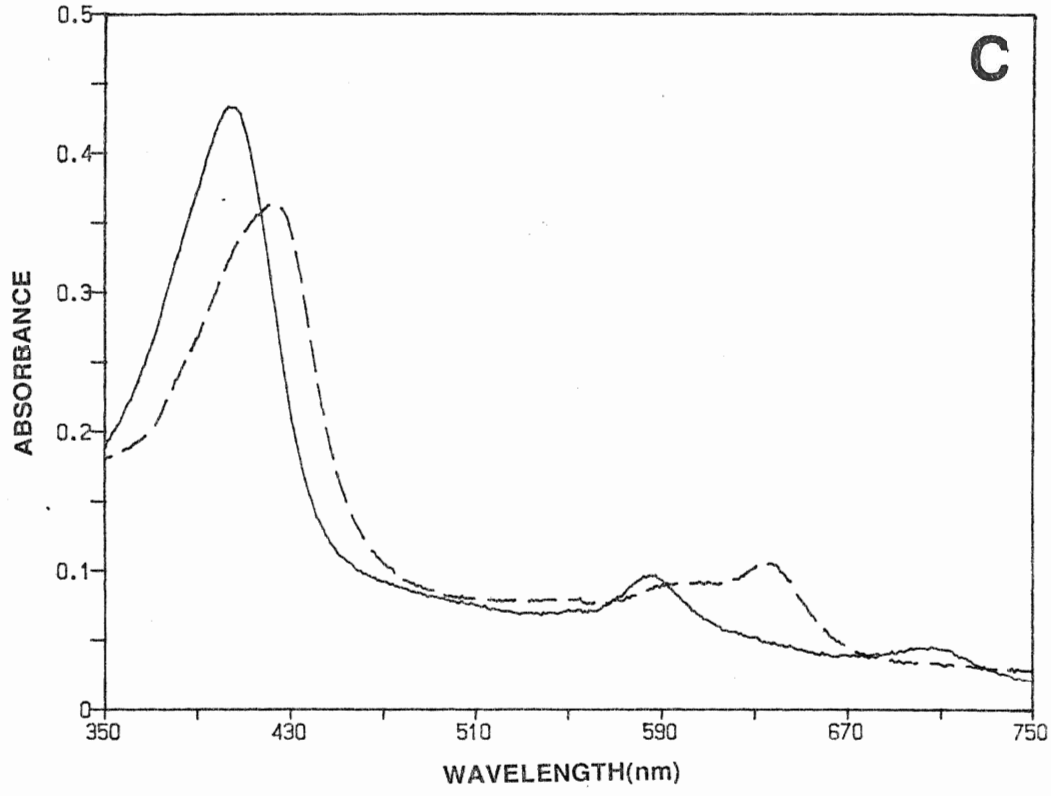
C
ABSORBANCE
0.5
0.4
0.3
0.2
0.1
0
350
430
510
590
670
750
WAVELENGTH(nm)

Figure 31. Formate complexes of HPII N201 mutant proteins. (A)3μM hematin N201Q in 50mM potassium phosphate, pH 6.5, 25 degrees. Spectrum of untreated protein (solid line) versus spectrum of protein to which was added 120mM HCOONa (broken line). (B)5μM hematin N201A. Conditions as in A. Spectrum of untreated protein (solid line) versus spectrum of protein to which was added 160mM HCOONa

Figure 31

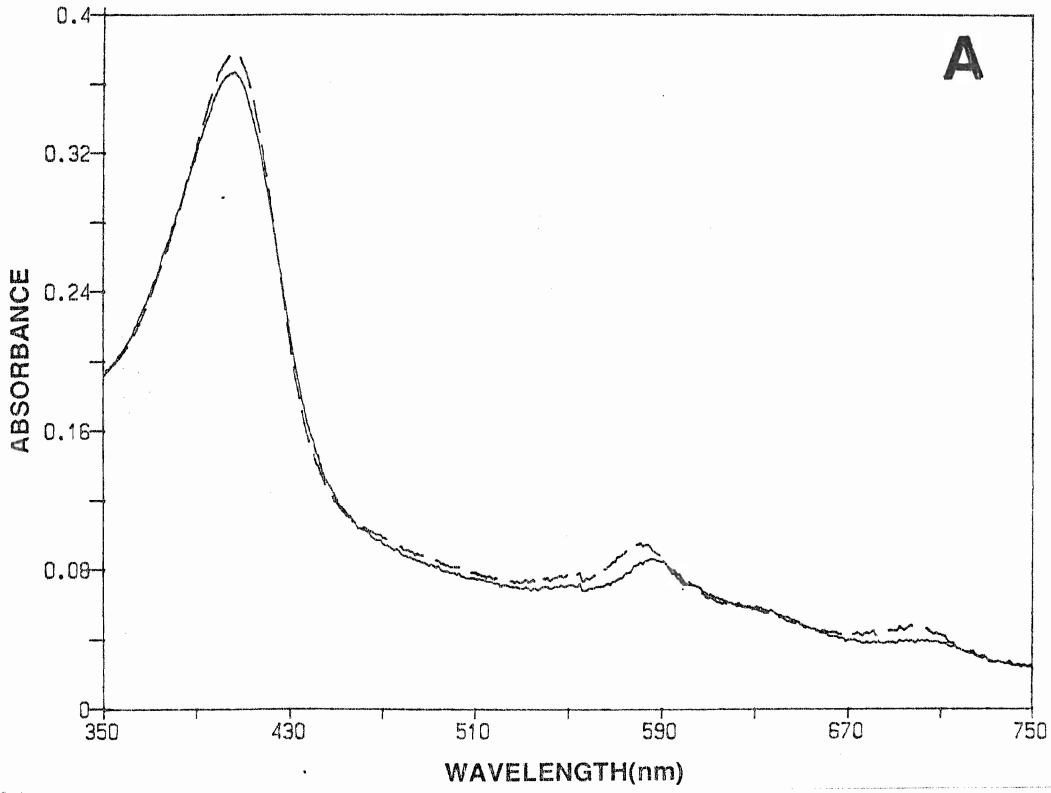
A
0.4
0.32
0.24
0.16
0.08
0
ABSORBANCE
350
430
510
590
670
750
WAVELENGTH(nm)

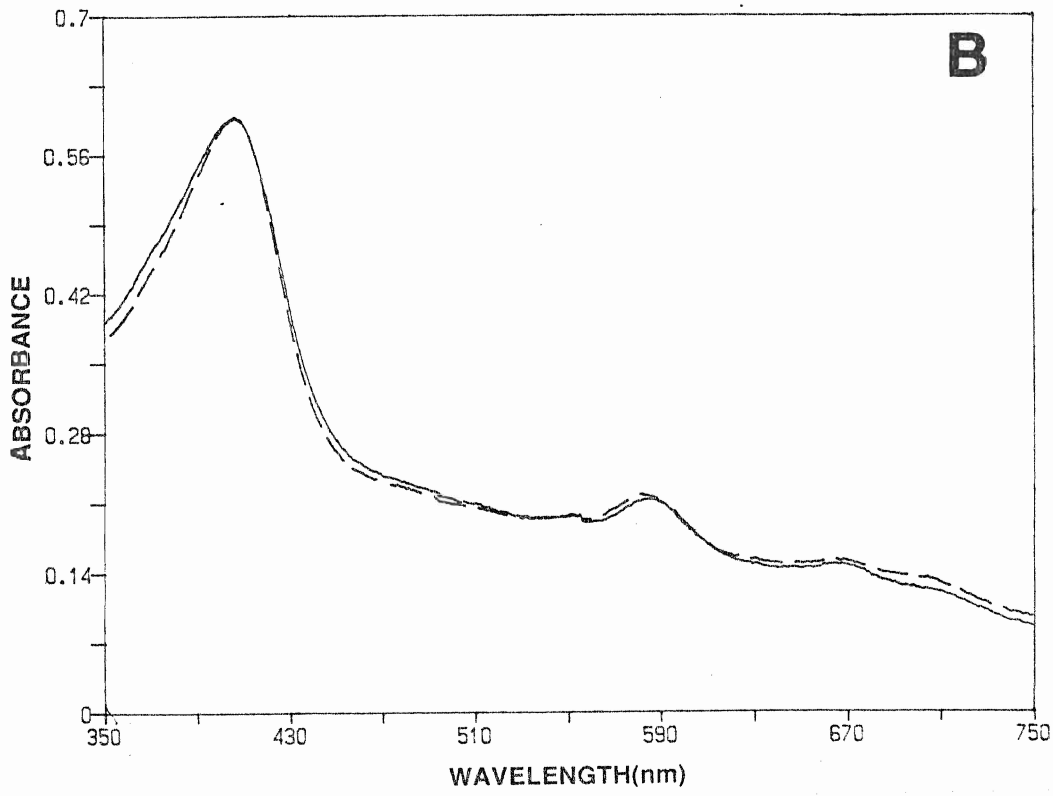
B
0.7
0.56
0.42
0.28
0.14
0
ABSORBANCE
350
430
510
590
670
750
WAVELENGTH(nm)

Figure 32

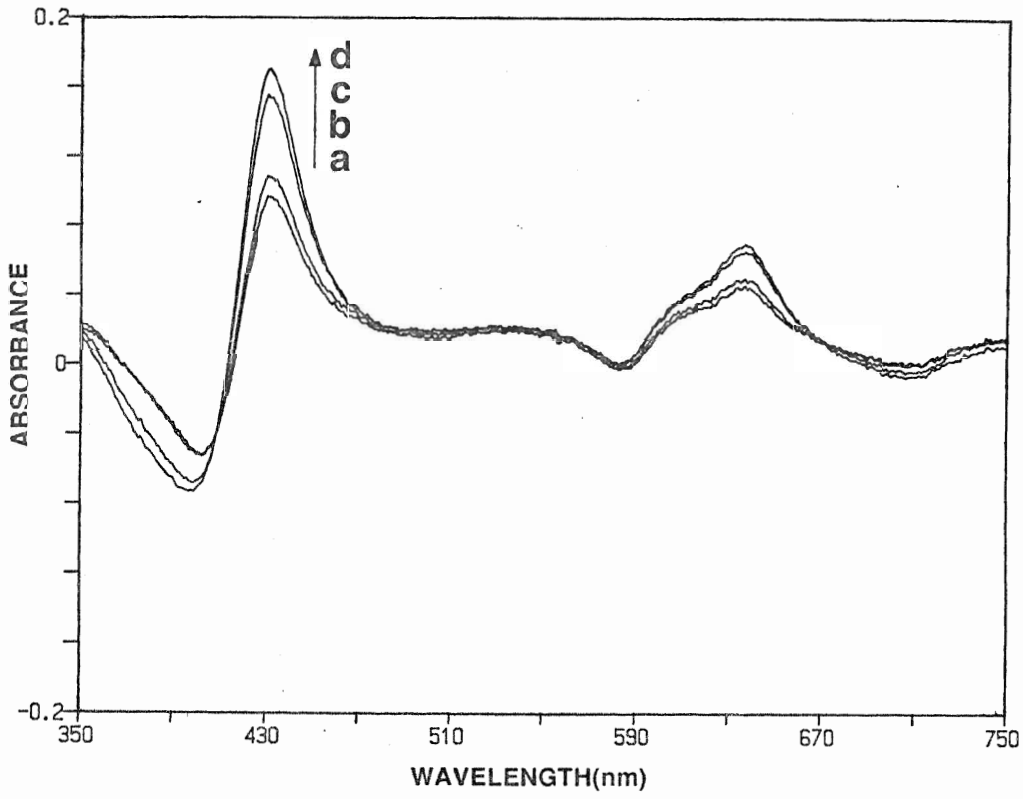

Figure 32. Representative difference spectra for titration of HPII mutant N201Q with cyanide.
3.8μM hematin N201Q. Titration conditions as stated in Materials and Methods. Difference spectra for HPII N201Q-HCN complexes at increasing concentration of KCN (**a**: 271μM, **b**: 611μM, **c**: 16.9mM, and **d**: 34.5mM) minus untreated protein.

Figure 33. Titration of HPII N201Q mutant protein with cyanide: secondary plots.
(**A**) Double Reciprocal Plot of Soret wavelength titration derived data versus concentration of HCN. (**B**) Hill Plot of Soret wavelength titration derived data versus concentration of HCN superimposed with fitted curve for double binding of ligand prepared on the Multifit™ fitting program for the Apple Macintosh™ computer. Dissociation constants of the ligand (HCN) from the binding populations and their estimated proportions are shown inset.

Figure 33

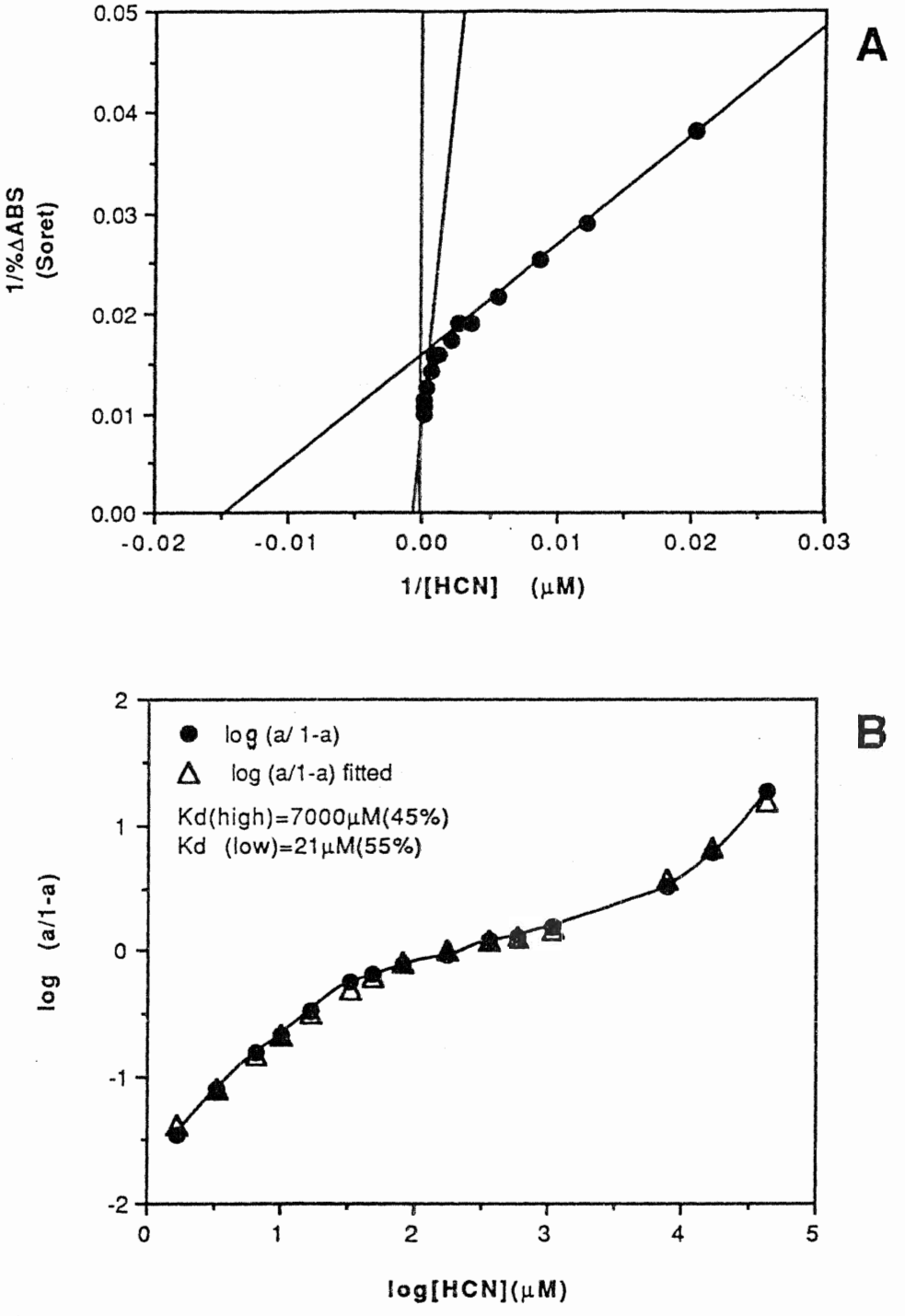
A
0.05
0.04
0.03
0.02
0.01
0.00
1/%ΔABS
(Soret)
-0.02
-0.01
0.00
0.01
0.02
0.03
1/[HCN] (μM)
B
log (a/ 1-a)
log (a/1-a) fitted
Kd(high)=7000μM(45%)
Kd (low)=21μM(55%)
2
1
0
-1
-2
log (a/1-a)
0
1
2
3
4
5
log[HCN](μM)

titration, indicating more than one phase of ligand binding. Figure 33 shows the double reciprocal plot (Fig. 33A)and Hill plot (Fig. 33B) for the titration of N201Q with cyanide. The results show biphasicity of cyanide binding suggested by the difference spectra. The proportion of lower affinity species compared to higher affinity species approaches equality in this case, based upon fitting to a double binding curve . Representative difference spectra obtained for the titrations of N201A mutant protein with cyanide are shown in Figure 34. The corresponding double reciprocal plots and Hill plots generated from the titration are shown in figure 35. Similarly, representative difference spectra obtained for the titrations of N201H mutant protein with cyanide are shown in Figure 36, with the corresponding double reciprocal plots and Hill plots generated from the titration shown in figure 37. Titration plots for the differences between appropriate wavelength pairs are shown in Appendix B. The degree of biphasicity of binding is highly divergent for the three N201 mutants, with the fraction of low affinity species for the N201A and N201H mutants estimated at 75% and 17%, respectively. The estimated dissociation constants and fractional contributions are summarized in TABLE II. The existence of (at least) two binding species in these mutants further suggests the presence of two heme populations.

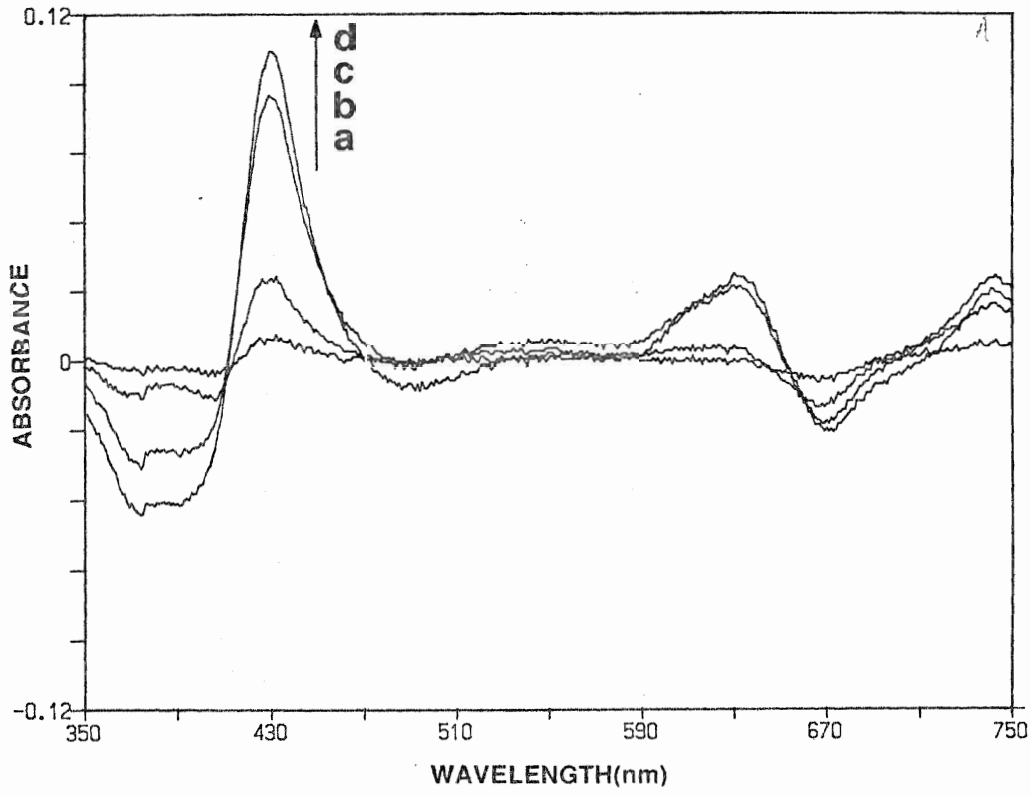

Figure 34. Representative difference spectra for titration of HPII mutant N201A with cyanide.
3.9μM hematin N201A. Titration conditions as stated in Materials and Methods. Difference spectra for HPII N201A-HCN complexes at increasing concentration of ligand (**a**: 415μM, **b**: 696μM, **c**: 15mM, and **d**: 38.9mM) minus untreated protein.

Figure 35. Titration of HPII N201A mutant protein with cyanide: secondary plots.
(**A**) Double Reciprocal Plot of Soret wavelength titration derived data versus concentration of HCN and (**B**), Hill Plot of Soret wavelength titration derived data versus concentration of HCN superimposed with fitted curve for double binding of ligand prepared on the Multifit™ fitting program for the Apple Macintosh™ computer. Dissociation constants of the ligand (HCN) from the binding populations and their estimated proportions are shown inset.

Figure 35

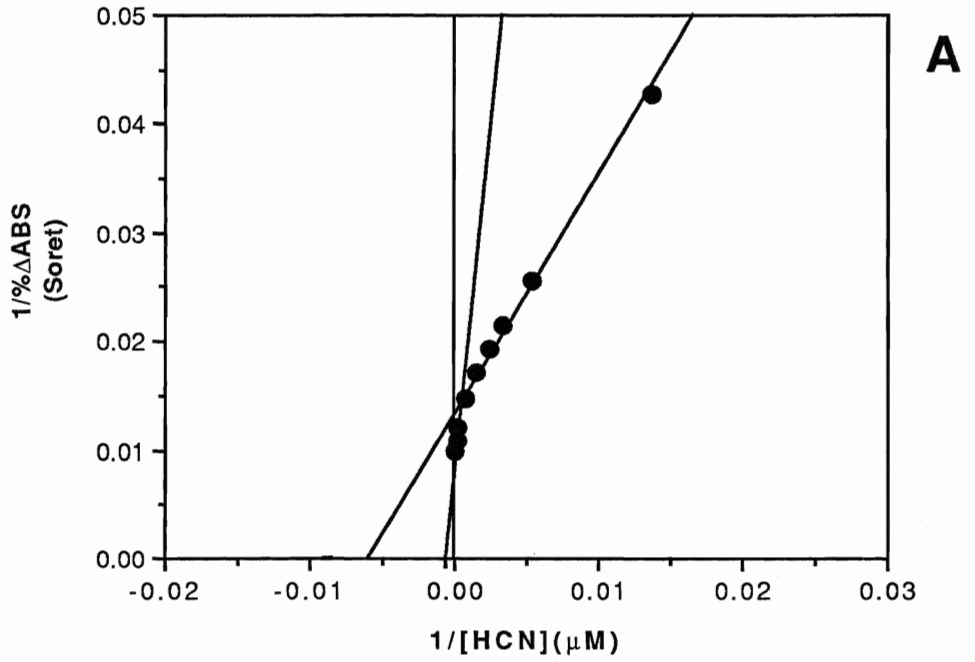
A
0.05
0.04
0.03
0.02
0.01
0.00
1/%ΔABS
(Soret)
-0.02
-0.01
0.00
0.01
0.02
0.03
1/[HCN](μM)

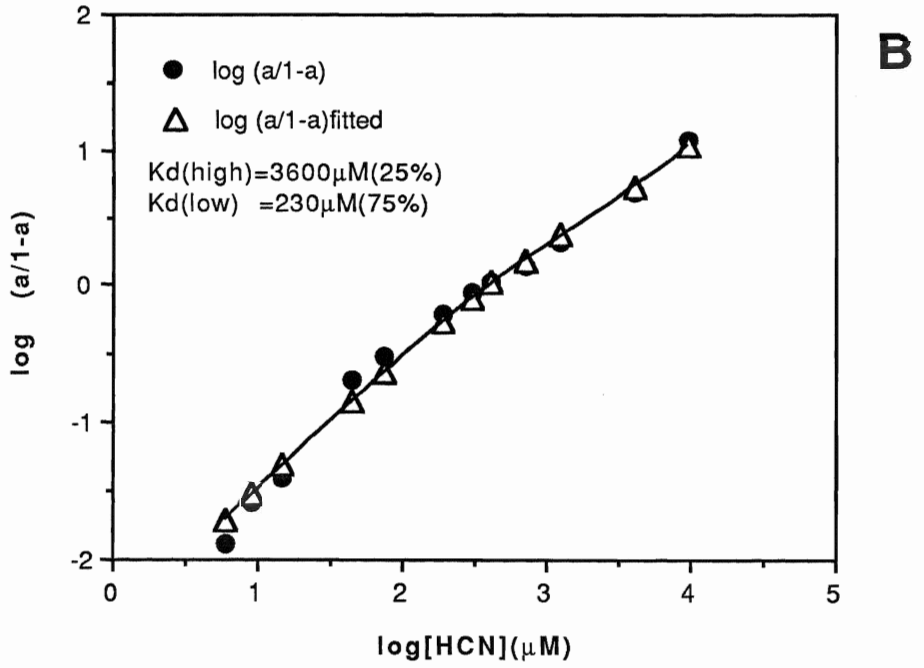
B
log (a/1-a)
log (a/1-a)fitted
Kd(high)=3600μM(25%)
Kd(low) =230μM(75%)
2
1
0
-1
-2
log (a/1-a)
0
1
2
3
4
5
log[HCN](μM)

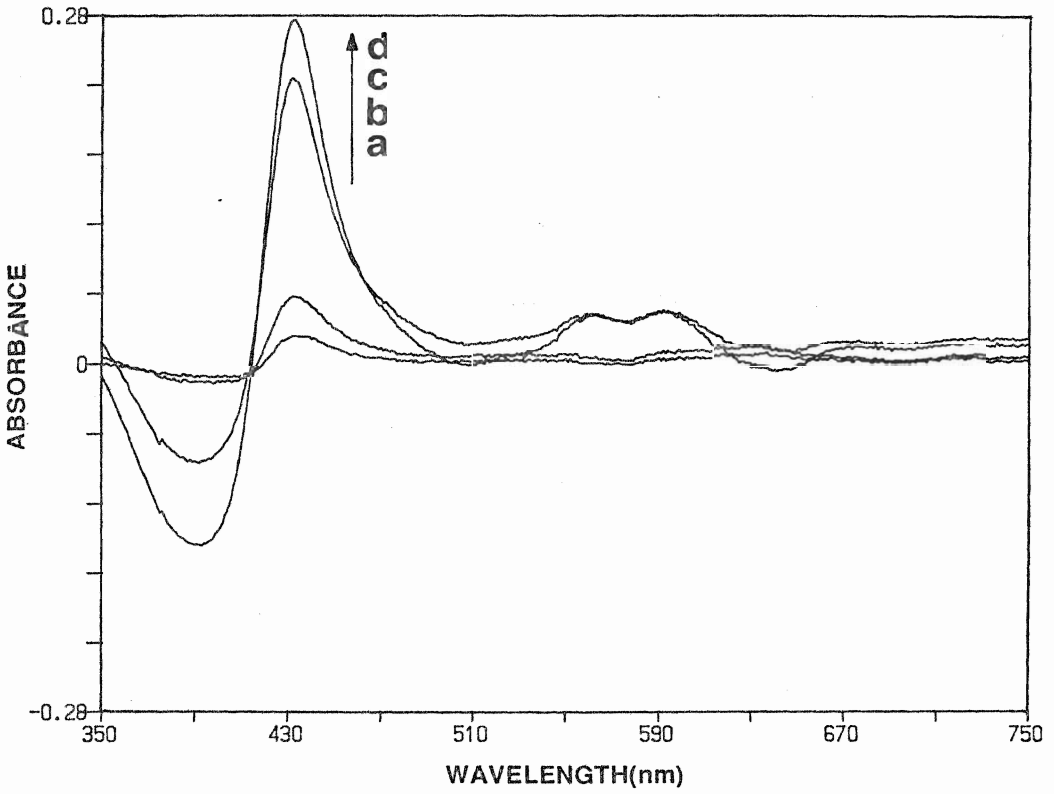

Figure 36. Representative difference spectra for titration of HPII mutant N201H with cyanide.
5 μM hematin N201H. Titration conditions as stated in Materials and Methods. Difference spectra for HPII N201H-HCN complexes at increasing concentration of ligand (**a**: 9.9μM, **b**: 33μM, **c**: 2mM, and **d**: 14.1mM) minus untreated protein.

Figure 37. Titration of HPII N201H mutant protein with cyanide: secondary Plots.
(**A**) Double Reciprocal Plot of Soret wavelength titration derived data versus concentration of HCN and (**B**), Hill Plot of Soret wavelength titration derived data versus concentration of HCN superimposed with fitted curve for double binding of ligand prepared on the Multifit™ fitting program for the Apple Macintosh™ computer. Dissociation constants of the ligand (HCN) from the binding populations and their estimated proportions are shown inset.

Figure 37

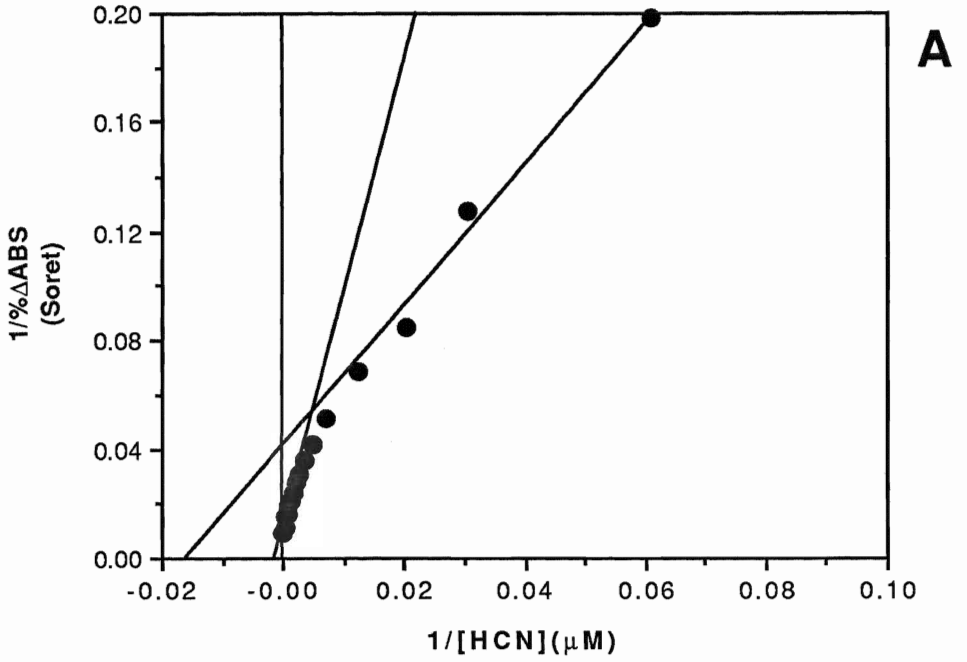
A
0.20
0.16
0.12
0.08
0.04
0.00
1/%ΔABS
(Soret)
-0.02
-0.00
0.02
0.04
0.06
0.08
0.10
1/[HCN](μM)

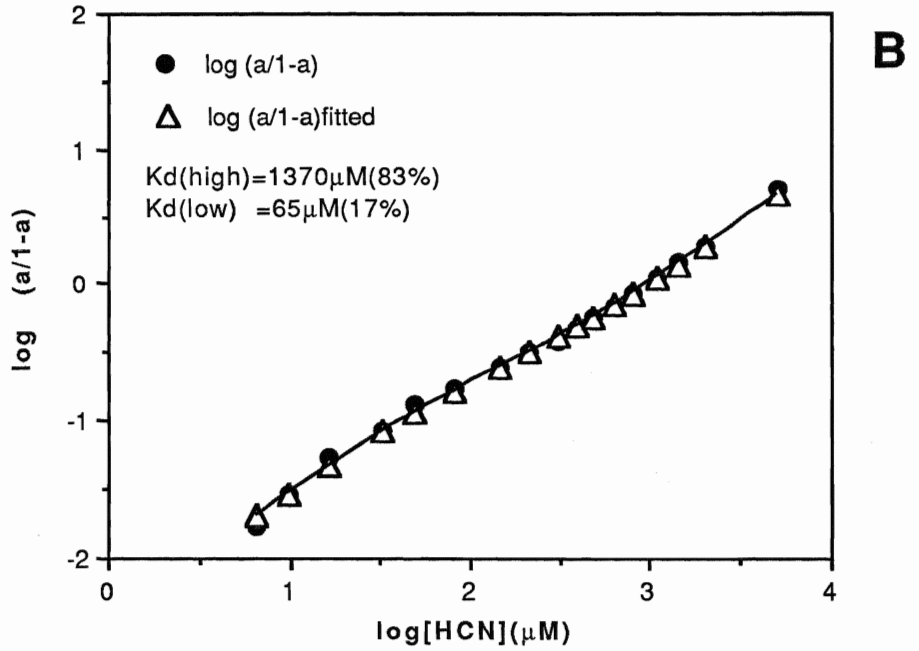
B
log (a/1-a)
log (a/1-a)fitted
Kd(high)=1370μM(83%)
Kd(low) =65μM(17%)
2
1
0
-1
-2
log (a/1-a)
0
1
2
3
4
log[HCN](μM)

TABLE II. Summary of cyanide binding for HPII wild type catalase and mutant proteins.

HEMOPROTEIN	CYANIDE BINDING (pH 6.5) [proportion]*
HPII wild type	MONOPHASIC
	K_d=87μM
H128A	K_d>>100mM
H128N	NONE
N201Q	BIPHASIC
	K_d=7mM [45%]
	K_d=21μM [55%]
N201A	BIPHASIC
	K_d=3.6mM [25%]
	K_d=230μM [75%]
N201H	BIPHASIC
	K_d=1.4mM [83%]
	K_d= 65μM [17%]

* Estimated via a curve fitting program

iii. Induction of spectral shifts in the HPII mutant N201H

Timkovich and Bondoc (1990) proposed that the original heme incorporated into some unusual microbial catalases is in fact ferriprotoporphyrin IX (protoheme), which undergoes self-modification in a pre-enzyme via reactions with free radical species generated during the initial turnovers of the pre-enzyme, to form *d* type hemes. This *in situ* heme conversion thus results in the heme which is subsequently fully functional in the enzyme, according to the proposal. Figure 38 shows the slow conversion of the spectrum for the N201H mutant of HPII catalase under conditions where the protein is exposed to low levels of constantly generated hydrogen peroxide, provided by a glucose/ glucose oxidase system. The spectral shifts with time seen in either the Soret (Fig. 38A) or the visible region (Fig. 38B) are inconsistent with the formation of either inactive catalase-peroxide compound II or compound III, which would be expected to show maxima at approximately 565nm (compound II) or 550nm and 580nm (compound III), respectively. An initial decrease in Soret absorbance attributable to formation of a protoheme peroxide compound I analogue is present, with no evidence of a maximum near 425nm characteristic of the formation of the inactive secondary peroxide compound, although the Soret peak *is* slightly red-shifted. The results suggest, however, the disappearance of the protoheme signal and its replacement by a spectrum characteristic of a *d* type heme, though the extent of contributions to such spectral shifts by the compound I analogue of this enzyme has not been investigated. These results will be compared with other observations in the following chapter.

Figure 38. Spectral conversion of HPII N201H in presence of generated H_2O_2.

11 μM hematin HPII in 10mM aerobic potassium phosphate, pH 6.5., 2nM glucose oxidase, 0.4ml final volume, 25 degrees. 4mM glucose was added to initiate formation of H_2O_2.Direction of spectral shifts as indicated by arrows. (**A**) Soret and (**B**) the visible regions of the spectrum shown at 0min, 1min, 30min (solid lines **a**, **b**, and **c** respectively), and 60min (broken line) after addition of glucose.

Figure 38

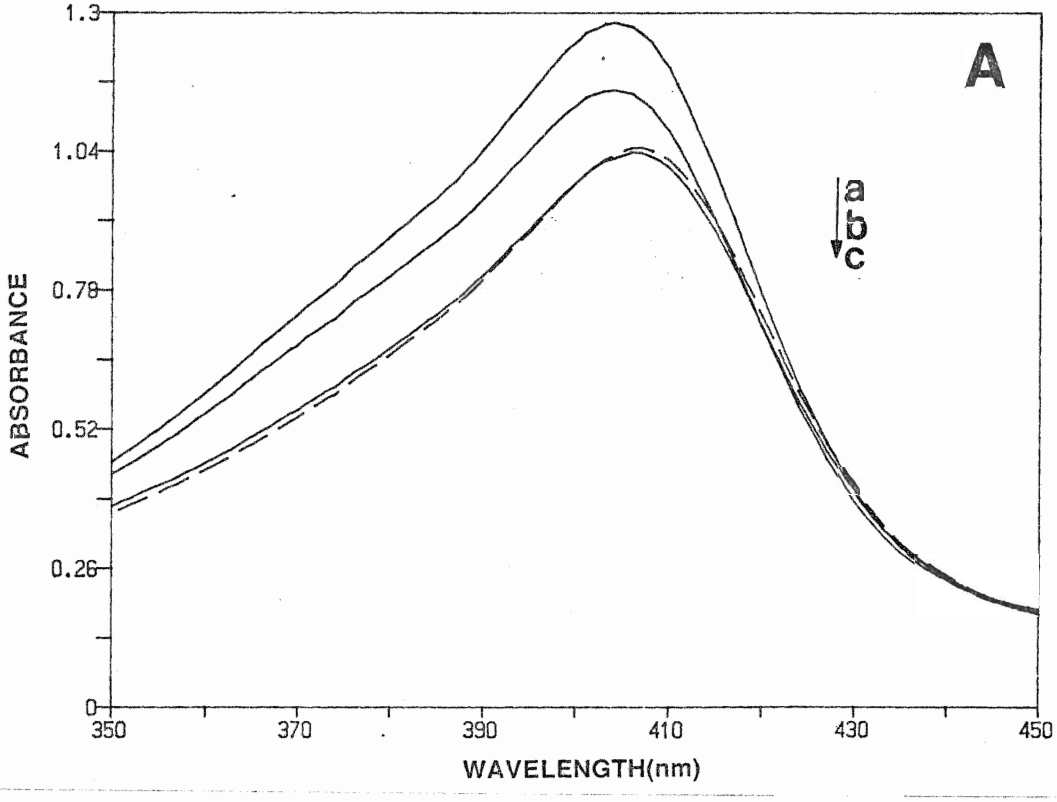
A
1.3
1.04
0.78
0.52
0.26
0
ABSORBANCE
350
370
390
410
430
450
WAVELENGTH(nm)
a
b
c

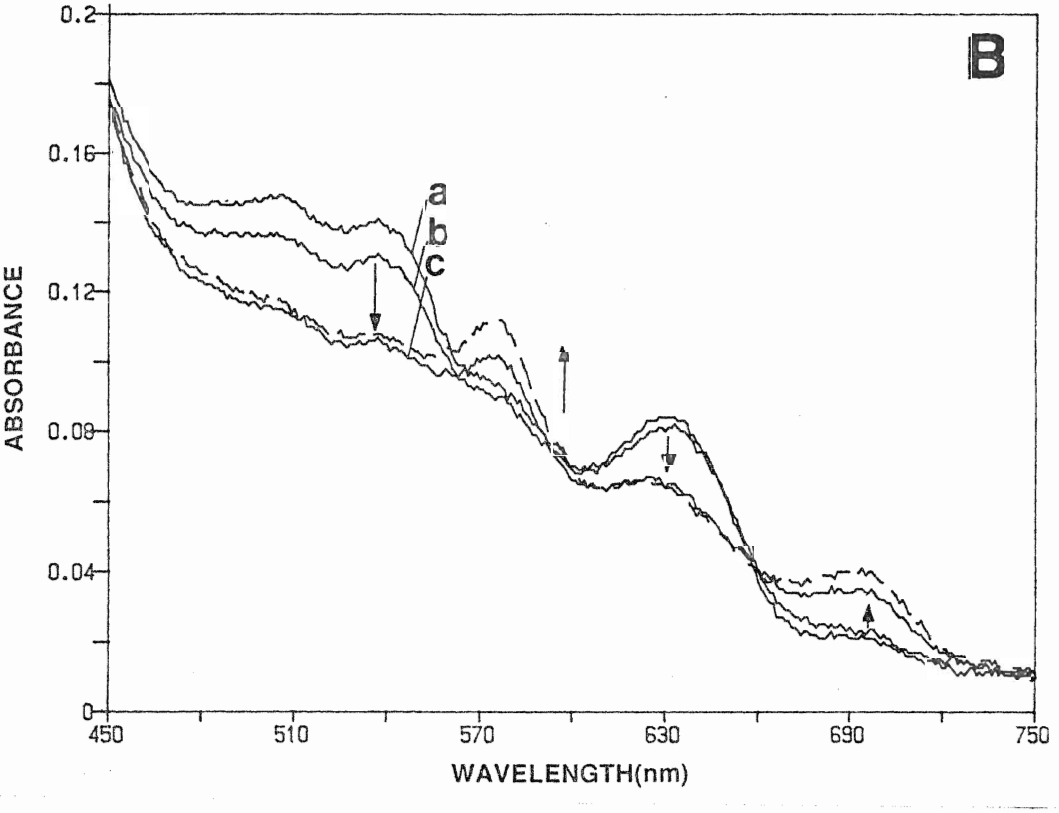
B
0.2
0.16
0.12
0.08
0.04
0
ABSORBANCE
450
510
570
630
690
750
WAVELENGTH(nm)
a
b
c

D. Catalase binding of Nicotinamide Adenine Dinucleotides

i. Affinity chromatography of BLC, HPII, SCCT, and SCCA proteins

Jouve *et al.* (1986) demonstrated that dye-linked affinity chromatography was a suitable technique with which to probe catalase proteins for the presence of dinucleotide "folds" (Thompson *et al.* 1975). The Cibacron™ F3GA dye is similar in chemical structure to nicotinamide adenine dinucleotides in open conformation (Fig. 9), allowing the NAD/NADP binding proteins to be retained by the dye-dextran linked matrix of the column. The elution pattern for BLC from an affinity column specific for NAD/NADP binding proteins shown in Figure 39A is typical of that expected for a dinucleotide binding protein containing little or no native-bound dinucleotide. The elutions were monitored spectrophotometrically at 405nm and 340nm, the absorbance maxima of catalase heme and (near UV) NADPH, respectively.

Monitoring the 280nm maxima was not possible due to the interference of dinucleotide ultraviolet absorbance with the protein maxima. Both ADP and NADPH were used as wash aliquots, and gave significant elution of Soret absorbance, the major peak eluting with the NADPH peak (Fig. 39A). This differs from other results reported for the bovine liver protein in which a significant fraction, α , elutes with the buffer used. The α fraction represents dinucleotide loaded catalase which does not bind the gel. The remaining β fractions elute with dinucleotide or with sufficiently high salt concentrations (Jouve *et al.* 1986). The degree of elution is dependent on the dinucleotide eluant used, as the binding of NADPH to catalase is normally very tight.

Figure 39. Elution profiles of BLC and HPII wild type proteins from Affi-gel Blue® affinity column.
Column prepared and ran as described in Materials and Methods, procedure #7. Starting and elution buffer was 50mM potassium phosphate , pH 7.0. Temperature was 4 degrees. For each elution, 300μg catalase protein was applied to the column. 1mM ADP and 10μM NADPH added in 2.5ml and 1ml washes at points shown. Hemoprotein (405nm) and reduced dinucleotide (340nm) absorbances were monitored. (**A**) Elution profile of BLC. (**B**) Elution profile of HPII wild type protein.

Figure 39

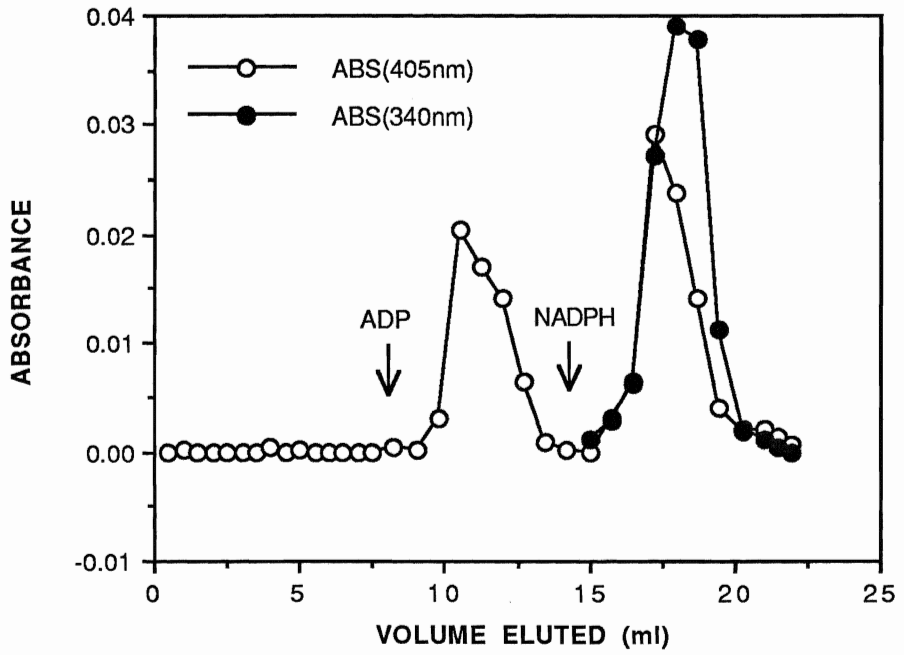
0.04
0.03
0.02
0.01
0.00
-0.01
ABSORBANCE
ABS(405nm)
ABS(340nm)
ADP
NADPH
0
5
10
15
20
25
VOLUME ELUTED (ml)

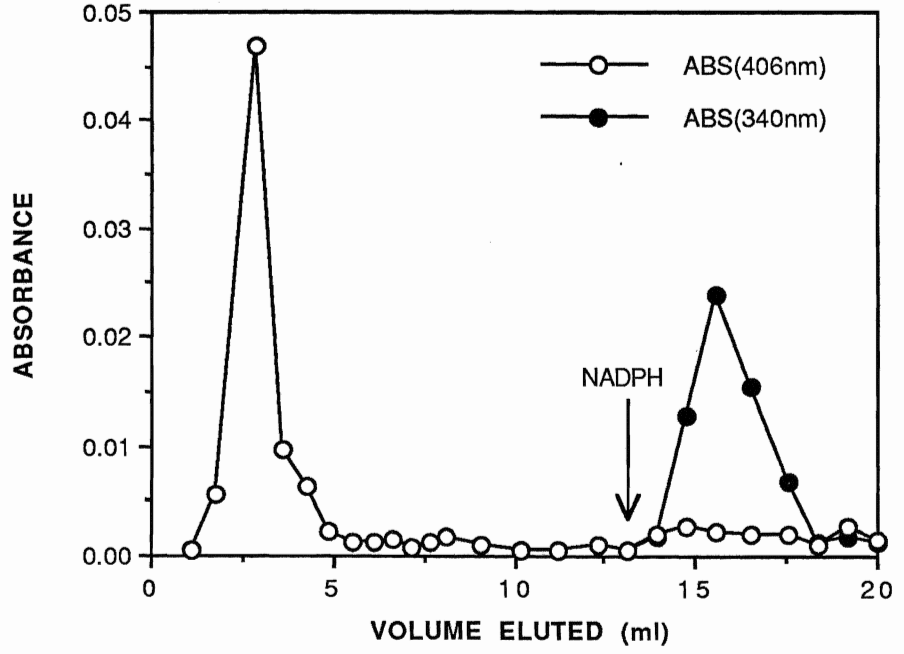
0.05
0.04
0.03
0.02
0.01
0.00
ABSORBANCE
ABS(406nm)
ABS(340nm)
NADPH
0
5
10
15
20
VOLUME ELUTED (ml)

Figure 40. Elution profiles of SCCT and SCCA proteins from Affi-gel Blue® affinity column.
Column prepared and ran as described in Materials and Methods, procedure #7. Starting and elution buffer was 50mM potassium phosphate , pH 7.0. Temperature was 4 degrees. For each elution, 300μg catalase protein was applied to the column. 1mM ADP and 10μM NADPH added in 2.5ml and 1ml washes at points shown. Hemoprotein (405nm) and reduced dinucleotide (340nm) absorbances were monitored. (**A**) Elution profile of SCCT. (**B**) Elution profile of SCCA protein.

Figure 40

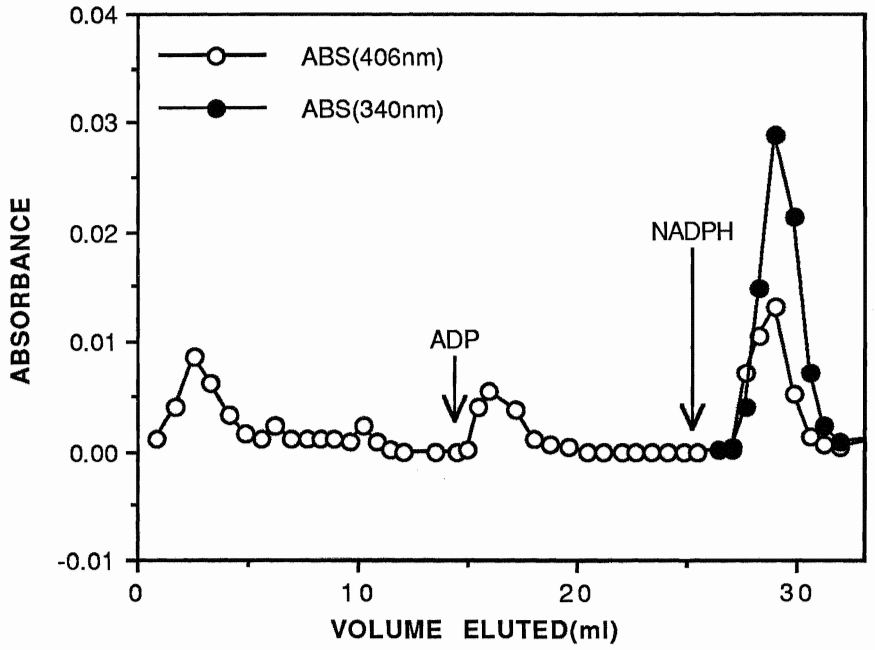
0.04
0.03
0.02
0.01
0.00
-0.01
ABSORBANCE
ABS(406nm)
ABS(340nm)
NADPH
ADP
0
10
20
30
VOLUME ELUTED(ml)

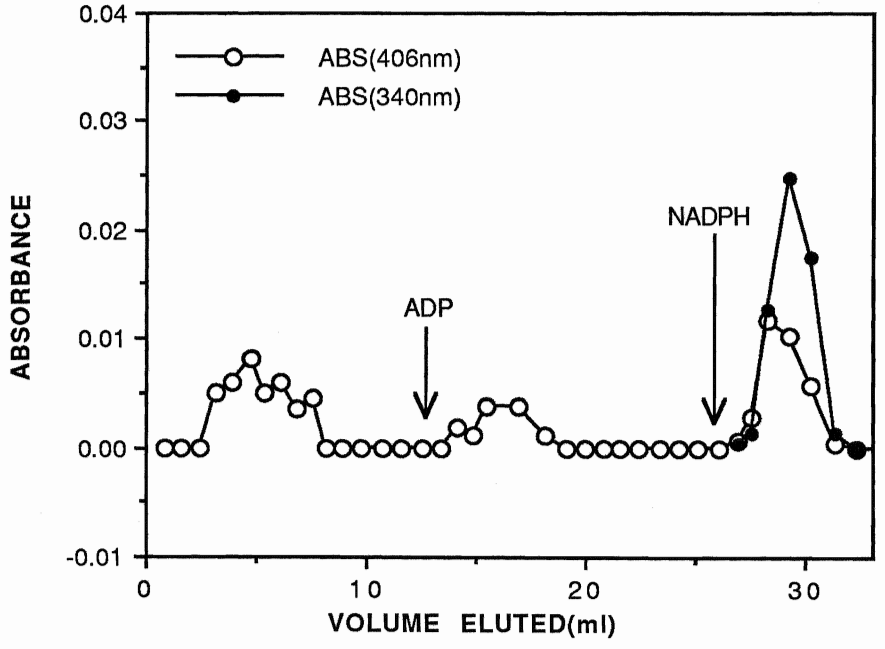
0.04
0.03
0.02
0.01
0.00
-0.01
ABSORBANCE
ABS(406nm)
ABS(340nm)
NADPH
ADP
0
10
20
30
VOLUME ELUTED(ml)

The elution profile for HPII catalase is shown in Figure 39B. The profile is typical of that for a non-dinucleotide binding protein. All the Soret absorbance is apparently eluted with the sample buffer, with none eluting even in the following wash of at least one bed volume of sample buffer. Dinucleotide binding was considered unlikely for this protein and only elution with the presumably definitive eluant for catalase was attempted. The NADPH peak elutes without appreciable Soret absorbance, as indicated in the figure.

Figures 40A and 40B show the comparative elution patterns for the two fractions of catalase isolated and purified from *Saccharomyces cerevisiae*, SCCT and SCCA. In both cases, α and β fractions were eluted. The apparent α fractions may however, be due to other protein components copurified with the catalases. Elution patterns with ADP and with NADPH nonetheless confirm that at least a portion of the samples contain dinucleotide binding hemoproteins, the most prominent peaks eluting with the NADPH containing fractions, as with BLC.

ii. Fluorescence emission spectra of BLC, HPII, SCCT, and SCCA proteins

Figure 41 shows the absolute fluorescence emission spectra obtained for BLC, HPII, and SCCT protein fractions (see Methods and Materials section #8, for procedural details). Excitation was at 340nm,: the absorbance maximum in the near ultraviolet region for reduced dinucleotides. It is apparent that a broad band probably indicative of NADPH is present in the spectrum obtained for commercial BLC protein, but absent in the native preparations of the remaining catalases. This is not surprising, as the loss or oxidationof NADPH would be expected during enzyme purification or during storage in buffer. Fresh commercial BLC samples have, however, been found with reduced dinucleotide present even after purification, due to the tight binding of the cofactor (Kirkman and Gaetani, 1984).

Binding properties of the proteins were examined fluorimetrically by exposure of the different catalases to NADPH in solution for 30minutes, followed by removal of the free NADPH by sample filtration on a G-25 Sephadex column. The fluorescence spectra of pre-exposure samples were subtracted from those of post-exposure samples. The resultant difference spectra at identical catalase concentrations are shown in Figure 42.

Figure 41. Absolute fluorescence emission spectra for catalase proteins.
All protein samples at 1μM hematin in 2.5ml final volume. Temperature was 30 degrees. Other conditions as described in Materials and Methods, procedure # 8. Absolute spectra with excitation at 340nm for **a**: BLC, **b**: NADPH at 0.5μM, **c**: HPII wild type protein, and **d**: SCCT.

Figure 41

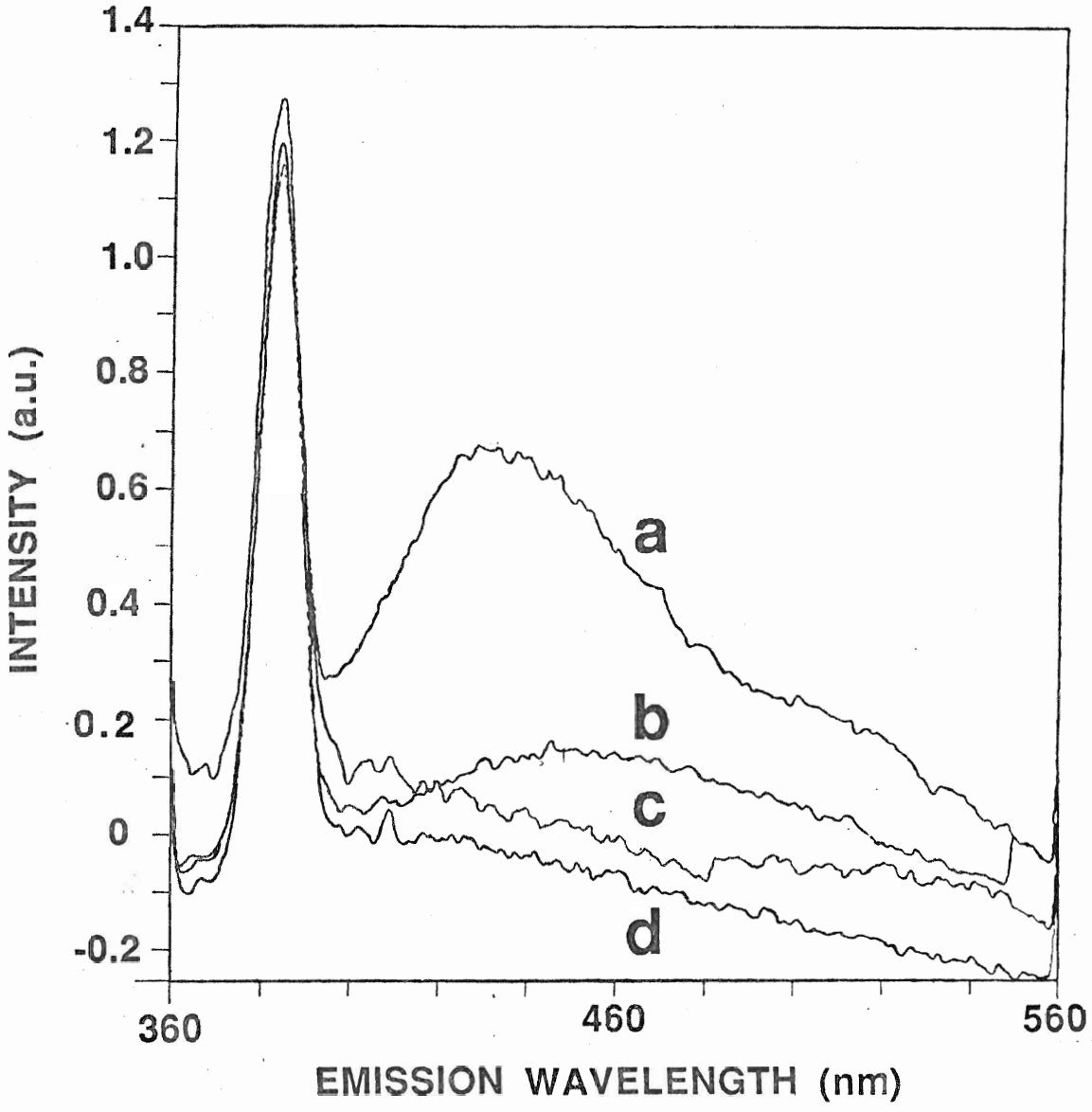
1.4
1.2
1.0
0.8
0.6
0.4
0.2
0
-0.2
INTENSITY (a.u.)
a
b
c
d
360
460
560
EMISSION WAVELENGTH (nm)

Figure 42. Fluorescence emission difference spectra for catalase proteins.
Spectra of BLC (**a**,**b**), HPII (**d**,**e**) and SCCT(**c**) proteins with background buffer emission signal subtracted. Excitation wavelength was 340nm. All samples at 0.2μM in 2.7ml final volume. Temperature was 30 degrees. Other conditions as described in Materials and Methods, procedure # 8 . Spectra **b**, **e** are for the untreated proteins, Spectra **a**, **c**,and **d** are for the proteins incubated for 30min with 50μM NADPH in the fluorometric sample buffer, and then passed over a Sephadex G-25 column (0.9x10cm) for removal by filtration of excess NADPH.

Figure 42

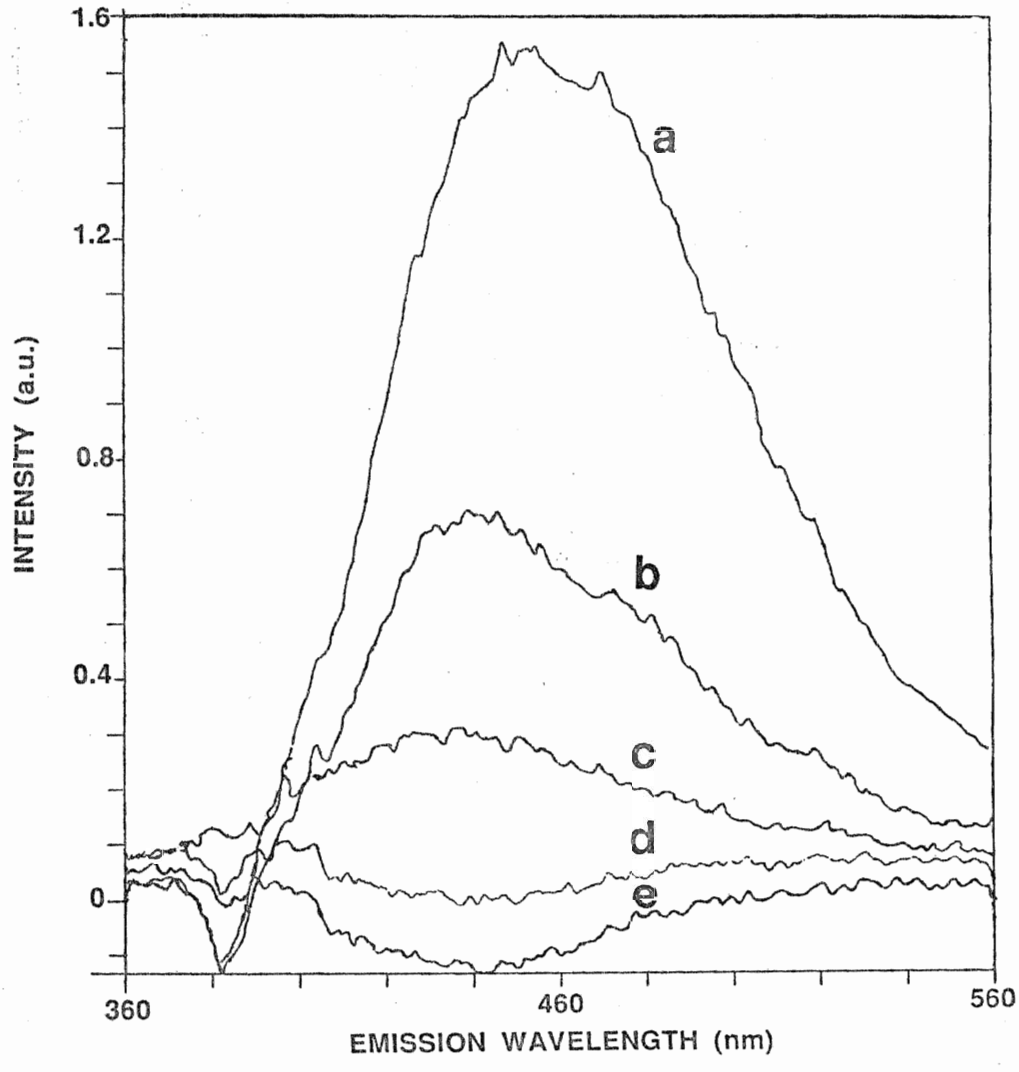
1.6
1.2
0.8
0.4
0
INTENSITY (a.u.)
a
b
c
d
e
360
460
560
EMISSION WAVELENGTH (nm)

E. Effects of NADPH on the Formation and Decomposition of BLC, SCCT and SCCA Secondary Peroxide Compounds

i. Time courses for BLC and SCCT compound II formation under conditions of constant H_2O_2 generation

Figures 43A and 43B show the effect of exposure of BLC to a low level of constantly generated hydrogen peroxide on its absorption spectra in the Soret and visible regions, respectively. The experiment of Figure 43 reproduces experimental results previously obtained by Kirkman *et al.* (1987) for the bovine enzyme. Formation of the compound I and compound II complexes; as evidenced by the decline in intensity of the band at 403nm and the slow red shift of the spectrum as the 425nm absorbance maximum of compound II appears in the Soret region. Using the millimolar extinction coefficients for catalase hematin (Nicholls and Schonbaum, 1963) as employed by Kirkman and co-workers, the proportion of catalase compound II after 60 minutes of peroxide generation can be estimated at 56%. The remaining spectra indicate the progressive formation of both compounds I and II over the one hour period. A rapid decline in absorbance maximum at 403nm may be compared to the absorbance increase at 425nm in the first 12 minutes, indicating a more rapid formation of compound I than compound II.

Figure 43B compares the visible spectra, showing the catalase/ glucose oxidase system before peroxide generation was initiated and after 60 minutes of constant exposure to H_2O_2. Inspection of the maxima reveals that the main bands for ferricatalase at 622nm and 540nm have been replaced by absorbance maxima at 568nm and 537nm characteristic of compound II with no evidence of the double peak of compound III (at approx. 550nm) in the spectrum after 60 minutes.

Figure 43. Time course of formation of BLC peroxide compounds.
Absorbance spectra in the (**A**) Soret region and (**B**) visible region for bovine liver catalase (4.3μM hematin) in aerobic 10mM potassium phosphate, pH 6.5 with 2.0 nM glucose oxidase, 25 degrees, final volume 1 ml. Generation of hydrogen peroxide initiated by addition of 4mM glucose. Arrows indicate direction of spectral shifts from zero minutes to 60minutes at times: **a**: 0min , **b**: 12min , **c**: 24min , **d**:36min , **e**:48min, **f**:60min in (**A**) and at times: **a**: 0min , **b**: 60min in (**B**).

Figure 43

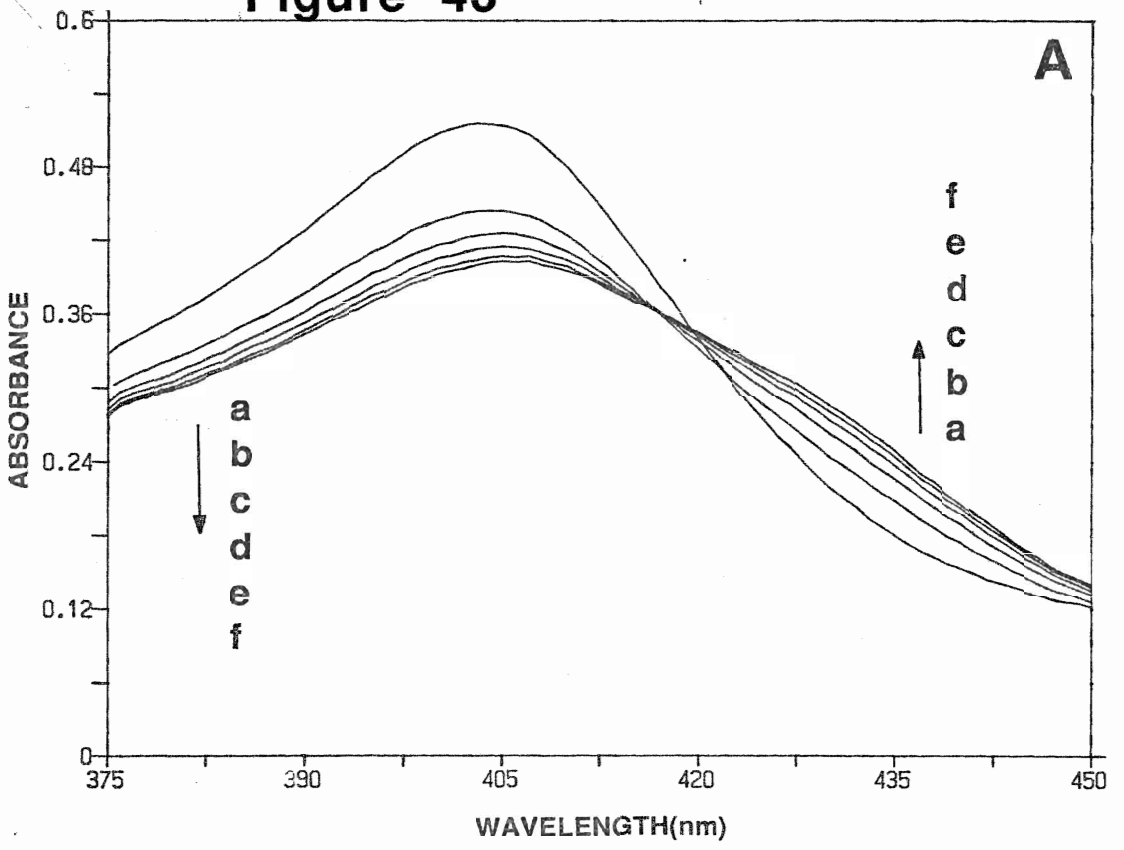
A
ABSORBANCE
0.6
0.48
0.36
0.24
0.12
0
375
390
405
420
435
450
WAVELENGTH(nm)
a
b
c
d
e
f
f
e
d
c
b
a

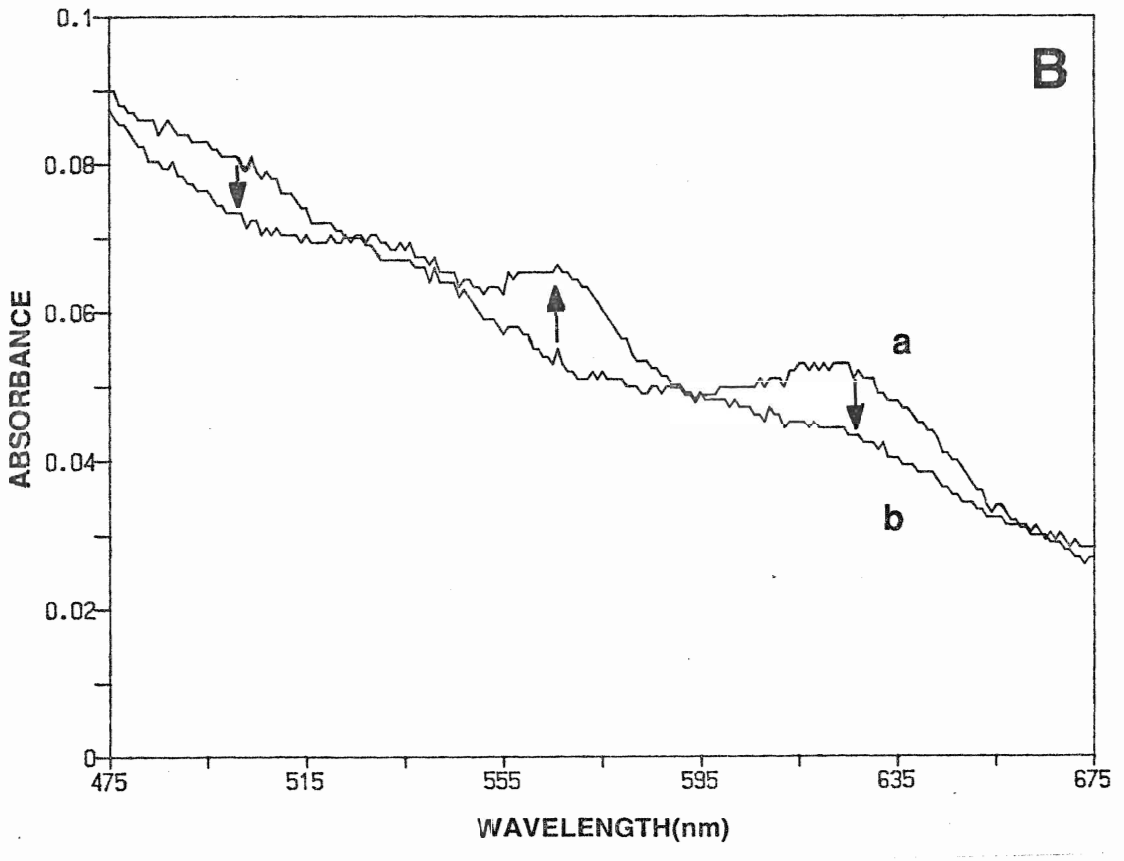
B
ABSORBANCE
0.1
0.08
0.06
0.04
0.02
0
475
515
555
595
635
675
WAVELENGTH(nm)
a
b

ii. Time courses for BLC compound II formation: effects of donors

Ferrocyanide is one of a class of electron donors which specifically promote the formation of compound II from compound I, without donating reducing equivalents to compound II to regenerate ferricatalase (Nicholls and Schonbaum, 1963). The effect of this donor on catalase compound I and II generation can be seen in the spectra of Figure 44, which shows that after only one minute of hydrogen peroxide generation, both compound I and compound II are formed. After 30 minutes under these conditions, no further compound I or compound II generation occurs. At thirty minutes after peroxide generation began, 65% of the total catalase was estimated to be in the form of compound II. This enhanced level of compound II formation was the only effect of the ferrocyanide on the catalase, as the visible spectrum (Figure 44B) indicates.

Figure 45A shows the time course of a reaction in which catalase pre-incubated with NADPH is exposed to hydrogen peroxide under conditions of constant generation. Both the Soret and the near-ultraviolet regions of the spectra are indicated, to demonstrate concomitant NADPH oxidation as the reaction proceeds. It is apparent that the NADPH prevents formation of compound II and that NADPH is progressively but slowly oxidized during the course of the reaction as indicated by the decline in the absorbance at 340nm. Upon the near-complete oxidation of the added NADPH, the formation of compound II begins, as evidenced by the increased red-shifted absorbance indicative of the maximum at 425nm. These events are represented in the form of secondary plots of the changes at 340nm and 435nm with time in

Figure 44. Time course of formation of BLC peroxide compounds in presence of ferrocyanide.
Experimental conditions as described in Figure 43. Pre-incubation of reaction mixture with $K_4Fe(CN)_6$ at initial concentration of 10μM. Arrows indicate direction of spectral shifts from zero minutes to 30minutes (**a**:0min, **b**:1min, **c**:2min, and **d:** 30min) in the Soret region (**A**) and at **a**: 0min and **b**: 30min in the visible region (**B**) of the spectrum.

Figure 44

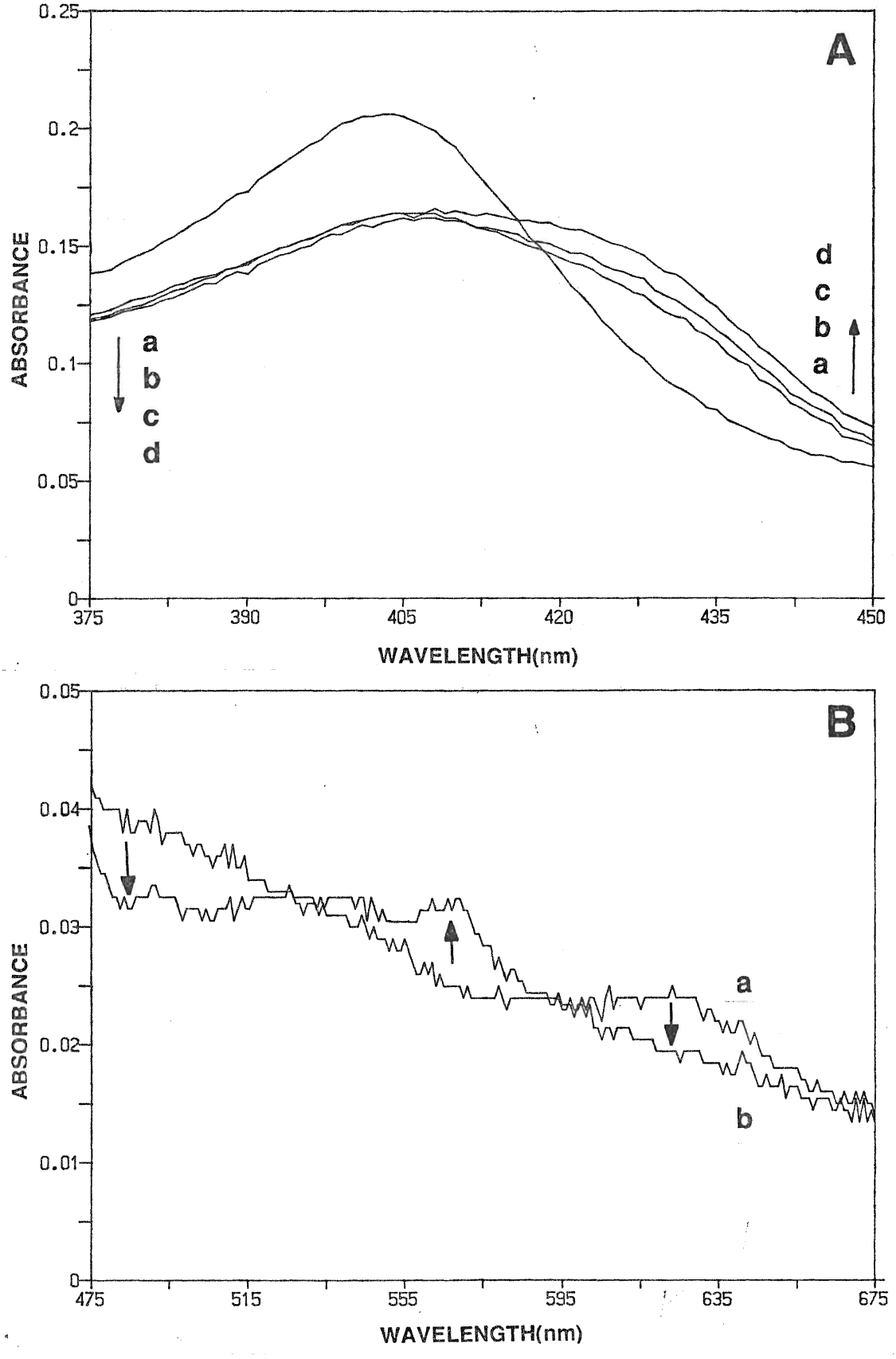
A
ABSORBANCE
0.25
0.2
0.15
0.1
0.05
0
375
390
405
420
435
450
WAVELENGTH(nm)
a
b
c
d
d
c
b
a
B
ABSORBANCE
0.05
0.04
0.03
0.02
0.01
0
475
515
555
595
635
675
WAVELENGTH(nm)
a
b

Figure 45. Time course for the oxidation of exogenously added NADPH by BLC.
(**A**) Bovine liver catalase (3.0 μM hematin) in aerobic 10 mM potassium phosphate, pH 6.5, plus 2nM glucose oxidase, at 25 degrees, final volume 0.2 ml. Pre-incubation with 10μM NADPH following initial spectrum (solid line). Glucose at 2 mM initiated reaction. Arrows indicate direction of representative spectral shifts from zero minutes to 70minutes after addition of glucose, at 0min, 12min,and 24min (large broken lines) prior to initiation of compound II formation and at 45min and 70min (small broken line) upon formation of compound II. (**B**) Secondary plot of data from Fig. 45(**A**) at 340nm and 435nm. Note that absorbance change at 340nm is in the negative direction from figure (**A**)

Figure 45

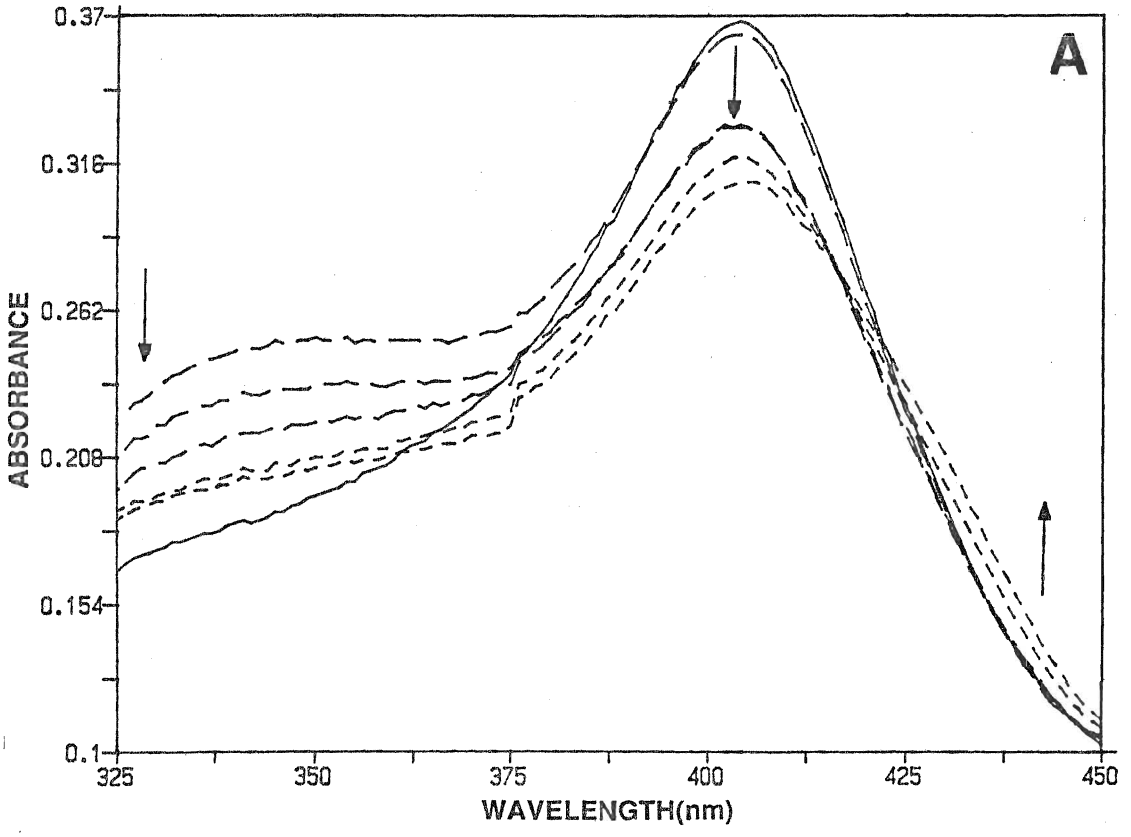
A
0.37
0.316
0.262
0.208
0.154
0.1
ABSORBANCE
325
350
375
400
425
450
WAVELENGTH(nm)

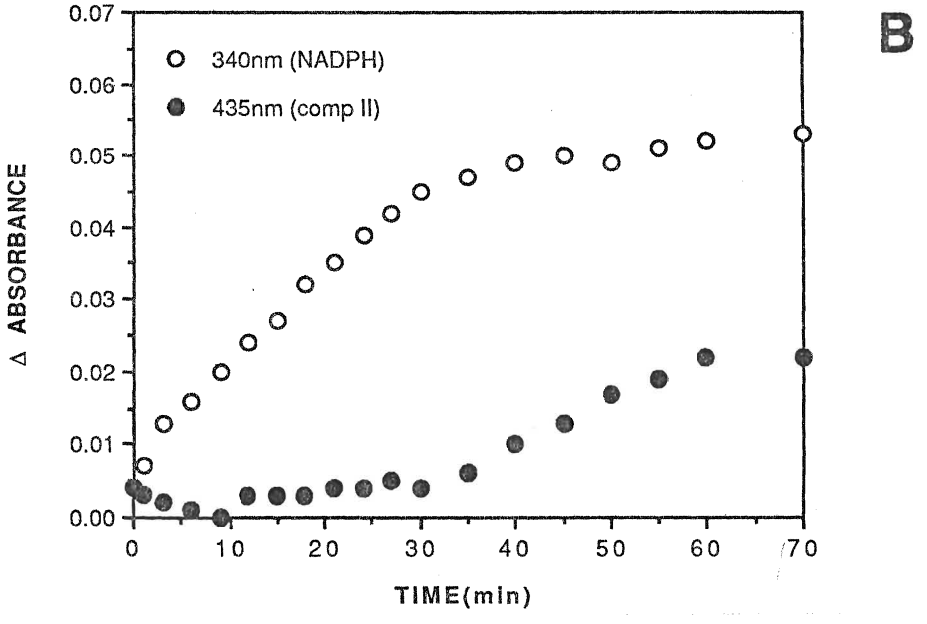
B
340nm (NADPH)
435nm (comp II)
0.07
0.06
0.05
0.04
0.03
0.02
0.01
0.00
Δ ABSORBANCE
0
10
20
30
40
50
60
70
TIME(min)

Figure 45B. The initial rate of NADPH oxidation is constant, with the concomitant rate of compound II formation being zero. Upon the approach of full oxidation of the NADPH, compound II formation is initiated rapidly but declines constantly as the rate approches the compound II steady state level.

iii. Steady-state kinetics of BLC compound II: effects of classical donors and nicotinamide adenine dinucleotides

Figure 46A (trace a) shows the slow formation of BLC compound II due to "endogenous donors" (uncharacterized donor groups on the protein) occurring under conditions of continuous hydrogen peroxide formation, which were similar to those for the spectral time courses shown previously. The absorbance change was monitored at 435nm, a wavelength at which compound I and ferricatalase are isobestic, thus allowing unambiguous observation of the formation of compound II. Conditions (indicated in the legend, see Methods and Materials for details) were similar to those used previously (Kirkman *et al*, 1987). The estimated rate constant of formation for compound II under these conditions was $5.7 \times 10^{-3} s^{-1}$. Nicholls (1964) observed similar rates of formation (rate constants from $1.6 \times 10^{-3} s^{-1}$ to $2.6 \times 10^{-3} s^{-1}$) under conditions utilizing 20μM hematin catalase.The rate may be modified by increasing or decreasing the concentration of glucose oxidase. To ensure reasonably rapid formation of the secondary complex and maintain constant peroxide generation, concentrations of glucose oxidase at 2nM or higher were typically employed.

The remaining traces in Figure 46A show the effects of ethanol and NADPH upon formation of compound II when pre-incubated with the catalase/glucose oxidase system prior to glucose addition (traces b and

Figure 46. Effects of NADPH and ethanol on the formation or depletion of BLC compound II.
Bovine liver catalase (4.0μM hematin) in aerobic 10mM potassium phosphate, pH 6.5 with 2.0 nM glucose oxidase, 25 degrees, final volume 0.8ml. Generation of hydrogen peroxide initiated by addition of 4mM glucose (single arrowhead). (**A**) Compound II formation in presence of pre-added NADPH at 20μM (TRACE **b**), ethanol at 20mM (TRACE **c**), and control experiment (TRACE **a**).(**B**) Compound II depletion at steady state upon addition of (TRACE **a**)40mM ethanol or (TRACE **b**) 40μM NADPH (double arrowhead).

Figure 46

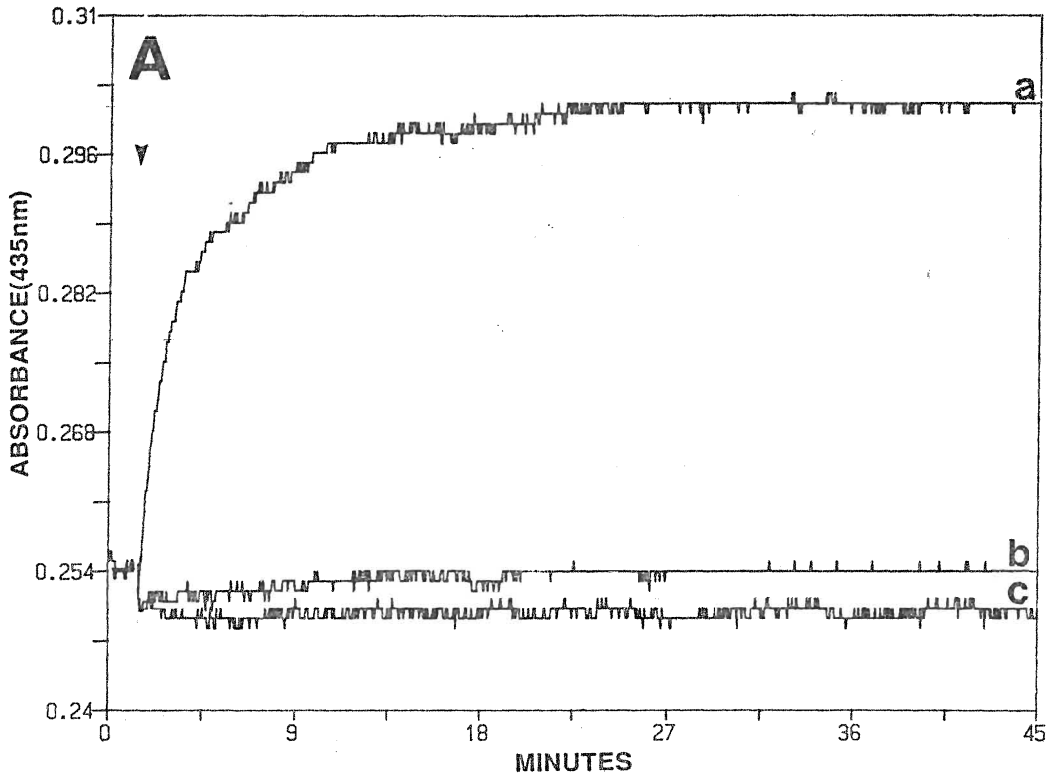
A
a
b
c
0.31
0.296
0.282
0.268
0.254
0.24
ABSORBANCE(435nm)
0
9
18
27
36
45
MINUTES

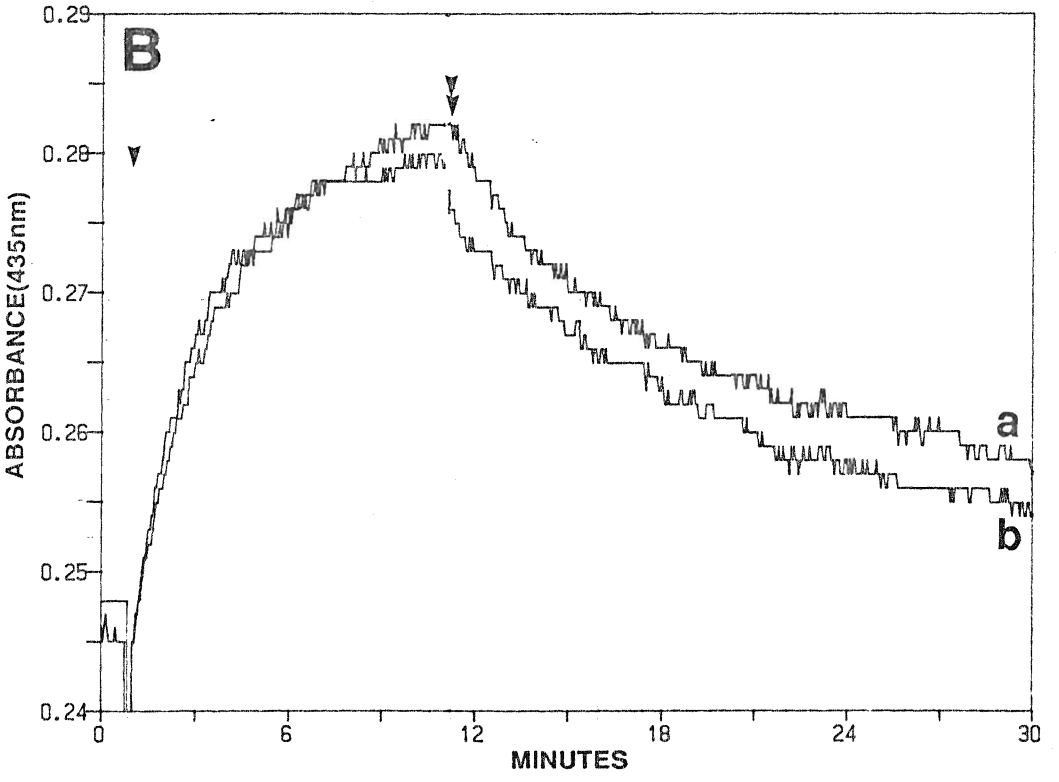
B
a
b
0.29
0.28
0.27
0.26
0.25
0.24
ABSORBANCE(435nm)
0
6
12
18
24
30
MINUTES

c). When added to the system upon compound II reaching its steady state concentration, the latter declines (Figure 46B; traces a and b). It is apparent that ethanol and NADPH induce almost identical effects in both experiments. These results confirm the previous findings that showed NADPH to be effective in the prevention of compound II formation as well as in its depletion (Kirkman *et al.* 1987).

Investigations of the effect of NADPH concentration on compound II formation were conducted. NADPH was ineffective in removing compound II under conditions where the initial concentration was approximately stoichiometric with the catalase hematin concentration. At higher NADPH concentrations however, the results for pre-incubation followed by constant hydrogen peroxide generation were as shown in Figure 47A, traces b, c, and d. In this approximate titration, a lag phase is typically seen during which compound II formation is absent (compare with Figure 45A, trace a) and NADPH oxidation occurs. Upon full oxidation of the bound NADPH, compound II formation is initiated. The lag phase was absent when the NADPH initially present was less than stoichiometric with catalase hematin concentration and appeared distinctly when NADPH was approximately stoichiometric with hematin group concentration. A plot of lag times against initial NADPH pre-incubation concentration is presented in Figure 47B and includes data from Fig. 47A. The duration of the lag phase is proportional to the NADPH concentration when the latter has risen above a certain minimal level. It is of the same order of magnitude as the time taken to produce an equivalent amout of compound II in the absence of NADPH. These results confirm previous findings that the rate of NADPH oxidation is slow

Figure 47. Compound II formation by BLC in the presence of increasing amounts of NADPH.
(**A**) Bovine liver catalase (4.3μM hematin) in aerobic 10 mM potassium phosphate buffer, pH 6.5 plus 2nM glucose oxidase, 25 degrees, final vol. 1.0 ml. Effects of (**a**) 0; (**b**) 3.3; (**c**) 6.6 and (**d**)10.5 μM NADPH indicated by the four traces. Glucose at 4 mM (arrowhead) initiated compound II formation. (**B**) Lag times from experiments analogous to those in Fig. 47(**A**) are plotted against the initial NADPH concentration.

Figure 47

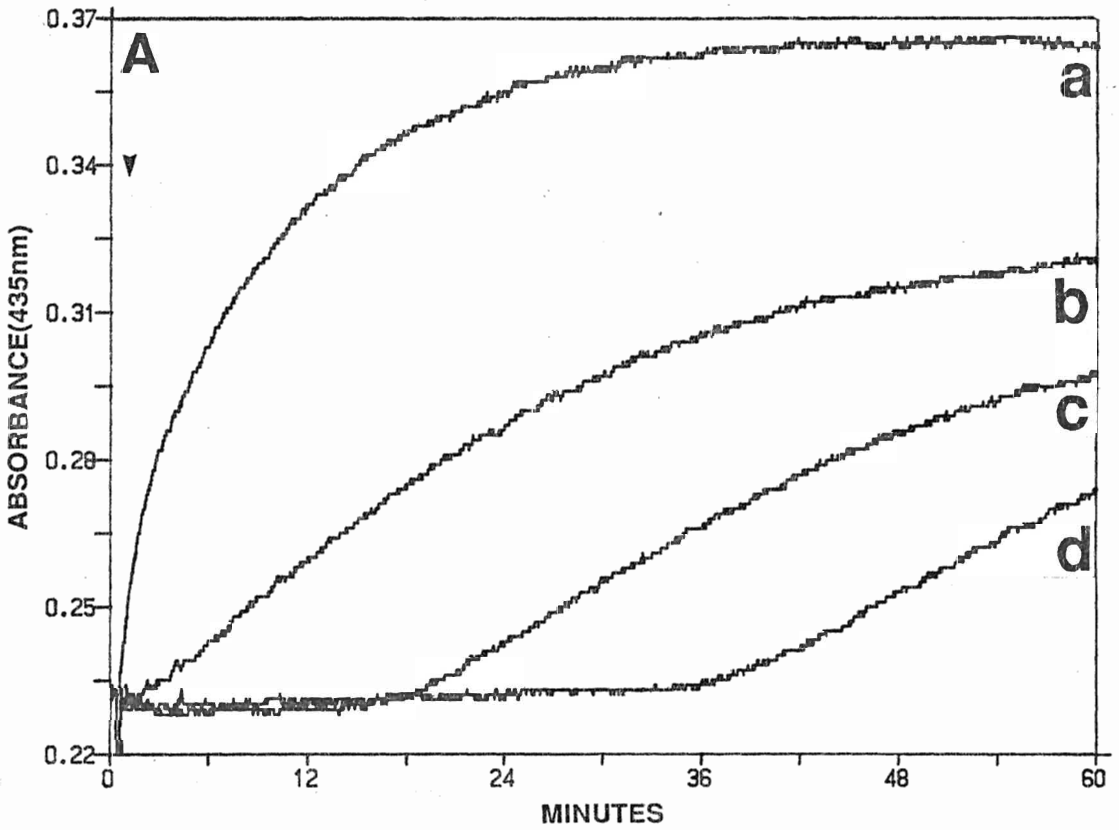
A
a
b
c
d
0.37
0.34
0.31
0.28
0.25
0.22
ABSORBANCE(435nm)
0
12
24
36
48
60
MINUTES

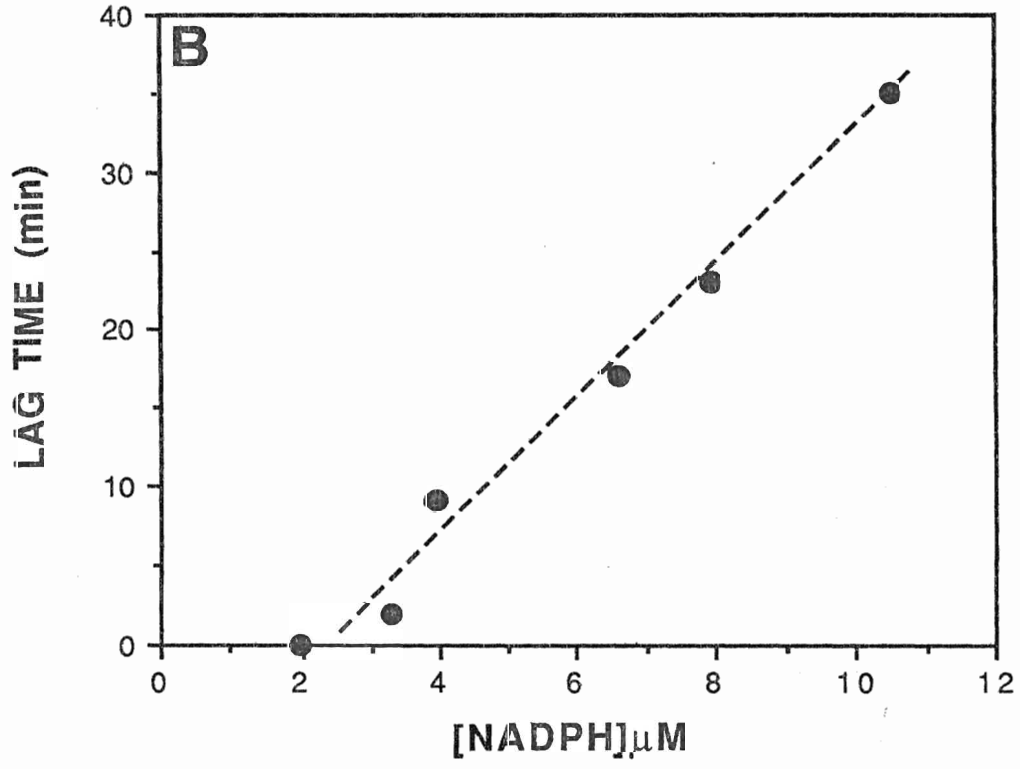
B
40
30
20
10
0
LAG TIME (min)
0
2
4
6
8
10
12
[NADPH]μM

Figure 48. Comparison of the effects of NADPH and other nicotinamide adenine dinucleotides on the formation of BLC compound II.

BLC at a concentration of 3.0μM hematin in aerobic potassium phosphate, pH 6.5 with 2nM glucose oxidase, at 25 degrees, final volume, 1ml. Glucose at 4mM initiated formation of compound II. Pre-incubations with NADP+ (**a**), NAD+ (**b**), NADH (**d**), NADPH (**e**), each at 5μM dinucleotide concentration, or with no addition (**c**) as control.

Figure 48

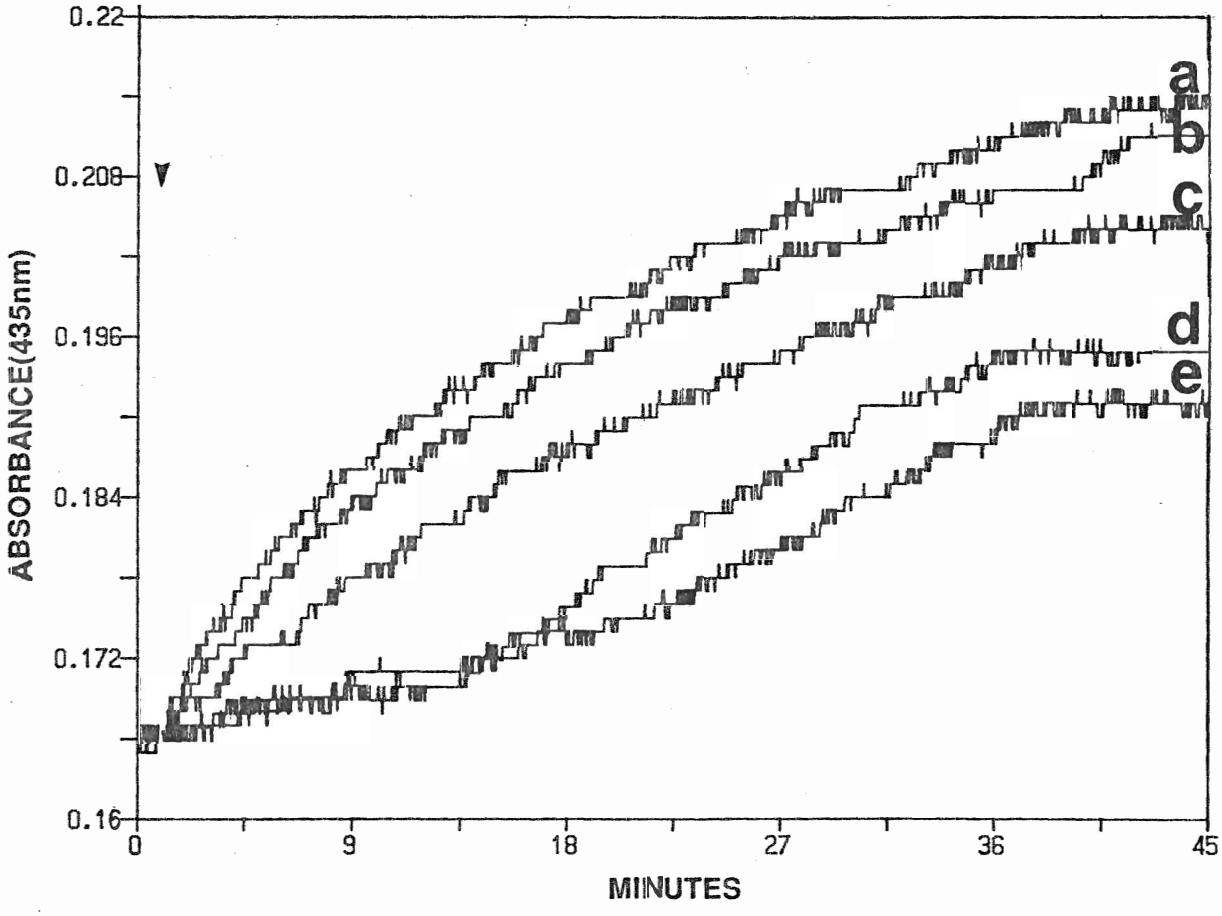
0.22
0.208
0.196
0.184
0.172
0.16
ABSORBANCE(435nm)
0
9
18
27
36
45
MINUTES
a
b
c
d
e

(Kirkman *et al.* 1987) and of the same order of magnitude as the rate of compound II formation in the absence of exogenous donors.

The results of a control experiment for the incubations of NADPH with the system investigated are shown in Figure 48. In this case preadditions consisted of other nicotinamide adenine dinucleotides. Only the preaddition of reduced forms of the dinucleotides induced the typical lag, and a sigmoidal shape of the kinetic trace. NADPH was superior in the initial suppression of compound II formation but had a faster rising initial rate of absorbance increase following the lag as did NADH. The oxidized forms of the dinucleotides, $NADP^+$ and NAD^+, were ineffective in delaying the formation of compound II.

Figure 49A shows the depletion of compound II by ethanol and NADPH upon reaching steady state following pre-incubation of the system with ferrocyanide. Both donors are effective and have similar rate constants estimated to be 3.2×10^{-3} s^{-1} for ethanol and 3.2×10^{-3} s^{-1} for NADPH, respectively. Previous experiments of this type have yielded similar results (Kirkman *et al.* 1987).

Figure 49B shows the effect of pre-incubation of $K_4Fe(CN)_6$ alone, and in conjunction with the donors ethanol and NADPH, on the formation of compound II. Ferrocyanide stimulates the formation of compound II via one-electron reduction of compound I (Nicholls and Schonbaum, 1963). As can be seen from trace a, ferrocyanide accelerates the rate of formation of compound II markedly within the initial 60 seconds after addition of glucose as compared with the control (trace b). When the system is pre-incubated with ferrocyanide in presence of NADPH, however (trace d), the formation of compound II is virtually eliminated, although pre-incubation with ethanol gives a steady state compound II concentration approximately one third that of

Figure 49 Ethanol, ferrocyanide , and NADPH effects on BLC compound II formation and decay.
Bovine liver catalase (2.0 μM hematin) in aerobic 10 mM potassium phosphate, pH 6.5, plus 2nM glucose oxidase, at 25 degrees, final volume 1.0 ml. Glucose at 4 mM (single arrowheads) initiated compound II formation.
(A) Ethanol and NADPH induced decompositions of compound II.Compound II formation in the presence of 11μM $K_4Fe(CN)_6$. Additions of (**b**) 82 mM ethanol or (**c**)17.5 μM NADPH as indicated (double arrowhead) with (**a**) serving as control.
(B) Ferrocyanide-induced compound II formation with or without NADPH.Compound II formation in the presence (**a,c,d**) or absence (**b**) of 11 μM $K_4Fe(CN)_6$ as indicated, with prior addition of (**c**) 82 mM ethanol or (**d**)17.5 μM NADPH, with (**a**) serving as control.

Figure 49

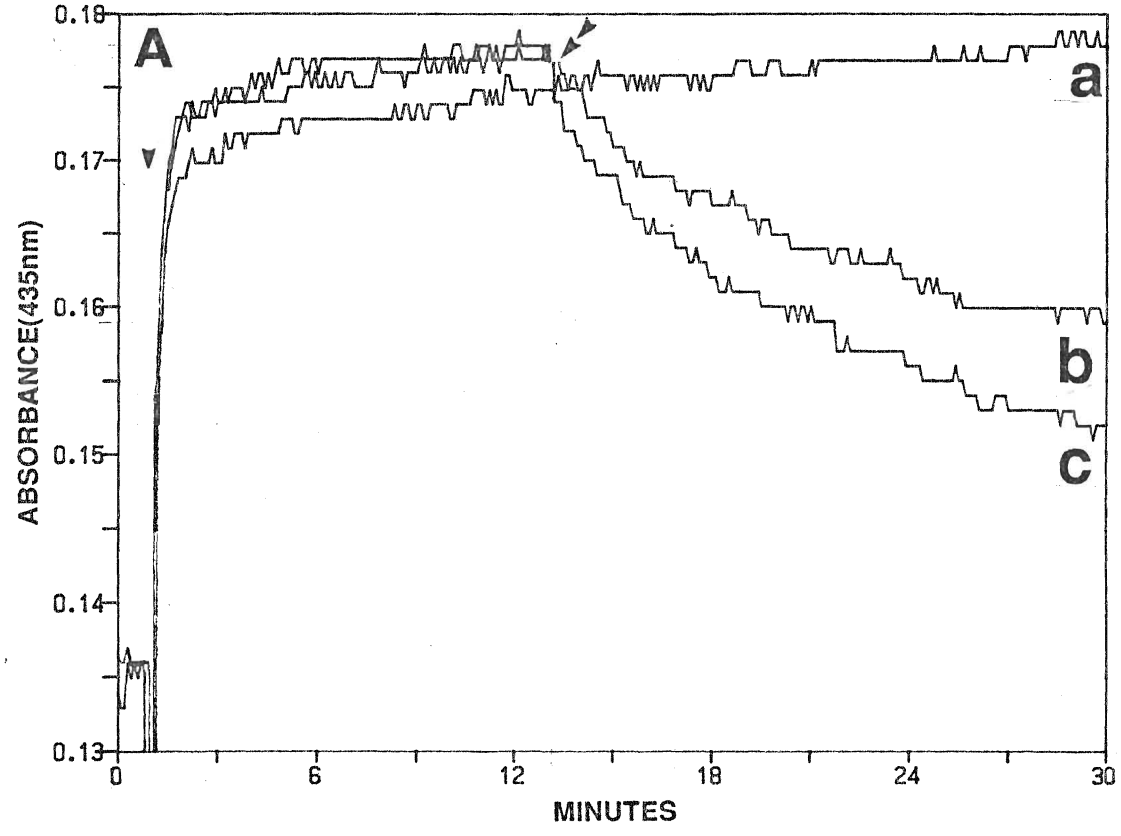
A
a
b
c
ABSORBANCE(435nm)
0.18
0.17
0.16
0.15
0.14
0.13
0
6
12
18
24
30
MINUTES

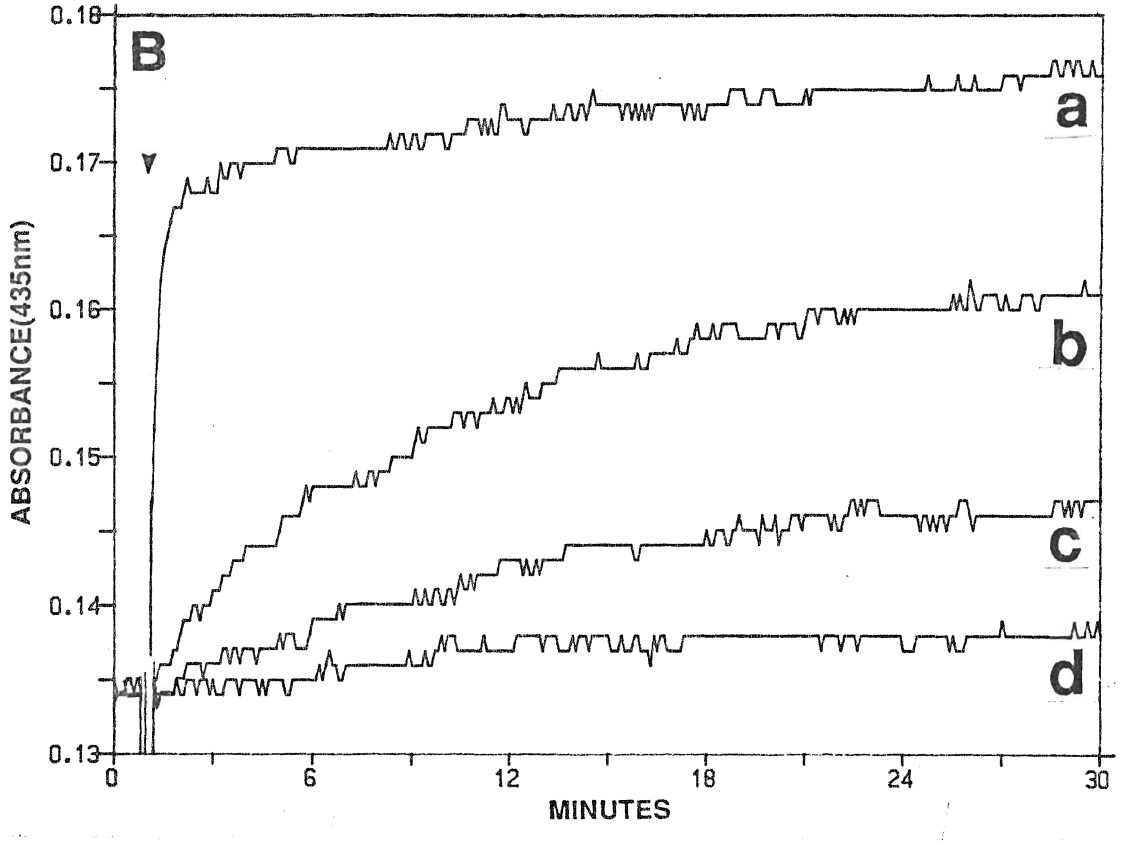
B
a
b
c
d
ABSORBANCE(435nm)
0.18
0.17
0.16
0.15
0.14
0.13
0
6
12
18
24
30
MINUTES

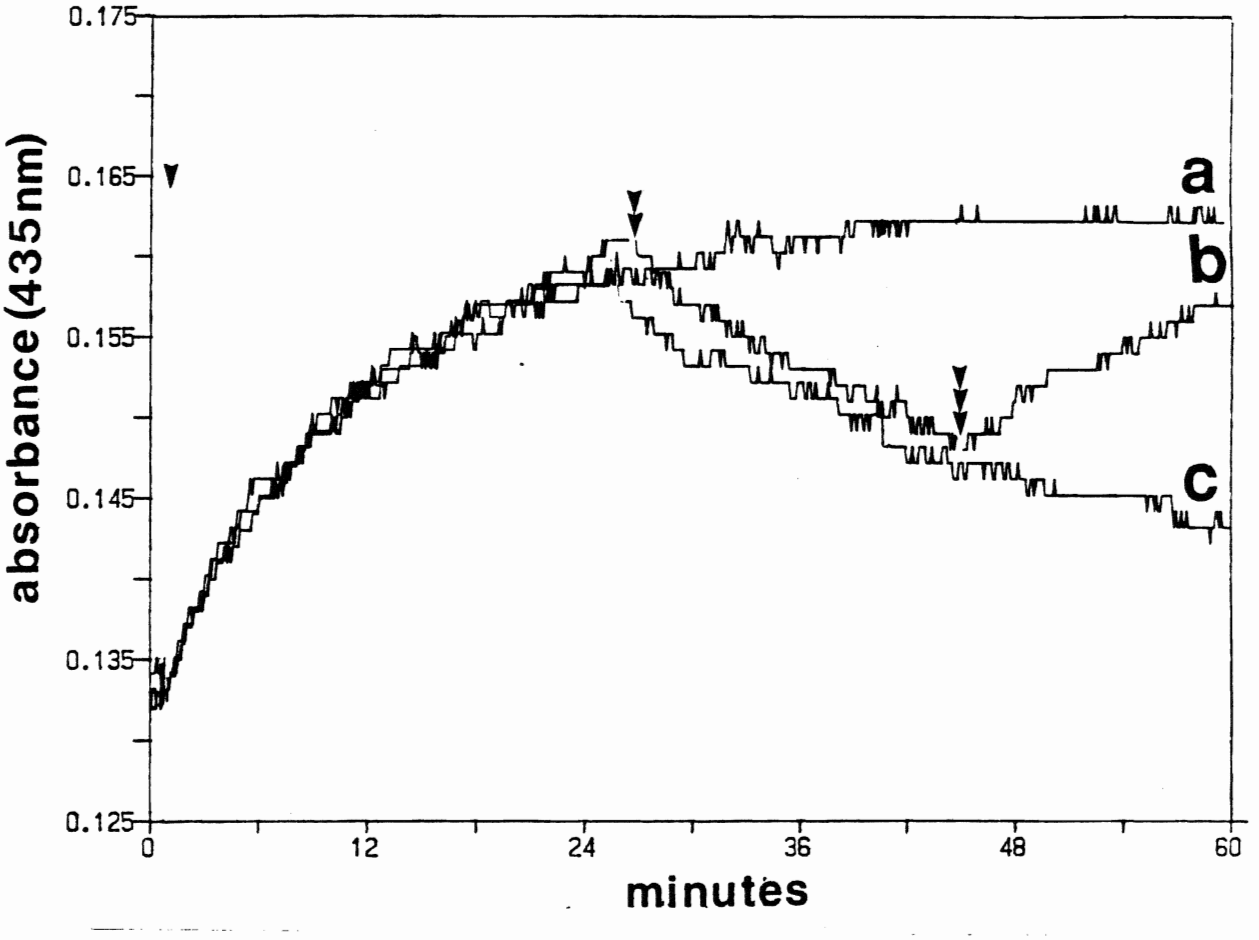

Figure 50. Effect of the order of addition of hydrogen donors to BLC compound II.
Experimental conditions as described in Fig. 49. Glucose (4mM) added to system (single arrowhead) initiated compound II formation. 200mM ethanol (**b**) or 18μM NADPH (**c**)added exogenously (double arrowheads) with final addition of 10μM $K_4Fe(CN)_6$ (triple arrowheads), and with control (**a**) as shown.

the control. NADPH is thus a more potent inhibitor of compound II formation than ethanol, although the concentrations of the two donors used differ by over three orders of magnitude.

To ensure that the order of addition of the donors did not affect the experimental results, the experiment shown in Figure 50 was performed. Upon reaching the approximate steady state level for compound II, either ethanol (trace a) or NADPH (trace b) was added to the system. Depletion of compound II was monitored for at least fifteen minutes before ferrocyanide was added as well. Ferrocyanide thus induces the formation of more compound II even in the presence of ethanol while ferrocyanide is ineffective in forming compound II in the presence of NADPH. In conjunction with the results shown in Figure 49, therefore, it appears that electron donation by ferrocyanide is effectively blocked by NADPH.

iv Steady-state kinetics of SCCT and SCCA compound II: effects of ferrocyanide and NADPH

The Soret spectrum of SCCT was monitored under conditions of continuous hydrogen peroxide generation as indicated in Fig. 51. As shown in the figure, the 405nm band of the SCCT declined with a concomitant red-shifted increase in absorbance after thirty minutes (small broken line spectrum), a pattern identical to that seen in Figure 34 for the bovine liver enzyme. To determine whether these spectral shifts were the results of compound I and compound II formation, sequential additions of ferrocyanide and ethanol were made after thirty minutes of hydrogen peroxide generation . Ferrocyanide addition increased the red-shifted absorbance region with little effect on the 403nm absorbance band one minute after addition (large broken line spectrum). Ethanol immediately restored the band at 403nm to almost

the original absorbance level of the ferricatalase, with no decay of the red-shifted region of the spectrum (dotted line spectrum). The effects of these donors thus indicate the existence of peroxide compounds analogous to those of the bovine liver enzyme.

Figure 52A (trace a) shows the slow formation of compound II (monitored at 435nm) for *Saccharomyces cerevisiae* catalase "T" fraction in the presence of the glucose oxidase/glucose system generating hydrogen peroxide at a constant rate. The rate constant under these conditions was estimated to be $3.8 \times 10^{-3} s^{-1}$. The effect of preaddition of NADPH is shown in trace b, with the typical NADPH oxidation-dependent lag phase apparent. The effect of ferrocyanide addition to the samples is also shown following the attainment of steady state levels of compound II. Trace a indicates an increased formation of compound II due to the one electron reduction of compound I by ferrocyanide. Trace b shows a corresponding susceptibility of catalase to ferrocyanide reduction, subsequent to the complete oxidation of the preadded NADPH.

Figure 52B shows the effect of ferrocyanide preaddition and the subsequent effect of NADPH addition to a sample of *Saccharomyces cerevisiae* catalase "A", under conditions of constant hydrogen peroxide generation. Similar to the case of BLC, ferrocyanide preaddition accelerates the formation of compound II, and NADPH addition causes its depletion. A slow rise in compound II concentration is then apparent following oxidation of the added NADPH. A role of NADPH in preventing compound II formation, and an ability to deplete the steady state level of the compound, for the catalases of the yeast *Saccharomyces cerevisiae*, thus would appear to be similar to that of the BLC.

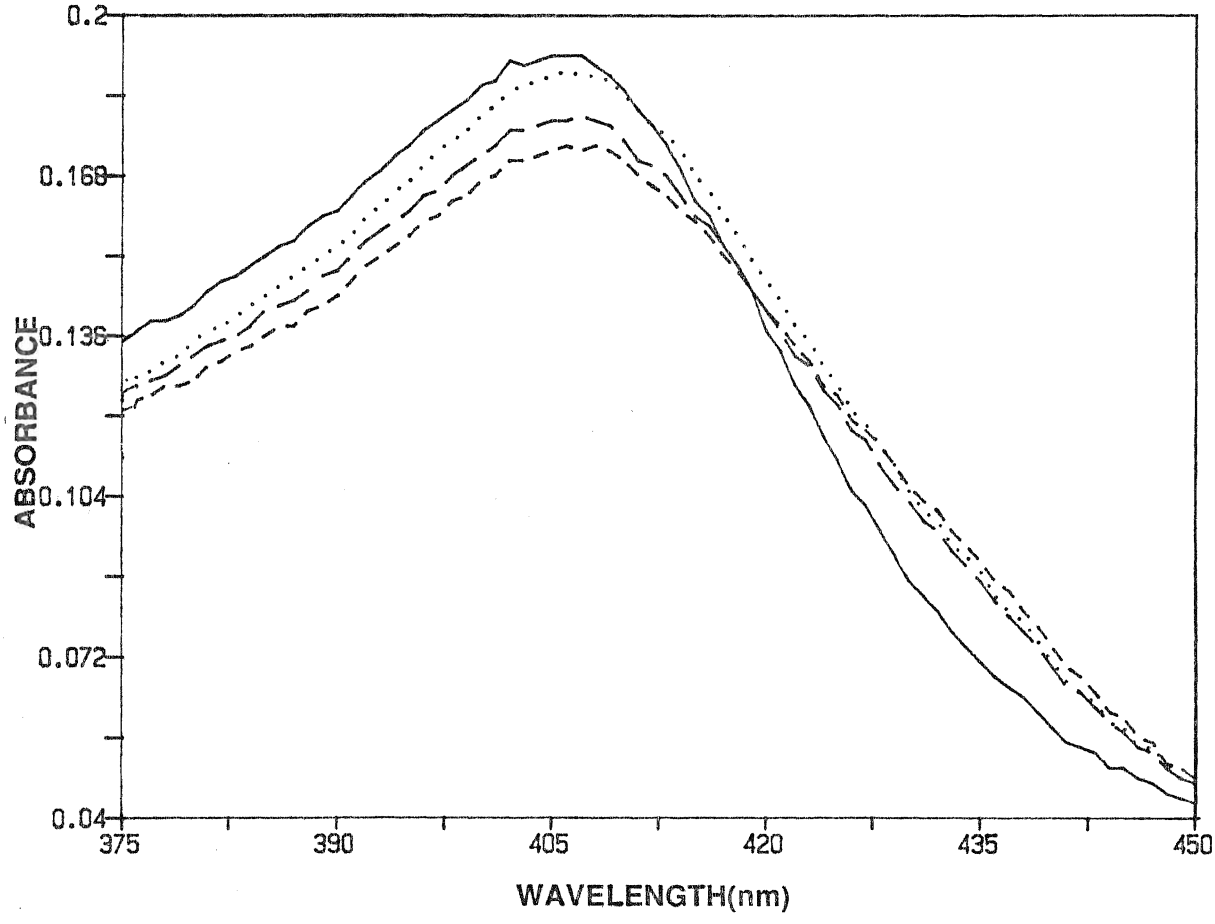

Figure 51. Time course of formation of SCCT peroxide compounds.
Soret spectra for 3μM hematin SCCT in 10mM aerobic potassium phosphate, pH 6.5, glucose oxidase at 4nM, to a final volume of 0.3ml. Glucose (4mM) initiated the formation of compound II. Spectrum prior to glucose addition at t=0min. (solid line) shown versus spectra at 30min after addition of glucose (large broken line), at 45min after 15min. exposure to ferrocyanide at t=30min (small broken line), and at 45min with exposure to 1M ethanol for 1min (dotted line).

Figure 52. Effects of Ferrocyanide and NADPH on the formation and decay of compound II of the *Saccharomyces cerevisiae* catalases.
(**A**) SCCT (4 μM hematin catalase) in aerobic 10 mM potassium phosphate, pH 6.5, plus 5nM glucose oxidase, at 25degrees, final volume 0.2ml. Glucose at 4 mM (single arrowhead) initiated compound II formation. Preaddition of 13μM NADPH (trace **a**) with subsequent additions of 16μM $K_4Fe(CN)_6$ (double arrowheads), with trace **b** serving as control. (**B**) SCCA (2.3 μM catalase) under conditions as described in Fig. 52A, final volume 0.2ml. Pre-incubation with 25μM $K_4Fe(CN)_6$. Glucose at 4 mM (single arrowhead) initiated compound II formation with 20μM NADPH (double arrowhead) added upon formation of compound II formation. Trace smoothed using Savitz-Golay function over 15 data points per calculation.

Figure 52

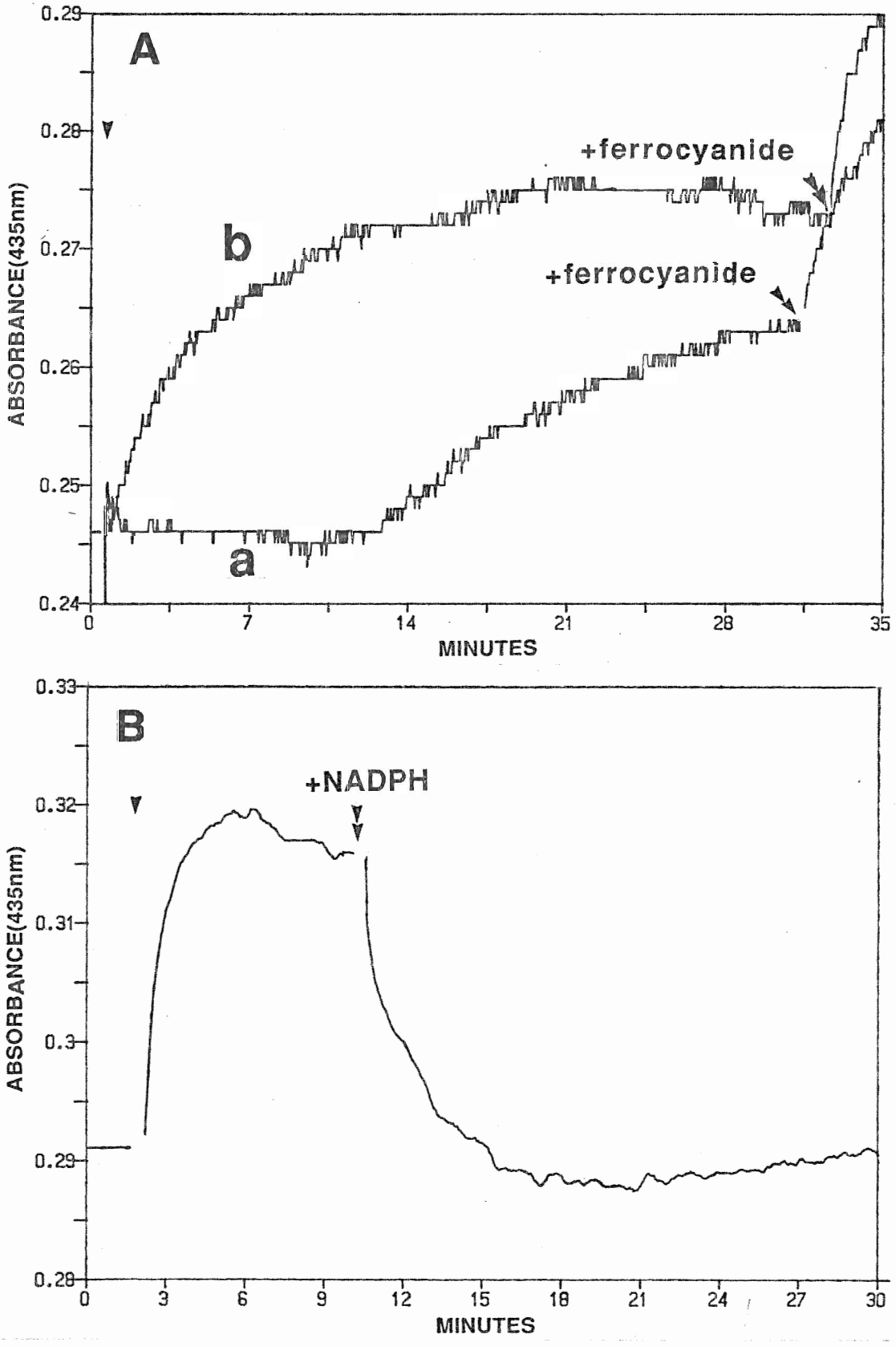
A
+ferrocyanide
b
+ferrocyanide
a
ABSORBANCE(435nm)
0.29
0.28
0.27
0.26
0.25
0.24
0
7
14
21
28
35
MINUTES
B
+NADPH
ABSORBANCE(435nm)
0.33
0.32
0.31
0.3
0.29
0.28
0
3
6
9
12
15
18
21
24
27
30
MINUTES

CHAPTER IV. DISCUSSION

A. EVIDENCE FOR THE REPLACEMENT OF HEME *d* BY PROTOHEME IN HPII MUTANT CATALASE PROTEINS

i. Nature of the catalase hemes

The replacement of heme *d* in HPII site directed mutant proteins with protoheme has been demonstrated. Comparisons have been made with results obtained for the HPII wild type protein and the BLC, SCCT, and SCCA proteins by three methods:

(a) Absorption spectroscopy of unmodified catalase proteins;
(b) Absorption spectroscopy of reduced alkaline pyridine hemochromes; and
(c) Monitoring absorption changes during titrimetric addition of classical heme ligands (cyanide and formate).

The results confirm that BLC is a typical protoheme enzyme. The spectrum of the native protein (Fig. 10) has maxima at wavelengths that correspond closely to those obtained previously (Nicholls and Schonbaum, 1963; Samejima and Yang, 1963). The spectrum of the reduced alkaline pyridine hemochrome of BLC (Fig. 15) has diagnostic maxima (α and β bands) indicating the sole presence of protoheme (ferriprotoporphyrin IX) , in accordance with results previously obtained (Stern, 1936). Titration of BLC with cyanide results in spectral shifts indicative of a high to low spin transition in the

coordination of the heme iron; i.e. a decrease in Soret band intensity with a red shift and replacement of the main band in the visible region with a blue shifted band. Values at specific wavelengths were used to prepare secondary plots of the data in the form of double reciprocal and Hill plots (see Appendix A). Titration of BLC with cyanide gave both a linear double reciprocal and a linear Hill plot (Fig. 22), indicating that the titrated species behaved as a homogeneous ligand binding population. The titration of BLC with formate resulted in spectral shifts indicative of a high spin perturbation of the heme iron, i.e., an intensification of the absorption and a slight blue shift in the visible region (Fig. 17). Double reciprocal and Hill plots prepared from these data were also linear, indicating that the titrated protein species behaved as an homogeneously monophasic ligand binding population. These investigations characterize BLC as containing only one ligand binding species, protoheme.

The spectra for both SCCT and SCCA proteins (Fig. 10) correspond closely to those obtained in previous characterizations (Seah and Kaplan, 1973; Seah *et al.* 1973). Major differences in the spectra between the two catalases are absent. Comparison of the SCCT and SCCA spectra with that of BLC shows similarity in both the positions of the bands and their relative intensities. This correspondence between spectral characteristics extends to the reduced alkaline pyridine hemochromes. The α and β bands diagnostic of protoheme are present in the spectra for the SCCT and SCCA, as they are for BLC (Fig. 15). SCCT and SCCA therefore also contain protoheme. The SCCT and SCCA proteins may be differentiated, however, on the basis of both their SDS denatured PAGE profiles (Fig. 14), and their specific catalatic reaction rates (Fig. 13, Appendix B)

Titration of SCCT and SCCA with cyanide produced results similar to those obtained for the analogous titration of BLC. Secondary plots based on the data indicate that the two catalases titrate monophasically with cyanide. Both the double reciprocal plot and the Hill plot for each catalase show a linear relationship (Figs. 24, 25). SCCA has a greater affinity for HCN than does SCCT, based on the dissociation constants estimated from the secondary plots (Table III), but these values do not differ greatly between the two catalases, nor between them and BLC. Formate binding by SCCT and SCCA was weak under present titration conditions, and may be attributed in part to the sensitivity of the ligand to pH. Partial titrations for these proteins suggest that the binding is monophasic, but this remains to be confirmed. In comparison with BLC, results of both cyanide and formate binding with *Saccharomyces cerevisiae* catalases, in conjunction with the other spectral characterizations, indicate that all these catalases contain a homogeneous population of protoheme prosthetic groups.

The spectrum of the HPII catalase of *E. coli* is different from that of BLC (Fig. 10). A difference is also apparent when comparing the spectrum of the HPII wild type reduced alkaline pyridine hemochrome with that of BLC (Fig. 16 cf. Fig. 15). The reduced pyridine hemochrome shows that the principal heme present in the catalase is not protoheme, but that of a chlorin, or *d* type heme. This characterization compares reasonably with spectral studies carried out previously (Claiborne *et al.* 1979), although the broad hemochrome band at 607nm is two nm blue shifted with respect to the same band in the earlier work, and apparently 6nm blue shifted compared with other reported results (Barrett, 1956; Chiu *et al.* 1989). Heme *d* isolated from the terminal oxidase complex of *E. coli*, however, yields a reduced pyridine

hemochrome with only one peak at 602nm in the visible region (Vavra *et al.* 1986). Variation in the mode of hemochrome preparation may be the cause of these discrepancies.The reduced alkaline pyridine hemochrome of HPII also had two additional absorption peaks that were not previously reported. Whether these are due to the presence of other heme species in lesser quantities or whether these peaks are artefactual due to the method of hemochrome preparation, remains uncertain.

Titration of HPII with cyanide gave results similar to those obtained for the cyanide titration of BLC, SCCT, and SCCA. Data replotted in double reciprocal and Hill plots both indicate a simple relationship between ligand concentration and spectral shift monitored in the Soret region (Fig. 28). The estimated dissociation constant of the HPII-cyanide complex is similar to the values obtained for the other catalase proteins (Table III). Titration of HPII with formate is likewise similar to the results indicated for BLC. The complex formed is spectroscopically indistinct, but the secondary plots also show monophasic binding (Fig. 29). Therefore, titrations of HPII with both cyanide and formate indicate the presence of a single heme population which is predominantly heme *d*.

The modification of the HPII catalase via site-directed mutagenesis yields proteins that differ from the wild type in terms of characteristic absorbances (Figs. 11,12), specific rate constants (Table I), and heme ligand binding properties (summarized in Table III). A qualitative evaluation of the reduced pyridine hemochrome spectra as well as the absolute absorbance spectra of the proteins shows that at least two different species of heme prosthetic group appear to be present in the proteins. HPII normally contains a *d* type

TABLE III. Summary of ligand binding properties of catalases and HPII mutant proteins

CATALASE	CYANIDE BINDING (pH 6.5)	FORMATE BINDING (pH 6.5)
Bovine liver	MONOPHASIC	MONOPHASIC
	K_d 12μM (8μM[1])	K_d ≈3mM (4mM[1])
Saccharomyces A	MONOPHASIC	Small Spectral Shift
	K_d 11μM	(K_d >400mM)
Saccharomyces T	MONOPHASIC	Small Spectral Shift
	K_d 110μM	
HPII wild type	MONOPHASIC	MONOPHASIC
	K_d>> 87μM	K_d ≈100mM
H128A	K_d>> 100mM	NONE
H128N	NONE	NONE
N201Q	BIPHASIC	Small Spectral Shift
	K_d7mM 45%	
	K_d21μM 55%	
N201A	BIPHASIC	Small Spectral Shift
	K_d3.6mM 25%	
	K_d230μM 75%	
N201H	BIPHASIC	Small Spectral Shift?
	K_d1.4mM 83%	
	K_d 65μM 17%	

1: (Nicholls and Schonbaum, 1963)

heme (Figs. 10,16), characterized as heme d_{cis} (the designation indicates the position of the hydroxyl groups relative to the plane of the heme on the C pyrrolic ring of the porphyrin). Heme d_{trans} is found in the terminal oxidase ba_1d complex of *E. coli*. The stereoisomers (Fig. 53) are specific to the systems they are found in. The unusual incorporation of protoheme in the mutant proteins of HPII, is sometimes nearly exclusive (Fig. 16; N201H), sometimes partial (Fig. 16, N201A), and sometimes not apparent at all (Fig. 16, N201Q and wild type HPII), based on the spectra of the reduced alkaline pyridine hemochromes for the HPII mutant proteins compared to the alkaline pyridine hemochrome spectrum of HPII (also see Table III). Replacement by oligonucleotide-directed mutagenesis of the critical histidine axial ligand of the heme in HPII (H128) results in the apparent substitution of the hemed_{cis} with protoheme and the functional inactivation of the enzyme (Figs. 11,16, Table III). Replacement by mutagenesis of the putative "essential" asparagine residue (N201) of HPII results in the replacement of hemed_{cis} in some proteins with protoheme in various proportions. Changing this asparagine residue yielded mutants ranging in activity from poor to undetectable compared to the catalatic activity of the wild type protein (Table I). The asparagine residue would therefore seem not to be essential to the function of the protein as a catalase, but to be important in the role of orienting the substrate, H_2O_2, for proper reaction at the heme's catalytic site. A possibility exists that the functionality of the relevant N201 mutant proteins derives from a very small population of the proteins that incorporate the heme *d*. Limits to the sensitivity of absorbance spectrophotometry and other techniques as employed in these investigations makes it

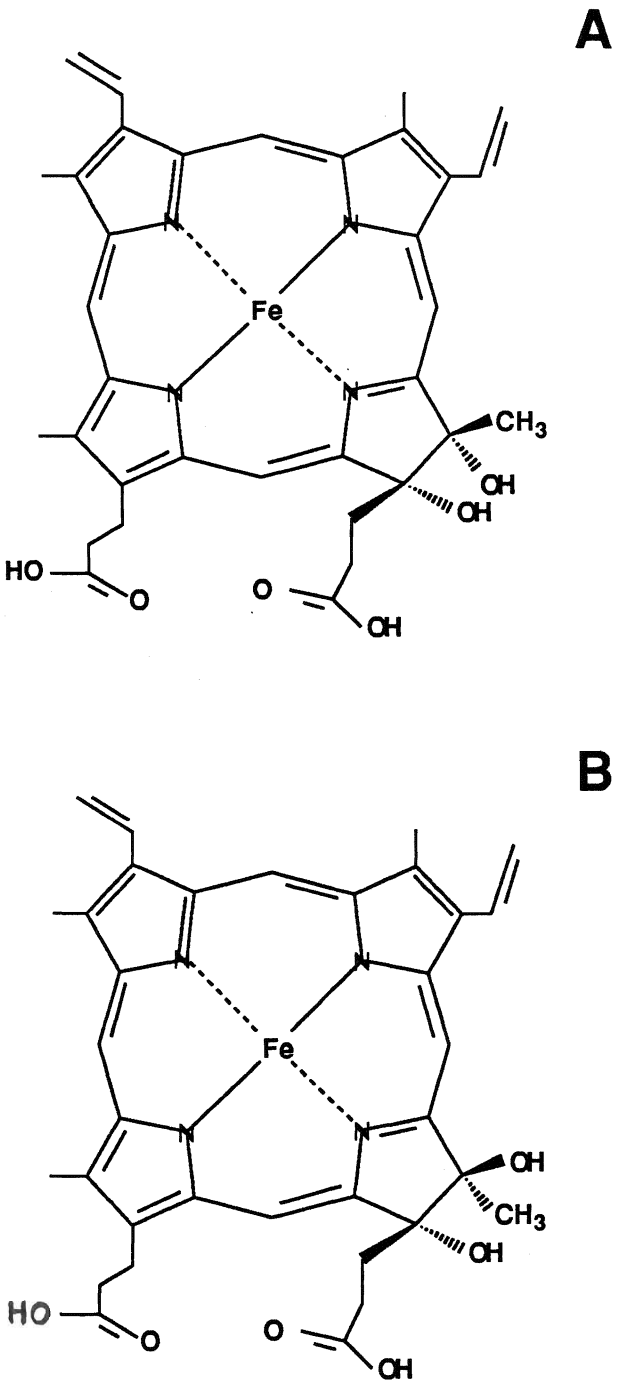

Figure 53. Stereoisomers of heme *d*
(**A**) Structural representation of heme d_{cis} (**B**) Structural representation of heme d_{trans}

difficult to determine if such a phenomenon were indeed taking place.

The cyanide titration of the HPII wild type compared to that of the N201 mutant proteins provided corroboration of the presence of a heterogeneous heme population (TABLE III, Fig. 28 cf. Figs. 33, 35, 37). The populations of low and high affinity ligands present, however, did not coincide with the estimated population of each heme from the reduced alkaline pyridine hemochrome spectra; this may reflect the presence of other binding species of similar affinity to those estimated by cyanide titration. In all cases, formate binding was of very low affinity in all trials, except for that of the wild type. The hypothesis that the structure of the heme crevice solely determines the heme that will be incorporated is unsatisfying. Thus, the mutant proteins, apart from the H128 family, incorporate not just a replacement heme, but a mixture of the wild type heme *d* and protoheme. One possibility is that the hemes are incorporated at different times during synthesis, so that a heterogeneous population of ligand binding proteins arises. Timkovich and Bondoc (1990) have recently proposed another hypothesis that would explain this phenomenon -that of a heme d_{cis} "self-biosynthesis" from a precursor heme (i.e., protoheme) incorporated into the catalase subunits during formation of the holoenzyme. The attractive feature of this hypothesis is that it eliminates the need for two different enzymes, which would be necessary in the formation of heme d_{cis} and heme d_{trans}. During the first or first few turnovers of the protoheme containing pre-enzyme in this scheme (Fig 54), reactions with oxygen, or peroxides, in the HPII catalase case, would generate oxy or peroxy radicals that attack the β-pyrrolic bond of ring C of the porphyrin (Fig. 54, first reaction), forming an epoxide (Fig. 54, second reaction).

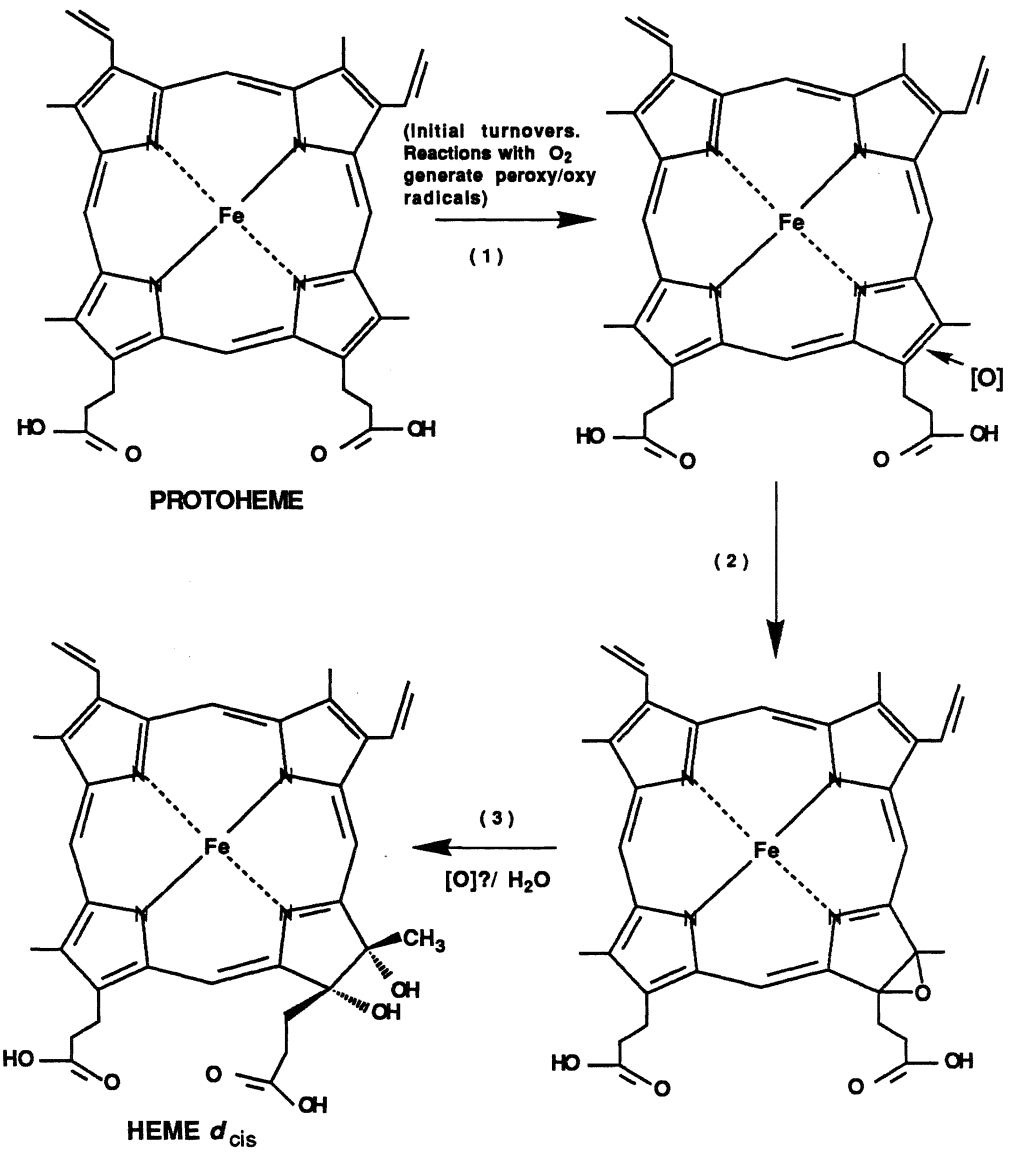

Figure 54. Hypothetical mechanism of heme conversion from protoheme to heme *d*.
Scheme adopted from Timkovich and Bondoc (1990). In the initial reaction **(1)**, the protoheme reacts with hydrogen peroxide, leading to other reactions generating oxy/ peroxy radicals. The radicals formed attack the heme at ring III (C), causing epoxidation **(2)**. The epoxide may then further react with other radicals or add water to form the heme d_{cis} diol **(3)**.

Subsequent reactions, possibly also implicating radicals or a hydrolysis, could then open the epoxide into a diol, the regiospecificity and isomerism of which would be governed specifically by the heme pocket of the surrounding protein (Fig. 54, third reaction). The protein may then rearrange the heme pocket to accomodate the newly structured heme and thus become the functional catalase, or, in the case of heme d_{trans}, the functional terminal oxidase. Such a scheme could provide the explanation for the heme mixture that appears in several of the mutant proteins of HPII catalase. If protoheme were intercalated to give the pre-enzyme suggested, in a system that has the heme pocket pre-modified via mutagenesis, to decrease the likelihood of formation of the final modifications to the heme (i.e. formation of heme d_{cis} via the route proposed above), then only a random proportion of the protoheme containing proteins would be converted to heme *d* catalases, perhaps only accidently achieving the final heme structure necessary to carry out the catalytic reactions. Mixtures of the pre-enzyme (protoheme containing protein) and functional enzyme (heme *d* containing protein) could then be recovered in proportions depending on how disruptive the residue modification in the heme pocket is to the process of heme conversion. Two types of result indicate that this is the case. Firstly, the characterizations of the HPII mutant proteins (Figs. 11,12, 16, TABLE III), secondly, the results with the HPII mutant protein N201H showed that it underwent a spectral shift indicative of the formation of a *d* type heme from a predominantly protoheme population, when the protein was exposed to H_2O_2, generated constantly at low levels by a glucose oxidase/ glucose system (Fig. 38). Similar spectral changes have been observed with the same mutant HPII catalase after 24 hours in the presence of ascorbate (von Ossowski *et*

al, in press). These data are also in accordance with the observation that hemoproteins treated with ascorbate form green pigments such as verdohemochrome and biliverdin-apoprotein complexes via coupled oxidation reactions (see Takeda *et al.* (1980), for a discussion).

ii. Future Investigations

In order to understand the phenomenon of *in situ* heme conversion as probed by studies of the HPII mutant proteins, and to justify the assumption that the presence of heterogeneous heme populations in the N201 proteins are results of such heme conversions, further investigations must be undertaken. Of primary importance would be the extraction of heme from the proteins for more detailed analysis. Structure probing techniques such as isotope exchange NMR spectroscopy and infra-red spectroscopy as employed in previous investigation of the HPII wild type prosthetic group (Chiu *et al.* 1989) would provide evidence for or against the Timkovich and Bondoc proposal. Should the phenomenon be validated, a second question must be answered; how does the nature of the heme pocket of the enzyme govern the specificity of the conversion of the heme? Further investigation of the problem using other site-directed mutants of HPII catalase with appropriately altered residues in the region of the heme pocket could provide additional insights into the mechanistic aspects of heme conversion or catalysis of the enzyme, as has already been provided by the H128 and N201 mutants as part of this study.

Perhaps the most difficult aspect of the heme conversion hypothesis to explain would be the case of formation of the terminal oxidase complex of *E. coli,* containing the ba_1d heme cluster. While

HPII is inducible under conditions of aerobic oxidation stress, and heme *d* could be readily formed due to the presence of excess peroxide in the cytosol, the terminal oxidase under identical conditions utilizes a heme *o* rather than the heme *d* containing system. In fact, the ba_1d complex is only produced when the *E. coli* strains are grown under severely limiting oxygen conditions (Timkovich and Bondoc, 1990). It is unclear as to how heme *d* could be efficiently produced by heme conversion for the terminal oxidase under such conditions, nor does it make sense that two enzyme systems induced under opposite conditions would utilize hemes so structurally similar. The possibility has been raised by Timkovich and Bondoc (1990) that heme *d* or its possible biosynthetic enzymes are constitutive. Further biochemical and physiological studies are necessary to determine whether either of these is in fact the case, or whether formation of heme *d* in all instances is due to a heme conversion process.

B. INTERACTION OF NADPH WITH THE CATALASES

NADPH is bound by BLC, as shown both by dye-linked affinity chromatography (Fig. 39A) and the fluorescence emission spectrum of the enzyme when excitation at 340nm is employed (Fig. 41). The binding of NADPH to BLC has been previously well characterized by several techniques (Kirkman and Gaetani, 1984; Fita and Rossmann, 1984) including dye-linked affinity chromatography (Jouve *et al.* 1986), but prior to the present, results had not been directly sought via fluorimetry. Both SCCT and SCCA also bind NADPH, as shown by dye-linked affinity chromatography (Fig. 40A,B) and probably by the fluorescence emission difference spectra for SCCT after exposure of the enzyme to excess NADPH (Fig. 42). This is the first time that NADPH has been reported to bind eukaryotic catalases other than the mammalian enzymes from bovine liver, human blood, and canine tissue (Kirkman and Gaetani, 1984).

In contrast to the results with the eukaryotic catalases, HPII wild type protein has been shown to be non-NADPH binding by dye-linked affinity chromatography (Fig. 39B). Fluorescence emission of the protein with excitation at 340nm, even after exposure to excess NADPH, also gave no indication of bound NADPH (Fig. 42). Jouve *et al.* (1989) have carried out the only other investigation of NADPH interaction with prokaryotic catalases, although crystallographic data indicates NADPH is bound to the catalase of *Micrococcus lysodeikticus* (Jouve *et al.* 1991). Their study of the catalases from *Proteus mirabilis* PR (Peroxide Resistant) strains showed that the PR catalase tightly bound NADPH. The phenomenon was similar to that observed for the BLC,

with two enzyme fractions of the *Proteus* enzyme recovered via anion exchange chromatography that differed only with respect to the quantity of NADPH bound. Though no data regarding the nature of the heme prosthetic group via pyridine hemochrome formation or other methodology has been published for the the *Proteus* enzyme, the absorbance spectrum (Jouve *et al*, 1983) indicates that the protein most likely contains protoheme. This alone reinforces that the HPII enzyme (heme *d* containing) is fundamentally different from *Proteus mirabilis* catalase and gives added weight to the argument that HPII would not be expected to bind NADPH.

The finding that the SCCT and the SCCA proteins bind NADPH is anticipated, as the characterization of these proteins by spectroscopic methods has shown them to be similar to the BLC (Figs 10, 15) However, this obviously eliminates the possibility that these isozymes are distinguishable by their ability to bind NADPH. *Aspergillus niger* catalase, though unusual in that it is a glycoprotein, has spectroscopic similarity to BLC and indeed has been shown to contain protoheme. This catalase, however, has also been shown to be non-NADPH binding. Jouve and coworkers (1989) have proposed that NADPH binding to a catalase is intimately related to the propensity of the catalase to form an oxoferryl compound II species (Fe^{IV}=O), which is catalytically inactive. They predict that only catalases containing protoheme as the prosthetic group, capable of forming compound II species analogous to those observed in mammalian catalases, would bind NADPH. This is certainly the case for the *Saccharomyces cerevisiae* enzymes, which undergo spectral shifts analogous to those seen for compound II formation in BLC in the presence of steadily generated H_2O_2 (Figs. 51, 52). This would also explain why the *Aspergillus niger* and HPII

catalases do not bind NADPH, as neither enzyme exhibits the spectral shifts indicative of compound II formation. Further attempts at validation of this hypothesis with other protoheme containing catalases will provide a better understanding of the apparent evolutionary conservation of the NADPH binding site on catalases and its possible relationship to the prosthetic groups used by different catalases.

C. HYDROGEN DONOR MODULATION OF CATALASE SECONDARY PEROXIDE COMPOUND FORMATION

i.Comparison of donor effects: classification of NADPH and NADH as unique two-electron donors to catalase compound I

The formation of bovine catalase peroxide compounds (Figs. 43, 46) was followed under experimental conditions similar to those used previously (Chance, 1950A; Kirkman et al. 1987), employing glucose oxidase in presence of glucose to generate H_2O_2. The hydrogen peroxide steady state concentration in the presence of micromolar concentrations of catalase in this type of experiment has been estimated by Chance (1950A) to be on the order of 1nM. Catalase compound II formation is enhanced under these circumstances due to the "endogenous donors" on the protein contributing to reduce compound I after the initial two electron oxidation by a peroxide molecule.

The addition of exogenous hydrogen donors to the catalase/ glucose oxidase system affects the formation or the steady state concentration of compound II, depending on the type of donor added. Ethanol, a two electron donor, induces the disappearance of compound II by rapid reaction with compound I, allowing the endogenous donors present to react with the inactive secondary compound (Fig. 46A). NADPH, tentatively characterized as a two electron donor (Kirkman *et al.* 1987), also induces the disappearance of compound II at a rate of the same order of magnitude as that for ethanol (Fig. 46A). Pre-incubation of the system with either of these two exogenous donors prevents formation of compound II (Fig 46B). NADH is also effective in depleting compound II and preventing its formation, though the oxidized forms of either the NADPH or NADH are not (Fig. 48). Ferrocyanide, a one

electron donor, induces the accelerated formation of compound II by apparent reaction with compound I(Figs. 44, 49).

Several features exhibited by NADPH as an electron donor to catalase make it difficult to consider the cofactor as a two-electron donor analogous to ethanol. Firstly, NADPH is effective in preventing compound II formation and causing its removal at micromolar concentrations. Ethanol, in contrast, must be added at concentrations in the millimolar range in order to have comparable effect, as is indeed seen in Fig. 46. Secondly, were NADPH to react with catalase compound I with a rate constant similar to that of ethanol (estimated by Chance (1950B) to be 1×10^3 $M^{-1}s^{-1}$), then donation of electrons by micromolar concentrations of NADPH should be effective in preventing formation of compound II for several seconds at the most. As can be seen in Fig 45, 47, the oxidation of NADPH occurs over a period of tens of minutes. Similarly, the NADPH titration (Fig. 47) indicates that compound II formation is inhibited by exogenously added NADPH for periods extending for minutes and proportional to the NADPH concentration. Finally, ethanol and NADPH are not equally effective in preventing formation of compound II when preincubated with ferrocyanide (Fig. 49B) or when ferrocyanide is added following the addition of either ethanol or NADPH upon attainment of compound II steady state (Fig. 50). These features suggest that NADPH does not react directly with compound I.

The function of catalase bound NADPH has been shown to be prevention of the formation of compound II (Kirkman *et al*, 1987). NADPH however, must engage in a reaction that donates only one electron to the inactive compound II complex to regenerate ferricatalase, if the nucleotide is not reacting directly with compound

I. The paradox is that physiological NADPH oxidation is usually a two electron process, leaving the question open as to whether the reduced dinucleotide donors should be classified in one of the groups in the original scheme developed by Keilin and Nicholls (1958), or whether they belong to a new class of donor.

Of the six groups of hydrogen donors identified by Keilin and Nicholls, three contain members capable of preventing the formation of compound II. Group two donors are phenols. They both accelerate the formation of compound II and cause its decomposition. As NADPH and NADH do not accelerate compound II formation, they cannot be group two donors. Group three consists of alcohols and formate. Alcohols prevent the formation of compound II by donation of two reducing equivalents to compound I and also cause the decomposition of compound II at steady state by removal of compound I, but only at molar ratios to peroxide concentration of 1000 times or greater. NADPH causes the decomposition of the compound II steady state at a rate approximately that of ethanol (Fig. 46 and Kirkman *et al*, 1987). However, NADPH is effective at micromolar concentrations, implying that it must react with compound I with a bimolecular rate constant at least three orders of magnitude greater than that of ethanol. NADPH and NADH are therefore not group three donors. Group four consists of only nitrite. This donor is capable of decomposing compound II at a rate of 1.3×10^6 $M^{-1}s^{-1}$ (Nicholls and Schonbaum, 1963). The reaction has been characterized to take place in one-electron steps, although nitrite has two reducing equivalents available. In addition, nitrite can prevent the formation of compound II by donation of both reducing equivalents to compound I (Chance, 1950B). NADPH and NADH are incompatible with membership in this group because of their slow oxidation rates when

bound to catalase. Based on these arguments against the inclusion of NADPH/NADH in the classes of electron donors of Keilin and Nicholls, it must therefore be concluded that nicotinamide adenine dincleotide cofactors constitute an unique class of two-electron donors in the reaction cycles of catalase.

ii. A model for the mechanism of NADPH inhibition of compound II formation

The classification of reduced nicotinamide adenine dinucleotides as unique two-electron donors must also be accounted for by a general reaction scheme of catalase with such donors. The modified scheme must incorporate features that explain the following:

(a) why NADPH does not react with compound I directly (i.e. is not reacting similarly to ethanol),

(b) how NADPH blocks the rapid formation of compound II by ferrocyanide,

(c)and how NADPH is effective, yet its oxidation is approximately three orders of magnitude slower than the oxidation of other two-electron donors (such as ethanol).

A model incorporating all these features is shown in Figure 55. Radical migration and intramolecular electron transfer has been shown to occur in various hemoproteins, and is invoked in the model presented. A more detailed discussion of this phenomenon and its implications for catalase will be given in the following section of this chapter.
The model (Figure 55) postulates that a protein radical species is formed upon spontaneous decay of the compound I porphyrin radical. The oxidizing equivalent can then either oxidize some other component of the system in an irreversible reaction, or could be reduced by one of the NADPH's two available electrons, the other reducing the heme iron back to the ferric state. This process may involve a concerted mechanism or proceed via an additional radical intermediate. The hypothetical concerted mechanism is the more parsimonious and is thus favoured

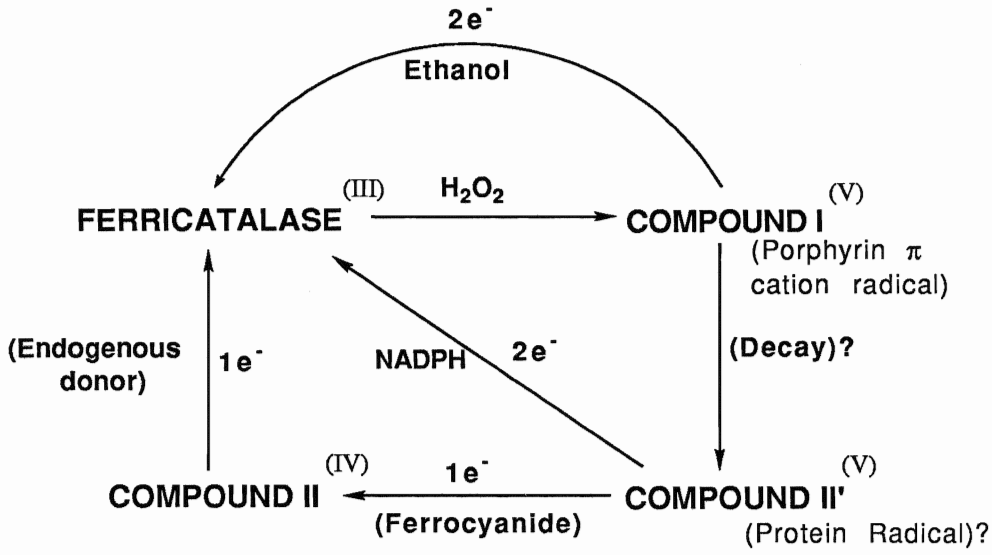

Figure 55. Scheme for NADPH oxidation by catalase and protection of the enzyme from inactivation through compound II formation.

Note the presence of a postulated protein radical species that both ferrocyanide and NADPH compete for.

here. With regard to the three features presented above, explanations can then be given as follows: a) NADPH reacts not with compound I *per se*, but with its immediate decay product (hypothesized to be a protein radical) as specified in the putative scheme. The oxidation of NADPH is probably a concerted process. b) Ferrocyanide and NADPH compete for the compound I decay product (as seen in Figs. 49, 50), but the binding affinity of catalase for NADPH is sufficiently high (a K_d on the order of 10nM (Kirkman and Gaetani, 1984)) to effectively eliminate ferrocyanide donation to the heme. Ferrocyanide is blocked by NADPH from donating its electron to the heme at any time before the co-factor is completely oxidized. c) NADPH/ NADH oxidation is slow because it is solely dependent upon the concentration of the compound II' species. This also explains why the oxidation rate is of the same order of magnitude as that for the achievement of compound II steady state. A lag phase is absent when the concentration of bound NADPH/NADH is equimolar or below the hematin concentration of enzyme, therefore, because the NADPH/NADH is reacting only with the iron-radical combination on its own subunit, as seen in Figs. 45, 47, and in agreement with previous results (Kirkman *et al.* 1987; Jouve *et al.* 1986).

iii. Formation of protein radicals and intramolecular electron transfer events: an adjunct hypothesis

The formation of a protein radical species via the decay of the compound I oxyferryl porphyrin radical of BLC, according to the scheme proposed above, satisfactorily explains the role NADPH plays in the catalytic cycles of the enzyme as a shunting pathway to prevent inactivation. It is unfortunate, however, that no direct evidence is

available showing electron density consistent with a protein radical centred away from the heme. Until recently, one major source of difficulty for investigations on catalase must certainly have been the fact that no crystalline structure of the protein to atomic resolution was available, as well as the fact that the enzyme is tetrameric and very large. These difficulties are absent for the hemoproteins myoglobin and cytochrome *c* peroxidase (CCP), both of which are well characterized biochemically, are single polypeptide proteins, relatively small, and are structurally known to atomic resolution. Large bodies of evidence accumulated show that the two hemoproteins react with hydrogen peroxide to produce protein radicals. Intricate details of the structure-function relationships of the proteins have been recently probed by sophisticated methods, including site-directed mutagenesis. Such studies have not only confirmed the presence of protein radicals centred of specific residues of the the proteins, but have also shown that they undergo electron transfers from one location in a protein to another. Aspects of the reactions of H_2O_2 with metmyoglobin and with CCP in forming protein radicals will be elaborated on in this discussion in order to present features of the processes that may be reflected in the catalatic reactions of the bovine, *Saccharomyces*, and other NADPH binding catalases. It should also be noted that protein radicals have now been implicated in the normal catalytic cycles of a number of other proteins including prostaglandin H synthase (DeGray *et al.* 1992), pyruvate lyase (Knappe *et al.* 1984), galactose oxidase (Whittaker and Whittaker, 1990), and the leghaemoglobin of soybean root nodules (Davies and Puppo, 1992)

The formation of a protein radical species in either metmyoglobin or CCP requires initial binding of a molecule of neutral hydrogen

peroxide at the heme iron. One of the peroxide hydrogens becomes co-ordinated to an axial ligand of the heme (His-52 imidazole of CCP (Poulos and Kraut, 1980) or the His-64 imidazole of metmyoglobin (Takano, 1977)). The hydrogen is then transferred to the terminal oxygen of the peroxide as the oxygen-oxygen bond is cleaved to yield the compound I oxo-heme species and one molecule of water. Two electrons are required for this cleavage, one of which comes from the iron atom, the other usually from the porphyrin ring of the heme.The π-cation porphyrin radical species thus formed may be reduced via a reaction with a second molecule of peroxide, or, as is of greatest interest in this discussion, quenched by a rapid electron transfer from the protein to form a protein radical species (Ortiz de Montellano, 1992). The resulting species would therefore be analogous to the formal oxidation level of compound II of catalase and peroxidases (i.e. Fe^{IV}).

Early work on the reaction of metmyoglobin with hydrogen peroxide and other substrates showed that the production of the oxyferryl heme species analogous to the compound II of peroxidases occurred in conjunction with rapid transfer of the remaining oxidizing equivalent of the peroxide away from the heme centre and onto the protein. EPR investigations suggested that the radical was centred on the side chain of an aromatic residue thought to be that of a tyrosine, though it was not initially certain that this was indeed the case (Harada and Yamazaki, 1987). Davies (1991) has recently shown that the protein radical initially formed upon electron transfer to the porphyrin is centred at Tyr-103 of equine myoglobin. This was accomplished by probing the accessibility and formation of the radical species by employing chemical scavengers and different substrates in

an investigation of the EPR spectrum. The Tyr-103 radical formed by equine myoglobin, and its counterpart in sperm whale myoglobin, are involved in other reactions apart from the electron transfer that occurs between the residue and the porphyrin. One reaction involves the epoxidation of styrene that occurs in presence of oxygen, which has led Ortiz de Montellano and Catalano (1985) to postulate that a tyrosine peroxyl radical is formed on the protein surface to take part in the reaction. Another reaction involves the formation of a dimer between two molecules of sperm whale metmyoglobin when reacted with H_2O_2, in which a cross-link forms between a Tyr-103 residue on the one protein molecule, and a Tyr-151 on another molecule. The latter reaction has been interpreted to imply an intramolecular electron-transfer occurring between Tyr-151 and Tyr-103 following formation of the Tyr-103 protein radical upon donation of an electron to the heme (Ortiz de Montellano *et al.* 1985). Direct evidence for a second protein radical formed upon reaction of metmyoglobin with H_2O_2 which is centred on Tyr-151 has recently given additional weight to this interpretation (Davies, 1991). It should also be noted, that the Tyr-103 protein radical apparently does not always react with a protein component of the system, as Catalano and colleagues (1989) have shown that the radical may also react again with the heme to yield a heme-protein crosslink.

Construction of recombinant myoglobin mutant proteins via techniques of site-directed mutagenesis to investigate the effects of amino acid alterations on the electron transfer events, has led to additional inferences regarding the role of tyrosine residues in these processes. By preparing all the possible tyrosine- phenylalanine mutants of sperm whale metmyoglobin (which has three Tyr residues:

Tyr-103, Tyr-146, and Tyr-151), Wilks and Ortiz de Montellano (1992) have demonstrated by EPR spectroscopy that when the mutants are reacted with hydrogen peroxide, the initial electron transfer event between the porphyrin and the protein implicates donation by Tyr-103. This residue is also involved in maintaining the structural integrity of the protein, and could only be replaced by phenylalanine when the Lys-102 residue was co-mutated to a glutamine residue. Two findings by these workers suggest that other loci apart from tyrosines are involved in the electron transfer events. Firstly, Tyr-103-Phe and Tyr-146-Phe double mutants were still capable of yielding protein dimers when reacted with H_2O_2 and secondly, mutant proteins in which all the tyrosines had been replaced by phenylalanines still showed free radical signals, albeit weaker than those observed in the wild type protein.

Studies done by Yonetani (1966) showed that CCP, when reacted with ethyl hydroperoxide, yielded an EPR signal consistent with the formation of free radical on a moiety within the protein, in the proportions of one radical equivalent per enzyme molecule. Much work since that discovery has been done in an attempt to identify unequivocally the locus of the electron density of the radical. A variety of spectroscopic techniques initially gave rise to the conclusion that the radical site is not allocated to a single amino acid side chain. Instead, it was proposed that a side chain cluster near the heme including Trp-191, Met-230, and Met-231 retained a delocalized radical, based on evidence that implicated a sulfur-containing residue and evidence implicating an aromatic residue (Bosshard *et al.* 1991). Probing the protein radical formed by electron nuclear double resonance (ENDOR) spectroscopy has led Sivaraja and co-workers (1989) to identify the site of the radical to be the Trp-191 residue. Work done by

Fishel and colleagues (1991), in which *Saccharomyces cerevisiae* CCP was altered by site directed mutagenesis to give a Trp-191 to Phe mutation, as well as mutations of the Met-230 and Met-231 residues implicated in the earlier radical cluster model for the CCP protein radical, has shown that the broad component of the EPR free radical signal disappeared when the Trp-191-Phe or the Asp-235-Asn mutations were examined for a compound I signal, and smaller perturbations in the EPR signal occurred for the Met-230/ Met-231 mutants. Though the evidence thus favours the involvement of the Trp-191 in forming the compound I radical species, the authors readily admit that the failure of Trp-191 mutations to eliminate EPR radical signals completely, indicates the presence of additional electron density centred on an as yet unknown site.

The electron migration patterns and protein residues both in the vicinity or considerably removed from the heme that implicate protein radicals in reactions of peroxides with myoglobins and CCP thus provide tenable evidence favouring the hypothesis that the same process occurs in catalases. Binding of NADPH may then be explained as an efficient donor system to either the ferryl heme and associated protein radical formed after the decay of a delocalized but unstable porphyrin cation radical species (as in the scheme in Figure 55). The NADPH would donate its electrons in a concerted reaction to reduce the system before the radical species generated could migrate and perhaps oxidize another component of the system irreversibly.

The closest approach of the heme's edge to the position of the NADPH when bound on the catalase has been found to be 13.7Å between the C4 atom of the nicotinamide ring and the vinyl and methyl groups of pyrrole ring II (B) of the heme (Fita and Rossmann, 1985B). The narrow

channel leading to the distal side of the heme in the catalase protein opens out into a large partially hydrophilic cavity lined by residues including Tyr 214. The narrow outer channel is associated with the NADP binding site such that the NADPH molecule can occupy this cavity. The cavity itself also leads to Asn147 in the heme pocket via a small internal channel consisting of a Val149, Gln194,Pro128,Asn148, and Thr149 and having an aperture less than 3Å in diameter (Fita and Rossmann,1985A). Electron transfer across 13.7Å would not appear to be prohibitive if the same process can occur between Tyr151 and the heme iron in myoglobin at approximately the same distance. In fact, electron transfer constants typical to biological systems with activation energies on the order of 100-300 meV, require separation of the redox partners to be between 10 and 20Å to obtain electron transfer rates in the range of 100 -1000 s^{-1} (Canters and van de Kamp, 1992), which is within the range of values estimated for the electron transfer events that occur in the CCP-cytochrome *c* complex (Bosshard *et al,* 1991).

The implication of tyrosine residues as the centres of radical density in myoglobin may be equally applicable to the case of BLC. One such tyrosine is available in the large cavity associated with NADPH binding (Tyr214) and several more are available from the β- barrel "walls" of the heme pocket. β-sheets are also favoured in electron transfer events over α helices in that they have a high degree of two dimensional connectivity via covalent and hydrogen bonding interactions, allowing conductivity across the sheet to be relatively independent of the sheet's starting point (Canters and van de Kamp, 1992) An additional interesting observation is that one of these β-barrel tyrosines is associated by hydrogen bonding with the "essential"

asparagine (Asn147 in BLC), a residue highly conserved in all catalases and implicated in function of the enzyme. This same asparagine also forms the end of the minor channel between the large cavity associated with the dinucleotide binding cleft in the protein and the heme pocket. Whether a pathway of electron migration follows the intersite channel or an intramolecular pathway utilizing tyrosine phenoxyl radical species based on the protein radical hypothesis proposed for catalase, remains to be evaluated.

Evidence for the hypothesis of electron transfer events in catalase has been recently obtained by the investigation of resonance Raman spectra obtained for compound I species of both HRP and BLC (Chuang and Van Wart, 1992). The Dv_{ox} shifts (the resonance Raman shifts on oxidation of the porphyrin ring) observed for HRP and BLC are about the same, but the magnitudes are smaller than those observed in the case of model porphyrins that do not have aromatic axial ligands, suggesting that the porphyrin radical in BLC compound is delocalized off the heme. In ferricatalase, the same researchers had noted that resonances of tyrosinate bands are enhanced in the 470-500nm region by ferric-tyrosinate charge transfer bands (Chuang *et al.* 1988). The finding that these modes were enhanced by excitation at 406.7nm in the compound I of BLC has led to the suggestion that a π-cation radical is delocalized onto the proximal Tyr-357 ligand, causing the enhancement. The modified catalytic reaction scheme proposed (Fig. 55) also resembles the mechanism specified by Miller *et al.* (1992) for the reaction of dioxygen with CCP. The latter studies involved reacting the dioxygen with ferrous rather than ferric CCP. The initial step in the reaction is similar to the reaction of CCP with H_2O_2, in which an iron-substrate complex is formed. The ferrous-dioxygen complex,

however, further reacts to give a species spectroscopically identical to compound I formed when ferric CCP is reacted with peroxide. Experiments done with site-directed mutant proteins of CCP in which the Trp-191 or Asp-235 residues are replaced, also form the dioxygen complex, but further reaction to an oxyferryl form is not observed. Miller *et al* (1992) propose that initial O-O heterolytic cleavage of the dioxygen in the ferric CCP gives an oxyferryl iron centre and a transient π- cation radical on the porphyrin which can then be reduced by endogenous donors to give a protein-based radical resulting in the heterogeneous enzyme population designated compound I'. As the formation of the oxyferryl heme is dependent on the critical residues Trp-191 and Asp-235 being present, this further reinforces the contention that Trp-191 is the site of the free radical generated, with Asp-235 important in influencing the local environment of the Trp-191 side chain. Similar to metmyoglobin, the compound I' conversion is also accompanied by crosslinking of residues between protein molecules to give homodimers and heterodimers with cytochrome *c*, indicating that the radical migrates to surface amino acid residues. The phenomenon is not observed when CCP and H_2O_2 are at equimolar concentrations, however, as is observed with metmyoglobins.Thus, not only does Miller's reaction scheme parallel the scheme proposed for catalase, it also involves the phenomenon of intramolecular electron transfer of radical density between loci within the protein.

Support for the mechanism by which NADPH prevents the formation of compound II in catalase according to the proposed scheme shown in Fig. 55 has recently come from work on metmyoglobin and HRP. Studies by Arduini and co-workers (1992) on the reduction of metmyoglobin ferryl species, indicate that the reducing agents

ascorbate, ergothioneine,and urate are capable of preventing the formation of the oxoferryl compound I and also prevent dimer formation when pre-incubated with metmyoglobin prior to addition of hydrogen peroxide. This suggests that these agents effectively reduce the ferryl heme and prevent protein radical formation, in much the same way as NADPH is postulated to reduce the compound II' species in the scheme(Fig. 55). The work of De Sandro *et al.*(1991) studying the mechanism of NADPH oxidation catalyzed by HRP and the 2,4- diacetyl-[^{2}H]heme (DHRP) substituted enzyme, has shown that the compound I species produced in either HRP or DHRP by reaction with H_2O_2 catalyses the oxidation of NADPH by a single electron transfer, which is inferred to yield an NADP radical species which then reduces O_2 to O_2^-. This process occurs in the presence of the mediating compound, scopoletin, in the case of compound I. In the absence of a mediating molecule however, the compound II formed by either the HRP or the DHRP catalayzed a slow and direct two-electron transfer from NADPH to give $NADP^+$. Though the HRP (and probably the DHRP) compound I species is somewhat different from that of catalase and peroxidases in that the heme structure is characterized to be an extraordinarily stable oxyferryl porphyrin radical, it is interesting to note that two electron transfer from NADPH occurs only by reaction with the compound II species. The authors have yet to detail fully the mechanism for the reactions observed in the systems employed.

iv. Future Investigations

The role of NADPH in the hypothetical free radical quenching mechanism for the reaction of catalases with hydrogen peroxide, as

well as the hypothesis of a protein free radical generated in the process, could be supported by stopped flow or freeze-quench EPR studies of the protein to show free radical electron densities in the vicinity of the heme or the bound NADPH molecule. Supporting evidence could be procured by biochemical methodologies such as selectively modifying groups in the heme pocket and observing the effects both on the kinetics of compound II formation and on the free radical centre(s), if they can be shown to exist. Similarly, well designed site-directed mutagenesis studies on the enzyme could also give a better indication as to whether the tyrosine residues or other residues are implicated directly, if at all, in the formation and intramolecular migration of protein free radicals in eukaryotic catalases. Such work, apart from that mentioned above involving myoglobins and CCP, and the obvious example of HPII catalase, has been done for a number of other proteins (Mauk, 1991). The finding that the *Saccharomyces cerevisiae* catalases are NADPH binding allows this phenomenon to be investigated in a system that is both well characterized in terms of its molecular genetics and gene expression systems, and that serves as a useful model for the analogous proteins of other eukaryotes. Additional characterization of the catalases from this source in terms of other aspects of their biochemistry, as well as characterization of catalases isolated from as yet unstudied sources, would provide a more complete survey of the role that NADPH plays in the mechanisms of catalase reactions.

LITERATURE CITED

Adachi, S., Nagano, S., Watanabe, Y., Ishimori, K., and Morishima, I. (1991) Alteration of human myoglobin proximal histidine to cysteine or tyrosine by site-directed mutagenesis: Characterization and their catalytic activities. Biochemical and Biophysical Research Communications. 180: (1): 138-144.

Adachi, S., Nagano, S., Ishimori, K., Watanabe, Y., Morishima, I., Egawa, T., Kitigawa, T., and Makino, R. (1993) Roles of proximal ligand in heme proteins: replacement of proximal histidine of human myoglobin with cysteine and tyrosine by site-directed mutagenesis as models for P-450, chloroperoxidase, and catalase. Biochemistry. 32: 241-252.

Alderman, J., Takagi, T., and Lieber, C.S. (1987) Ethanol-metabolizing pathways in deermice. Journal of Biological Chemistry. 262(16): 7497-7503.

Alderman, J., Kato, S., and Lieber, C.S. (1989) The microsomal ethanol oxidizing system mediates metabolic tolerance to ethanol in deermice lacking alcohol dehydrogenase. Archives of Biochemistry and Biophysics. 187(2): 464-475.

Allgood, G.S. and Perry, J.J. (1986) Characterization of a manganese-containing catalase from the obligate thermophile *Thermoleophilum album*. Journal of Bacteriology. 168: 563-567.

Ames, B.N. and Shigenaga, M.K. (1992) DNA damage by endogenous oxidants and mitogenesis as causes of aging and cancer. In: (Scandalios, ed.) *Molecular Biology of Free Radical Scavenging Systems*. pp 1-22. Cold Spring Harbour, Plainview, N.Y.

Ammerer, G., Richter, K., Hartter, E. and Ruis, H. (1981) Synthesis of *Saccharomyces cerevisiae* catalase A *in vitro*. European Journal of Biochemistry. 113: 327-331.

Arduini, A., Mancinelli, G., Radatti, G.L., Damonti, W., Hochstein, P., and Cadenas, E. (1992) Reduction of sperm whale ferrylmyoglobin by endogenous reducing agents: potential reducible loci of ferrylmyoglobin. Free Radical Biology & Medicine. 13: 449-454.

Barrett, J. (1956) The Prosthetic Group of Cytochrome a_2 . Biochemical Journal. 64: 626-639.

Beaumont, F., Jouve, H.M., Gagnon, J., Gaillard, J., and Pelmont, J. (1990) Purification and properties of a catalase from potato tubers (*Solanum tuberosum*). Plant Science. 72: 19-26.

Beers, R.F. and Sizer, I.W. (1952) A spectrophotometric method for measuring the breakdown of hydrogen peroxide by catalase. Journal of Biological Chemistry. 195: 133-137

Belazzi, T., Wagner, A., Wieser, R., Schanz, M., Adam, G.,Hartig, A., and Ruis,H. (1991) Negative regulation of transcription of the *Saccharomyces cerevisiae* catalase T (*CTT1*) gene by cAMP is mediated by a positive control element. EMBO Journal. 10(3) :585-592.

Bewley, G.C., Mackay, W.J., and Cook, J.L. (1986) Temporal variation for the expression of catalase in *Drosophila melanogaster*: correlations between rates of enzyme synthesis and levels of translatable catalase-messenger RNA. Genetics. 113: 919-938.

Böck, P., Kramar, R., and Pavelka, M. (1980) *Peroxisomes and Related Particles in Animal Tissues.* pp.28-31/191-193. Springer-Verlag, New York.

Bosshard, H.R., Anni, H., and Yonetani, T. (1991) Yeast cytochrome c peroxidase. In: (Everse, J. *et al*, eds.) *Peroxidases in Chemistry and Biology, Vol. II.* pp. 51-84. CRC Press, Boca Raton.

Bradford, M. M. (1976) A rapid and sensitive method for quantification of microgram quantities of protein utilizing the principle of protein-dye binding. Analytical Biochemistry. 72: 248-254.

Brown, G.L. (1953) A Study of Yeast Catalase. Acta Chemica Scandinavica, 7: 435-440.

Cadenas, E. and Sies, H. (1982) Low level chemiluminescence of liver microsomal fractions initiated by tert-butyl hydroperoxide. European Journal of Biochemistry. 124: 349-356.

Canters, G.W. and van de Kamp. M. (1992) Protein-mediated electron transfer. Current Opinion in Structural Biology. 2: 859-869.

Cantz, M., Morikofer-Zwez, S., Bossi, E., Kaufmann, H., von Wartburg, J.P., and Aebi, H. (1968) Alternative molecular forms of erythrocyte catalase. Experientia, 24(2): 119-121.

Catalano, C.E., Choe, Y.S., and Ortiz de Montellano, P.R. (1989) Reactions of the protein radical in peroxide-treated myoglobin. Journal of Biological Chemistry. 264(18): 10534-10541.

Chance, B. (1947) An intermediate compound in the catalase-hydrogen peroxide reaction. Acta Chemica Scandinavica. 1: 236-267.

Chance, B. (1949).The interaction of catalase and cyanide. Journal of Biological Chemistry.179:1299-1308.

Chance, B. (1950A) The reactions of catalase in the presence of the notatin system. Biochemical Journal. 46: 387-402.

Chance, B. (1950B) On the reaction of catalase peroxides with acceptors. Journal of Biological Chemistry. 182: 649-658.

Chance, B. (1952).The state of catalase in the respiring cell. Science. 116: 202-203.

Chance,B., Oshino,N., Sugano, T., and Jamieson, D. (1974) Role of catalase in ethanol metabolism. In: (Thurman *et al*, eds.) *Alcohol and Aldehyde Metabolizing Systems*. pp. 169-182. Academic Press, New York.

Chiu, J. T., Loewen, P.C., Switala, J., Gennis, R.B., and Timkovich, R. (1989) Proposed structure for the prosthetic group of the catalase HPII from *Escherichia coli*. Journal of the American Chemical Society. 111(18):7046-7050.

Chuang, W-J., Johnson, S., and Van Wart, H.E.(1988) Resonance Raman spectra of bovine liver catalase: Enhancement of proximal tyrosinate vibrations. Journal of Inorganic Biochemistry. 34: 201-219.

Chuang, W-J and Van Wart, H.E. (1992) Resonance Raman spectra of horseradish peroxidase and bovine liver catalase compound I species. Journal of Biological Chemistry. 267(19):13293-13301.

Claiborne,A. and Fridovich, I. (1979) Purification of the o-dianisidine peroxidase from *Escherichia coli* B. Physicochemical characterization and analysis of its dual catalatic and peroxidatic activities. Journal of Biological Chemistry. 254: 4245-4252.

Claiborne, A., Malinowski, D.P., and Fridovich, I. (1979)Purification and characterization of hydroperoxidase II of *Escherichia coli*. B. Journal of Biological Chemistry. 254(22):11664-11668

Cohen,G., Fessl, F., Traczyk, A., Rytka, J., and Ruis, H. (1985) Isolation of the catalase A gene of *Saccharomyces cerevisiae* by complementation of the *cta1* mutation. Molecular and General Genetics. 200: 74-79.

Cohen,G., Rapatz, W., and Ruis, H.E. (1988) Sequence of the *Saccharomyces cerevisiae CTA1* gene and amino acid sequence of catalase A derived from it. European Journal of Biochemistry. 176: 159-163.

Davies, M.J. (1991) Identification of a globin free radical in equine myoglobin treated with peroxides. Biochimica et Biophysica Acta. 1077: 86-90.

Davies, M. J. and Puppo, A. (1992) Direct detection of a globin-derived radical in leghaemoglobin treated with peroxides. Biochemical Journal. 281: 197-201.

Dawson, J.H., Bracete, A.M., Huff, A.M. Kadkhodayan, S., Zeitler, C.M., Sono, M.,Chang, C. K., Loewen, P.C. (1992) The active site structure of *E. coli* HPII catalase. FEBS Letters. 295(1,2,3):123-126.

de Duve, C. (1974) Intracellular localization, biosynthesis, and functions of rat liver catalase. In: (Thurman *et al*, eds.) *Alcohol and Aldehyde Metabolizing Systems*. pp. 161-168. Academic Press, New York,

DeGray, J.A., Lassman, G., Curtis, J.F., Kennedy, T.A., Marnett, L.J.,Eling, T.E., and Mason, R.P. (1992) Spectral Analysis of the protein-derived tyrosyl radicals from prostaglandin H synthase. Journal of Biological Chemistry. 267(33): 23583-23588.

De Sandro,V., Dupuy, C., Kaniewski,J., Ohayon, R., Deme, D., Virion, A., and Pommier, J. (1991) Mechanism of NADPH oxidation catalyzed by horse-radish peroxidase and 2,4-diacetyl-[^{2}H]heme-substituted horse-radish peroxidase. European Journal of Biochemistry. 201: 507-515.

Distel, B., Veenhuis, M., and Tabak, H. (1987) Import of alcohol oxidase into peroxisomes of *Saccharomyces cerevisiae*. EMBO Journal. 6: 3111-3116.

Dolphin,D., Forman,A., Borg,D.C., Fajer, B., and Felton, R.H. (1971) Compounds I of catalase and horseradish peroxidase: π-cation radicals. Proceedings of the National Academy of Sciences, USA. 68 (3): 614-618.

Dunford, H.B. (1991) Horseradish peroxidase: Structure and kinetic properties. In: (Everse, J *et al*, eds.) *Peroxidases in Chemistry and Biology , Vol. II.* pp. 2-24. CRC Press, Boca Raton,Fla.

Eaton, J.W., Boraas, M., and Etkin, N.L. (1972) Catalase activity and red cell metabolism. In: (Taylor, N. ed.) *Advances in Experimental Medicine and Biology*, Vol. 28, pp.121-131. Plenum, New York.

Eisenstark, A. and Perrot, G. (1987) Catalase has only a minor role in protection against near-ultraviolet radiation damage in bacteria. Molecular and General Genetics. 207: 68-72.

Fishel, L.A., Farnum, M.F., Mauro,J.M., Miller, M.A., Kraut, J., Liu, Y., Tan, X., and Scholes, C.P. (1991) Compound I radical in site-directed mutants of cytochrome *c* peroxidase as probed by electron paramagnetic resonance and electron-nuclear double resonance. Biochemistry, 30: 1986-1996.

Fita, I and Rossmann, M. G. (1985A) The active center of catalase. Journal of Molecular Biology. 185 :21-37.

Fita, I. and Rossmann, M.G.(1985B) The NADPH binding site on beef liver catalase. Proceedings of the National Academy of Sciences, USA. 82: 1604-1608.

Furata, S. and Hayashi, H.M.G. (1990) Purification and properties of recombinant rat catalase produced in *Escherichia coli*. Journal of Biochemistry (Tokyo). 107: 708-713.

Fuhrhop, J.H. and Smith, K.M. (1975) Laboratory Methods (19.7.3.) In: (K.M. Smith, ed.) *Porphyrins and Metalloporphyrins*, pp. 304-307 Elsevier,Amsterdam.

Goldberg, I and Hochman, A. (1989) Three different types of catalase in *Klebsiella pneumoniae*. Archives of Biochemistry and Biophysics. 268: 124-128.

Goth, L. (1991) Serum catalase: reversibly formed charge isoform of erythrocyte catalase. Clinical Chemistry. 37(12):2043-2047.

Gould, S.J., Keller, G.-A., Hosken, N., Wilkinson, J. and Subramani, S. (1989) A conserved tripeptide sorts proteins to peroxisomes. Journal of Cell Biology. 108: 1657-1664.

Guemouri, L., Artur, Y., Herbeth, B., Jeandel, C., Cuny, G., and Siest, G. (1991) Biological variability of superoxide dismutase, glutathione peroxidase, and catalase in blood. Clinical Chemistry. 37(11): 1932-1937.

Haas, A., Brehm, K,, Kreft, J.,, B.W., and Goebel, W. (1991) Cloning, characterization, and expression in *Escherichia coli* of a gene encoding *Listeria seeligeri* catalase, a bacterial enzyme highly homologous to mammalian catalases. Journal of Bacteriology, 173(16):5159-5167.

Handler, J.A., Bradford, B.U., Glassman,E., Ladine, J.K., and Thurman, R.G. (1986) Catalase-dependent ethanol metabolism *in vivo* in deermice lacking alcohol dehydrogenase. Biochemical Pharmacology. 35(24): 4487-4492.

Hansen, H. and Roggenkamp, R. (1989) Functional complementation of catalase-defective peroxisomes in a methylotrophic yeast by import of the catalase A from *Saccharomyces cerevisiae*. European Journal of Biochemistry. 184: 173-179.

Harada, K. and Yamazaki, I. (1987) Electron spin resonance spectra of free radicals formed in the reaction of metmyoglobin with Ethylhydroperoxide. Journal of Biochemistry (Tokyo). 101: 283-286.

Hartig, A. and Ruis,H. (1986) Nucleotide sequence of the *Saccharomyces cerevisiae CTT1* gene and deduced amino-acid sequence of yeast catalase T. European Journal of Biochemistry. 160: 487-490.

Hartig, A. Ogris, M., Cohen, G., and Binder, M. (1990) Fate of highly expressed proteins destined to peroxisomes in *Saccharomyces cerevisiae*. Current Genetics. 18: 23-27.

Heimberger, A. and Eisenstark, A. (1988) Compartmentalization of catalases in *Escherichia coli*. Biochemical and Biophysical Research Communications. 154(1): 392-397.

Hörtner,H., Ammerer,G., Hartter,E., Hamilton,B., Rytka,J., Bilinski,T., and Ruis,H. (1982) Regulation of synthesis of catalases and iso-1-

cytochrome *c* in *Saccharomyces cerevisiae* by glucose, oxygen, and heme. European Journal of Biochemistry. 128 : 179-184.

Ingelman-Sundberg, M. and Jörnvall, H. (1984) induction of the ethanol-inducible form of rabbit liver microsomal cytochrome P-450 by inhibitors of alcohol dehydrogenase. Biochemical and Biophysical Research Communications. 124(2): 375-382.

Issajew, W.(1904) Über die hefekatalase. Hoppe-Seyler's Zeitschrift fur Physiologisches Chemie. 42: 102-116.

Jones, G.L. and Masters, C.J. (1976). On the comparative characteristics of mammalian catalases. Comparative Biochemistry and Physiology. 55B: 511-518.

Jones, P. and Wilson, I. (1978). Catalases and iron complexes with catalase-like properties. In: (Sigel, H. ed.) *Metal Ions in Biological Systems, Vol. 7.* pp.185-240. Marcel Dekker Inc., New York.

Jouve, H.M., Pelmont, J.,and Gaillard, J. (1986) Interaction between pyridine adenine dinucleotides and bovine liver catalase: A chromatographic and spectral study. Archives of Biochemistry and Biophysics. 248(1): 71-79.

Jouve, H.M., Beaumont, F., Leger, I., Foray, J., and Pelmont, J. (1989) Tightly bound NADPH in *Proteus mirablis* PR catalase. Biochemistry and Cell Biology. 67(6): 271-277.

Jouve, H.M., Gouet, P., Boudjada, N., Buisson, G., Kahn, R., and Duee, E. (1991) Crystallization and crystal packing of *Proteus mirablis* PR catalase. Journal of Molecular Biology. 221: 1075-1077.

Keilin, D. and Hartree, E.F. (1936) Coupled oxidation of alcohol. Proceedings ofthe Royal Society (London). B119: 141-149.

Keilin, D. and Hartree, E.F. (1945) Properties of catalase. Catalysis of coupled oxidation of alcohols. Biochemical Journal. 39: 293-301.

Keilin, D. and Hartree, E. F. (1955) Catalase, peroxidase and metmyoglobin as catalysts of coupled peroxidatic reactions. Biochemical Journal, 60: 310-325.

Keilin, D. and Nicholls, P. (1958) Reactions of catalase with hydrogen peroxide and hydrogen donors. Biochimica et Biophysica Acta. 29: 302-307.

Kikuchi-Torii, K., Hayashi, S., Nakamoto, H., and Nakamura, S. (1982) Properties of *Aspergillus niger* catalase. Journal of Biochemistry (Tokyo). 92 :1449-1456.

Kirkman, H.N. and Gaetani, G.F. (1984) Catalase: A tetrameric enzyme with four tightly bound molecules of NADPH.Proceedings of the National Academy of Sciences, USA. 81 :4343-4347.

Kirkman, H.N., Galiano, S., and Gaetani, G.F.(1987) The function of catalase-bound NADPH. Journal of Biological Chemistry. 262(2): 660-666.

Knappe, J., Neugebauer, F.A., Blaschkowski, H.P., and Ganzler, M. (1984) Post-translational activation introduces a free radical in pyruvate formate-lyase. Proceedings of the National Academy of Sciences of the USA. 81: 1332-1335.

Kono, Y. and Fridovich, I. (1983) Isolation and characterization of the pseudocatalase of *Lactobacillus plantarum.* Journal of Biological Chemistry. 258(10): 6015-6019.

Laemmli, U.K. (1970) Cleavage of structural proteins during the assembly of the head of bacteriophage T4. Nature. 227: 680-685.

Lazarow, P.B., and Fujiki, Y. (1985) Biogenesis of peroxisomes. *Annual Review of Cell Biology,* Vol. 1 (1985), pp. 489-530.

Loew, O. (1901) Catalase, A new enzyme of general occurrence with special reference to the tobacco plant. U.S. Dept. of Agriculture Report **#68**. p. 47.

Loewen, P.C. (1992) Regulation of bacterial catalase synthesis. In: (Scandalios, ed.) *Molecular Biology of Free Radical Scavenging Systems*, pp.97-115. Cold Spring Harbour Press, Plainview, N.Y.

Loewen, P.C. and Switala, J. (1986) Purification and characterization of catalase HPII from *Escherichia coli* K12. Biochemistry and Cell Biology. 64: 638-646.

Loewen, P.C., Switala, J., and Triggs-Raine, B.L. (1985A) Catalases HPI and HPII in *Escherichia coli* are induced independently. Archives of Biochemistry and Biophysics. 243(1):144-149.

Loewen, P.C., Triggs, B.L., George, C.S. and Hrabarchuk, B.E (1985B) .Genetic mapping of *katG* , a locus that affects synthesis of the bifunctional catalase-peroxidase hydroperoxidase I in *Escherichia coli.* Journal of Bacteriology. 162(2):661-667.

Lowry, O.H., Roberts, N.A., and Kapphahn,J.I. (1957) The fluorometric measurement of pyridine nucleotides. Journal of Biological Chemistry, 224: 1047-1064.

Ma, M., and Eaton, J.W. (1992) Multicellular oxidant defense in unicellular organisms. Proceedings of the National Academy of Siences, U.S.A. 89: 7924-7928.

Mashino, T. and Fridovich, I. (1988) NADPH mediates the inactivation of bovine liver catalase by monochloroamine. Archives of Biochemistry and Biophysics. 265 (2):279-285.

Mauk, A.G. (1991) Electron transfer in genetically engineered proteins. The cytochrome c paradigm. In: (Palmer, G.A. ed.) *Structure and Bonding 75: Long-Range Electron Transfer in Biology.* pp. 130-157. Springer-Verlag, New York.

Melik-Adamyan, W.R., Barynin, V.V., Vagin, A. A., Borisov, V.V., Vainshtein, B.K., Fita, I., Murthy, M.R.N., and Rossmann, M.G. (1986) Comparison of beef liver and *Penicillium vitale* catalases. Journal of Molecular Biology. 188: 63-72.

Miller, M.A., Bandyopadhyay, D., Mauro, J.M., Traylor, T.G., and Kraut, J. (1992) Reaction of ferrous cytochrome *c* peroxidase with dioxygen: Site-directed mutagenesis provides evidence for rapid reduction of dioxygen by intramolecular electron transfer from the compound I radical site. Biochemistry. 31: 2789-2797.

Morikofer-Zwez, S., Cantz, M., Kaufmann, H., von Wartburg, J.P., and Aebi, H. (1969) Heterogeneity of erythrocyte catalase. European Journal of Biochemistry. 11 :49-57.

Mosavi-Movahedi, A.A., Wilkinson, A.E., and Jones, M.N. (1987) Characterization of *Aspergillus niger* catalase. International Journal of Biological Macromolecules. 9: 327-332.

Murthy, M.R.N., Reid, T.J., Sicignano, A., Tanaka, N., and Rossmann, M.G. (1981) Structure of beef liver catalase. Journal of Molecular Biology. 152: 465-499.

Nelson, D.P. and Kiesow, L.A. (1972) Enthalpy of decomposition of hydrogen peroxide by catalase at 25 degrees (with molar extinction co-efficients of H_2O_2 solutions in the ultraviolet). Analytical Biochemistry. 49: 474-478.

Ni, W. and Trelease, R.N., Geer, B.W.(1991) Two genes encode the two subunits of cottonseed catalase. Archives of Biochemistry and Biophysics. 289 (2): 237-243.

Nicholls, P. (1962) The reaction between aminotriazole and catalase. Biochimica et Biophysica Acta. 59: 414-420

Nicholls, P. (1964) The formation and catalytic role of catalase peroxide compound II. Biochimica et Biophysica Acta. 81: 479-495.

Nicholls, P. and Schonbaum, G.R..(1963) Catalases. In: (Lardy *et al*, eds.) *The Enzymes*, Vol. 2, pp. 147-222. Academic Press, New York.

Oakes, J. (1986) ^{1}H and ^{19}F Nuclear Magnetic Resonance investigation of the active site of catalase. Journal of the Chemical Society of London, Faraday Transactions I. 82: 2079-2087.

Ogura, Y. (1955) Catalase activity at high concentrations of hydrogen peroxide. Archives of Biochemistry and Biophysics. 57: 288-300.

Okada,H., Ueda, M., Sugaya, T., Atomi,H., Mozaffar,S., Hishida,T., Teranishi,Y., Okazaki,K., Takechi, T., Kamiryo,T., and Tanaka,A. (1987) Catalase gene of the yeast *Candida Tropicalis* . European Journal of Biochemistry. 170: 105-110.

Orii, Y., Sakai, Y., and Ozawa, K. (1989) Ubiquitous formation of catalase compound II in hemoglobin. free perfused rat liver and detection of novel spectral species. Biochemical and Biophysical Research Communications. 162(3): 1272-1278.

Orr, W.C. and Sohal, R.S. (1992) The effects of catalase gene overexpression on life span and resistance to oxidative stress in transgenic *Drosophila melanogaster.* Archives of Biochemistry and Biophysics. 297(1): 35-41.

Ortiz de Montellano, P. R. (1992) Catalytic sites of hemoprotein peroxidases. *Annual Review of Pharmacology and Toxicology.* Vol. 32: pp. 89-107.

Ortiz de Montellano, P. R. and Catalano, C.E. (1985) Epoxidation of styrene by hemoglobin and myoglobin. Journal of Biological Chemistry. 260: 9265-9271.

Oshino, N. and Chance,. B(1977) , Properties of glutathione release observed during reduction of organic hydroperoxide, demethylation of aminopyrine and oxidation of some substances in perfused rat liver, and their implications for the physiological function of catalase. Biochemical Journal. 162 : 509-525.

Palaniappan, V. and Terner, J. (1990) Resonance Raman spectroscopic characterization of horseradish peroxidase intermediates. In: (Reddy, C.C. *et al*, eds.) *Biological Oxidation Systems, vol. I*, pp.487-503. Academic Press.,San Diego.

Percy, M.E. (1984) Catalase: an old enzyme with a new role? Canadian Journal of Biochemistry and Cell Biology. 62 :1006-1014.

Pichorner, H., Jessner, G., and Ebermann, R. (1993) tBOOH Acts as a suicide substrate for catalase. Archives of Biochemistry and Biophysics. 300(1): 258-264.

Poulos, T.L. and Kraut, J. (1980) Stereochemistry of peroxidase catalysis. Journal of Biological Chemistry. 255(17): 8199-8205.

Radi, R., Bush, K.M., and Freeman, B.A. (1993) The role of cytochrome *c* and mitochondrial catalase in hydroperoxide-induced heart mitochondrial lipid peroxidation. Archives of Biochemistry and Biophysics. 300(1): 409-415.

Radi,R., Turrens, J.F., Chang, L.Y., Bush, K.M., Crapo, J.D., and Freeman, B.A. (1991) Detection of catalase in rat heart mitochondria. Journal of Biological Chemistry. 266(32): 22028-22034.

Reid, T.J., Murthy, M.R.N., Sicignano, A., Tanaka,N., Musick, W.D., and Rossmann, M.G. (1981) Structure and heme environment of beef liver catalase at 2.5Å resolution. Proceedings of the National Academy of Sciences of the USA. 78(8): 4767-4771.

Ruis, H. and Hamilton, B. (1992) Regulation of yeast catalase genes. In: (Scandalios, ed.) *Molecular Biology of Free Radical Scavenging Systems*, pp.153-172. Cold Spring Harbour Press. Plainview, N.Y.

Samejima,T. and Yang, J. (1963) Reconstitution of acid-denatured catalase. Journal of Biological Chemistry. 238(10): 3256-3261.

Scandalios, J.G. (1992) Regulation of the antioxidant defense genes *Cat* and *Sod* of maize. In: (Scandalios, ed.) *Molecular Biology of Free Radical Scavenging Systems*, pp.117-152. Cold Spring Harbour Press. Plainview, N.Y.

Schonbaum, G.R. and Chance, B. (1976) Catalase. In: (Boyer, P.D. ed.) *The Enzymes,* vol. XIII pt. C, third edition. pp. 363-408. Academic Press, London.

Schroeder, W.A., Shelton, J.R., Shelton, J.B., Robberson, B., Apell, G., Fang, R.S., and Bonaventura, J. (1982) The complete amino acid sequence of bovine liver catalase and the partial sequence of bovine erythrocyte catalase. Archives of Biochemistry and Biophysics. 214(1): 397-421.

Seah, T.C.M. and Kaplan, J. .G(1973) Purification and properties of the catalase of bakers' yeast. Journal of Biological Chemistry. 248(8): 2889-2893.

Seah, T.C.M., Bhatti, A.R., and Kaplan,J.G.(1973) Novel catalatic proteins of bakers' yeast. I. An atypical catalase. Canadian Journal of Biochemistry. 51:1551-1554.

Sharma, K.D., Andersson, L.A., Loehr, T.M., Terner, J., Goff, H.M. (1989) Comparative spectral analysis of mammalian, fungal, and bacterial catalases. Journal of Biological Chemistry. 264(22): 12772-12779.

Sichak, S.P. and Dounce, A.L. (1986) Analysis of the peroxidatic mode of action of catalase. Archives of Biochemistry and Biophysics. 249(2): 286-295.

Sies, H. (1974) Organ spectrophotometry of catalase compound I in the study of hydrogen peroxide and hydrogen donor metabolism in hemoglobin-free perfused rat liver. In: (Thurman *et al*, eds.) *Alcohol and Aldehyde Metabolizing Systems*, Academic Press, New York, pp. 183-197.

Sivaraja, M., Goodin, D.B., Smith, M., and Hoffman, B.M. (1989) Identification of ENDOR of Trp^{191} as the free radical site in cytochrome *c* peroxidase compound ES. Science. 245: 738-740.

Skoneczny, M., Chelstowska, A. R., and Rytka,J.(1988) Study of the coinduction by fatty acids of catalase A and acyl-CoA oxidase in

standard and mutant *Saccharomyces cerevisiae* strains. European Journal of Biochemistry. 174 : 297-302.

Spevak, W., Fessl, F., Rytka, J., Traczyk, A., Skoneczny, M., and Ruis, H. (1983) Isolation of the catalase T structural gene of *Saccharomyces cerevisiae* by functional complementation. Molecular and Cellular Biology. 3: 1545-1552.

Starke, P.E. and Farber, J.L. (1985) Endogenous defences against the cytotoxicity of hydrogen peroxide in cultured rat hepatocytes. Journal of Biological Chemistry. 260(1): 86-92.

Stern, K. G.(1936).The prosthetic group of catalase. Journal of Biological Chemistry. 112: 661-665.

Storz, G., Tartaglia, L.A., and Ames, B.N. (1990) Transcriptional regulator of oxidative stress-inducible genes: Direct activation by oxidation. Science. 248: 189-196.

Sugita, Y., Tobe, T., Sakamoto, T., and Higashi, T. (1982) Immature precursor catalase in subcellular fractions of rat liver. Journal of Biochemistry(Tokyo) 92: 509-515.

Sumner, J.B. (1941) The chemical nature of catalase. *Advances in Enzymology.* Vol 1. pp. 163-176.

Sumner and Dounce (1937) Crystallization of beef liver catalase. Journal of Biological Chemistry. 121: 217-226.

Susani, M., Zimniak, P., Fessl, F., Ruis, H.(1976) Localization of catalase A in vacuoles of *Saccharomyces cerevisiae*: evidence for the vacuolar nature of isolated "yeast peroxisomes". Hoppe-Seyler's Zeitschrift fur Physiologiches Chemie. 357: 961-970.

Takano, T. (1977) Structure of myoglobin refined at 2.0Å resolution. Journal of Molecular Biology. 110: 537-568.

Takeda, A., Miyahara, T., Hachimori,A., and Samejima, T.(1980) The interactions of thiol compounds with porcine erythrocyte catalase. Journal of Biochemistry (Tokyo). 87: 429-439.

Thompson, S.T., Cass, K.H., Stellwagen, E.(1975) Blue dextran-sepharose: An affinity column for the dinucleotide fold in proteins. Proceedings of the National Academy of Sciences of the USA. 72(2): 669-672.

Thurman, R.G., Ley, H.G., and Scholz,R. (1972) Hepatic microsomal ethanol oxidation. European Journal of Biochemistry. 25: 420-430.

Timkovich, R. and Bondoc, L.L. (1990) Diversity in the structure of hemes. In: *Advances in Biophysical Chemistry* ,Vol. 1., pp. 203-247.

Tolbert, N.E. (1978) Peroxisomal redox enzymes. *Methods in Enzymology*, Vol. 52. pp. 493-505.

Vainshtein, R.K., Melik-Adamyan, W.R., Barynin, V.V., Vagin, A.A., Grebrenko, A.I., Borisov, V.V., Bartels, K.S., Fita, I., and Rossmann, M.G. (1986) Three-dimensional structure of catalase from *Penicillium vitale* at 2.0Å resolution. Journal of Molecular Biology. 188: 49-61.

van der Zel, A., Dadoo, R., Geer, B.W., and Heinstra, P.W.H. (1991) The Involvement of catalase in alcohol metabolism in *Drosophila melanogaster* larvae. Archives of Biochemistry and Biophysics. 287(1): 121-127.

Vavra, M.R., Timkovich, R., Yap, F. S. , and Gennis, R.B .(1986) Spectroscopic studies on heme *d* in the visible and infrared. Archives of Biochemistry and Biophysics. 250(2): 461-468.

Veenhuis, M., Mateblowski, M. ,Kunau, W.H. and Harder, E. (1987) Proliferation of microbodies in *Saccharomyces cerevisiae* . Yeast. 3: 77-84.

Verduyn,C., Giuseppin, M.L.F., Scheffers, W.A.,and van Dijken,J.P. (1988) Hydrogen peroxide metabolism in yeasts. Applied and Environmental Microbiology. 54: 2086-2090.

von Ossowski, I., Mulvey, M.R., Leco, P.A., Borys,A., and Loewen, P.C. (1991) Nucleotide sequence of *Escherichia coli kat* E , which encodes catalase HPII. Journal of Bacteriology. 173(2): 514-520.

Vuillaume, M., Lafont, R., Hubert, M., Jouve, H., Calvayrac, R., Best-Belpomme, M. (1988) A new property of catalase: The concerted synthesis of nucleotide triphosphates. Bioelectrochemistry and Bioenergetics. 19: 541-556.

Wayne, L.G. and Diaz, G.A.(1988) Detection of a novel catalase in extracts of *Mycobacterium avium* and *Mycobacterium intracellulare*. Infection and Immunity. 56(4): 936-941.

Wen, J-W., Osumi, T., Hashimoto, T., and Ogata, M. (1990) Molecular analysis of human acatalasemia. Journal of Molecular Biology. 211: 383-393.

Whittaker, M.M. and Whittaker, J.W. (1990) A Tyrosine-derived free radical in apogalactose oxidase. Journal of Biological Chemistry. 265: 9610-9613.

Wieser,R., Adam, G., Wagner, A., Schuller,C., Marchler, G., Ruis, H., Krawiec, Z., and Bilinski,T.(1991) Heat shock factor-independent control of transcription of the *CTT1* gene encoding the cytosolic catalase T of *Saccharomyces cerevisiae*. Journal of Biological Chemistry. 266(19): 12406-12411.

Wilks, A. and Ortiz de Montellano, P. R. (1992) Intramolecular translocation of the protein radical formed in the reaction of recombinant sperm whale myoglobin with H_2O_2. Journal of Biological Chemistry. 267(13): 8827-8833.

Winkler, H., Adam, G.,Mattes, E., Schanz,M., Hartig,A., and Ruis,H. (1988) Co-ordinate control of synthesis of mitochondrial and non-mitochondrial hemoproteins: a binding site for the HAP1 (CYP1) protein in the UAS region of the yeast catalase T gene (*CTT1*). EMBO Journal. 7(6):1799-1804.

Yonetani, T. (1966) Studies on cytochrome *c* peroxidase. IV. A comparison of peroxide-induced complexes of horseradish and cytochrome c peroxidase. Journal of Biological Chemistry. 241: 2562-2571.

Zhang,Y., Heym, B., Allen, B.,Young, D. (1992) The catalase-peroxidase gene and isoniazid resistance of *Mycobacterium tuberculosis*. Nature. 358: 591-593.

Zimniak, P., Hartter, E., Woloszczuk, W. (1976) Catalase biosynthesis in yeast: Formation of catalase A and catalase T during oxygen adaptation of *Saccharomyces cerevisiae*. European Journal of Biochemistry. 71: 393-398.

APPENDIX A

Calculation of Catalase Activities

Experiments were performed according to the procedure specified in Materials and Methods, chapter III. The parameters for estimation of the specific rate constants per catalase hematin are given in Table A-I, below. These were derived via analysis of time courses of H_2O_2 decomposition as shown in the representative traces of Fig. 13, chapter III. Assay conditions as in legend to Fig. 13. Rate constants were calculated as follows:

$$k_0 = \frac{\ln 2}{t\frac{1}{2}} \qquad \text{(eq. A-1)}$$

where k_0 is the rate constant in reciprocal seconds and $t\frac{1}{2}$ is the time required for hydrogen peroxide absorbance at 240nm to fall to one half its initial value. The specific rate constant is calculated as:

$$k_0' = \frac{k_0}{[\text{hematin catalase}]} \qquad \text{(eq. A-2)}$$

where k_0' is given in units of $M^{-1}s^{-1}$.

TABLE A-I. Parameters and calculated rate constants for determination of catalase activities.

Catalase	Trial#	[Catalase heme] (nM)	$t_{1/2}$ (s)	k_1 (x $10^{-3}s^{-1}$)	k_1' (heme) (x 10^6 $M^{-1}s^{-1}$)
Bovine Liver	1	2.75	52	1.33	4.8
	2	1.37	78	8.88	6.5
	3	2.75	37	18.9	6.9
	4	2.75	34	20.4	7.4
	5	2.75	38	18.2	6.6
HPII(wild type)	1	13.3	44	15.7	1.2
	2	6.68	72	9.62	1.4
	3	13.3	56	1.23	0.92
	4	13.3	44	15.7	1.2
HPII(N201A)	1	74.8	50	13.8	0.18
	2	60.0	70	9.90	0.16
	3	13.4	234	2.96	0.22
HPII(N201H)		88.4	462	1.50	0.017
SCCT	1	0.77	114	6.05	7.8
	2	1.55	82	8.45	5.5
	3	2.33	47	1.49	6.4
SCCA	1	3.92	30	2.31	5.9
	2	7.84	14	5.09	6.5

Appendix B

Data for catalase titrations with heme ligands

Figures B-1(**A** through **I**) show titration plots for the catalase proteins obtained via plotting the percent absorbance difference for selected wavelength pairs as indicated against ligand concentration.

Figure B-1. Titration plots for catalase ligand titrations. Titrations were in 50mM potassium phosphate, pH 6.5, at 25 degrees.(**A**) Titration plot for BLC (15μM hematin) with HCN. (**B**) Titration plot for BLC (15μM hematin) with HCOOH. (**C**) Titration plot for SCCT (3μM hematin) with HCN. (**D**) Titration plot for SCCA (1μM hematin) with HCN. (**E**) Titration plot for HPII (5μM hematin) with HCN. (**F**) Titration plot for HPII (5μM hematin) with HCOOH. (**G**) Titration plot for HPII N201A mutant protein (3.9μM hematin) with HCN. (**H**) Titration plot for HPII N201Q mutant protein (3.8μM hematin) with HCN. (**I**) Titration plot for HPII N201H mutant protein (5μM hematin) with HCN.

Figure B-1

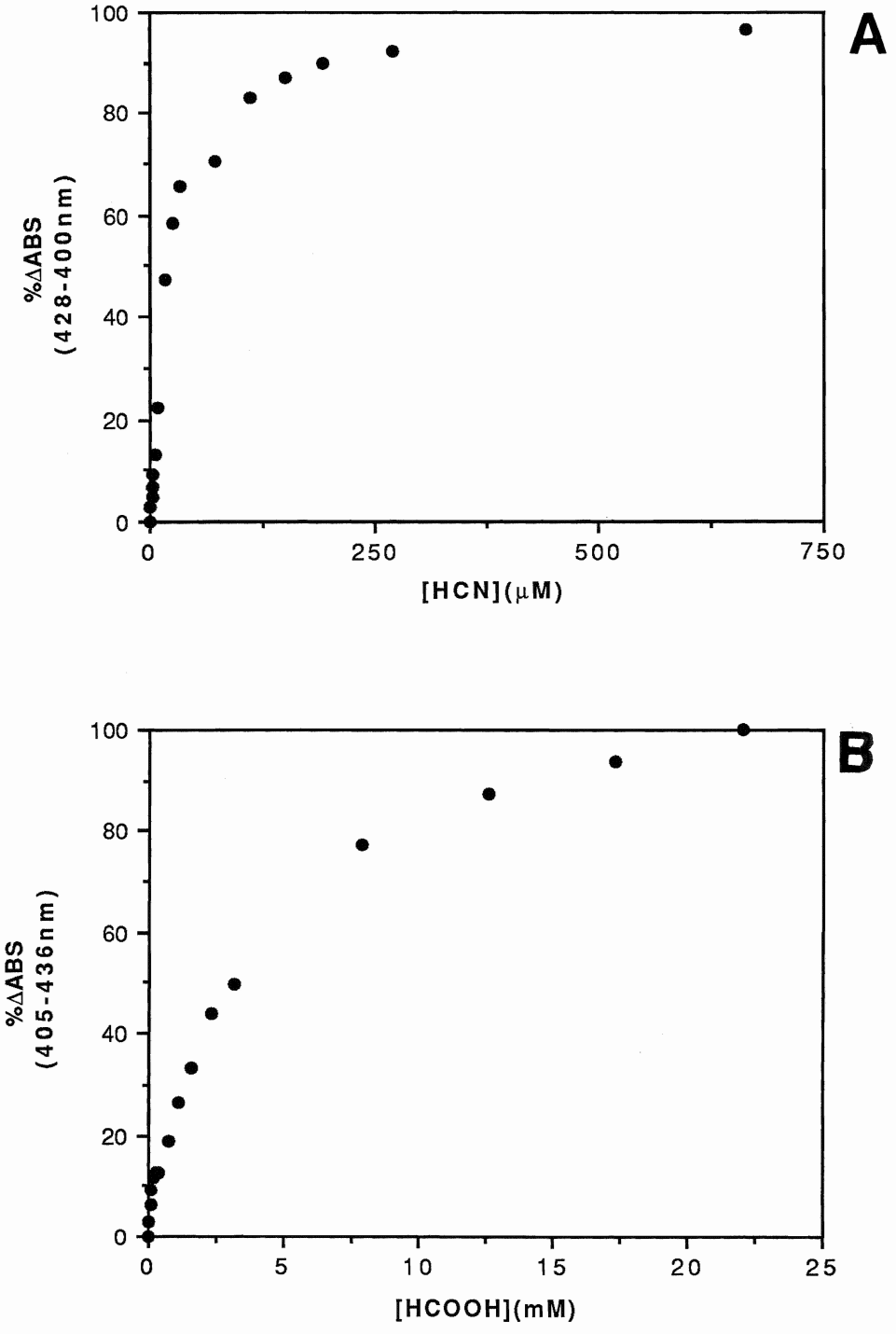
A
%ΔABS
(428-400nm)
100
80
60
40
20
0
0
250
500
750
[HCN](μM)
B
%ΔABS
(405-436nm)
100
80
60
40
20
0
0
5
10
15
20
25
[HCOOH](mM)

Figure B-1

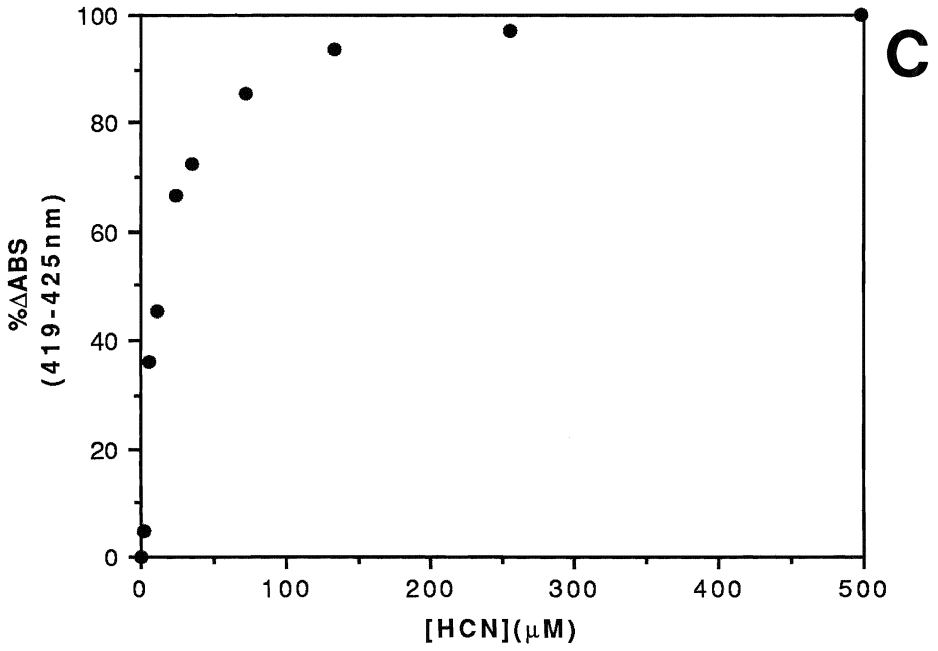
C
%ΔABS
(419-425nm)
100
80
60
40
20
0
0
100
200
300
400
500
[HCN](μM)

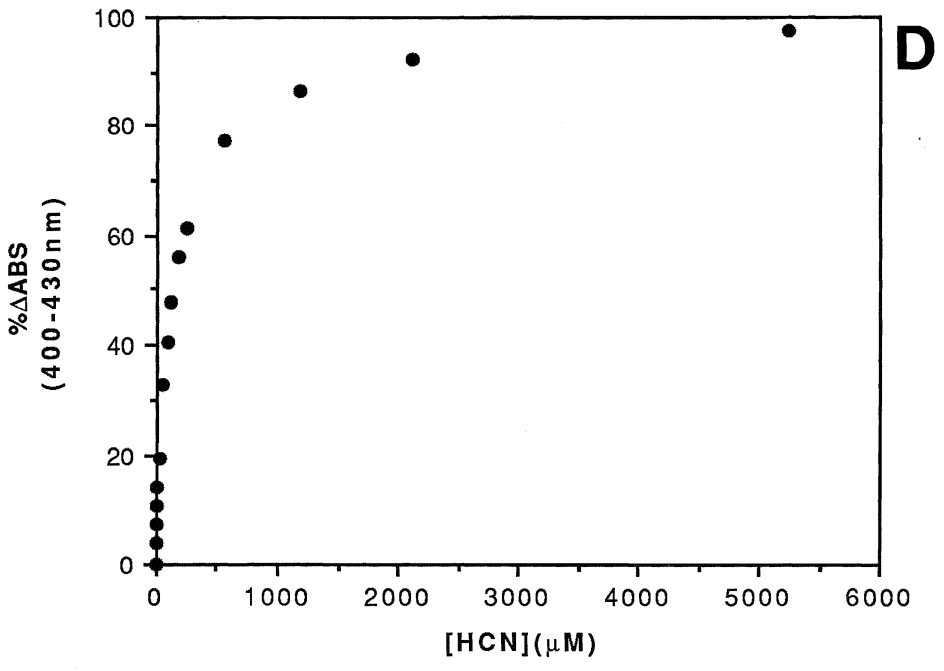
D
%ΔABS
(400-430nm)
100
80
60
40
20
0
0
1000
2000
3000
4000
5000
6000
[HCN](μM)

Figure B-1

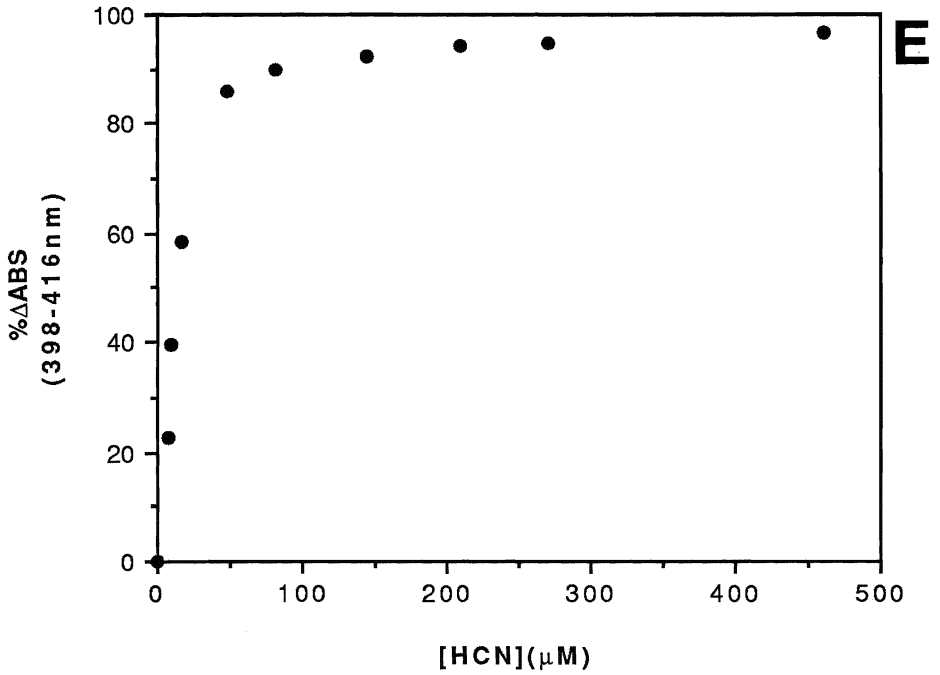
E
%ΔABS
(398-416nm)
100
80
60
40
20
0
0
100
200
300
400
500
[HCN](μM)

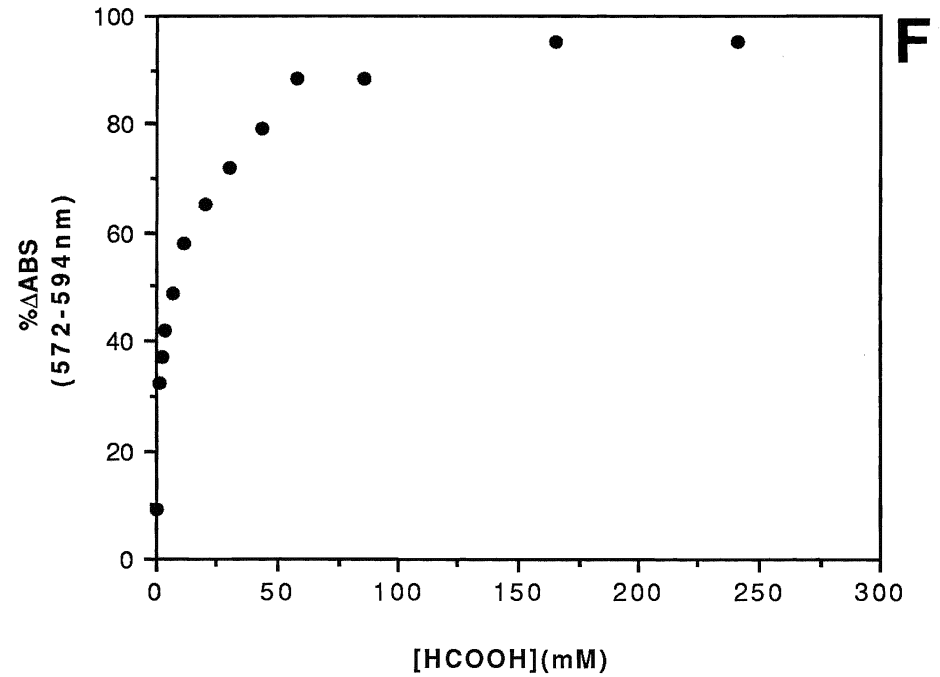
F
%ΔABS
(572-594nm)
100
80
60
40
20
0
0
50
100
150
200
250
300
[HCOOH](mM)

Figure B-1

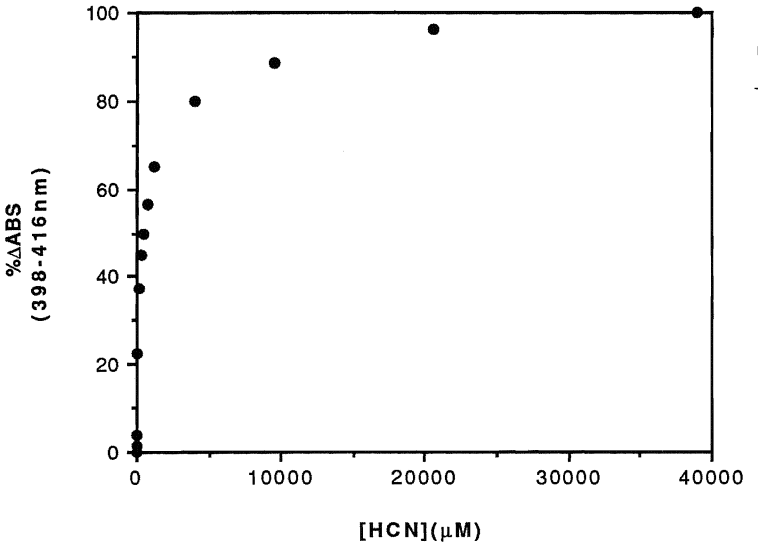

G

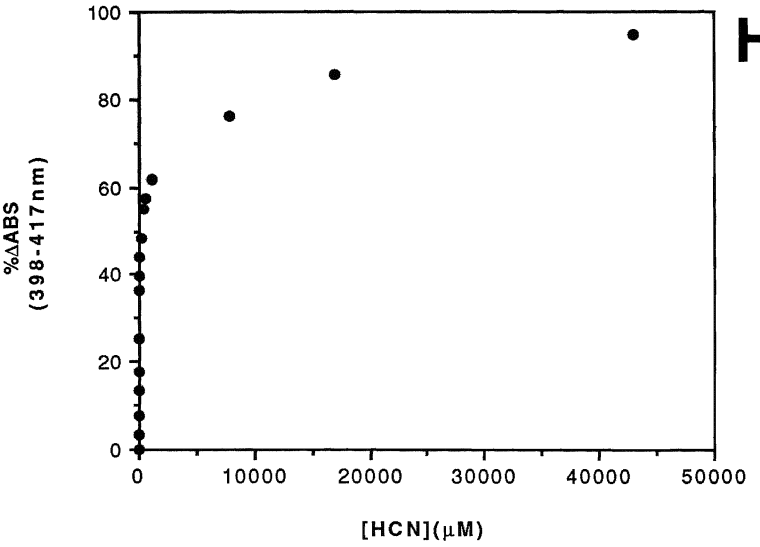

H

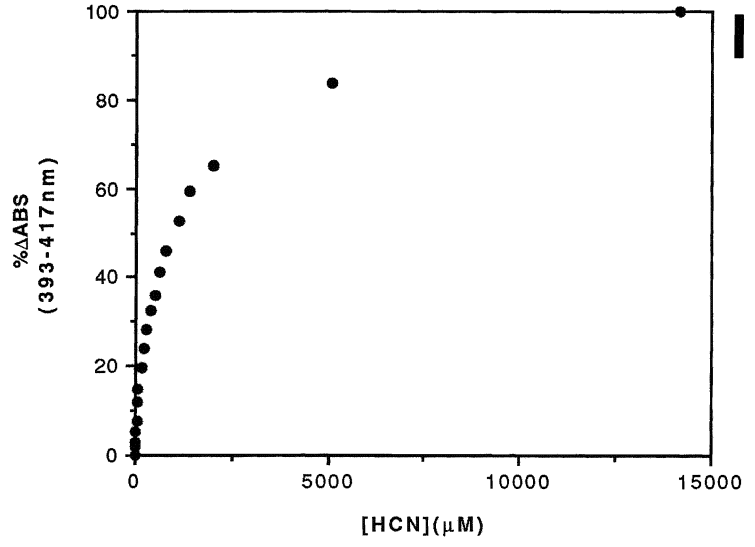

I